Jnclassified
ecurity Classification of this page

REPORT DOCUMENTATION PAGE

1a Report Security Classification: Unclassified	1b Restrictive Markings
2a Security Classification Authority 2b Declassification/Downgrading Schedule	3 Distribution/Availability of Report Approved for public release; distribution is unlimited.
4 Performing Organization Report Number(s)	5 Monitoring Organization Report Number(s)
6a Name of Performing Organization Naval Postgraduate School — 6b Office Symbol *(if applicable)* AA/PL	7a Name of Monitoring Organization Naval Postgraduate School
6c Address *(city, state, and ZIP code)* Monterey CA 93943-5000	7b Address *(city, state, and ZIP code)* Monterey CA 93943-5000
8a Name of Funding/Sponsoring Organization — 6b Office Symbol *(if applicable)*	9 Procurement Instrument Identification Number
Address *(city, state, and ZIP code)*	10 Source of Funding Numbers Program Element No / Project No / Task No / Work Unit Accession No

11 Title *(include security classification)* A COMPUTATIONAL AND EXPERIMENTAL INVESTIGATION OF INCOMPRESSIBLE OSCILLATORY AIRFOIL FLOW AND FLUTTER PROBLEMS

12 Personal Author(s) Riester, Peter J.

13a Type of Report	13b Time Covered	14 Date of Report *(year, month, day)*	15 Page Count
Master's Thesis	From To	1993, June	160

16 Supplementary Notation The views expressed in this thesis are those of the author and do not reflect the official policy or position of the Department of Defense or the U.S. Government.

17 Cosati Codes			18 Subject Terms *(continue on reverse if necessary and identify by block number)*
Field	Group	Subgroup	Flutter,Theodorsen comparison with panel code U2DIIF,Enhanced lift, Flow visualization.

19 Abstract *(continue on reverse if necessary and identify by block number)*

In this thesis several incompressible oscillatory flow and flutter problems were investigated. First, a previously developed unsteady panel code was modified so that systematic comparisons with Theodorsen's classical theory could be accomplished. It was found that the panel code is in excellent agreement with the Theodorsen results. Second, the panel code was applied to the analysis of bending-torsion flutter. Again, general agreement with Theodorsen's flutter predictions was obtained. In the experimental part of the thesis two flow visualization experiments were performed. First, the vortical flow patterns generated by an airfoil executing harmonic plunge oscillations were visualized. In the second experiment, the interference effects between a stationary airfoil and a small vane executing plunge oscillations were explored.

20 Distribution/Availability of Abstract xx__ unclassified/unlimited __ same as report __ DTIC users	21 Abstract Security Classification Unclassified	
22a Name of Responsible Individual M. F. Platzer	22b Telephone *(include Area Code)* 408 656 2058	22c Office Symbol AA/PL

DD FORM 1473,84 MAR — 83 APR edition may be used until exhausted — security classification of this page

All other editions are obsolete — Unclassified

Approved for public release; distribution is unlimited.

A COMPUTATIONAL AND EXPERIMENTAL INVESTIGATION OF INCOMPRESSIBLE OSCILLATORY AIRFOIL FLOW AND FLUTTER PROBLEMS

by

Peter J. Riester
Lieutenant Commander, United States Navy
B.S., United States Naval Academy, 1981

Submitted in partial fulfillment
of the requirements for the degree of

MASTER OF SCIENCE IN AERONAUTICAL ENGINEERING

from the

NAVAL POSTGRADUATE SCHOOL
June 1993

ABSTRACT

In this thesis several incompressible oscillatory flow and flutter problems were investigated. First, a previously developed unsteady panel code was modified so that systematic comparisons with Theodorsen's classical theory could be accomplished. It was found that the panel code is in excellent agreement with the Theodorsen results. Second, the panel code was applied to the analysis of bending-torsion flutter. Again, general agreement with Theodorsen's flutter predictions was obtained. In the experimental part of the thesis two flow visualization experiments were performed. First, the vortical flow patterns generated by an airfoil executing harmonic plunge oscillations were visualized. In the second experiment, the interference effects between a stationary airfoil and a small vane executing plunge oscillations were explored.

TABLE OF CONTENTS

TABLE OF SYMBOLS

a elastic axis position taken from the midchord

b half chord

C_α spring constant for pitch

C_h spring constant for plunge

C_D drag coefficient

C_L lift coefficient

$C_{L\alpha}$ lift coefficient as a result of pitch

C_{Lh} lift coefficient as a result of plunge

$C_{M\alpha}$ moment coefficient as a result of pitch

C_{Mh} moment coefficient as a result of plunge

h plunge amplitude

i denotes complex number

I_α mass moment of inertia

I_L denotes imaginary part of lift

I_M denotes imaginary part of moment

Im Imaginary part

K_p reduced frequency used in panel code

K_t reduced frequency used in Theodorsen analysis

κ mass ratio $(1/\mu)$

L lift force per unit span

L_α, L_β, L_h aerodynamic coefficients used for Theodorsen analysis

M moment

M_h, M_α aerodynamic coefficients used for Theodorsen analysis

q dynamic pressure

Re real part

R_L real part of lift

R_M real part of moment

S_α static moment about the elastic axis

t nondimensional time

U freestream velocity

AOA angle of atack

α pitch amplitude

ρ density

ϕ phase angle between force and motion

$\phi_{L\alpha}$ phase angle between lift force and pitch motion

ϕ_{Lh} phase angle between lift force and plunge motion

$\phi_{M\alpha}$ phase angle between moment and pitch motion

ϕ_{Mh} phase angle between moment and plunge motion

ω frequency of harmonic oscillation (rad/sec)

ω_α natural frequency of system for pitch

ω_h natural frequency of system for plunge

ACKNOWLEDGEMENTS

The research for this thesis was conducted using the facilities of the Department of Aeronautics and Astronautics at the Naval Postgraduate School. I would like to give my sincere appreciation to professors M. F. Platzer and S. K. Hebbar, my thesis advisor and co-advisor, for their guidance, encouragement and many hours of council that led to the completion of this work. In addition I would like to thank Dr. E. Tuncer for helping me modify the U2DIIF panel code through his gifted knowledge of computers in the department.

I would also like to thank the staff of the Department of Aeronautics and Astronautics, in particular Mr. John Molton, Mr. Ron Ramaker, Mr Don Meeks, Mr. Rick Stills, Mr. Ted Best, Mr Pat Hickey and Mr. Jack King. Their technical assistance was instrumental in enabling my experiment to be a success.

Special thanks go to the Department of Physics, in particular Dr. Robert Keolian for helping me with the smoke tunnel phase of my research. The use of Dr. Keolian's shaker table and design suggestions proved to be extremely helpful

Finally, I would like to thank my beautiful and gifted wife, Nancy, for her endless support both throughout my tour here and finally in the typing of this thesis.

I. INTRODUCTION

A. GENERAL

In this thesis, several numerical methods were used to analyze the flow about an airfoil performing unsteady motion in an inviscid incompressible fluid. First, the unsteady motion of a single airfoil was analyzed after modifying the U2DIIF code [ref.2]. The primary purpose was to verify the code against the proven theory of Theodorsen for analyzing the phenomenon of flutter. To accomplish this the U2DIIF code was modified to calculate aerodynamic values over a range of reduced frequencies and then apply these values to the flutter analysis.

Next, the propulsive effects of a plunging airfoil were verified through experimental methods using a low speed plexiglas wind tunnel.

Finally, an exploratory test was conducted in the department's smoke tunnel to study the interaction between a plunging airfoil and a stationary large airfoil.

B. SCOPE

Chapter II contains the modification of the single airfoil U2DIIF code into the code UPOT.f and extensive verification of this code against results produced by Theodorsen. Chapter III describes the UPOT code and explains the modifications which

were added to solve the flutter determinant. In chapter IV the flow visualization experiment is described which was performed to study the vortical wake patterns produced by a plunging airfoil. In chapter V a second experiment is described which was performed to explore a plunging airfoil's potential for control of flow separation.

II. SINGLE AIRFOIL ANALYSIS

A. U2DIFF PANEL CODE

1. Geometry

Figure 2.1 shows a representation of the system that is analyzed using the panel code. Shown are the values for h (plunge) and α (AOA).

2. U2DIFF

The U2DIIF code was developed by TENG [ref.2] for the study of unsteady inviscid and incompressible flow over a single airfoil. The code is based on the extension of the panel method, developed by Hess & Smith [ref.4] for steady potential flow problems, to include the unsteady motion of the airfoil that is continuously shedding vortices into the trailing wake. This vortex shedding process is nonlinear in that the wake vortices influence the flow over the airfoil which in turn alters the vortex shedding as the airfoil proceeds in time.

The non-linearity of the unsteady flow makes this problem different from the steady flow problem which requires only simple Gaussian elimination. Teng developed a code that used an iterative type of solution. Typical program output includes the airfoil pressure distribution, force and moment coefficients, and the trailing vortex wake pattern. No

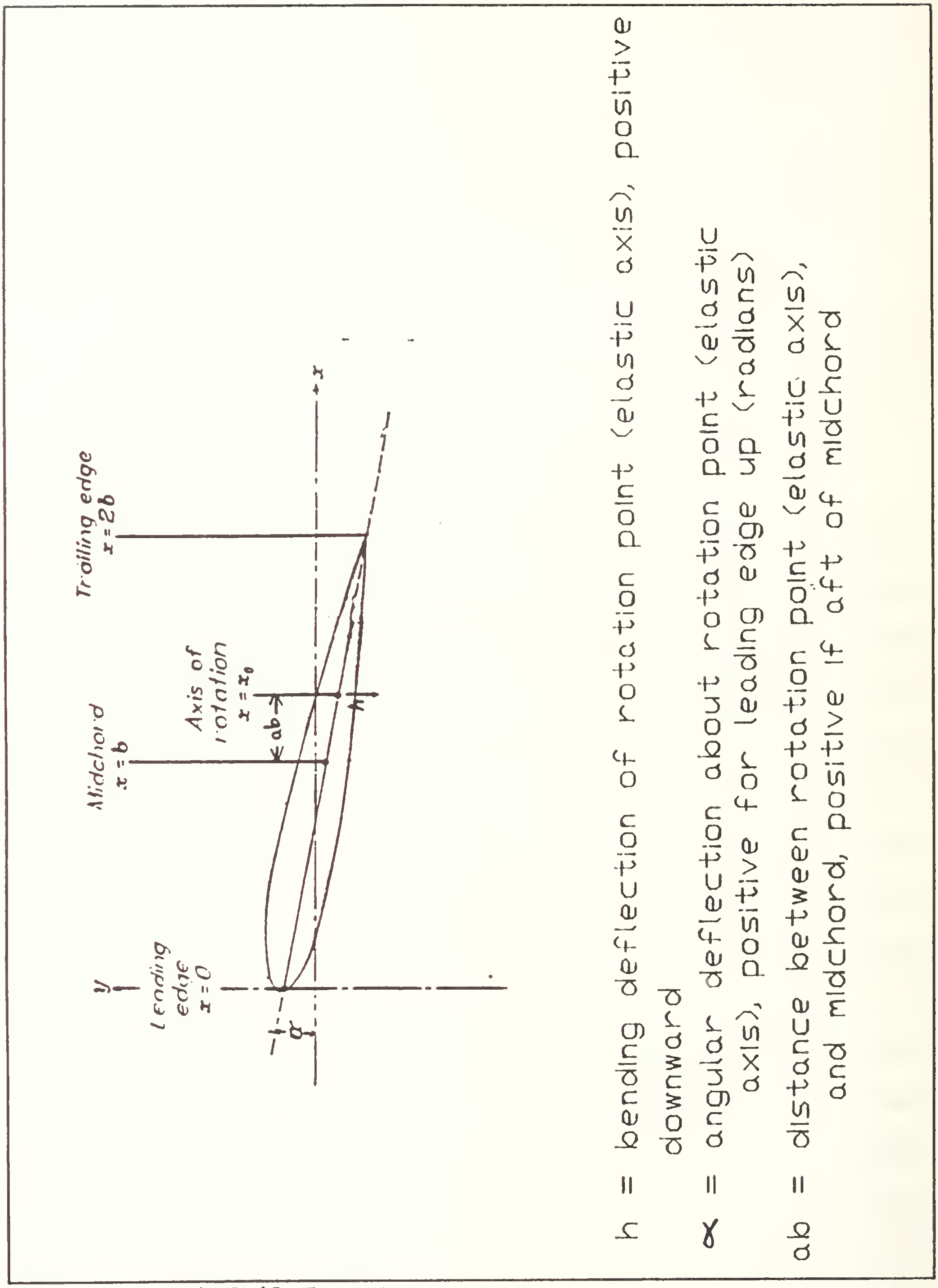

Figure 2.1 Airfoil Geometry

attempt is made here to reproduce the work of Teng or to explore the operation of the U2DIIF code, but the reader is encouraged to review reference 2.

B. PHASE PROGRAM

The phase program was put through some verification by Neace [ref.9] and modified slightly in order to present results for harmonic motion. The code PHV3.f (phaseshift) was written by Neace to convert the time dependent output of lift and moment histories to harmonic output using an iterative curve fit algorithm:

$$F(t)=Amp*Sin(\omega t+\phi) \qquad (2.1)$$

where Amp = amplitude of motion, ω = frequency, and ϕ = phase angle between motion and the aerodynamic forces. One primary output of this program was the values of phaseshift (ϕ) between the AOA and coefficients of lift (C_L) and moment (C_M) for the pitching airfoil and the phaseshift between the plunge value (h/2b) and the C_L and C_M for the plunging airfoil. The other output was the amplitude of C_L and C_M for the pitching or plunging case.

C. MODIFICATION OF U2DIIF AND PHASE PROGRAM

In an attempt to make the above mentioned codes more "user friendly", the two codes were combined into a single code named UPOT.f. The modification involved a new input file

called UPOT.in which gives the user several options of operation. The input file can call for the analysis of steady flow only, straight and modified ramp motion, pitch oscillation, plunge oscillation, and the capability of performing the oscillation analysis over a series of reduced frequencies. A sample input file is shown in Figure (2.2).

1. Output

Outputs from the code have been limited to reduce the amount of computer space taken up by the code operation. A sample calculation was run using the input from Figure (2.2) and the on-screen output is shown in Figure (2.3). Of course, the user can modify the output portions of the code to minimize output. The following list describes the input/output files and the data they contain.

a. UPOT.IN: The input file figure (2.2).

b. CL.d: This file contains the various AOA values along with its corresponding C_L for each time step.

c. CM.D: This file contains the various AOA values along with its corresponding C_M for each time step.

d. PHASE.d: This file contains the values of non dimensional time (t), AOA, C_L, C_M, for each time step.

e. FOR015.DAT: This file contains the values of non dimensional AOA, curve fit for C_L, curve fit for C_M, (used in the phase portion of program).

f. CPSS.d: This file contains the steady state pressure coefficient for the mid point locations of all the air foil panels.

g. CPU005.d: This file contains the unsteady pressure coefficient for the mid point location of all airfoil

panels. (in this case the values are for an AOA equal to 5 degrees).

h. PHZSWP.d: This file contains the phase information of the reduced frequency sweep portion for the program. The file contains the phase angle of C_L, and C_M, and the amplitude of C_L, C_M.

i. FLUTTER.IN: This file contains information that can be used to solve the flutter determinant. It contains K_p, C_L Re, C_L Im, C_M Re, C_M Im for the pitch or plunge case.

stdin Page 1

```
 4
.................................................................
      AIRFOIL TYPE : NACA 0012 AIRFOIL
      NLOWER = 50 , NUPPER = 50
.................................................................
IFLAG  NLOWER  NUPPER
0        50     50
AIRFOIL TYPE
 7
IRAMP  IOSCIL   ALPI      ALPMAX       PIVOT
  0      1      -3.0       3.0          0.37
FREQ   RFQSTP  RFQFNL
.68      0.01     .7
IGUST  UGUST   VGUST
  0     0.      0.
ITRANS  DELHX  DELHY DELI  PHASE
0        .00     .0    .0   0.00
CYCLE  NTCYCLE     TOL
 2       60        0.005
naot &  naot X aoa values multiplied by 10 (integer)
 2      05 10  20 25 39 50


Comments...

IRAMP  0: n/a              RFREQ is based on full chord
       1: Straight ramp
       2: Modified ramp

IOSCIL 0: n/a              RFREQ is based on full chord
       1: Sinusoidal pitch, motion starts at min Aoa

ITRANS 0: n/a
       1: Translational harmonic oscillation

ALPI/ALPMAX   Minimum/MAX  AOA in degrees for IRAMP/ITRANS/IOSCIL
              MAX does not apply for ITRANS
PIVOT  Location of Elastic Axis as a fraction of full chord
FREQ   Initial reduced frequency for program
RFQSTP Reduced freq step size for a sweep of freq.'s(enter 0.0 if only one calcu
   lation is desired.)
RFQFNL Final freq for the sweep
DELHX  Translational amount in the chordwise direction (dist/full chord)
DELHY  Max Translational amount in the vertical direction (h/fullchord(b))
DELI   Min Translational amount in the vertical direction (h/b)
CYCLE  : # of cycles for oscillatory motions
        -In case of ramp, cycle=1.5 denotes airfoil is held
         at max aoa for the duration of .5 cycle
        -For steady state solution set it to 0

NTCYCLE: # of time steps for each cycle
          CYCLE*NTCYCLE is limited to 200 currently.
TOL     Tolerance for convergence of the unsteady solution.(recommend using not
    less than .001)
NAOT: # of input aoa for cp output
       - angles should be in increasing order,
       - for oscilatory motions angles should increase
         first, then decrease. Decreasing angles are for
         the return cycle..
```

Figure 2.2 UPOT.IN

```
stdin                                                    Page 1

     4
   ****************************************************************
         AIRFOIL TYPE : NACA 0012 AIRFOIL
         NLOWER = 50 , NUPPER = 50
   ****************************************************************



   =======================================
   IFLAG    (0:NACA, 1:INPUT)     =     0
   NO. PANELS UPPER SURFACE       =    50
   NO. PANELS LOWER SURFACE       =    50
   =======================================
     7
   OSCILLATORY MOTION, IOSCIL      =              1
   INITIAL ANGLE OF ATTACK        =    -3.0000
   FINAL   ANGLE OF ATTACK        =     3.0000
   REDUCED FREQ. FOR OSCIL        =     0.6800
   REDUCED FREQ. STEP       =     0.0100
   FINAL REDUCED FREQ.            =     0.7000
   PIVOT POINT                    =     0.3700
   =======================================
   TOTAL # OF CYCLES              =     2.0000
   # of TIME STEPS PER CYCLE      =    60
   TOLERANCE FOR CONVERGENCE      =     0.0050
   =======================================



 FREQ SWEEP
 FREQ =    0.680000


  STEADY FLOW SOLUTION AT ALPHA =  -3.000000

     1  0.999507 -1.116717 -0.086820  0.280753 -0.848084
     2  0.997535 -1.108171 -0.086820  0.213074 -0.887088
     3  0.993600 -1.100064 -0.086820  0.168200 -0.912031
     4  0.987718 -1.092523 -0.086820  0.134381 -0.930386
     5  0.979910 -1.085444 -0.086820  0.106525 -0.945238
     6  0.970208 -1.078820 -0.086820  0.082353 -0.957939
     7  0.958651 -1.072610 -0.086820  0.060678 -0.969186
     8  0.945283 -1.066794 -0.086820  0.040815 -0.979380
     9  0.930159 -1.061323 -0.086820  0.022307 -0.988783
    10  0.913336 -1.056157 -0.086820  0.004851 -0.997572
    11  0.894883 -1.051250 -0.086820 -0.011780 -1.005873
    12  0.874870 -1.046545 -0.086820 -0.027772 -1.013791
    13  0.853379 -1.041994 -0.086820 -0.043274 -1.021408
    14  0.830493 -1.037547 -0.086820 -0.058416 -1.028793
    15  0.806302 -1.033154 -0.086820 -0.073319 -1.036011
    16  0.780903 -1.028773 -0.086820 -0.088096 -1.043118
    17  0.754395 -1.024362 -0.086820 -0.102850 -1.050167
    18  0.726883 -1.019887 -0.086820 -0.117685 -1.057206
    19  0.698476 -1.015315 -0.086820 -0.132698 -1.064283
    20  0.669285 -1.010628 -0.086820 -0.147973 -1.071435
    21  0.639427 -1.005803 -0.086820 -0.163603 -1.078704
    22  0.609018 -1.000836 -0.086820 -0.179660 -1.086122
    23  0.578179 -0.995714 -0.086820 -0.196223 -1.093720
    24  0.547031 -0.990441 -0.086820 -0.213352 -1.101523
    25  0.515698 -0.985017 -0.086820 -0.231108 -1.109553
    26  0.484302 -0.979449 -0.086820 -0.249545 -1.117830
    27  0.452969 -0.973745 -0.086820 -0.268710 -1.126370
    28  0.421821 -0.967910 -0.086820 -0.288653 -1.135188
    29  0.390982 -0.961956 -0.086820 -0.309418 -1.144298
    30  0.360573 -0.955883 -0.086820 -0.331061 -1.153716
    31  0.330715 -0.949692 -0.086820 -0.353649 -1.163464
    32  0.301524 -0.943373 -0.086820 -0.377267 -1.173570
    33  0.273117 -0.936907 -0.086820 -0.402032 -1.184074
    34  0.245605 -0.930250 -0.086820 -0.428106 -1.195034
    35  0.219097 -0.923337 -0.086820 -0.455707 -1.206527
    36  0.193698 -0.916066 -0.086820 -0.485152 -1.218668
    37  0.169507 -0.908273 -0.086820 -0.516866 -1.231611
    38  0.146621 -0.899722 -0.086820 -0.551434 -1.245566
```

Figure 2.3a UPOT output

stdin Page 2

39	0.125130	-0.890054	-0.086820	-0.589671	-1.260822
40	0.105117	-0.878738	-0.086820	-0.632708	-1.277774
41	0.086664	-0.864972	-0.086820	-0.682121	-1.296966
42	0.069841	-0.847530	-0.086820	-0.740144	-1.319145
43	0.054717	-0.824472	-0.086820	-0.810000	-1.345363
44	0.041349	-0.792611	-0.086820	-0.896386	-1.377093
45	0.029792	-0.746398	-0.086820	-1.006151	-1.416387
46	0.020090	-0.675433	-0.086820	-1.148872	-1.465903
47	0.012282	-0.558323	-0.086820	-1.334727	-1.527981
48	0.006399	-0.346398	-0.086820	-1.554189	-1.598183
49	0.002465	0.075008	-0.086820	-1.656311	-1.629819
50	0.000493	0.854855	-0.086820	-0.999986	-1.414209
51	0.000493	1.561213	-0.086820	0.449705	-0.741819
52	0.002465	1.669507	-0.086820	0.997431	-0.050689
53	0.006399	1.558290	-0.086820	0.875814	0.352401
54	0.012282	1.445845	-0.086820	0.674864	0.570207
55	0.020090	1.357269	-0.086820	0.513069	0.697804
56	0.029792	1.287651	-0.086820	0.392567	0.779380
57	0.041349	1.231267	-0.086820	0.302348	0.835256
58	0.054717	1.184229	-0.086820	0.233416	0.875548
59	0.069841	1.144055	-0.086820	0.179673	0.905719
60	0.086664	1.109153	-0.086820	0.137083	0.928933
61	0.105117	1.078474	-0.086820	0.102934	0.947136
62	0.125130	1.051316	-0.086820	0.075364	0.961580
63	0.146621	1.027193	-0.086820	0.053053	0.973112
64	0.169507	1.005756	-0.086820	0.035030	0.982329
65	0.193698	0.986749	-0.086820	0.020565	0.989664
66	0.219097	0.969966	-0.086820	0.009091	0.995444
67	0.245605	0.955241	-0.086820	0.000149	0.999926
68	0.273117	0.942428	-0.086820	-0.006640	1.003314
69	0.301524	0.931390	-0.086820	-0.011593	1.005780
70	0.330715	0.921993	-0.086820	-0.014984	1.007464
71	0.360573	0.914106	-0.086820	-0.017049	1.008488
72	0.390982	0.907597	-0.086820	-0.017994	1.008957
73	0.421821	0.902331	-0.086820	-0.018001	1.008960
74	0.452969	0.898173	-0.086820	-0.017221	1.008574
75	0.484302	0.894989	-0.086820	-0.015784	1.007861
76	0.515698	0.892645	-0.086820	-0.013805	1.006879
77	0.547031	0.891016	-0.086820	-0.011369	1.005668
78	0.578179	0.889982	-0.086820	-0.008545	1.004263
79	0.609018	0.889434	-0.086820	-0.005387	1.002690
80	0.639427	0.889276	-0.086820	-0.001926	1.000962
81	0.669285	0.889426	-0.086820	0.001821	0.999089
82	0.698476	0.889824	-0.086820	0.005855	0.997068
83	0.726883	0.890423	-0.086820	0.010190	0.994892
84	0.754395	0.891196	-0.086820	0.014851	0.992547
85	0.780903	0.892138	-0.086820	0.019880	0.990010
86	0.806302	0.893264	-0.086820	0.025328	0.987255
87	0.830493	0.894605	-0.086820	0.031258	0.984247
88	0.853379	0.896208	-0.086820	0.037745	0.980946
89	0.874870	0.898136	-0.086820	0.044881	0.977302
90	0.894883	0.900467	-0.086820	0.052775	0.973255
91	0.913336	0.903280	-0.086820	0.061567	0.968728
92	0.930159	0.906675	-0.086820	0.071417	0.963630
93	0.945283	0.910746	-0.086820	0.082565	0.957828
94	0.958651	0.915603	-0.086820	0.095332	0.951141
95	0.970208	0.921351	-0.086820	0.110175	0.943306
96	0.979910	0.928123	-0.086820	0.127830	0.933900
97	0.987718	0.936086	-0.086820	0.149558	0.922194
98	0.993600	0.945516	-0.086820	0.177698	0.906809
99	0.997535	0.957020	-0.086820	0.217400	0.884647
100	0.999507	0.971841	-0.086820	0.280753	0.848084

```
***************************************
***  BEGIN UNSTEADY FLOW SOLUTION  ****
***************************************
```

istep	alpha	time	nitr	cl,	cd,	cm
1	-3.0000	0.0000	1	-0.3479	0.0002	-0.0403
2	-2.9836	0.1540	0	-0.3372	-0.0005	-0.0424
3	-2.9344	0.3080	0	-0.3247	-0.0012	-0.0434
4	-2.8532	0.4620	0	-0.3101	-0.0019	-0.0441

Figure 2.3b UPOT output

stdin Page 3

5	-2.7406	0.6160	0	-0.2935	-0.0027	-0.0444
6	-2.5981	0.7700	0	-0.2751	-0.0033	-0.0444
7	-2.4271	0.9240	0	-0.2549	-0.0039	-0.0441
8	-2.2294	1.0780	0	-0.2332	-0.0044	-0.0434
9	-2.0074	1.2320	0	-0.2101	-0.0047	-0.0424
10	-1.7634	1.3860	0	-0.1858	-0.0048	-0.0410
11	-1.5000	1.5400	0	-0.1605	-0.0048	-0.0393
12	-1.2202	1.6940	0	-0.1345	-0.0046	-0.0373
13	-0.9271	1.8480	0	-0.1080	-0.0043	-0.0350
14	-0.6237	2.0020	0	-0.0812	-0.0038	-0.0323
15	-0.3136	2.1560	0	-0.0545	-0.0031	-0.0295
16	0.0000	2.3100	1	-0.0280	-0.0023	-0.0264
17	0.3136	2.4640	0	-0.0021	-0.0014	-0.0231
18	0.6237	2.6180	0	0.0230	-0.0004	-0.0197
19	0.9271	2.7720	0	0.0471	0.0006	-0.0161
20	1.2202	2.9260	0	0.0699	0.0016	-0.0124
21	1.5000	3.0800	1	0.0911	0.0025	-0.0087
22	1.7634	3.2340	0	0.1107	0.0034	-0.0050
23	2.0074	3.3880	0	0.1284	0.0042	-0.0013
24	2.2294	3.5420	0	0.1440	0.0048	0.0024
25	2.4271	3.6960	0	0.1573	0.0053	0.0059
26	2.5981	3.8500	1	0.1683	0.0056	0.0093
27	2.7406	4.0040	0	0.1769	0.0057	0.0126
28	2.8532	4.1580	0	0.1829	0.0056	0.0156
29	2.9344	4.3120	0	0.1863	0.0054	0.0184
30	2.9836	4.4660	0	0.1872	0.0050	0.0210
31	3.0000	4.6200	0	0.1855	0.0045	0.0232
32	2.9836	4.7740	0	0.1812	0.0038	0.0252
33	2.9344	4.9280	0	0.1745	0.0031	0.0268
34	2.8532	5.0820	0	0.1653	0.0024	0.0280
35	2.7406	5.2360	1	0.1538	0.0016	0.0289
36	2.5981	5.3900	0	0.1402	0.0008	0.0295
37	2.4270	5.5440	0	0.1246	0.0002	0.0296
38	2.2294	5.6980	0	0.1071	-0.0004	0.0294
39	2.0074	5.8520	0	0.0880	-0.0009	0.0288
40	1.7634	6.0060	0	0.0676	-0.0012	0.0278
41	1.5000	6.1600	0	0.0459	-0.0014	0.0265
42	1.2202	6.3140	0	0.0234	-0.0014	0.0249
43	0.9270	6.4680	0	0.0001	-0.0013	0.0229
44	0.6237	6.6220	0	-0.0235	-0.0010	0.0206
45	0.3136	6.7760	0	-0.0472	-0.0006	0.0181
46	0.0000	6.9300	1	-0.0709	0.0000	0.0153
47	-0.3136	7.0840	0	-0.0941	0.0006	0.0123
48	-0.6237	7.2380	0	-0.1166	0.0014	0.0092
49	-0.9271	7.3920	0	-0.1382	0.0021	0.0059
50	-1.2202	7.5460	0	-0.1586	0.0028	0.0025
51	-1.5000	7.7000	1	-0.1776	0.0035	-0.0010
52	-1.7634	7.8540	0	-0.1950	0.0041	-0.0045
53	-2.0074	8.0080	0	-0.2105	0.0047	-0.0080
54	-2.2294	8.1620	0	-0.2241	0.0051	-0.0114
55	-2.4271	8.3160	0	-0.2356	0.0053	-0.0147
56	-2.5981	8.4700	0	-0.2448	0.0054	-0.0179
57	-2.7406	8.6240	1	-0.2516	0.0053	-0.0210
58	-2.8532	8.7780	0	-0.2559	0.0051	-0.0239
59	-2.9344	8.9320	0	-0.2578	0.0047	-0.0265
60	-2.9836	9.0860	0	-0.2571	0.0042	-0.0289
61	-3.0000	9.2400	0	-0.2539	0.0035	-0.0309
62	-2.9836	9.3940	0	-0.2482	0.0028	-0.0327
63	-2.9344	9.5480	0	-0.2400	0.0020	-0.0342
64	-2.8532	9.7020	0	-0.2295	0.0011	-0.0353
65	-2.7406	9.8560	0	-0.2168	0.0003	-0.0360
66	-2.5981	10.0100	0	-0.2019	-0.0005	-0.0364
67	-2.4271	10.1640	0	-0.1851	-0.0012	-0.0365
68	-2.2294	10.3180	0	-0.1664	-0.0017	-0.0361
69	-2.0074	10.4720	0	-0.1463	-0.0022	-0.0354
70	-1.7634	10.6260	0	-0.1247	-0.0025	-0.0343
71	-1.5000	10.7800	0	-0.1020	-0.0026	-0.0329
72	-1.2202	10.9340	0	-0.0784	-0.0026	-0.0311
73	-0.9271	11.0880	0	-0.0542	-0.0024	-0.0290
74	-0.6237	11.2420	0	-0.0296	-0.0020	-0.0267
75	-0.3136	11.3960	0	-0.0050	-0.0015	-0.0240
76	0.0000	11.5500	0	0.0195	-0.0008	-0.0211
77	0.3136	11.7040	0	0.0436	-0.0001	-0.0181

Figure 2.3c UPOT output

```
                                   stdin                              Page 4

  78    0.6237 11.8580     0        0.0670     0.0007    -0.0148
  79    0.9270 12.0120     0        0.0894     0.0016    -0.0114
  80    1.2202 12.1660     1        0.1106     0.0024    -0.0079
  81    1.5000 12.3200     0        0.1304     0.0033    -0.0044
  82    1.7633 12.4740     0        0.1486     0.0040    -0.0008
  83    2.0074 12.6280     0        0.1649     0.0046     0.0028
  84    2.2294 12.7820     0        0.1792     0.0051     0.0063
  85    2.4270 12.9360     1        0.1913     0.0055     0.0097
  86    2.5981 13.0900     0        0.2012     0.0057     0.0130
  87    2.7406 13.2440     0        0.2087     0.0057     0.0161
  88    2.8532 13.3980     0        0.2137     0.0056     0.0191
  89    2.9344 13.5520     0        0.2161     0.0053     0.0218
  90    2.9836 13.7060     0        0.2160     0.0048     0.0242
  91    3.0000 13.8600     0        0.2134     0.0042     0.0263
  92    2.9836 14.0140     1        0.2083     0.0036     0.0282
  93    2.9344 14.1680     0        0.2007     0.0028     0.0297
  94    2.8532 14.3220     0        0.1907     0.0020     0.0309
  95    2.7406 14.4760     0        0.1785     0.0012     0.0317
  96    2.5981 14.6300     0        0.1641     0.0005     0.0321
  97    2.4271 14.7840     0        0.1478    -0.0002     0.0322
  98    2.2294 14.9380     0        0.1297    -0.0008     0.0319
  99    2.0074 15.0920     0        0.1100    -0.0013     0.0312
 100    1.7634 15.2460     0        0.0889    -0.0016     0.0302
 101    1.5000 15.4000     0        0.0666    -0.0017     0.0288
 102    1.2202 15.5540     0        0.0435    -0.0017     0.0271
 103    0.9271 15.7080     0        0.0197    -0.0016     0.0251
 104    0.6238 15.8620     0       -0.0044    -0.0013     0.0228
 105    0.3136 16.0160     0       -0.0287    -0.0008     0.0202
 106    0.0000 16.1700     0       -0.0528    -0.0002     0.0173
 107   -0.3136 16.3239     1       -0.0765     0.0005     0.0143
 108   -0.6237 16.4779     0       -0.0994     0.0012     0.0111
 109   -0.9270 16.6319     0       -0.1215     0.0020     0.0078
 110   -1.2202 16.7859     0       -0.1423     0.0028     0.0043
 111   -1.5000 16.9399     0       -0.1617     0.0035     0.0008
 112   -1.7633 17.0939     1       -0.1795     0.0042    -0.0027
 113   -2.0074 17.2479     0       -0.1955     0.0047    -0.0063
 114   -2.2294 17.4019     0       -0.2095     0.0052    -0.0097
 115   -2.4270 17.5559     0       -0.2212     0.0054    -0.0131
 116   -2.5981 17.7099     0       -0.2308     0.0056    -0.0164
 117   -2.7406 17.8639     0       -0.2379     0.0055    -0.0195
 118   -2.8532 18.0179     1       -0.2426     0.0053    -0.0224
 119   -2.9344 18.1719     0       -0.2447     0.0049    -0.0250
 120   -2.9836 18.3259     0       -0.2444     0.0044    -0.0274


                 PHASE SHIFT ANALYSIS
                  FREQ =    0.6800000

 AMPLITUDE;  clamp, cmamp :  0.2304234       3.4331881E-02
 PHASE;        clp,    cmp  :    184.9092       -37.54200
 AVERAGE DRAG, TOTAL DRAG :    1.5421067E-03   9.4068512E-02
 ETAS, WBAR                 :  -0.2168084       -7.1127615E-03



FREQ SWEEP
FREQ =    0.690000


 STEADY FLOW SOLUTION AT ALPHA =   -3.000000

    1  0.999507 -1.116717 -0.086820  0.280753 -0.848084
    2  0.997535 -1.108171 -0.086820  0.213074 -0.887088
    3  0.993600 -1.100064 -0.086820  0.168200 -0.912031
    4  0.987718 -1.092523 -0.086820  0.134381 -0.930386
    5  0.979910 -1.085444 -0.086820  0.106525 -0.945238
    6  0.970208 -1.078820 -0.086820  0.082353 -0.957939
    7  0.958651 -1.072610 -0.086820  0.060678 -0.969186
    8  0.945283 -1.066794 -0.086820  0.040815 -0.979380
    9  0.930159 -1.061323 -0.086820  0.022307 -0.988783
   10  0.913336 -1.056157 -0.086820  0.004851 -0.997572
   11  0.894883 -1.051250 -0.086820 -0.011780 -1.005873
   12  0.874870 -1.046545 -0.086820 -0.027772 -1.013791
```

Figure 2.3d UPOT output

13	0.853379	-1.041994	-0.086820	-0.043274	-1.021408
14	0.830493	-1.037547	-0.086820	-0.058416	-1.028793
15	0.806302	-1.033154	-0.086820	-0.073319	-1.036011
16	0.780903	-1.028773	-0.086820	-0.088096	-1.043118
17	0.754395	-1.024362	-0.086820	-0.102850	-1.050167
18	0.726883	-1.019887	-0.086820	-0.117685	-1.057206
19	0.698476	-1.015315	-0.086820	-0.132698	-1.064283
20	0.669285	-1.010628	-0.086820	-0.147973	-1.071435
21	0.639427	-1.005803	-0.086820	-0.163603	-1.078704
22	0.609018	-1.000836	-0.086820	-0.179660	-1.086122
23	0.578179	-0.995714	-0.086820	-0.196223	-1.093720
24	0.547031	-0.990441	-0.086820	-0.213352	-1.101523
25	0.515698	-0.985017	-0.086820	-0.231108	-1.109553
26	0.484302	-0.979449	-0.086820	-0.249545	-1.117830
27	0.452969	-0.973745	-0.086820	-0.268710	-1.126370
28	0.421821	-0.967910	-0.086820	-0.288653	-1.135188
29	0.390982	-0.961956	-0.086820	-0.309418	-1.144298
30	0.360573	-0.955883	-0.086820	-0.331061	-1.153716
31	0.330715	-0.949692	-0.086820	-0.353649	-1.163464
32	0.301524	-0.943373	-0.086820	-0.377267	-1.173570
33	0.273117	-0.936907	-0.086820	-0.402032	-1.184074
34	0.245605	-0.930250	-0.086820	-0.428106	-1.195034
35	0.219097	-0.923337	-0.086820	-0.455707	-1.206527
36	0.193698	-0.916066	-0.086820	-0.485152	-1.218668
37	0.169507	-0.908273	-0.086820	-0.516866	-1.231611
38	0.146621	-0.899722	-0.086820	-0.551434	-1.245566
39	0.125130	-0.890054	-0.086820	-0.589671	-1.260822
40	0.105117	-0.878738	-0.086820	-0.632708	-1.277774
41	0.086664	-0.864972	-0.086820	-0.682121	-1.296966
42	0.069841	-0.847530	-0.086820	-0.740144	-1.319145
43	0.054717	-0.824472	-0.086820	-0.810000	-1.345363
44	0.041349	-0.792611	-0.086820	-0.896386	-1.377093
45	0.029792	-0.746398	-0.086820	-1.006151	-1.416387
46	0.020090	-0.675433	-0.086820	-1.148872	-1.465903
47	0.012282	-0.558323	-0.086820	-1.334727	-1.527981
48	0.006399	-0.346398	-0.086820	-1.554189	-1.598183
49	0.002465	0.075008	-0.086820	-1.656311	-1.629819
50	0.000493	0.854855	-0.086820	-0.999986	-1.414209
51	0.000493	1.561213	-0.086820	0.449705	-0.741819
52	0.002465	1.669507	-0.086820	0.997431	-0.050689
53	0.006399	1.558290	-0.086820	0.875814	0.352401
54	0.012282	1.445845	-0.086820	0.674864	0.570207
55	0.020090	1.357269	-0.086820	0.513069	0.697804
56	0.029792	1.287651	-0.086820	0.392567	0.779380
57	0.041349	1.231267	-0.086820	0.302348	0.835256
58	0.054717	1.184229	-0.086820	0.233416	0.875548
59	0.069841	1.144055	-0.086820	0.179673	0.905719
60	0.086664	1.109153	-0.086820	0.137083	0.928933
61	0.105117	1.078474	-0.086820	0.102934	0.947136
62	0.125130	1.051316	-0.086820	0.075364	0.961580
63	0.146621	1.027193	-0.086820	0.053053	0.973112
64	0.169507	1.005756	-0.086820	0.035030	0.982329
65	0.193698	0.986749	-0.086820	0.020565	0.989664
66	0.219097	0.969966	-0.086820	0.009091	0.995444
67	0.245605	0.955241	-0.086820	0.000149	0.999926
68	0.273117	0.942428	-0.086820	-0.006640	1.003314
69	0.301524	0.931390	-0.086820	-0.011593	1.005780
70	0.330715	0.921993	-0.086820	-0.014984	1.007464
71	0.360573	0.914106	-0.086820	-0.017049	1.008488
72	0.390982	0.907597	-0.086820	-0.017994	1.008957
73	0.421821	0.902331	-0.086820	-0.018001	1.008960
74	0.452969	0.898173	-0.086820	-0.017221	1.008574
75	0.484302	0.894989	-0.086820	-0.015784	1.007861
76	0.515698	0.892645	-0.086820	-0.013805	1.006879
77	0.547031	0.891016	-0.086820	-0.011369	1.005668
78	0.578179	0.889982	-0.086820	-0.008545	1.004263
79	0.609018	0.889434	-0.086820	-0.005387	1.002690
80	0.639427	0.889276	-0.086820	-0.001926	1.000962
81	0.669285	0.889426	-0.086820	0.001821	0.999089
82	0.698476	0.889824	-0.086820	0.005855	0.997068
83	0.726883	0.890423	-0.086820	0.010190	0.994892
84	0.754395	0.891196	-0.086820	0.014851	0.992547
85	0.780903	0.892138	-0.086820	0.019880	0.990010

Figure 2.3e UPOT output

```
 86  0.806302  0.893264 -0.086820  0.025328  0.987255
 87  0.830493  0.894605 -0.086820  0.031258  0.984247
 88  0.853379  0.896208 -0.086820  0.037745  0.980946
 89  0.874870  0.898136 -0.086820  0.044881  0.977302
 90  0.894883  0.900467 -0.086820  0.052775  0.973255
 91  0.913336  0.903280 -0.086820  0.061567  0.968728
 92  0.930159  0.906675 -0.086820  0.071417  0.963630
 93  0.945283  0.910746 -0.086820  0.082565  0.957828
 94  0.958651  0.915603 -0.086820  0.095332  0.951141
 95  0.970208  0.921351 -0.086820  0.110175  0.943306
 96  0.979910  0.928123 -0.086820  0.127830  0.933900
 97  0.987718  0.936086 -0.086820  0.149558  0.922194
 98  0.993600  0.945516 -0.086820  0.177698  0.906809
 99  0.997535  0.957020 -0.086820  0.217400  0.884647
100  0.999507  0.971841 -0.086820  0.280753  0.848084

****************************************
***   BEGIN UNSTEADY FLOW SOLUTION   ****
****************************************

 istep  alpha    time      nitr        cl, cd, cm

  1    -3.0000  0.0000     1       -0.3479    0.0002   -0.0403
  2    -2.9836  0.1518     0       -0.3370   -0.0005   -0.0425
  3    -2.9344  0.3035     0       -0.3243   -0.0012   -0.0435
  4    -2.8532  0.4553     0       -0.3096   -0.0020   -0.0442
  5    -2.7406  0.6071     0       -0.2929   -0.0027   -0.0445
  6    -2.5981  0.7588     0       -0.2744   -0.0034   -0.0446
  7    -2.4271  0.9106     0       -0.2542   -0.0039   -0.0442
  8    -2.2294  1.0624     0       -0.2323   -0.0044   -0.0436
  9    -2.0074  1.2141     0       -0.2091   -0.0047   -0.0426
 10    -1.7634  1.3659     0       -0.1848   -0.0049   -0.0412
 11    -1.5000  1.5177     0       -0.1595   -0.0049   -0.0395
 12    -1.2202  1.6694     0       -0.1334   -0.0047   -0.0375
 13    -0.9271  1.8212     0       -0.1069   -0.0043   -0.0352
 14    -0.6237  1.9730     0       -0.0802   -0.0038   -0.0326
 15    -0.3136  2.1247     0       -0.0535   -0.0031   -0.0297
 16     0.0000  2.2765     1       -0.0271   -0.0023   -0.0267
 17     0.3136  2.4283     0       -0.0012   -0.0014   -0.0234
 18     0.6237  2.5801     0        0.0238   -0.0004   -0.0199
 19     0.9271  2.7318     0        0.0478    0.0006   -0.0164
 20     1.2202  2.8836     0        0.0704    0.0016   -0.0127
 21     1.5000  3.0354     1        0.0916    0.0026   -0.0090
 22     1.7634  3.1871     0        0.1110    0.0034   -0.0052
 23     2.0074  3.3389     0        0.1285    0.0042   -0.0015
 24     2.2294  3.4907     0        0.1439    0.0048    0.0022
 25     2.4271  3.6424     0        0.1571    0.0053    0.0057
 26     2.5981  3.7942     1        0.1679    0.0056    0.0092
 27     2.7406  3.9460     0        0.1763    0.0057    0.0124
 28     2.8532  4.0977     0        0.1822    0.0056    0.0155
 29     2.9344  4.2495     0        0.1855    0.0054    0.0183
 30     2.9836  4.4013     0        0.1862    0.0050    0.0209
 31     3.0000  4.5530     0        0.1843    0.0045    0.0231
 32     2.9836  4.7048     0        0.1799    0.0038    0.0251
 33     2.9344  4.8566     0        0.1729    0.0031    0.0267
 34     2.8532  5.0083     0        0.1636    0.0023    0.0280
 35     2.7406  5.1601     1        0.1520    0.0016    0.0289
 36     2.5981  5.3119     0        0.1383    0.0008    0.0295
 37     2.4271  5.4636     0        0.1226    0.0001    0.0296
 38     2.2294  5.6154     0        0.1050   -0.0005    0.0294
 39     2.0074  5.7672     0        0.0859   -0.0009    0.0288
 40     1.7634  5.9189     0        0.0654   -0.0013    0.0279
 41     1.5000  6.0707     0        0.0437   -0.0014    0.0266
 42     1.2202  6.2225     0        0.0211   -0.0014    0.0250
 43     0.9271  6.3742     0       -0.0021   -0.0013    0.0230
 44     0.6237  6.5260     0       -0.0257   -0.0010    0.0207
 45     0.3136  6.6778     0       -0.0494   -0.0006    0.0182
 46     0.0000  6.8295     1       -0.0729    0.0000    0.0154
 47    -0.3136  6.9813     0       -0.0960    0.0007    0.0125
 48    -0.6237  7.1331     0       -0.1185    0.0014    0.0093
 49    -0.9270  7.2849     0       -0.1399    0.0021    0.0060
 50    -1.2202  7.4366     0       -0.1602    0.0029    0.0026
 51    -1.5000  7.5884     1       -0.1791    0.0036   -0.0009
```

Figure 2.3f UPOT output

stdin Page 7

52	-1.7634	7.7402	0	-0.1963	0.0042	-0.0044
53	-2.0074	7.8919	0	-0.2117	0.0047	-0.0079
54	-2.2294	8.0437	0	-0.2251	0.0051	-0.0113
55	-2.4270	8.1955	0	-0.2364	0.0053	-0.0147
56	-2.5981	8.3472	1	-0.2454	0.0054	-0.0179
57	-2.7406	8.4990	0	-0.2520	0.0053	-0.0210
58	-2.8532	8.6508	0	-0.2562	0.0051	-0.0238
59	-2.9344	8.8025	0	-0.2578	0.0047	-0.0265
60	-2.9836	8.9543	0	-0.2570	0.0042	-0.0289
61	-3.0000	9.1061	0	-0.2536	0.0035	-0.0310
62	-2.9836	9.2578	0	-0.2477	0.0028	-0.0328
63	-2.9344	9.4096	0	-0.2394	0.0019	-0.0342
64	-2.8532	9.5614	0	-0.2288	0.0011	-0.0354
65	-2.7406	9.7131	0	-0.2159	0.0003	-0.0361
66	-2.5981	9.8649	0	-0.2009	-0.0005	-0.0365
67	-2.4271	10.0167	0	-0.1839	-0.0012	-0.0366
68	-2.2294	10.1684	0	-0.1652	-0.0018	-0.0362
69	-2.0074	10.3202	0	-0.1450	-0.0022	-0.0355
70	-1.7634	10.4720	0	-0.1233	-0.0025	-0.0345
71	-1.5000	10.6237	0	-0.1006	-0.0027	-0.0330
72	-1.2202	10.7755	0	-0.0770	-0.0026	-0.0313
73	-0.9271	10.9273	0	-0.0528	-0.0024	-0.0292
74	-0.6237	11.0790	0	-0.0282	-0.0020	-0.0269
75	-0.3136	11.2308	0	-0.0036	-0.0015	-0.0242
76	0.0000	11.3826	0	0.0209	-0.0008	-0.0213
77	0.3136	11.5343	0	0.0448	-0.0001	-0.0183
78	0.6237	11.6861	0	0.0681	0.0007	-0.0150
79	0.9270	11.8379	0	0.0904	0.0016	-0.0116
80	1.2202	11.9897	0	0.1115	0.0025	-0.0081
81	1.5000	12.1414	1	0.1311	0.0033	-0.0045
82	1.7634	12.2932	0	0.1493	0.0040	-0.0010
83	2.0074	12.4450	0	0.1654	0.0047	0.0026
84	2.2294	12.5967	0	0.1796	0.0052	0.0061
85	2.4270	12.7485	0	0.1915	0.0055	0.0095
86	2.5981	12.9003	1	0.2012	0.0057	0.0129
87	2.7406	13.0520	0	0.2085	0.0058	0.0160
88	2.8532	13.2038	0	0.2133	0.0056	0.0189
89	2.9344	13.3556	0	0.2156	0.0053	0.0217
90	2.9836	13.5073	0	0.2153	0.0048	0.0241
91	3.0000	13.6591	0	0.2125	0.0042	0.0263
92	2.9836	13.8109	0	0.2072	0.0036	0.0282
93	2.9344	13.9626	0	0.1995	0.0028	0.0297
94	2.8532	14.1144	0	0.1894	0.0020	0.0309
95	2.7406	14.2662	0	0.1770	0.0012	0.0317
96	2.5981	14.4179	1	0.1625	0.0005	0.0322
97	2.4271	14.5697	0	0.1461	-0.0002	0.0323
98	2.2294	14.7215	0	0.1279	-0.0008	0.0320
99	2.0074	14.8732	0	0.1081	-0.0013	0.0313
100	1.7634	15.0250	0	0.0870	-0.0016	0.0303
101	1.5000	15.1768	0	0.0647	-0.0018	0.0289
102	1.2202	15.3285	0	0.0415	-0.0018	0.0272
103	0.9271	15.4803	0	0.0178	-0.0016	0.0252
104	0.6237	15.6321	0	-0.0063	-0.0013	0.0229
105	0.3136	15.7838	0	-0.0305	-0.0008	0.0203
106	0.0000	15.9356	1	-0.0546	-0.0002	0.0175
107	-0.3136	16.0874	0	-0.0782	0.0005	0.0145
108	-0.6237	16.2391	0	-0.1011	0.0012	0.0113
109	-0.9270	16.3909	0	-0.1230	0.0020	0.0079
110	-1.2202	16.5427	0	-0.1437	0.0028	0.0044
111	-1.5000	16.6945	1	-0.1630	0.0035	0.0009
112	-1.7634	16.8462	0	-0.1807	0.0042	-0.0026
113	-2.0074	16.9980	0	-0.1965	0.0048	-0.0061
114	-2.2294	17.1498	0	-0.2103	0.0052	-0.0096
115	-2.4270	17.3015	0	-0.2219	0.0055	-0.0130
116	-2.5981	17.4533	1	-0.2312	0.0056	-0.0163
117	-2.7406	17.6051	0	-0.2382	0.0055	-0.0194
118	-2.8532	17.7568	0	-0.2427	0.0053	-0.0223
119	-2.9344	17.9086	0	-0.2446	0.0049	-0.0250
120	-2.9836	18.0604	0	-0.2441	0.0044	-0.0274

PHASE SHIFT ANALYSIS
FREQ = 0.6900000

Figure 2.3g UPOT output

stdin Page 8

```
AMPLITUDE;  clamp, cmamp :  0.2300964      3.4413978E-02
PHASE;      clp,   cmp   :   193.5791      -37.85255
AVERAGE DRAG, TOTAL DRAG :   1.5437672E-03  9.4169796E-02
ETAS, WBAR               :  -0.2118947     -7.2855391E-03
```

Figure 2.3h UPOT output

2. Difference Between UPOT and U2DIIF/Phase

The input file format was changed along with the following:

- The program can now analyze a pitch, plunge or ramp motion that starts from any minimum value of Alpha or plunge (h/2b). Previously, the program only accepted the initial position of zero. This program does not need to go through the origin.
- The phase portion of the program was changed to curve fit C_L and C_M to a cosine function:

$$F(t)=Amp*Cos(\omega t+\phi) \tag{2.2}$$

  where, Amp = amplitude of motion, ω = frequency of motion, ϕ = phase angle between motion and the aerodynamic forces. This was done since the alpha and plunge values were allowed to start from a new zero position.
- The phase portion uses the middle 180 degrees of the final 360 degree cycle specified in the UPOT.in file. This change was done to capture an all positive area of the cosine curve for phasing analysis. The program integrates this portion of the cosine curve, and for proper code operation the area under the curve must be kept to one sign. If the areas of integration were chosen to include both sides of the axis, then the code would produce errors near 90 and 270 degrees.

3. UPOT Verification

The code UPOT did not incorporate any drastic changes to the prior codes, but the original code had never been extensively compared to prior theories over a wide range of reduced frequencies. When conducting these comparisons, it is easy to become confused. This section will go through the comparisons slowly to help alleviate that problem.

a. *K_{panel} (K_p) vs. $K_{Theodorson}$ (K_t).*

The equation for reduced frequency is:

$$K_p=\frac{\omega 2b}{U} \qquad K_t=\frac{\omega b}{U} \tag{2.3}$$

where: ω = frequency of oscillation (rad/sec)

b = half chord (units to match U)

U = free stream velocity (units to match b).

The difference between K_p and K_t lies in the fact that K_p calls for the full chord and K_t calls for the half chord, hence, it is important to remember that K_p is twice K_t.

b. *Aerodynamic Forces*

The aerodynamic forces problem of simple harmonic motion about an equilibrium position was solved theoretically by Theodorsen in NACA TR-496 [ref.10] and outlined by Fung in [ref.5]. The complex equations were simplified using the simple harmonic motion equation and resulted in the following:

$$L=\pi\rho b^3\omega^2\left(L_h\frac{h}{b}+\left[L_\alpha-\left(\frac{1}{2}+a\right)L_h\right]\alpha+\left[L_\beta-(c-e)L_z\right]\beta\right)e^{i(\omega t+\phi_L)} \tag{2.4}$$

$$\begin{aligned} M=\pi\rho b^4\omega^2\Big(&\left[M_h-\left(\frac{1}{2}+a\right)L_h\right]\frac{h}{b}+\\ &\left[M_\alpha-\left(\frac{1}{2}+a\right)(L_\alpha+M_h)+\left(\frac{1}{2}+a\right)^2L_h\right]\alpha\\ &+\left[M_\beta-\left(\frac{1}{2}+a\right)L_\beta-(c-e)M_z+(c-e)\left(\frac{1}{2}+a\right)L_z\right]\beta\Big)e^{i(\omega t+\phi_M)}\end{aligned} \tag{2.5}$$

L, M are the lift and moment per unit span of the airfoil about the elastic axis, b, h/b, a and α (radians), are

shown in Figure (2.1)., L_h, L_α, L_β, and M_α are defined by Scanlan [ref.6,pp.412-424] for various values of K_t and e. This analysis will not cover airfoil aileron combinations. Therefore β becomes zero and equations 2.4 and 2.5 reduce to:

$$L=\pi\rho b^3\omega^2\left(L_h\frac{h}{b}+\left[L_\alpha-\left(\frac{1}{2}+a\right)L_h\right]\alpha\right)e^{i(\omega t+\phi_L)} \tag{2.6}$$

$$\begin{gathered}M=\pi\rho b^4\omega^2\left(\left[M_h-\left(\frac{1}{2}+a\right)L_h\right]\frac{h}{b}+\right.\\ \left.\left[M_\alpha-\left(\frac{1}{2}+a\right)\left(L_\alpha+M_h\right)+\left(\frac{1}{2}+a\right)^2L_h\right]\alpha\right)e^{i(\omega t+\phi_L)}\end{gathered} \tag{2.7}$$

The UPOT panel code used the following equations in defining lift and moment:

$$C_L=\frac{L}{2qb}=\sqrt{R_L^2+I_L^2}\,e^{i(\omega t+\phi L)} \qquad \phi_L=\tan^{-1}\frac{I_L}{R_L} \tag{2.8}$$

$$C_M=\frac{M}{4qb^2}=\sqrt{R_m^2+I_m^2}\,e^{i(\omega t+\phi m)} \qquad \phi_m=\tan^{-1}\frac{I_m}{R_m} \tag{2.9}$$

where R_L and I_L are the real and imaginary parts of C_L, and R_M and I_M are the real and imaginary parts of C_M. For the same conditions the lift (L) and moment (M) should be the same for both the panel code and Theodorsen. This fact allows for comparison of the magnitude, real, imaginary and phase of lift and moment.

For lift: L_t (eqn 2.6) equals L_p (eqn 2.8)

$$\pi\rho b^3\omega^2[L_h h/b+(L_\alpha-(½+a)L_h)\alpha]e^{i(\omega t+\phi_L)}=2qb\sqrt{R_L^2+I_L^2}e^{i(\omega t+\phi_L)} \quad (2.10)$$

After canceling $e^{i(\omega t+\phi L)}$:

$$\pi\rho b^3\omega^2[L_h(h/b)+(L_\alpha-(½+a)L_h)\alpha]=2qb\sqrt{R_L^2+I_L^2} \quad (2.11)$$

$$C_L=\sqrt{R_L^2+I_L^2}$$

For pitch case, h/b = 0, 2.11 reduces to:

$$\pi\rho b^3\omega^2[(L_\alpha-(½+a)L_h)\alpha]=2qbC_\alpha \quad (2.12)$$

Substitute K_t = $b\omega/U$ for ω^2 and q = $½\rho U^2$ into equation 2.12 which gives:

$$2\pi qbK_t^2(L_\alpha-(½+a)L_h)\alpha=2qbC_{L\alpha} \quad (2.13)$$

After cancelling and substituting K_p for K_t:

$$\frac{\pi K_p^2}{4}[L_\alpha-(½+a)L_h]\alpha=C_{L\alpha} \quad (2.14)$$

This relationship can be further broken down into the real and imaginary parts:

$$Imag: \quad \frac{\pi K_p^2}{4}[iL_\alpha-(½+a)iL_h]\alpha=C_{L\alpha}\sin(\phi_L) \quad (2.15)$$

Plunge Case: α=0 using equation 2.11 gives:

Real: $$\frac{\pi K_p^2}{4}[L_\alpha-(½+a)L_h]\alpha=C_{L\alpha}\cos(\phi_L) \tag{2.16}$$

$$\pi\rho b^3\omega^2 L_h\frac{h}{b}=2qbC_{Lh} \tag{2.17}$$

The panel code uses h/2b for analysis because it uses full chord vice half chord. Therefore equation 2.17 becomes:

$$2\pi\rho b^3\omega^2 L_h\left(\frac{h}{2b}\right)=2qbC_{Lh} \tag{2.18}$$

Substituting as before for ω:

$$2\pi qbK_t^2 L_h 2\left(\frac{h}{2b}\right)=2qbC_{Lh} \tag{2.19}$$

Cancel and substitute K_p:

$$\left(\frac{\pi K_p^2}{2}\right)\left(\frac{h}{2b}\right)L_h=C_{Lh} \tag{2.20}$$

This can also be broken up into imaginary and real parts as before.

MOMENT:

Equating equations 2.7 and 2.9 results in:

$$\pi\rho b^4\omega^2\left([M_h-(½+a)L_h]\frac{h}{b}+[M_\alpha-(½+a)(L_\alpha+M_h)+(½+a)^2L_h]\alpha\right) =4qb^2\sqrt{R_m^2+I_m^2} \tag{2.21}$$

For pitch: h/b = 0

$$M_p = 4qb^2\sqrt{R_m^2 + I_m^2}\, e^{i(\omega t + \phi_m)} \tag{2.22}$$

$$C_{M\alpha} = \sqrt{R_m^2 + I_m^2} \tag{2.23}$$

resulting in:

$$\pi\rho b^4\omega^2 ([M_\alpha - (½+a)(L_\alpha + M_h) + (½+a)^2 L_h]\alpha) = 4qb^2 C_{M\alpha} \tag{2.24}$$

After substituting and cancelling:

$$\frac{\alpha\pi K_p^2}{8}[M_\alpha - (½+a)(L_\alpha + M_h) + (½+a)^2 L_h] = C_{M\alpha} \tag{2.25}$$

REAL $M_h = ½$

$$\frac{\alpha\pi K_p^2}{8}[M_\alpha - (½+a)(L_\alpha + ½) + (½+a)^2 L_h] = C_{M\alpha}\cos(\phi_{M\alpha}) \tag{2.26}$$

IMAG: $M_h = 0$

$$\frac{\alpha\pi K_p^2}{8}[iM_\alpha - (½+a)(iL_\alpha) + (½+a)^2 iL_h] = C_{M\alpha}\sin(\phi_{M\alpha}) \tag{2.27}$$

For plunge, $\alpha = 0$, equation 21 reduces to :

REAL: $M_h = ½$

$$\frac{\pi}{4}K_p^2\left(\frac{h}{2b}\right)[M_h - (½+a)L_h] = C_{Mh}\cos(\phi_{Mh}) \tag{2.28}$$

IMAG: $M_h = 0$

$$\frac{\pi}{4}K_p^2\left(\frac{h}{2b}\right)(\tfrac{1}{2}+a)L_h=C_{Mh}\sin(\phi_{Mh}) \qquad \textbf{(2.29)}$$

Comparisons are shown for various cases of pitch and plunge. The tables include pitch values of 1 (Tables 2.2-2.3) and 6.7 degrees (Tables 2.4-2.5), plunge (h/2b) values of .01 (Table 2.8) and .0833 (Table 2.6-2.7). The graphs include 1 degree pitch (Figures 2.7-12, 2.13-20), 6.7 degree pitch (Figures 2.21-28,2.29-36), .01 h/2b plunge (Figures 2.53-56), and .0833 h/2b plunge (Figures 2.37-44, 2.45-52).

4. Results

The tables and graphs show that the panel code predicts the Theodorsen results accurately. An initial question that was first addressed for the comparisons was how many cycles to use for good consistent phase results. Initial runs were made at several different cycle values and the results are shown in Table 2.1. It can be seen that the panel code predicts Theodorsen's results, using a cycle number of three. Increasing the cycle number just takes more computer time and only results in marginal increases in accuracy.

The most glaring difference appears in the I_M c_{Mh} comparisons of Figures 2.47-48. The panel code drops off sharply at the higher end of the reduced frequency spectrum. The reason for this is believed to be due to the magnitude of h/2b chosen for the comparison. The code was rerun for a

	Comparison of Phase Calculations Using Various Cycles.				
		(Pitch, 6.7 deg., NACA 0007, .37c, 50 panels top and bottom)			
Kp	# Cycles	Cl Phase Angle	Cm Phase Angle	Cl Amplitude	Cm amplitude
1.00	1	182.0537	-54.409	0.4884	0.08937
1.00	2	208.1592	-46.424	0.5109224	0.083932
1.00	3	206.001	-44.313	0.51527	0.083169
% Diff. 2/3		1.05%	4.76%	0.84%	0.92%
1.00	4	204.9365	-43.33887	0.51668	0.082951
1.00	5	204.3955	-42.86817	0.5172907	0.082865
1.00	6	204.0596	-42.58497	0.517598	0.082822
1.00	7	203.8291	-42.3916	0.517776	0.082792
1.00	8	203.6031	-42.25684	0.51789	0.082784
% Diff. 7/8		0.11%	0.32%	0.02%	0.01%
3.60	2	264.44052	-59.79002	1.0931	0.212011
3.60	3	261.9737	-58.29977	1.09954	0.21936
% Diff. 2/3		0.94%	2.56%	0.59%	3.35%
3.60	4	260.17877	-57.4404	1.10271	0.21903
3.60	5	259.2686	-56.79395	1.104505	0.218845
3.60	6	258.5186	-56.3252	1.105599	0.218739
3.60	7	257.9483	-56.0098	1.106306	0.218673
3.60	8	257.6163	-55.380567	1.106764	0.218632
% Diff. 7/8		0.13%	1.14%	0.04%	0.02%

TABLE 2.1 PHASE CALCULATION VS CYCLE NUMBER

series of h/2b values and the percent difference for the panel code to Theodorsen was plotted in Figure 2.4. This chart shows that the h/2b value chosen has a tremendous impact on the code results. An h/2b value of .01 gave an acceptable error of 10% at K_p = 8. Runs were completed with a value of .01 h/2b and the favorable results are shown in Figures 2.53-56.

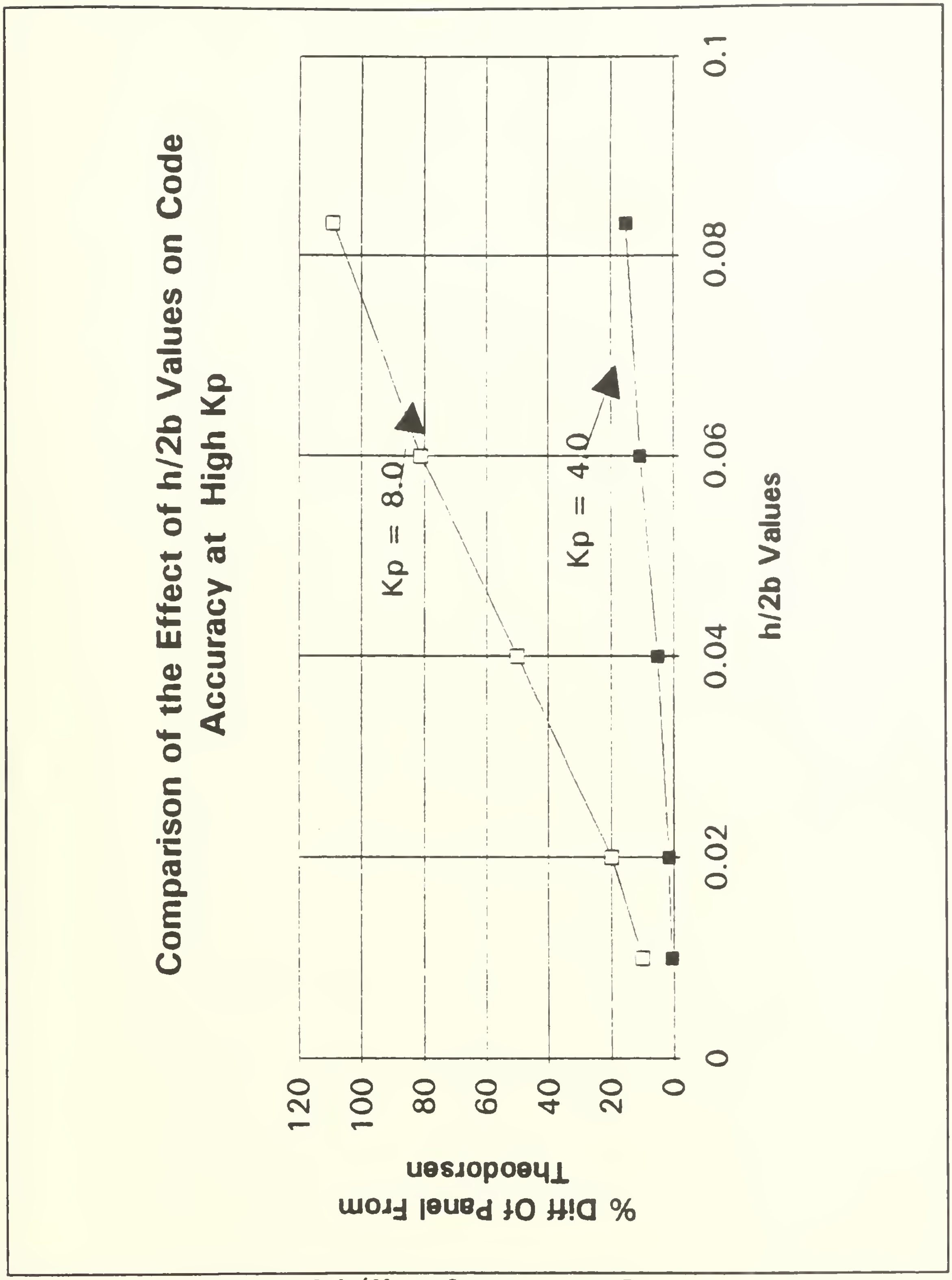

Figure 2.4 Effect of h/2b values on Im C_m

Comparison of Panel Cl Values with Theordorsen Results

(pitch, 1.0 deg., .37c, NACA 0007, 50 panels top and bottom.3cyc65calc.)

Kpanel (equal to 2 x Theordorsen Kt) %DIFF taken wrt Theordorsen values.

1/kt	Kpanel	Real pan.	Real theo.	% DIFF.	Imag Pan.	Imag Theo	% DIFF.	Mag Pan.	Mag Theo.	% DIFF.	Phase Pn.	Phase Th.	% DIFF.
18.67	0.11998	-0.10312	-0.098452	4.74%	0.01082	0.00788418	37.24%	0.1036881	0.0987874	4.98%	174.01008	175.42145	0.80%
12.5	0.16	-0.09954	-0.095343	4.40%	0.01094	0.00748657	46.52%	0.10013938	0.0958346	4.71%	173.72806	175.52214	1.02%
10	0.2	-0.09634	-0.092534	4.11%	0.0104	0.00647781	60.55%	0.09689972	0.0927608	4.46%	173.83872	175.9957	1.23%
8.33	0.24	-0.09354	-0.090022	3.91%	0.00944	0.00510646	84.86%	0.09401513	0.0901869	4.27%	174.23728	176.75341	1.42%
6.25	0.32	-0.08886	-0.085787	3.58%	0.00668	0.00182687	309.38%	0.08910923	0.085802	3.85%	175.71373	178.91357	1.79%
5	0.4	-0.08522	-0.082367	3.46%	0.00328	-0.0024119	235.99%	0.0852831	0.0824025	3.50%	177.79586	181.6773	2.14%
4.17	0.48	-0.08232	-0.079546	3.49%	-0.00048	-0.0067203	92.86%	0.0823214	0.0798296	3.12%	180.33408	184.82905	2.43%
3.75	0.53	-0.08084	-0.077883	4.09%	-0.00278	-0.0095731	70.98%	0.08088779	0.0782505	3.37%	181.96956	187.02715	2.70%
3.33	0.6	-0.07842	-0.076125	3.01%	-0.01178	-0.013414	12.33%	0.07929687	0.0772982	2.59%	188.52882	189.99348	0.77%
2.94	0.68	-0.07564	-0.074217	1.92%	-0.01832	-0.0179149	8.90%	0.07738057	0.0763489	1.35%	192.17543	193.57073	0.72%
2.5	0.8	-0.07272	-0.071761	1.34%	-0.02328	-0.0246748	5.65%	0.07635548	0.0758848	0.62%	197.75153	198.9752	0.61%
2	1	-0.06848	-0.068284	0.28%	-0.03466	-0.035806	3.20%	0.07673387	0.077102	0.48%	206.85223	207.87124	0.39%
1.67	1.2	-0.0648	-0.065233	0.97%	-0.04564	-0.0467313	2.34%	0.07909595	0.0802443	1.43%	215.24128	215.81696	0.17%
1.25	1.6	-0.05704	-0.059409	3.99%	-0.06658	-0.0680358	2.14%	0.08767245	0.0903233	2.93%	229.41288	228.8726	0.24%
0.83	2.4	-0.041693	-0.048737	10.38%	-0.106072	-0.1100687	3.63%	0.11404519	0.1195806	4.63%	248.44832	246.99297	0.59%
0.5	4	-0.002503	-0.008851	71.72%	-0.179738	-0.1888358	4.82%	0.17975643	0.1890431	4.91%	269.2022	287.31651	0.71%
0.25	8	0.1564088	0.1826884	3.86%	-0.358727	-0.3805373	5.73%	0.39134264	0.4138552	5.44%	293.55769	293.14781	0.14%
Values for Kp equal to 2.4,4,and 8 above were calculated using 200 panels top and bottom and 4 cycles of 100 calculations.													
The below values were calculated using 75 panes and 3cyc65calc.													
0.83	2.4	-0.0416	-0.048737	10.99%	-0.10518	-0.1100687	4.44%	0.11310788	0.1195805	5.41%	248.42059	246.99297	0.58%
0.5	4	-0.00498	-0.008851	43.73%	-0.17718	-0.1888358	6.18%	0.17722998	0.1890431	6.25%	288.38983	287.31651	0.40%
0.25	8	0.1382	0.1628884	18.28%	-0.35464	-0.3805373	6.81%	0.37989468	0.4138552	8.21%	291.00936	293.14781	0.73%

TABLE 2.2 1 DEGREE PITCH C_L

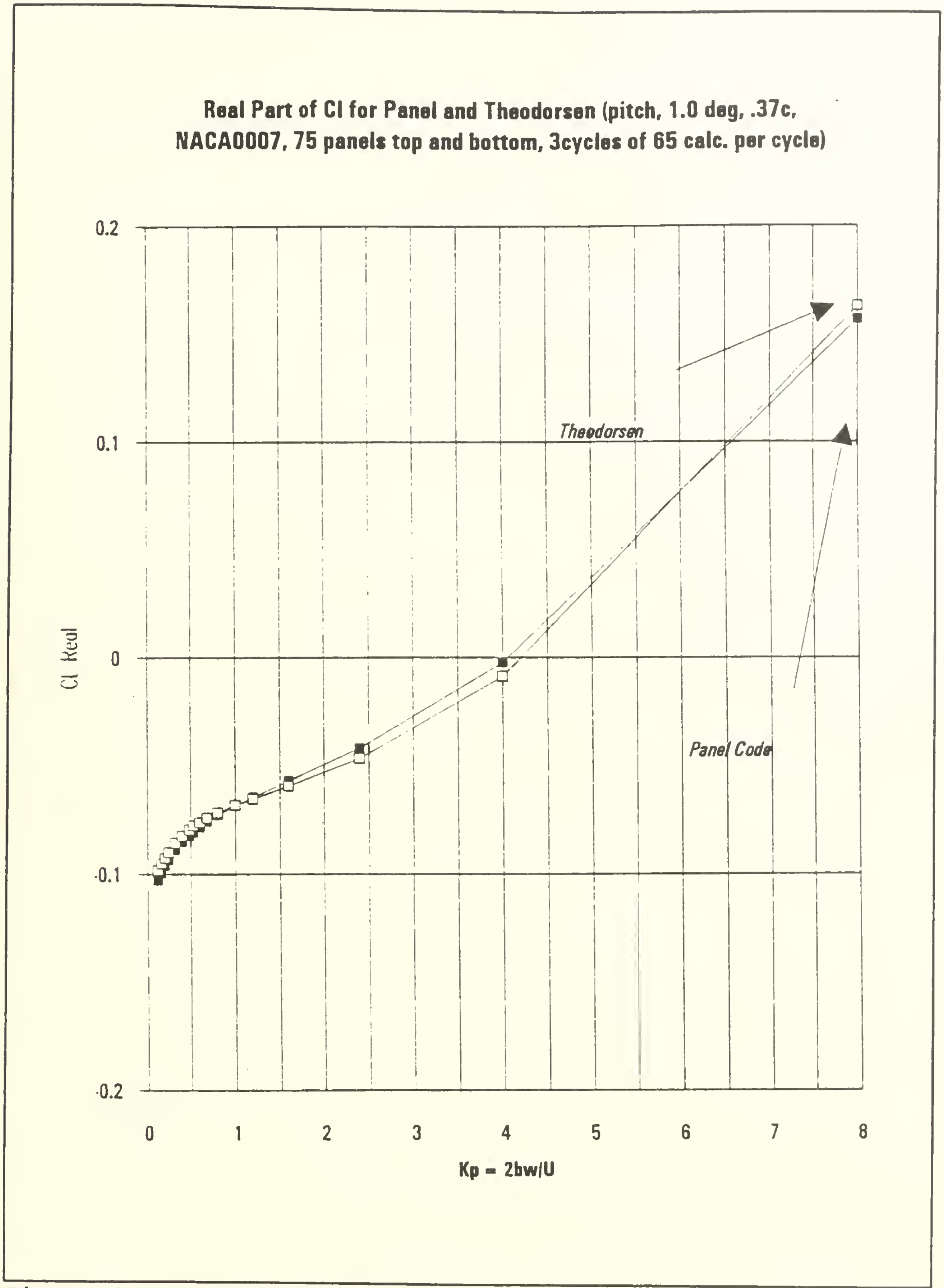

Figure 2.5 1 Degree pitch C_L Re

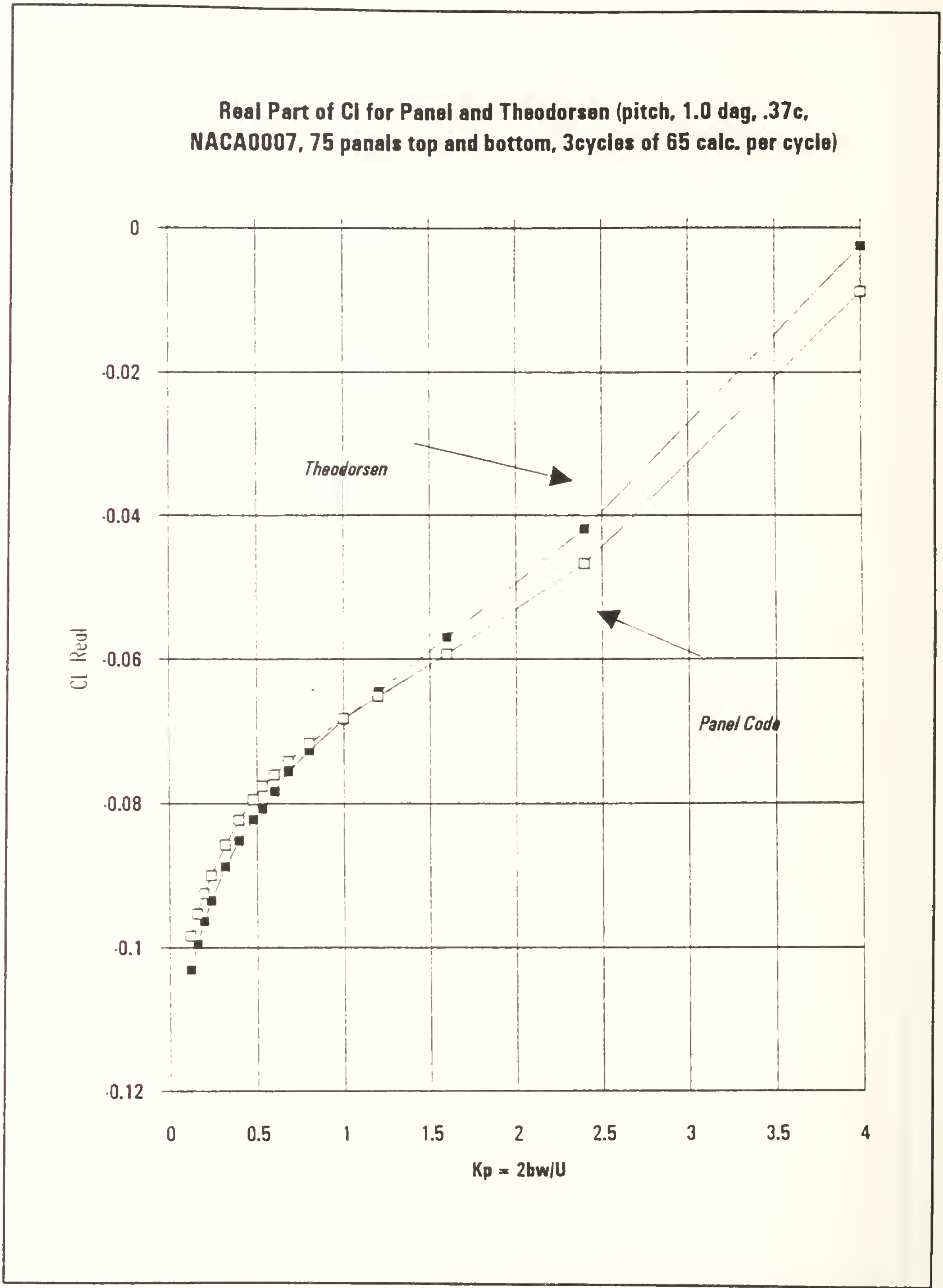

Figure 2.6 1 degree pitch C_L Re

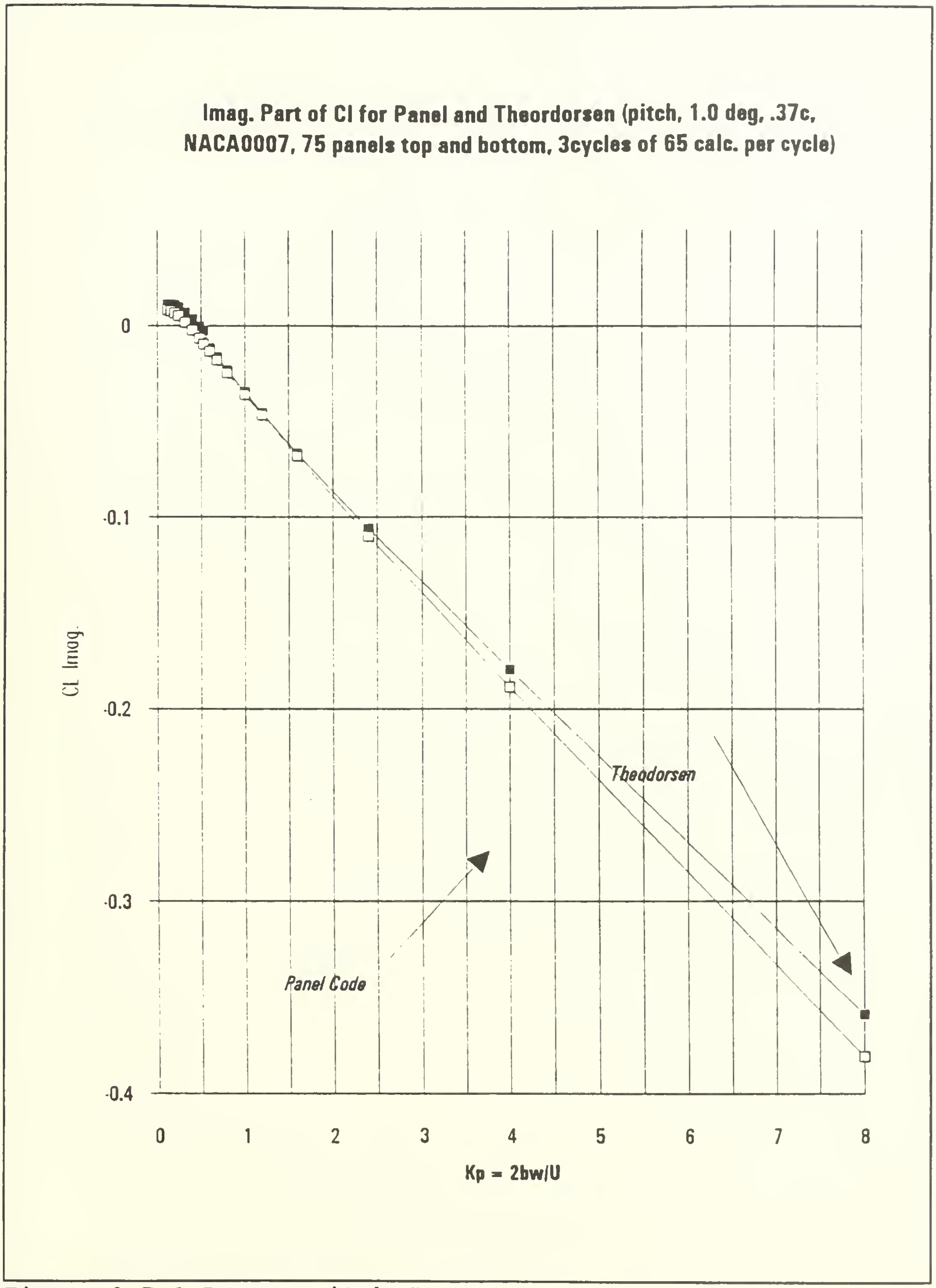

Figure 2.7 1 Degree pitch C_L Im

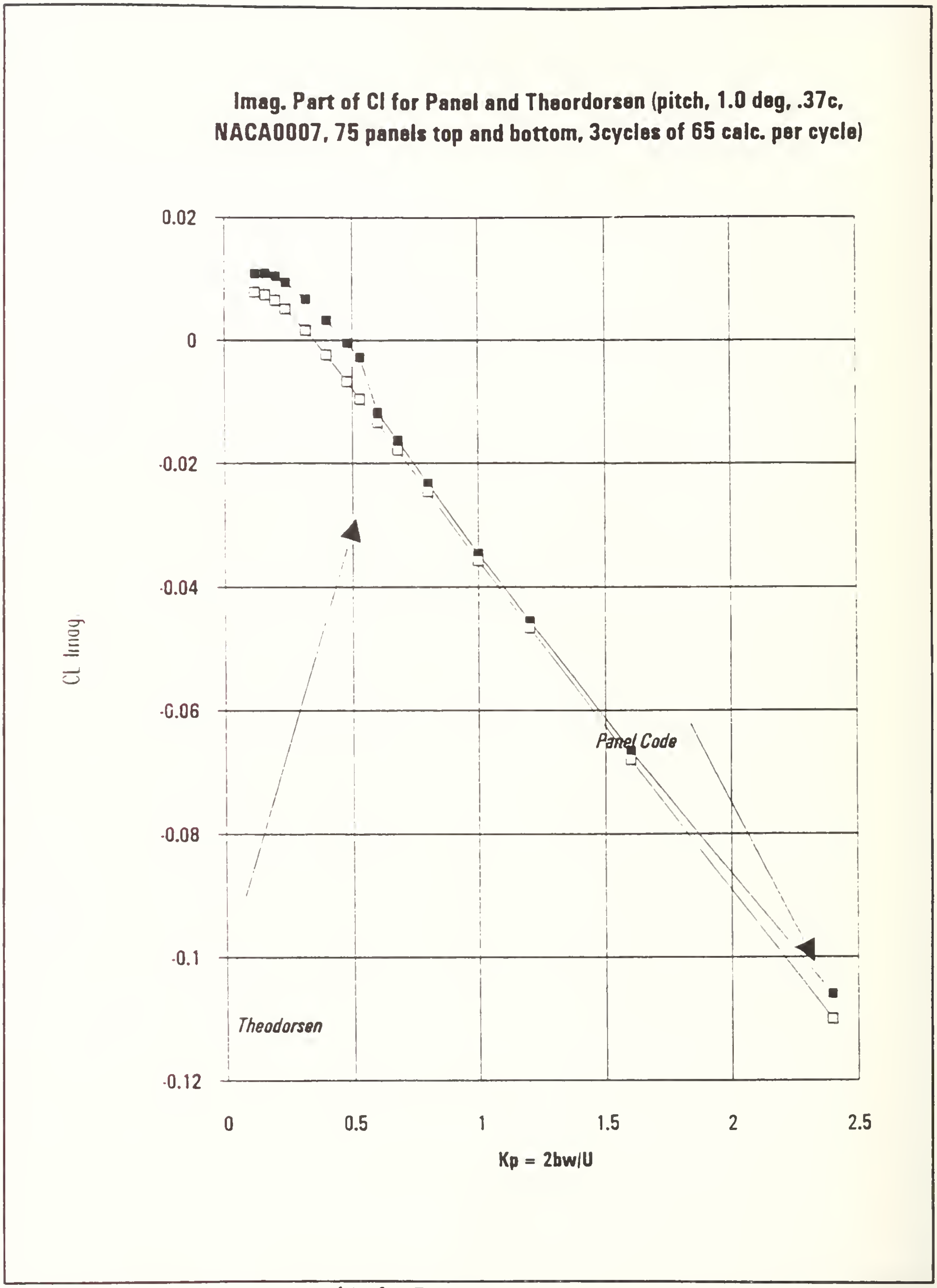

Figure 2.8 1 Degree pitch C_L Im

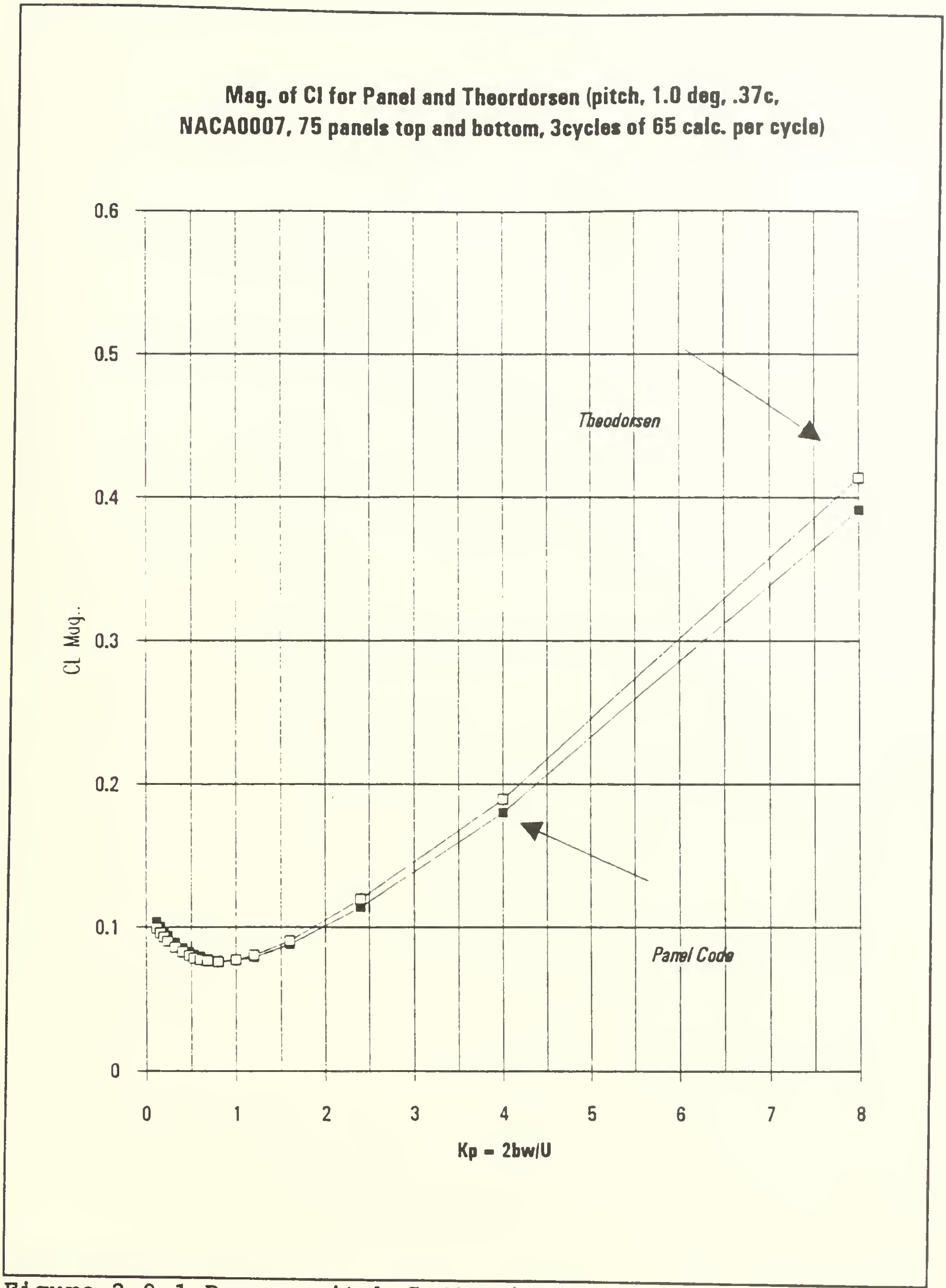

Figure 2.9 1 Degree pitch C_L Magnitude

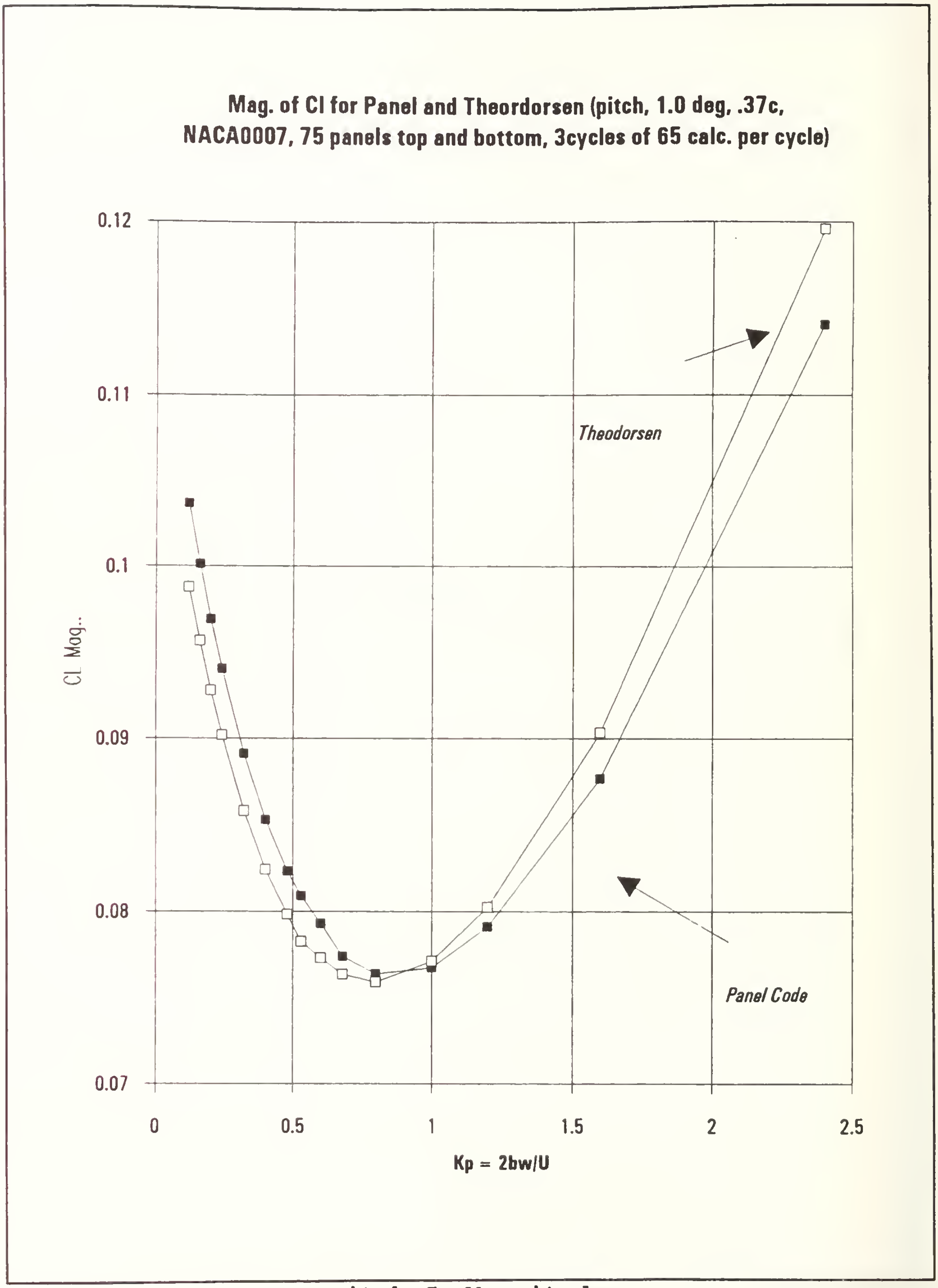

Figure 2.10 1 Degree pitch C_L Magnitude

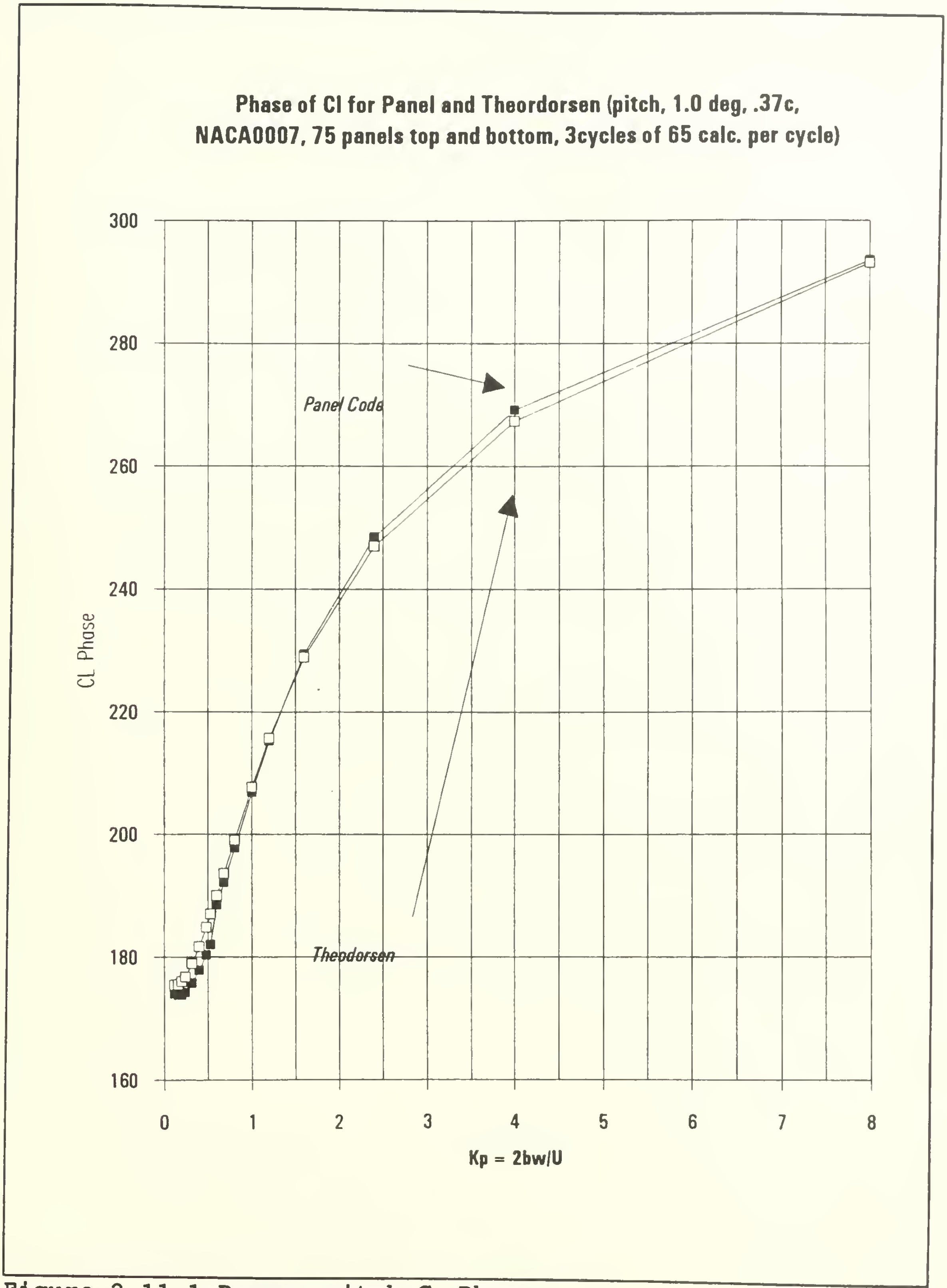

Figure 2.11 1 Degree pitch C_L Phase

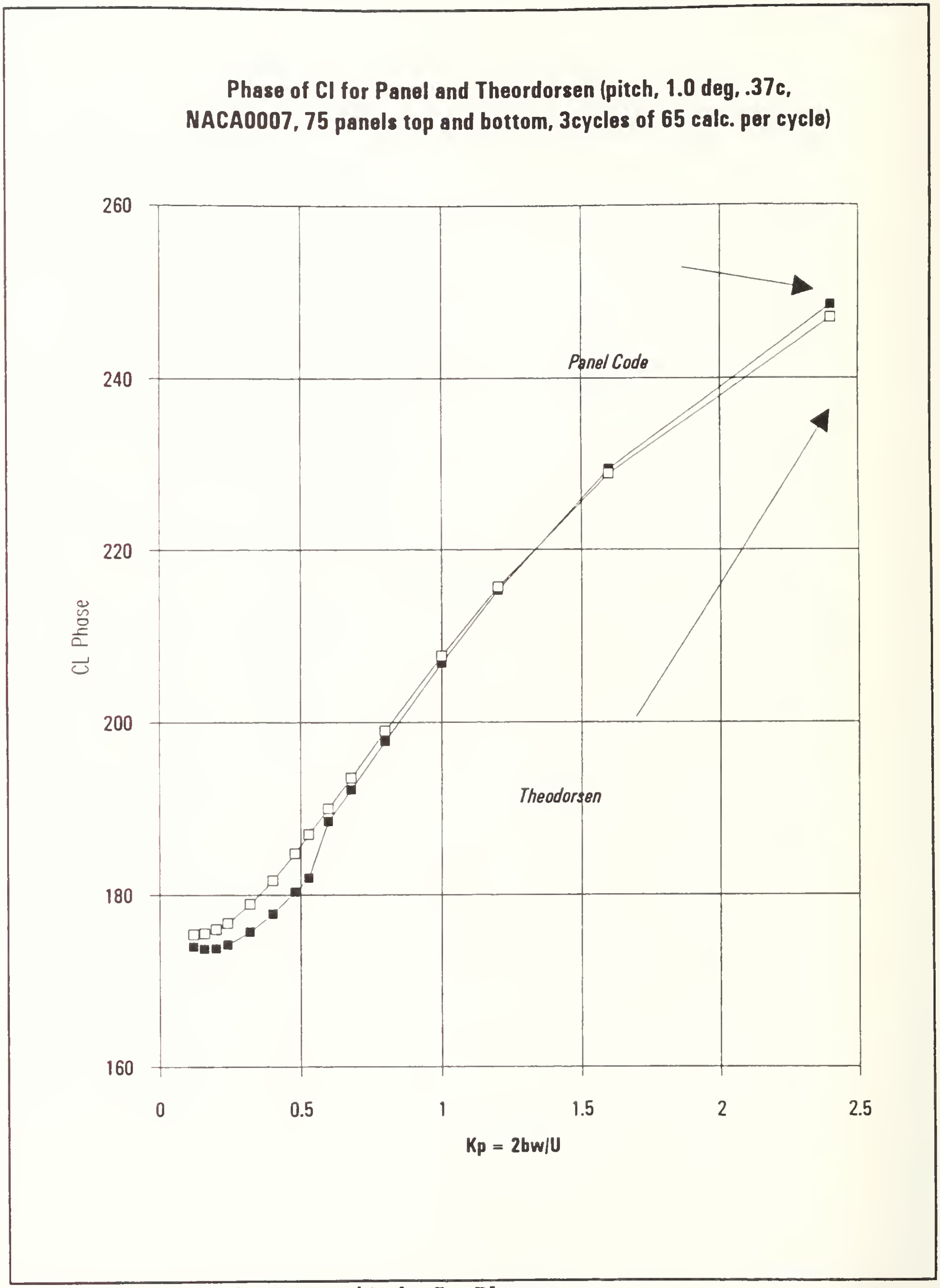

Figure 2.12 1 degree pitch C_L Phase

	Comparison of Panel Moment Aerodynamic Values (CM) with Theordorsen Results											
			(pitch, 1.0 deg., .37c, NACA 0007, 75 panels top and bottom)									
	Kpanel (equal to 2 x Theordorsen Kt)					Mh=.5						
1/kt	Kpanel	Rp	Rt	% DIFF	Imag Pan.	Imag t	% DIFF	Mag Pan.	Mag The.	% DIFF	Phase Pn.	Phase Th.	% DIFF
16.67	0.11996	0.01188	0.0116391	0.35%	-0.00262	-0.002591	1.14%	0.0121655	0.0121192	0.38%	347.56314	347.65745	0.03%
12.5	0.16	0.01147	0.0114656	0.14%	-0.0031	-0.003089	0.35%	0.0118815	0.0116938	0.10%	344.87599	344.9456	0.02%
10	0.2	0.01111	0.0111736	0.57%	-0.0035	-0.003519	0.54%	0.0116483	0.0117148	0.57%	342.51393	342.5197	0.00%
8.33	0.24	0.01081	0.0109116	0.93%	-0.00385	-0.003902	1.34%	0.0114751	0.0115886	0.96%	340.39656	340.32135	0.02%
6.25	0.32	0.0103	0.0104731	1.65%	-0.00447	-0.004619	7.23%	0.0112281	0.0115284	2.60%	336.54009	335.29353	0.37%
5	0.4	0.00993	0.0101633	2.30%	-0.00502	-0.005194	3.34%	0.0111268	0.0114134	2.51%	333.16163	332.93194	0.07%
4.17	0.48	0.00965	0.0099323	2.84%	-0.00554	-0.005773	4.04%	0.0111272	0.0114883	3.14%	330.14016	329.83193	0.09%
3.75	0.53	0.0095	0.0098269	3.33%	-0.00585	-0.006084	3.84%	0.0111567	0.0115576	3.47%	328.37568	328.23904	0.04%
3.33	0.6	0.00935	0.0097636	4.24%	-0.00629	-0.006615	4.91%	0.0112688	0.0117935	4.45%	326.0702	325.88165	0.06%
2.94	0.68	0.00922	0.0097216	5.16%	-0.0068	-0.007172	5.16%	0.0114564	0.0120806	5.17%	323.59022	323.58433	0.00%
2.5	0.8	0.00912	0.009729	6.26%	-0.00762	-0.008005	4.81%	0.0118844	0.0125991	5.67%	320.12036	320.55117	0.13%
2	1	0.00911	0.0099403	8.35%	-0.00884	-0.009412	6.08%	0.012694	0.0136892	7.27%	315.66177	316.56403	0.22%
1.67	1.2	0.00924	0.0103033	10.32%	-0.01017	-0.010842	6.20%	0.0137407	0.0149568	8.13%	312.25686	313.5406	0.41%
1.25	1.6	0.00992	0.0116031	14.51%	-0.01289	-0.013768	6.38%	0.0162653	0.0180056	9.67%	307.56146	310.12198	0.82%
0.83	2.4	0.013738	0.0156299	12.10%	-0.018818	-0.019796	4.94%	0.0232987	0.0252225	7.63%	306.13184	308.29271	0.70%
0.5	4	0.0250217	0.0290254	13.79%	-0.03081	-0.032172	4.23%	0.0396906	0.04333	8.40%	309.08103	312.05662	0.95%
0.25	8	0.0810345	0.0923334	12.24%	-0.062024	-0.063999	3.09%	0.1020471	0.1123447	9.17%	322.56932	325.27302	0.83%
Values for Kp equal to 2.4, and 8 above were calculated using 200 panels top and bottom and 4 cycles of 100 calculations.													
The below values were calculated using 75 panels and 3 cyc 65 calc.													
0.83	2.4	0.0125	0.0156299	20.02%	-0.01658	-0.019796	6.14%	0.0223934	0.0252225	11.22%	303.93134	308.29271	1.41%
0.5	4	0.0223	0.0290254	23.17%	-0.03046	-0.032172	5.32%	0.0377505	0.04333	12.88%	306.20614	312.05662	1.87%
0.25	8	0.0716	0.0923334	22.45%	-0.06212	-0.063999	2.94%	0.0947916	0.1123447	15.62%	319.05517	325.27302	1.91%

TABLE 2.3 1 DEGREE PITCH C_M COMPARISON

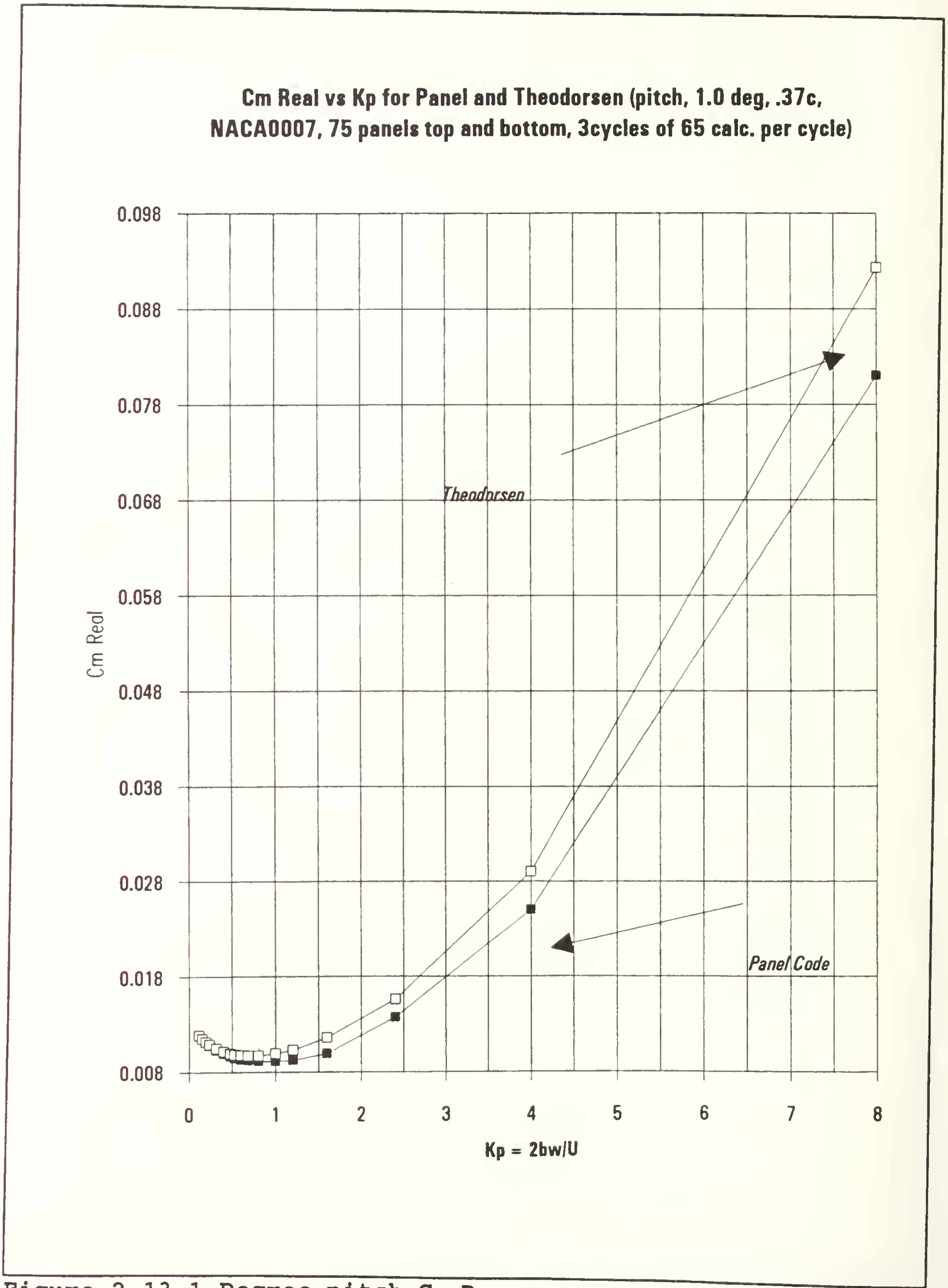

Figure 2.13 1 Degree pitch C_M Re

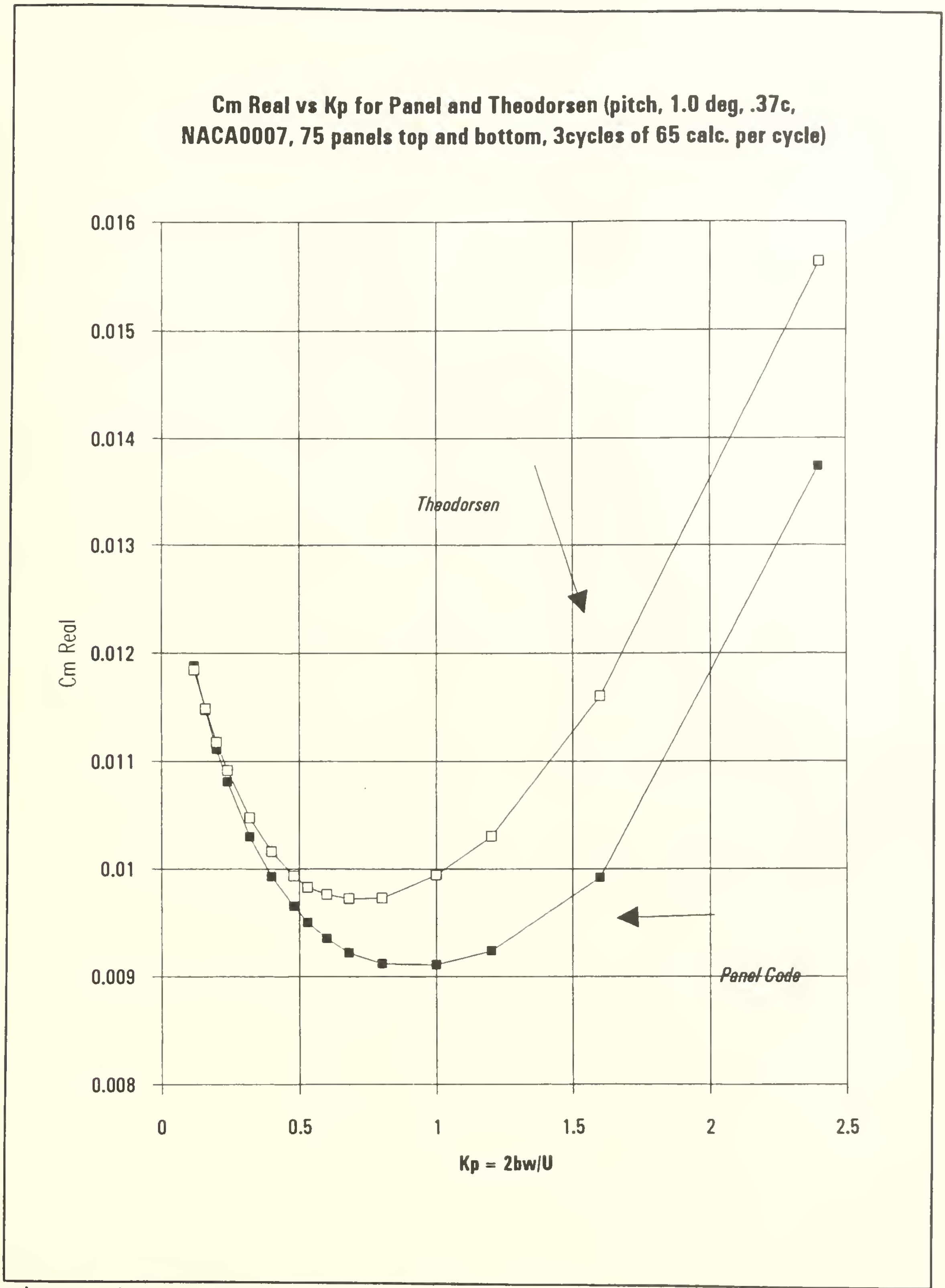

Figure 2.14 1 Degree pitch C_M Re

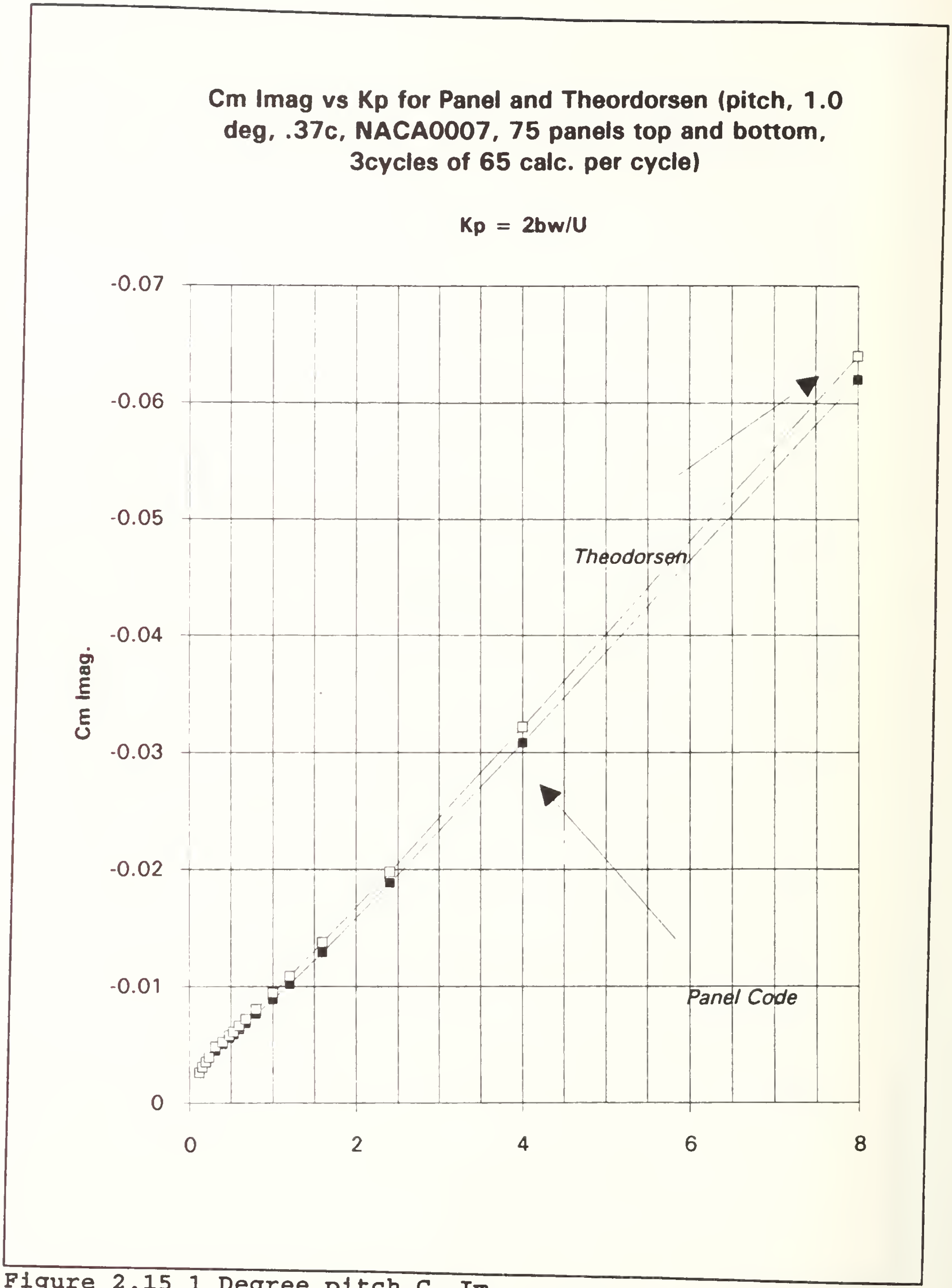

Figure 2.15 1 Degree pitch C_M Im

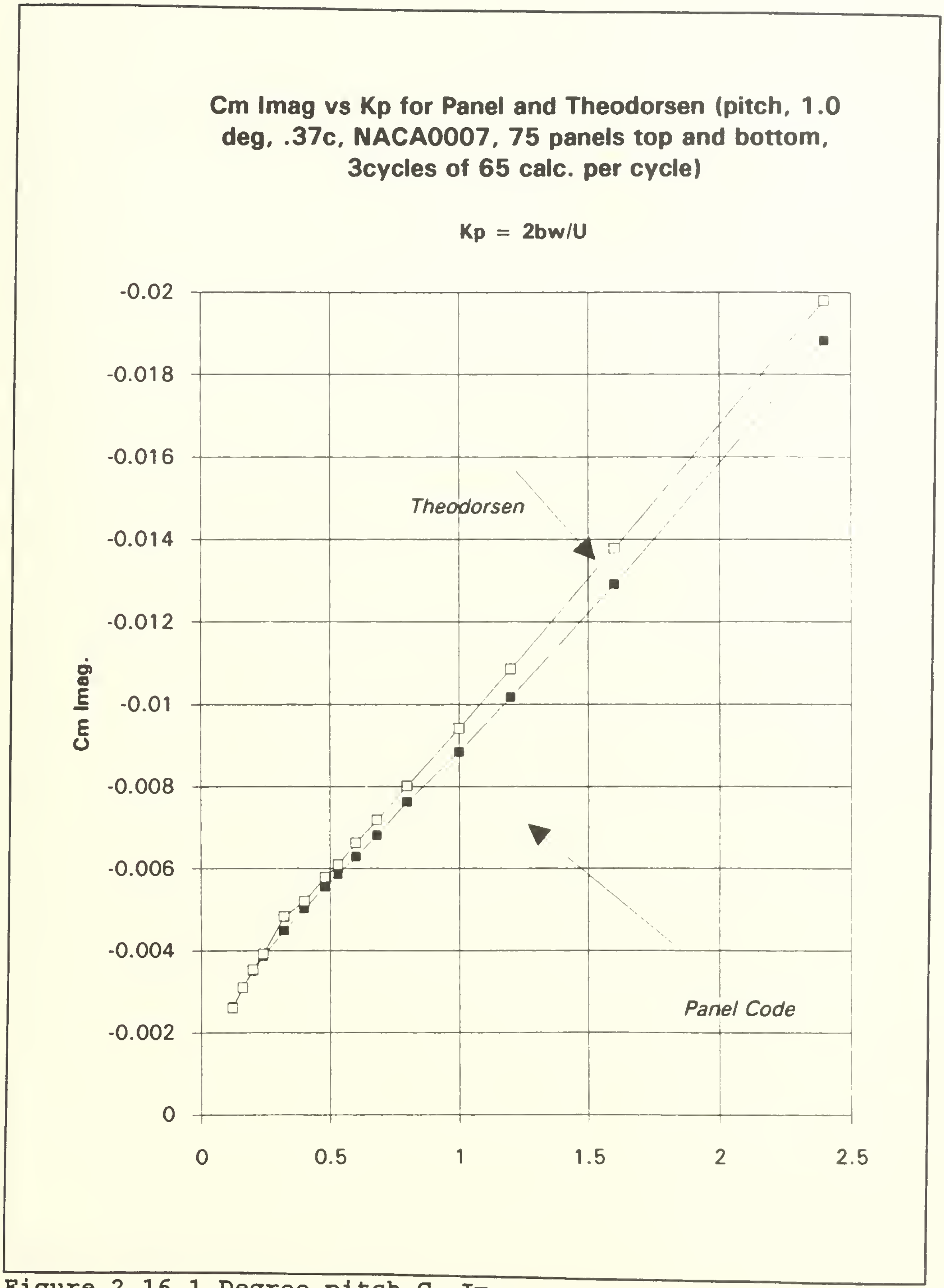

Figure 2.16 1 Degree pitch C_M Im

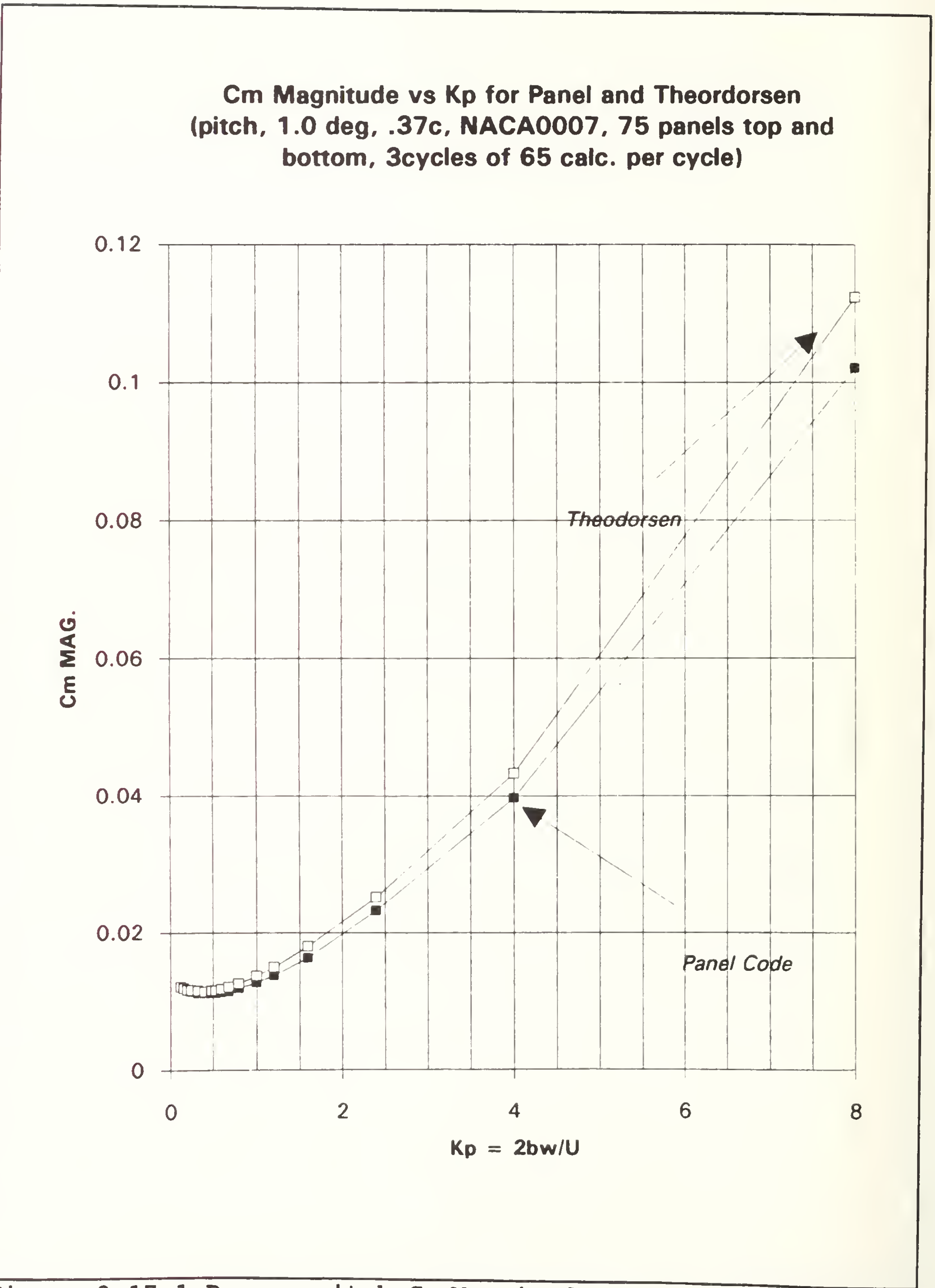

Figure 2.17 1 Degree pitch C_M Magnitude

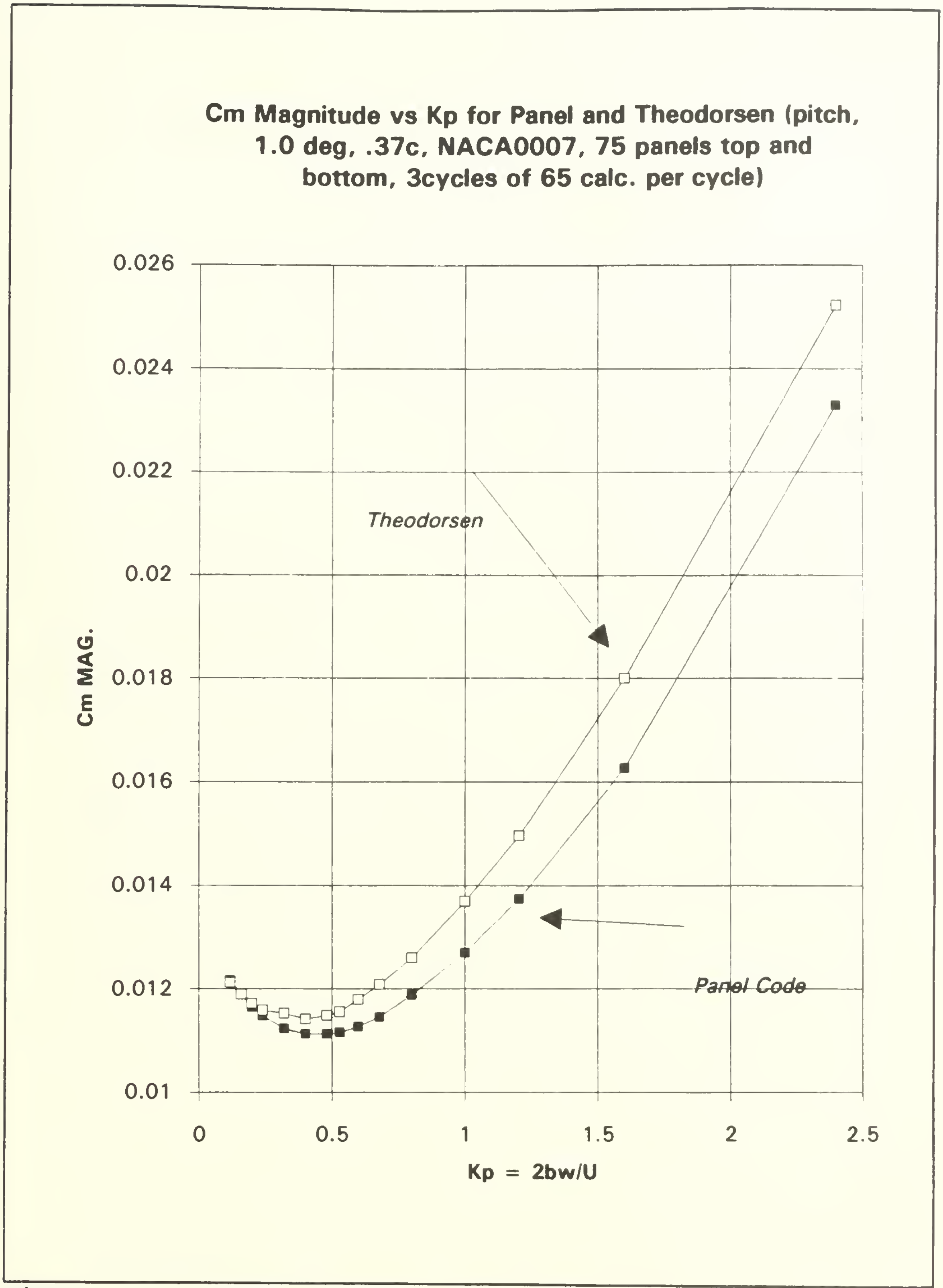

Figure 2.18 1 Degree pitch C_M Magnitude

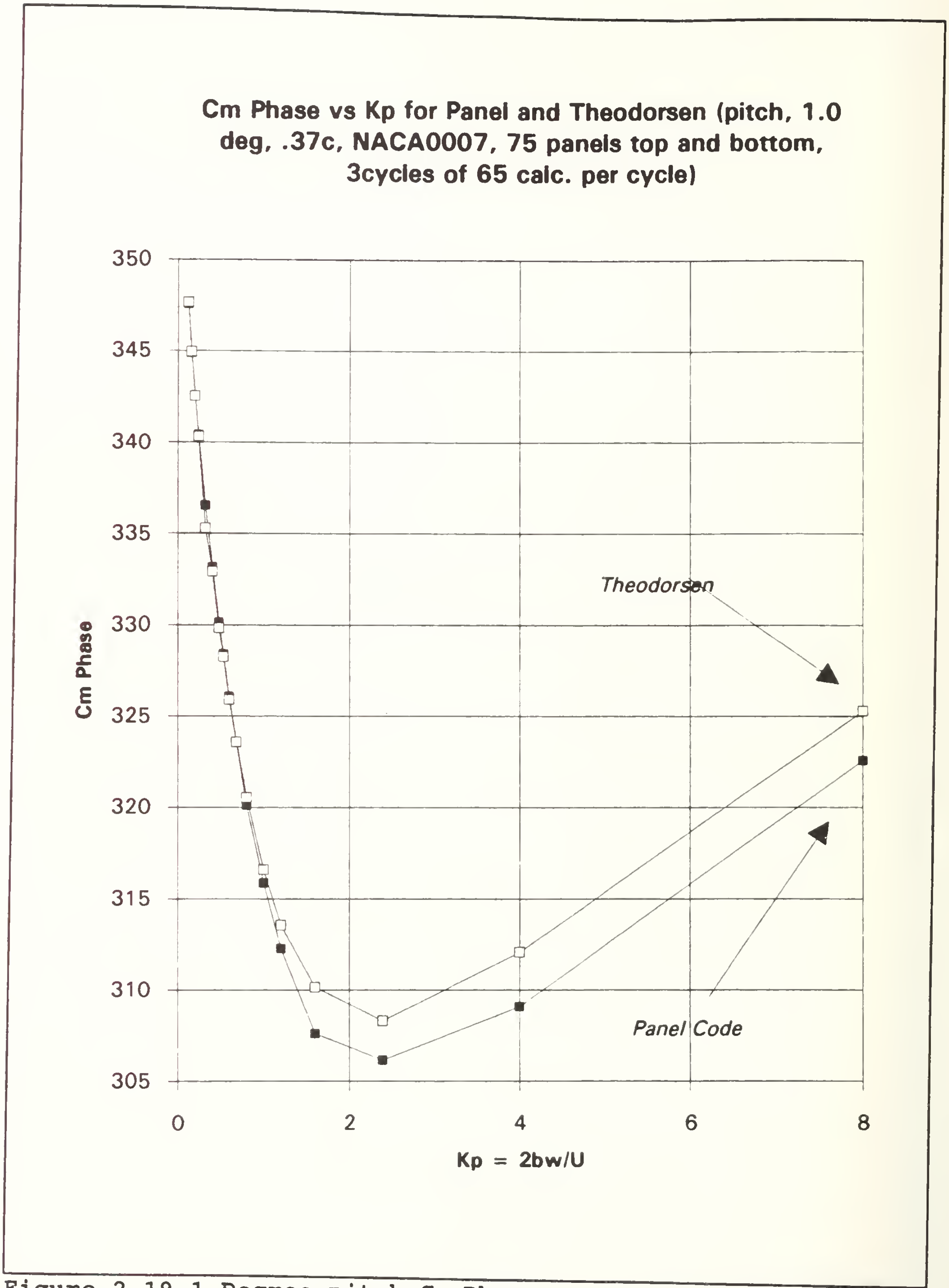

Figure 2.19 1 Degree pitch C_M Phase

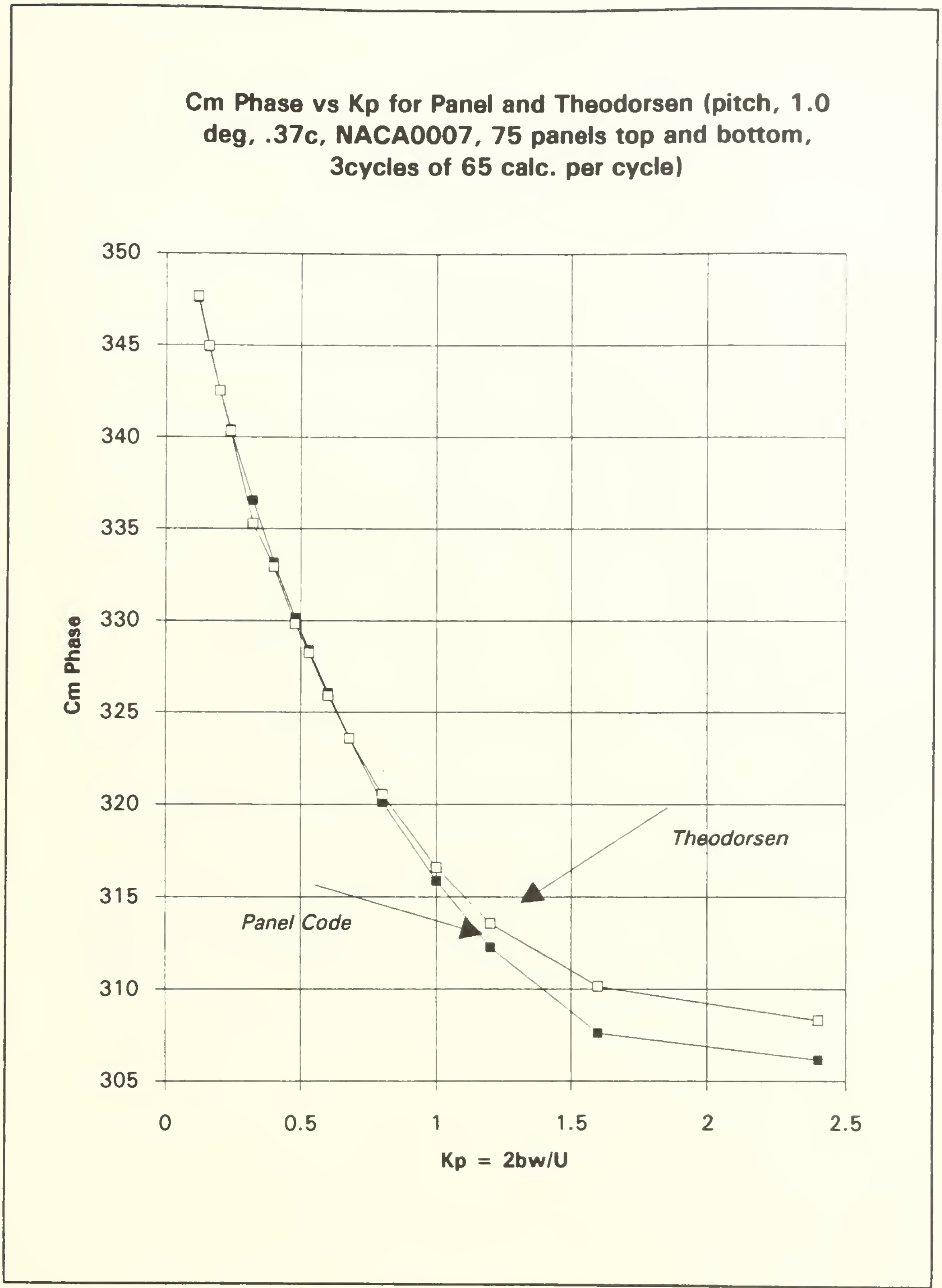

Figure 2.20 1 Degree pitch C_M Phase

		Comparison of Panel CL Values with Theordorsen Results											
		(pitch, 6.7 deg., .37c, NACA 0007, 75 panels top and bottom, 3cyc65calc.)											
		Kpanel (equal to 2 x Theordorsen Kt)				%DIFF taken wrt Theordorsen values.							
Kpanel	1/kt.	Real pen.	Real theo.	% DIFF.	Imag Pan.	Imag Theo.	% DIFF.	Mag Pan.	Mag Theo.	% DIFF.	Phase Pn.	Phase Th.	% DIFF.
0.11666	16.67	-0.66904	-0.65963	4.46%	0.07156	0.052624	35.51%	0.692748	0.6617417	4.69%	174.06616	175.42145	0.77%
0.16	12.5	-0.66442	-0.636766	4.01%	0.07227	0.050026	44.46%	0.668337	0.6407516	4.31%	173.79224	175.52214	0.66%
0.2	10	-0.64216	-0.61966	3.58%	0.07024	0.0434	61.84%	0.64569	0.6214672	3.94%	173.75776	175.9657	1.27%
0.24	6.33	-0.62342	-0.603148	3.36%	0.06214	0.0342133	61.63%	0.626506	0.604116	3.71%	174.30776	176.75341	1.36%
0.32	6.25	-0.59084	-0.57477	2.60%	0.043054	0.0106	294.36%	0.592407	0.5746733	3.05%	175.63227	176.61357	1.72%
0.4	5	-0.56526	-0.55166	2.43%	0.02292	-0.01616	241.83%	0.565744	0.5520666	2.47%	177.67614	181.6773	2.20%
0.48	4.17	-0.54524	-0.53296	2.30%	-0.023584	-0.045026	47.62%	0.54575	0.5348566	2.04%	182.47675	184.62905	1.27%
0.53	3.75	-0.53384	-0.52034	2.59%	-0.04174	-0.06414	34.92%	0.535469	0.5242782	2.13%	184.47076	167.02715	1.37%
0.6	3.33	-0.5204	-0.51004	2.03%	-0.06766	-0.066674	24.49%	0.524806	0.5176976	1.33%	187.42943	169.69348	1.35%
0.68	2.94	-0.50646	-0.497256	1.85%	-0.0672	-0.12003	16.02%	0.515703	0.5115376	0.61%	180.68413	193.57073	1.40%
0.6	2.5	-0.48666	-0.4808	1.70%	-0.13666	-0.16532	17.15%	0.507779	0.5084263	0.13%	195.84761	196.9752	1.67%
1	2	-0.46648	-0.4575	1.96%	-0.2067	-0.2366	13.01%	0.511037	0.5165833	1.07%	204.10342	207.67124	1.72%
1.2	1.67	-0.4482	-0.43706	2.55%	-0.27804	-0.3131	11.20%	0.527437	0.5376365	1.90%	211.61332	215.61696	1.76%
1.6	1.25	-0.41768	-0.39804	4.96%	-0.41216	-0.45584	9.58%	0.566941	0.605166	3.01%	224.60517	226.6725	1.66%
2.4	0.63	-0.36116	-0.31314	15.33%	-0.67442	-0.73746	6.55%	0.765035	0.6011661	4.51%	241.63042	246.99297	2.09%
4	0.5	-0.04413	-0.0593	25.56%	-1.25667	-1.2652	0.66%	1.257644	1.2665666	0.71%	267.96929	267.31651	0.25%
6	0.25	0.996234	1.090012	8.60%	-2.6321	-2.5496	11.06%	3.002211	2.77283	6.27%	266.38009	293.14761	1.29%
Values above for Kp of 4 and 6 were calculated using 200 panels and 4 cycles of 100 calculations per cycle.													
Below calculations were done with 75 panels and 3cyc of 65 calc.s													
4	0.5	-0.2076	-0.0593	250.42%	-1.1674	-1.2652	5.36%	1.215297	1.2665669	4.05%	260.15476	267.31651	2.68%
6	0.25	0.56564	1.060012	48.11%	-2.8049	-2.5466	10.01%	2.661366	2.77283	3.19%	261.40143	263.14761	4.01%

TABLE 2.4 6.7 DEGREE PITCH C_L COMPARISON

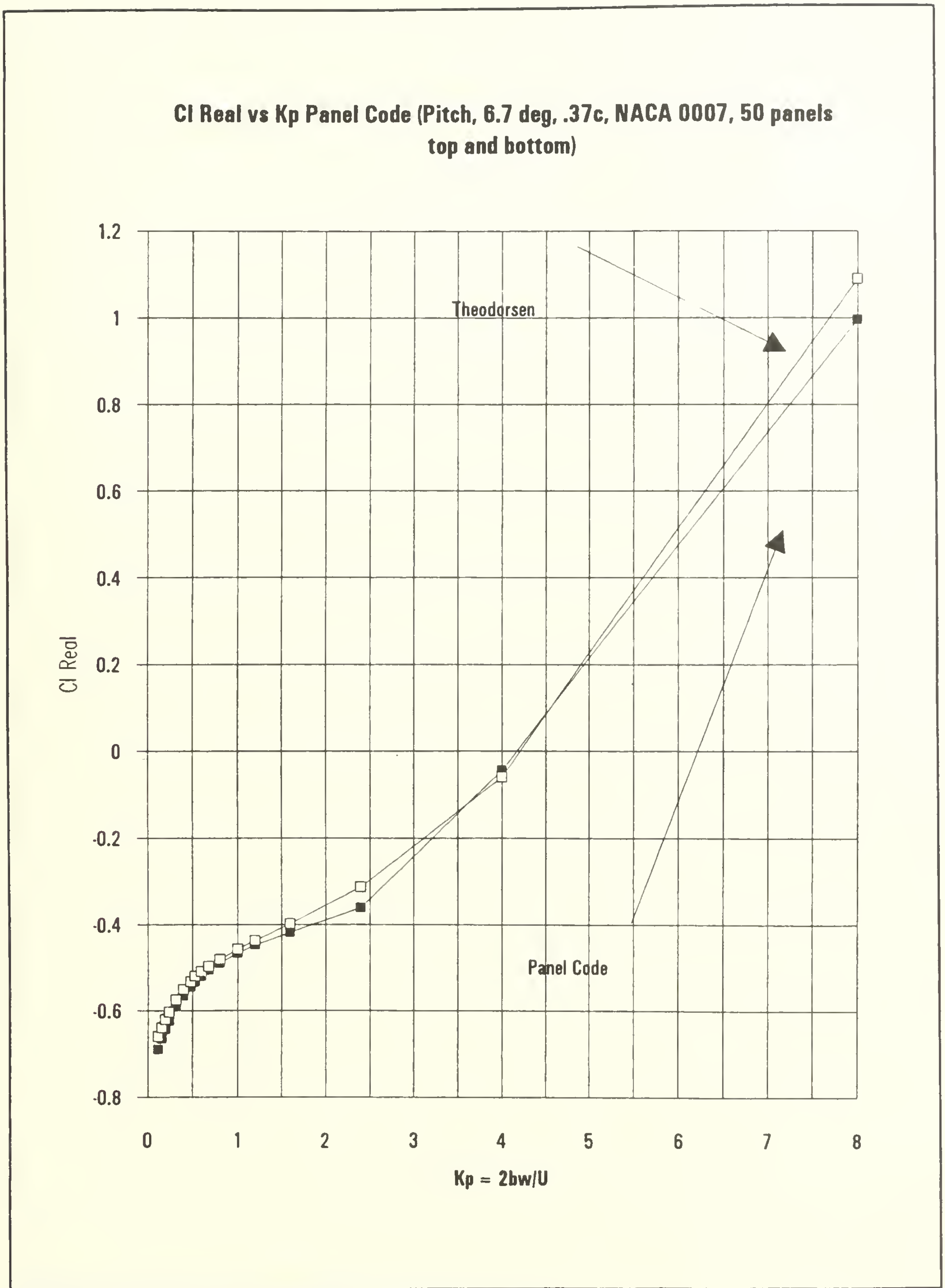

Figure 2.21 6.7 degrees pitch C_L Re

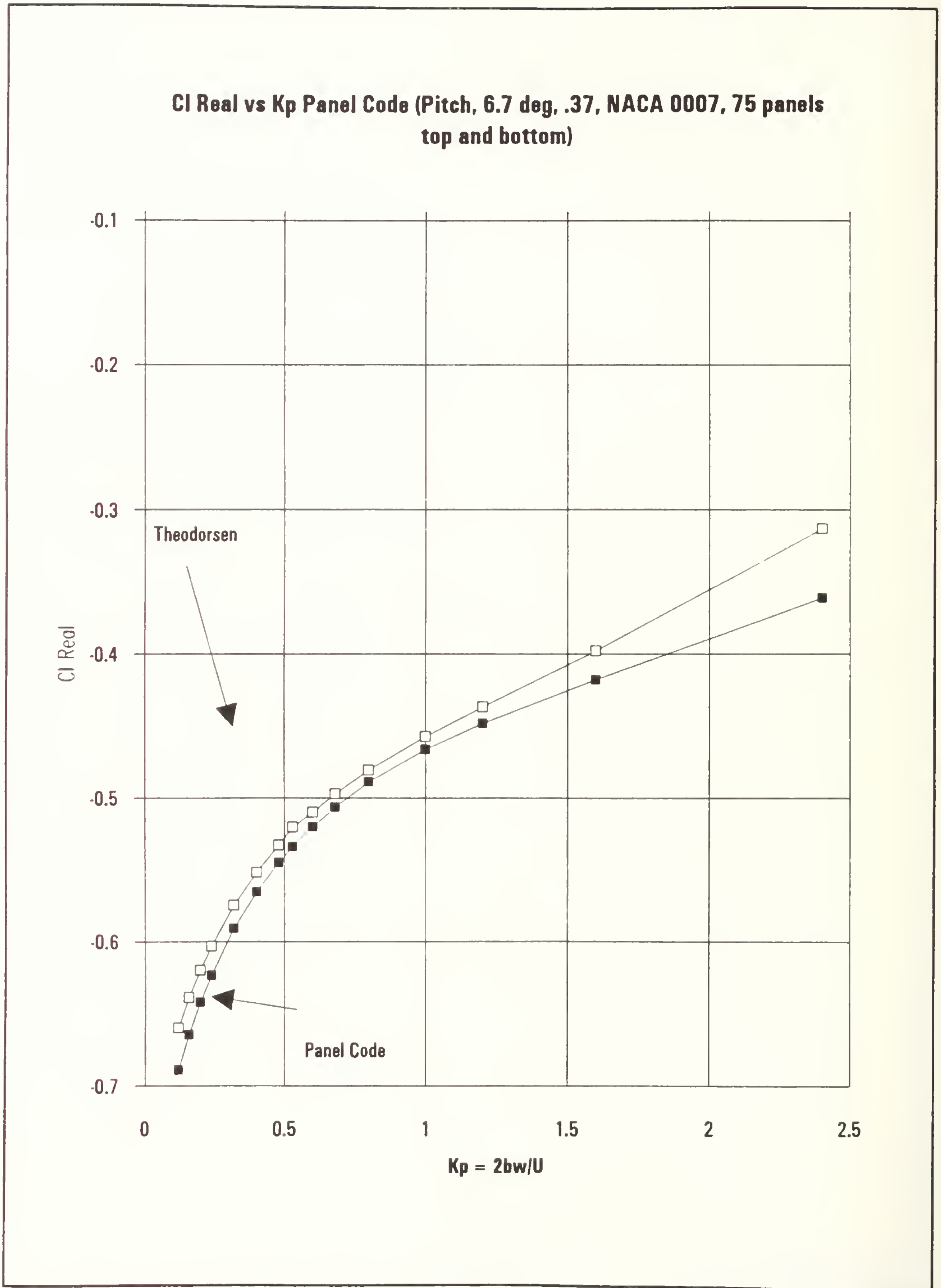

Figure 2.22 6.7 degrees pitch C_L Re

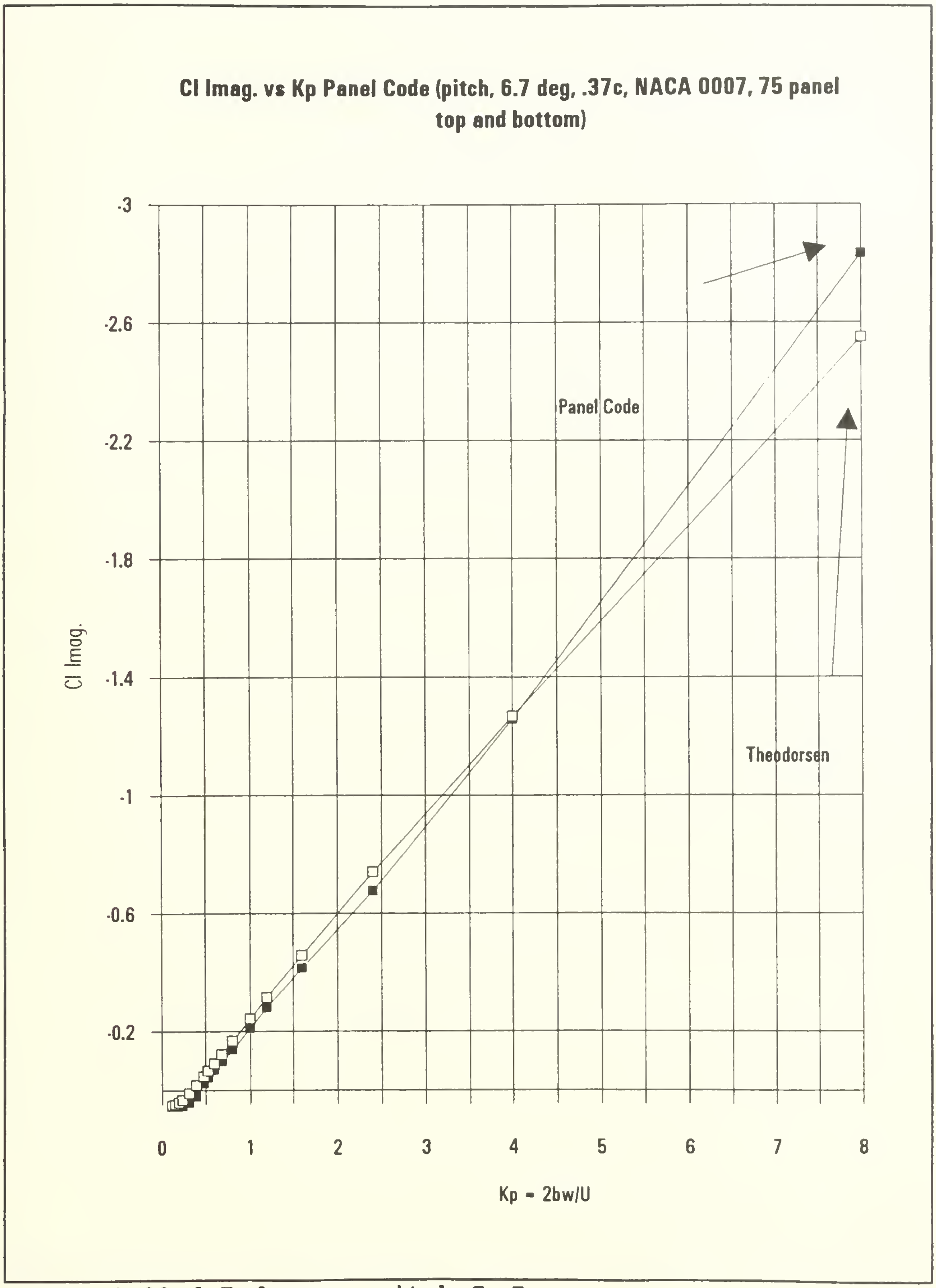

Figure 2.23 6.7 degrees pitch C_L Im

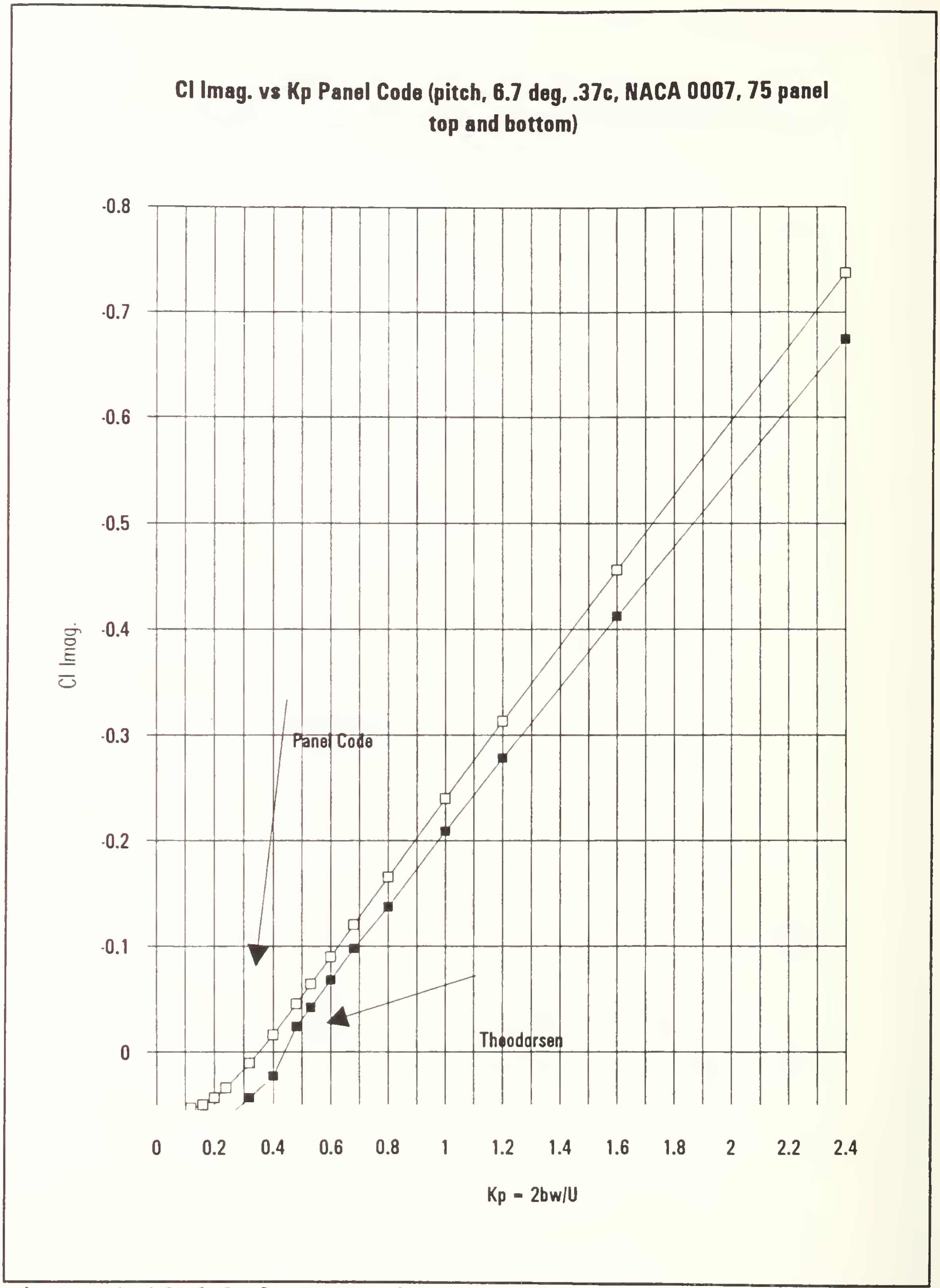

Figure 2.24 6.7 degrees pitch C_L Im

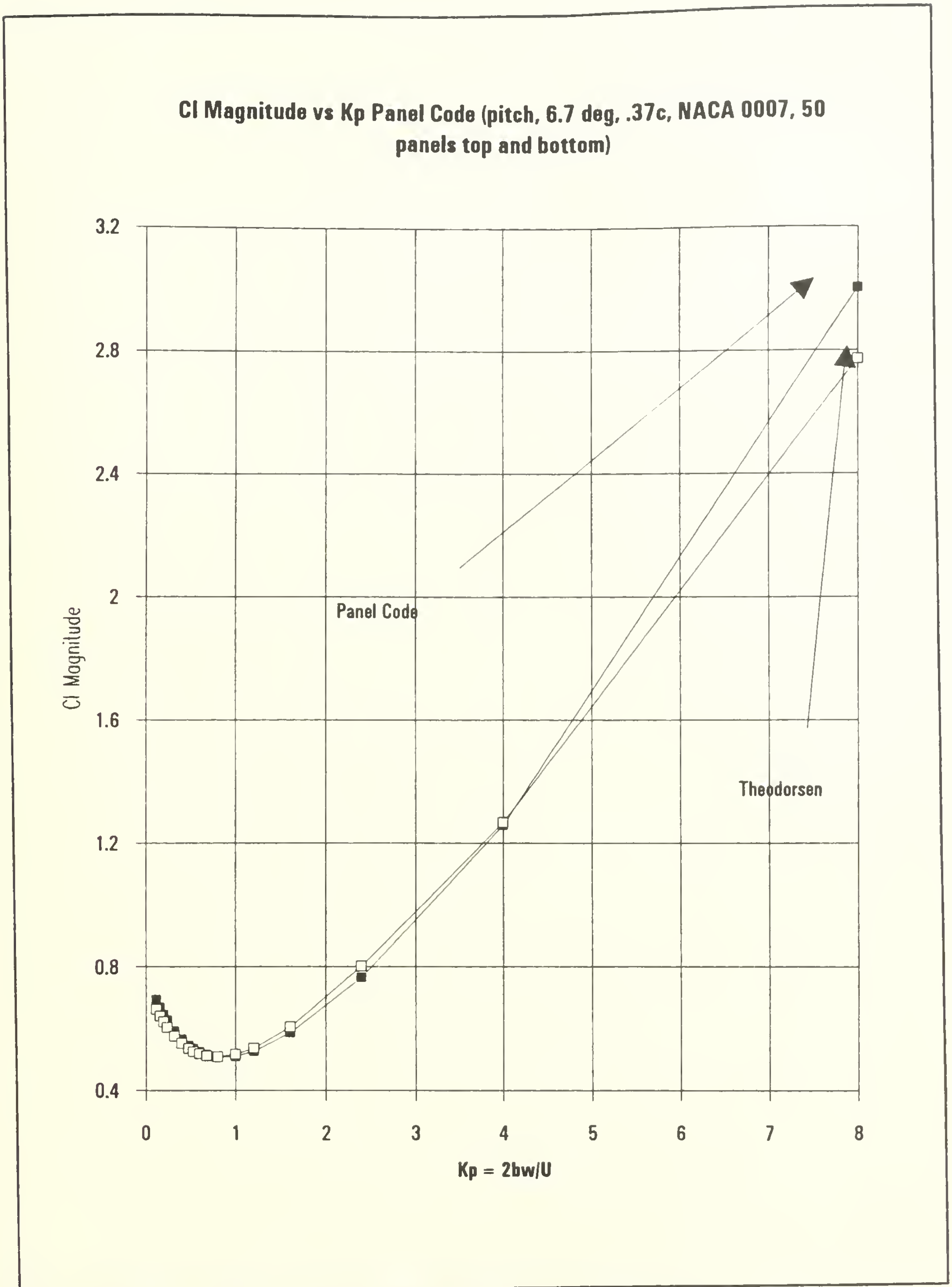

Figure 2.25 6.7 degrees pitch C_L Magnitude

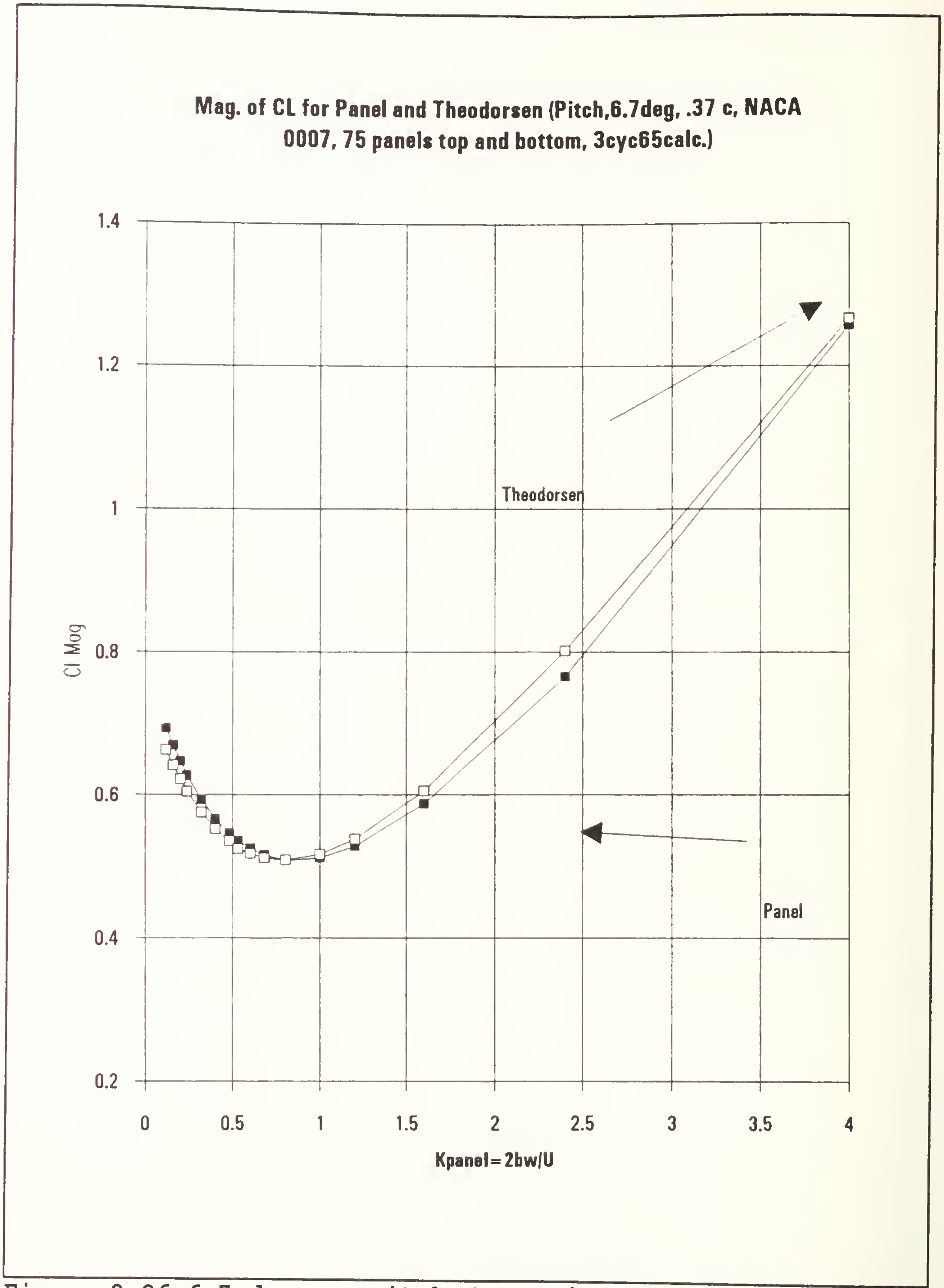

Figure 2.26 6.7 degrees pitch C_L Magnitude

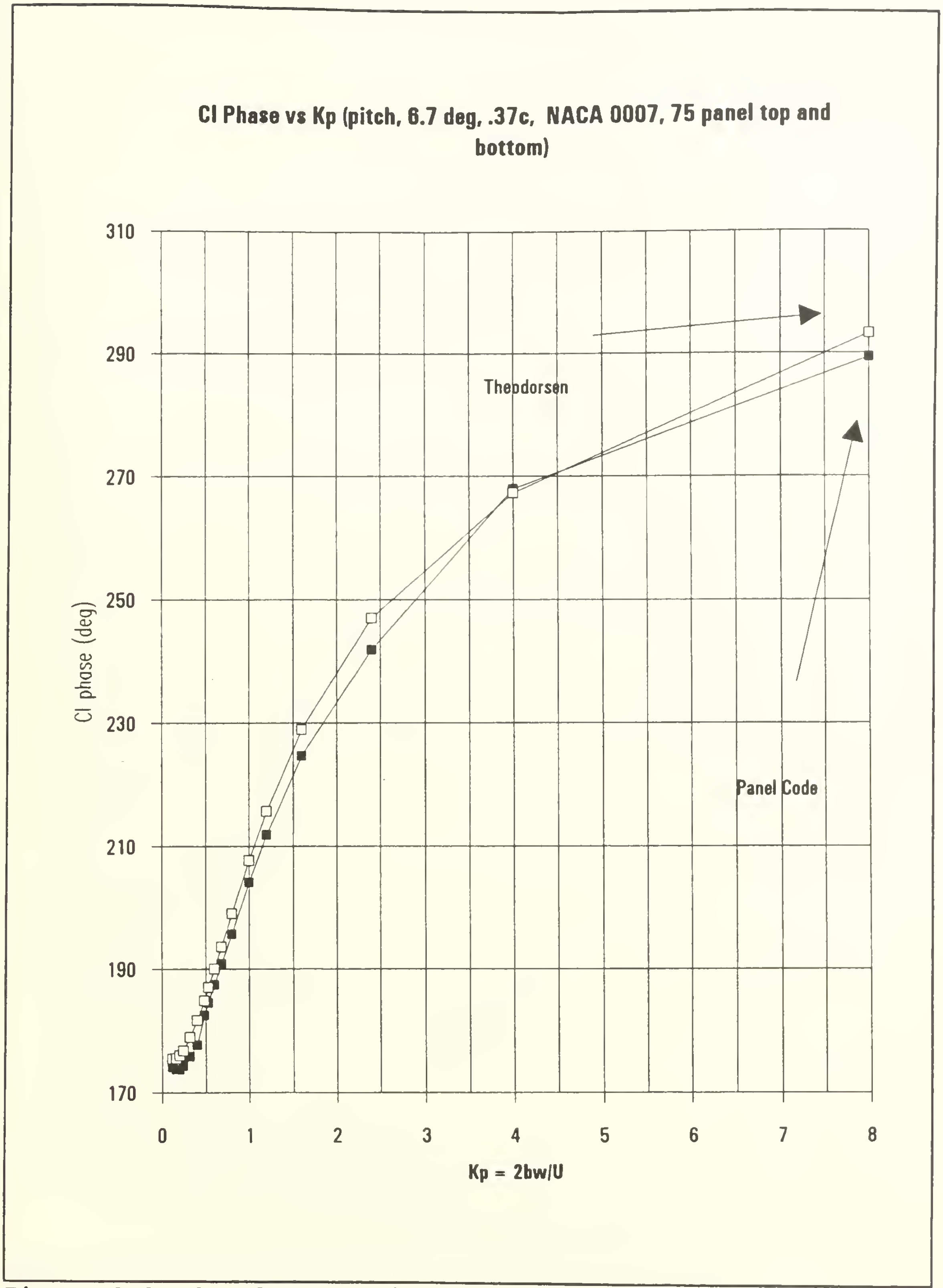

Figure 2.27 6.7 degrees pitch C_L phase

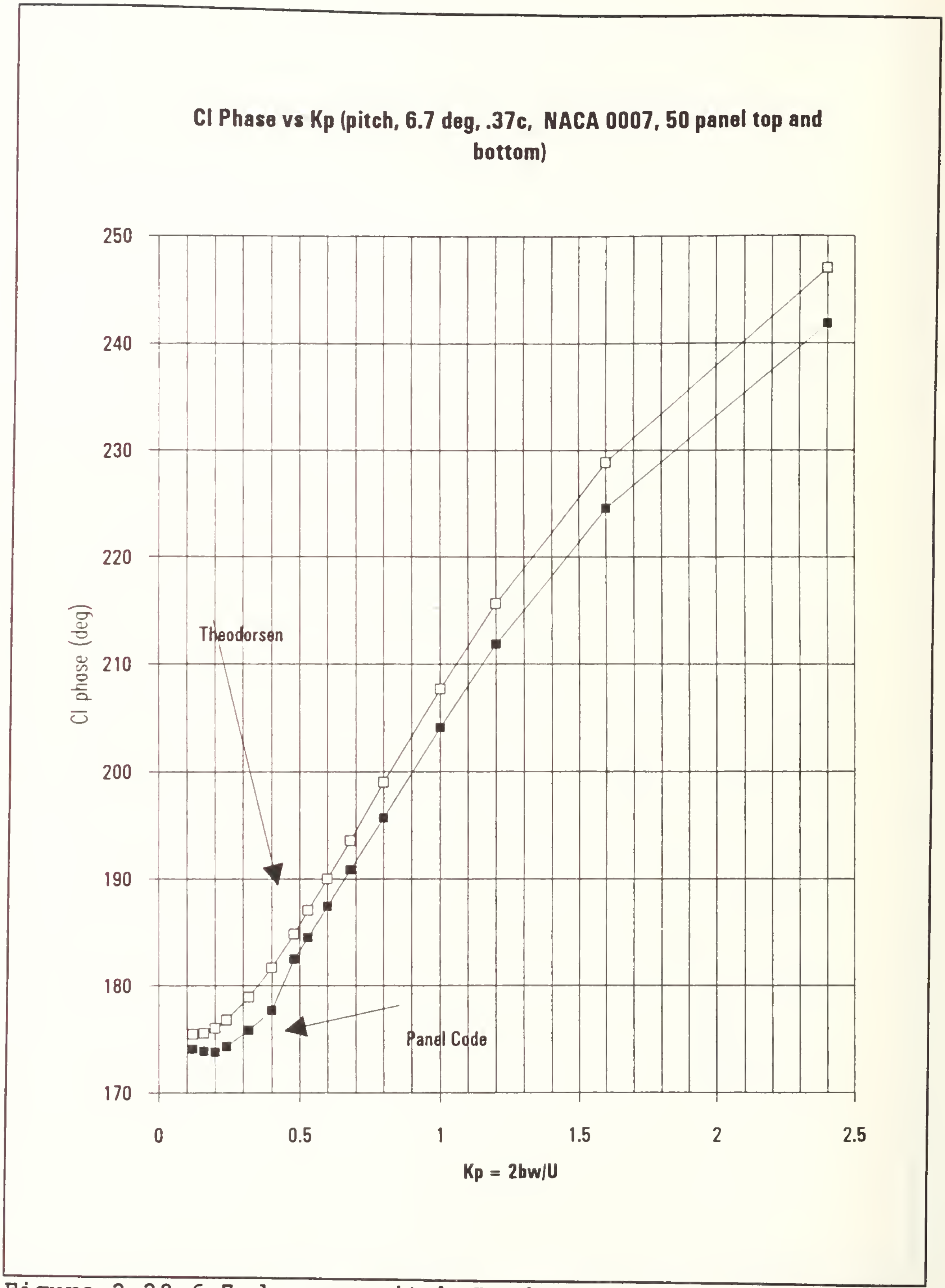

Figure 2.28 6.7 degrees pitch C_L Phase

1/kt	Kpanel	Rp	Rt	% DIFF	Imag Pan.	Imag Th.	% DIFF	Mag Pan.	Mag The.	% DIFF	Phase Pn.	Phase Th.	% DIFF
	Comparison of Panel Moment Aerodynamic Values (CM) with Theordorsen Results												
		(pitch, 6.7 deg., .37c, NACA 0007, 50 panels top and bottom,3cyc65calc.)											
	Kpanel (equal to 2 x Theordorsen Kt)					Mh = .5							
16.67	0.11996	0.079057	0.079322	0.33%	-0.016252	-0.017304	5.48%	0.081136	0.081188	0.06%	347	347.6938	0.20%
12.5	0.16	0.076019	0.076953	1.21%	-0.021796	-0.020696	5.32%	0.079083	0.079688	0.78%	344	344.9458	0.27%
10	0.2	0.071855	0.074864	4.02%	-0.023347	-0.023576	0.97%	0.075553	0.078469	3.74%	341.9999	342.5197	0.15%
8.33	0.24	0.072101	0.073109	1.38%	-0.024826	-0.026148	5.05%	0.076258	0.077644	1.79%	341.0004	340.3203	0.20%
6.25	0.32	0.068532	0.07017	2.33%	-0.029115	-0.030698	5.16%	0.07446	0.076591	2.78%	336.9821	338.3714	0.18%
5	0.4	0.065941	0.068094	3.16%	-0.032575	-0.034798	6.39%	0.073549	0.07647	3.82%	333.7106	332.932	0.23%
4.17	0.48	0.064013	0.066548	3.81%	-0.035849	-0.038681	7.32%	0.073367	0.076972	4.68%	330.7499	329.8319	0.28%
3.75	0.53	0.063055	0.06584	4.23%	-0.037946	-0.041223	7.95%	0.073592	0.07786	5.28%	326.9609	327.9488	0.31%
3.33	0.6	0.062071	0.065416	5.11%	-0.040477	-0.044321	8.67%	0.074103	0.079018	6.22%	326.8914	325.8817	0.31%
2.94	0.68	0.061259	0.065135	5.95%	-0.043608	-0.04806	9.24%	0.075195	0.08094	7.10%	324.5541	323.584	0.30%
2.5	0.8	0.060628	0.065184	6.99%	-0.048262	-0.053636	10.02%	0.077492	0.084414	8.20%	321.4786	320.5512	0.29%
2	1	0.060704	0.0668	6.85%	-0.0582	-0.063055	10.87%	0.082725	0.091714	9.80%	317.2064	316.5682	0.20%
1.67	1.2	0.061896	0.069032	10.34%	-0.064202	-0.072639	11.62%	0.08918	0.100209	11.01%	313.9523	313.5415	0.13%
1.25	1.6	0.066935	0.077741	13.90%	-0.08115	-0.092249	12.03%	0.105193	0.120638	12.80%	309.5167	310.1219	0.20%
0.83	2.4	0.084477	0.10472	19.33%	-0.117542	-0.132633	11.38%	0.14475	0.168991	14.34%	305.7047	308.2927	0.84%
0.5	4	0.183099	0.19447	16.13%	-0.21796	-0.215551	1.12%	0.272226	0.290311	6.23%	306.8074	312.0588	1.68%
0.25	8	0.534359	0.618634	13.62%	-0.52513	-0.428776	22.47%	0.7492	0.752699	0.46%	315.4991	325.2741	3.01%
Values for Kp equal to 4 and 8 above were calculated using 200 panels top and bottom and 4 cycles of 100 calculations.													
The below values were calculated using 75 panels and 3 cyc of 65 calc.													
0.5	4	0.144459	0.19447	25.72%	-0.200537	-0.215551	6.97%	0.247151	0.290311	14.87%	305.7676	312.0588	2.02%
0.25	6	0.446235	0.618634	27.54%	-0.495585	-0.428776	15.58%	0.668221	0.752699	11.22%	312.128	325.2741	4.04%

TABLE 2.5 6.7 DEGREES PITCH C_M COMPARISON

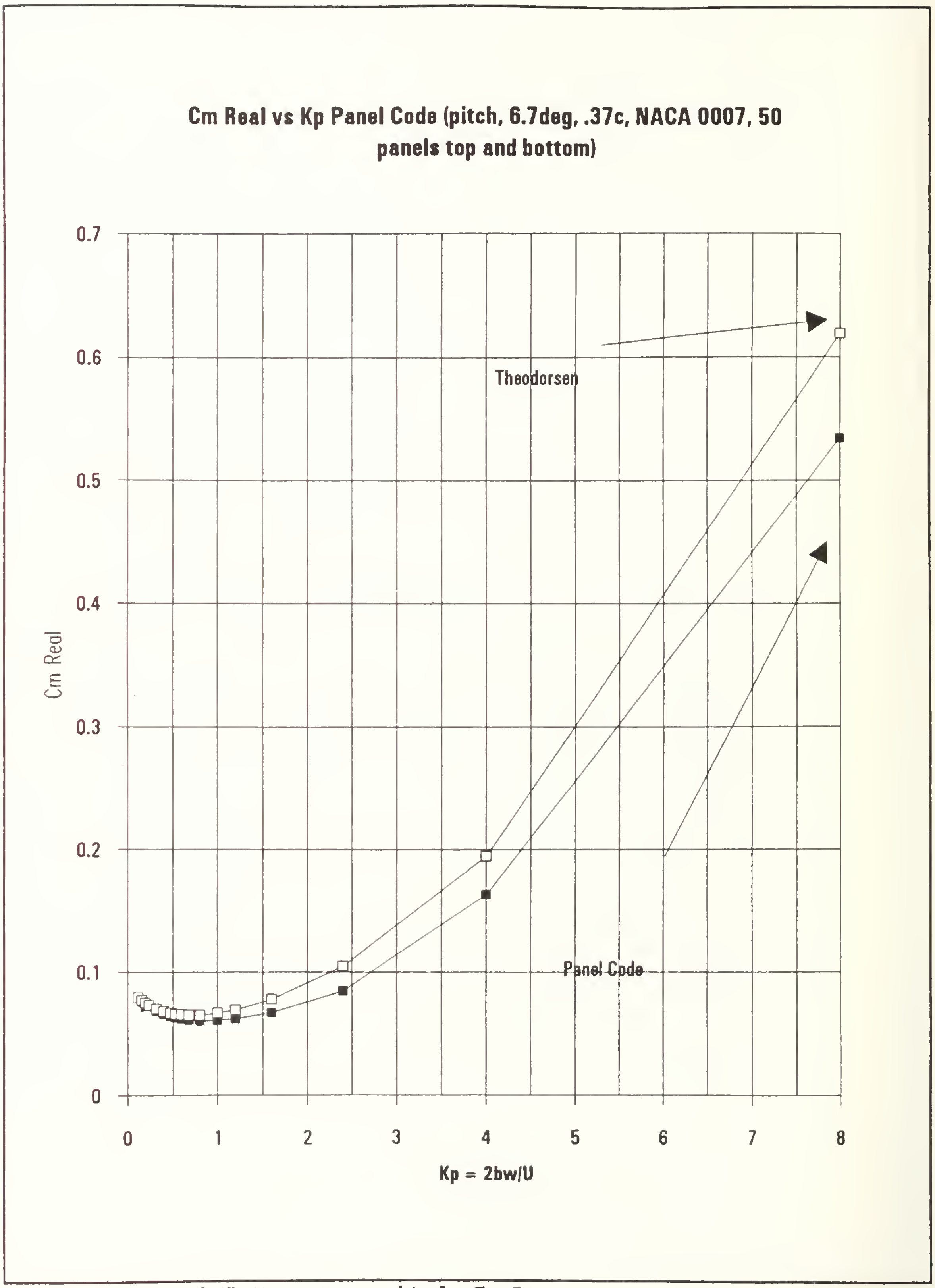

Figure 2.29 6.7 Degrees pitch C_M Re

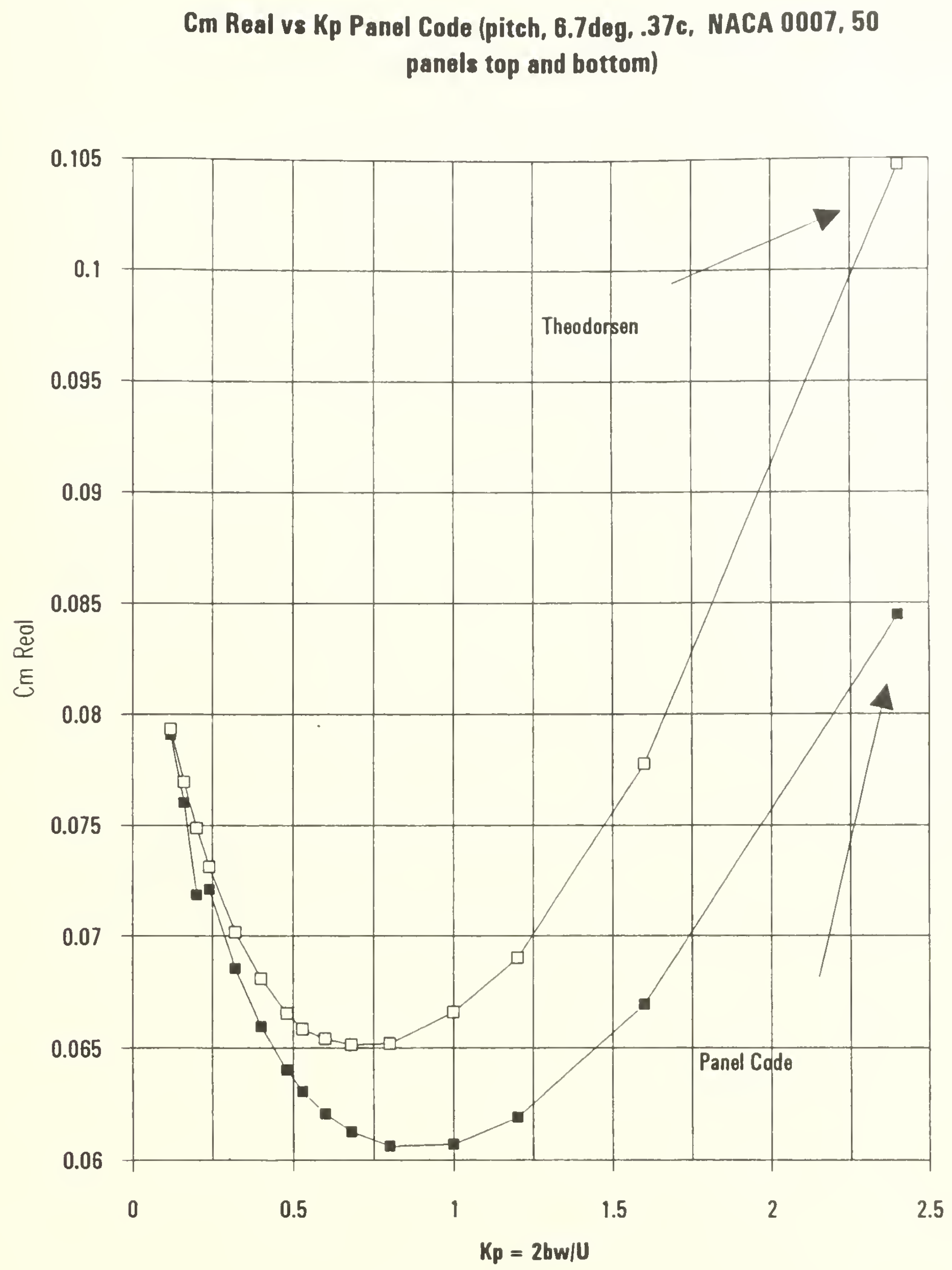

Figure 2.30 6.7 Degrees pitch C_M Re

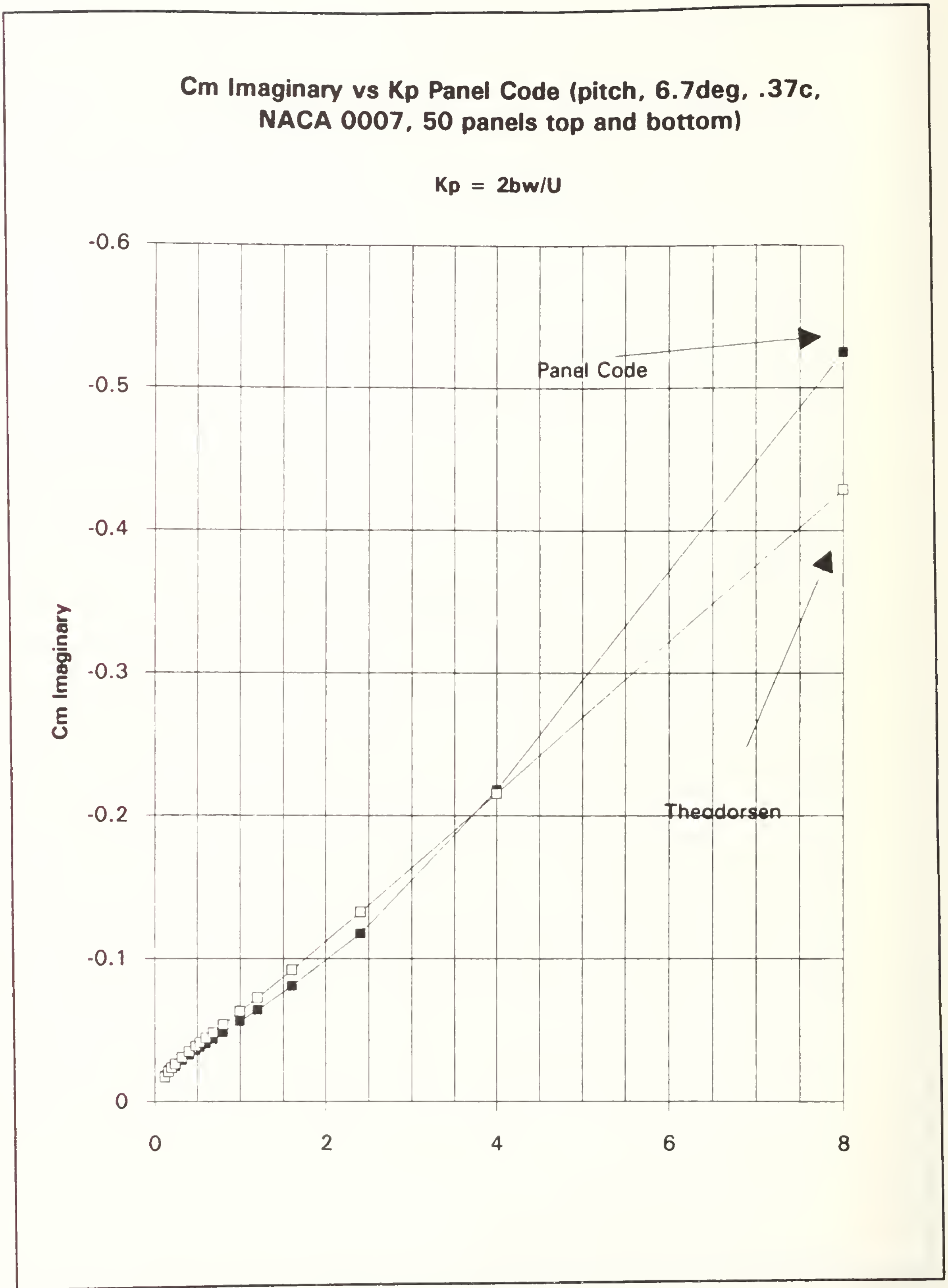

Figure 2.31 6.7 Degrees pitch C_M Im

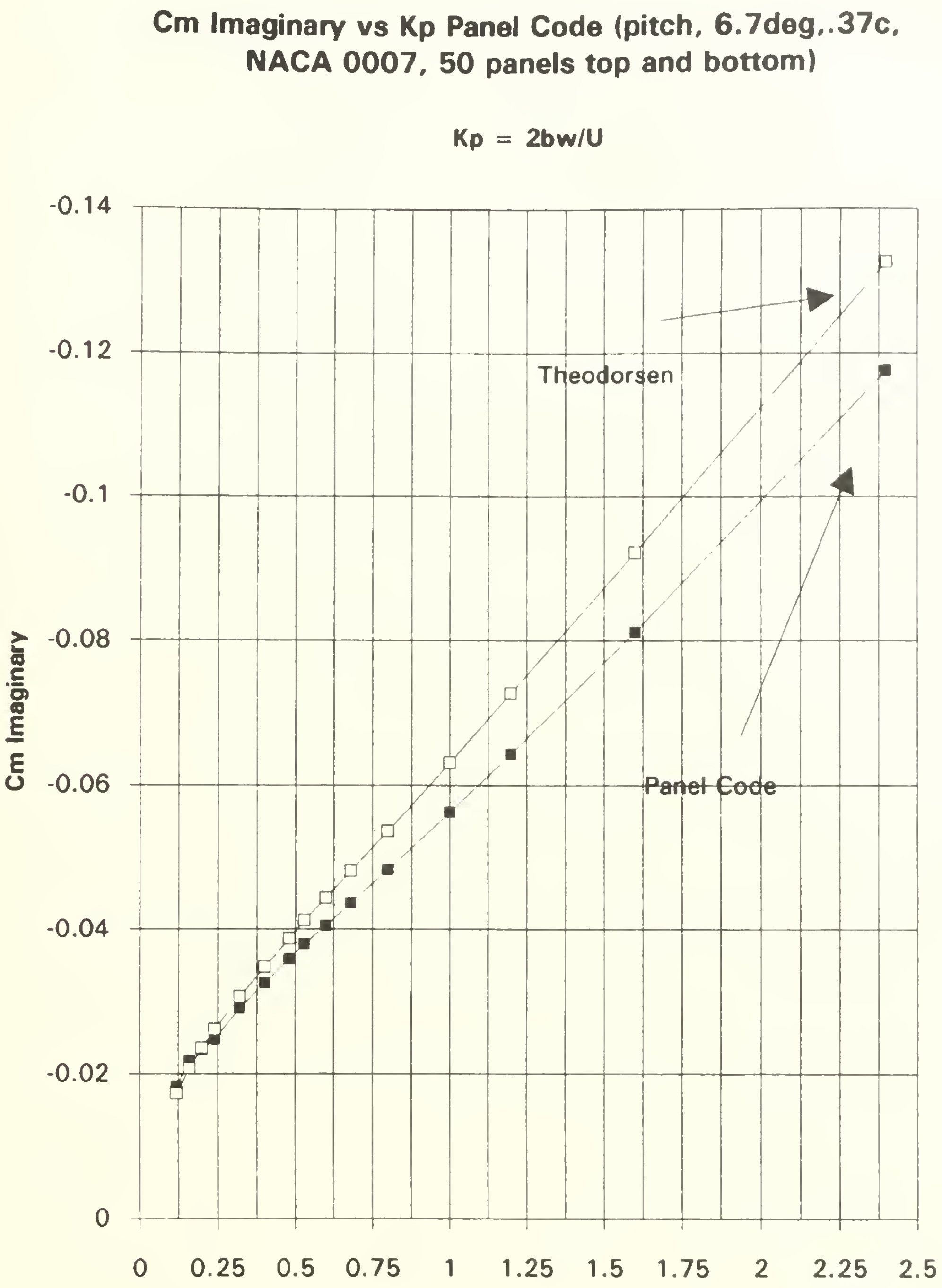

Figure 2.32 6.7 Degrees pitch C_M Im

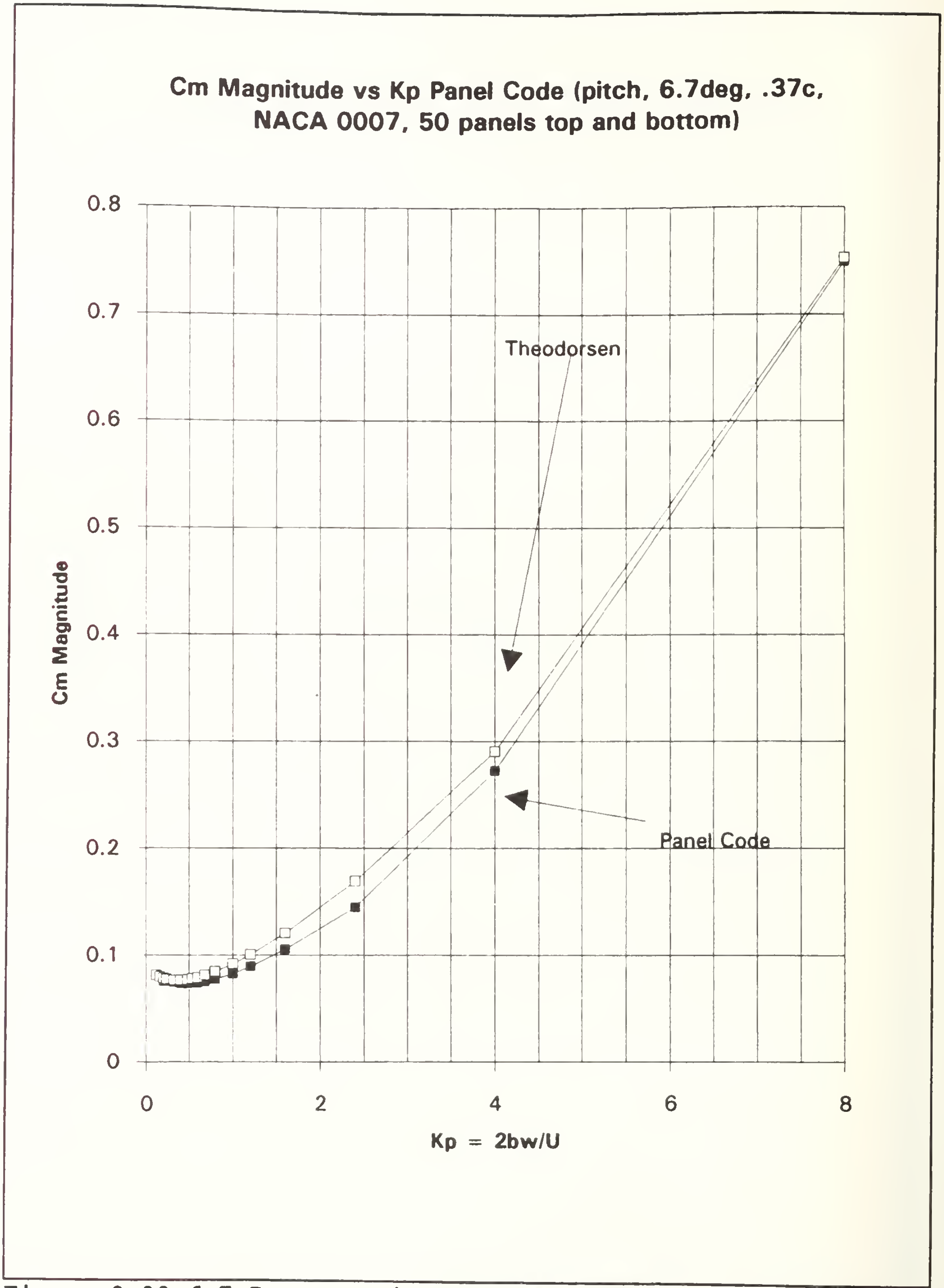

Figure 2.33 6.7 Degrees pitch C_M magnitude

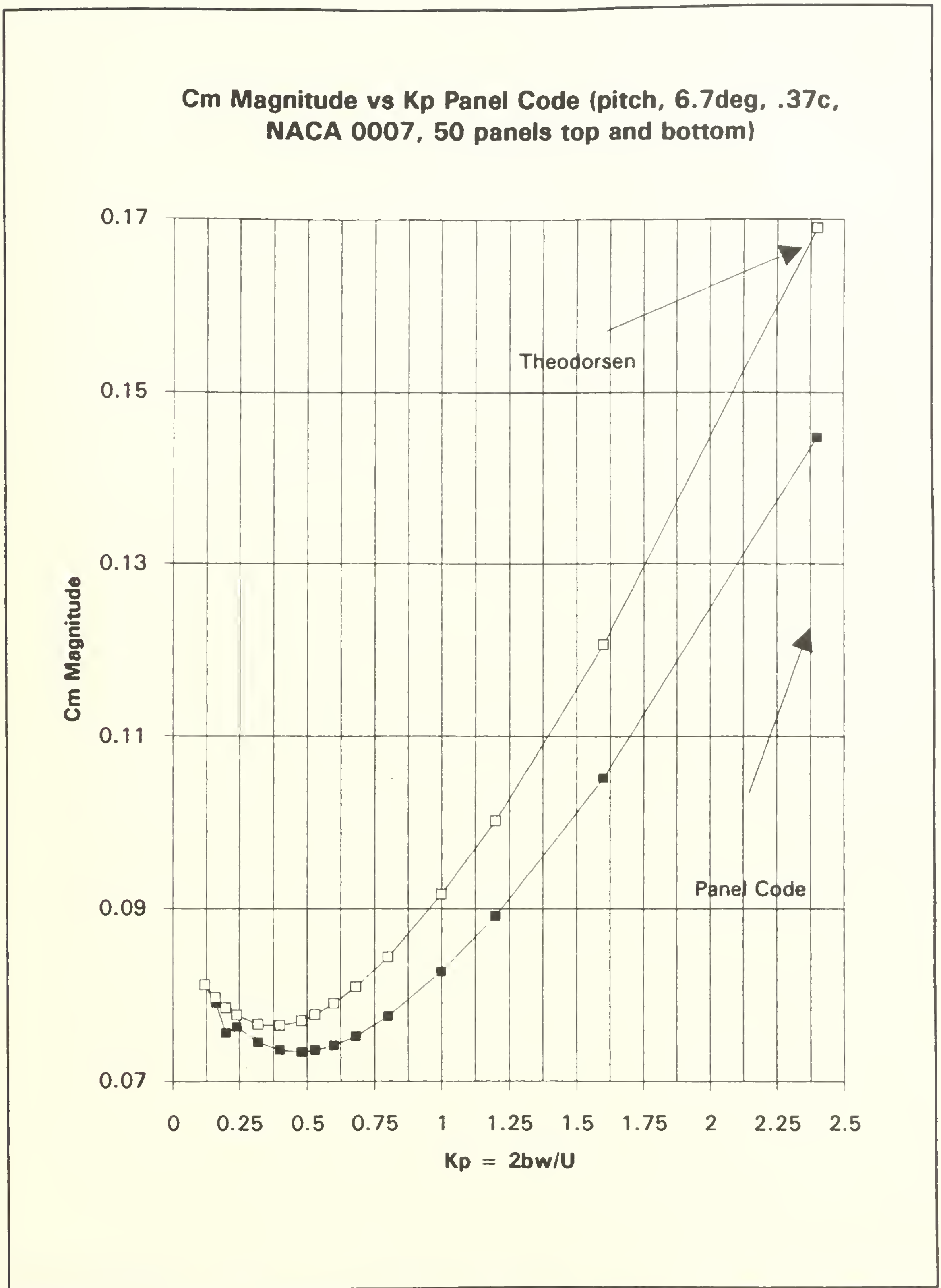

Figure 2.34 6.7 Degrees pitch C_M magnitude

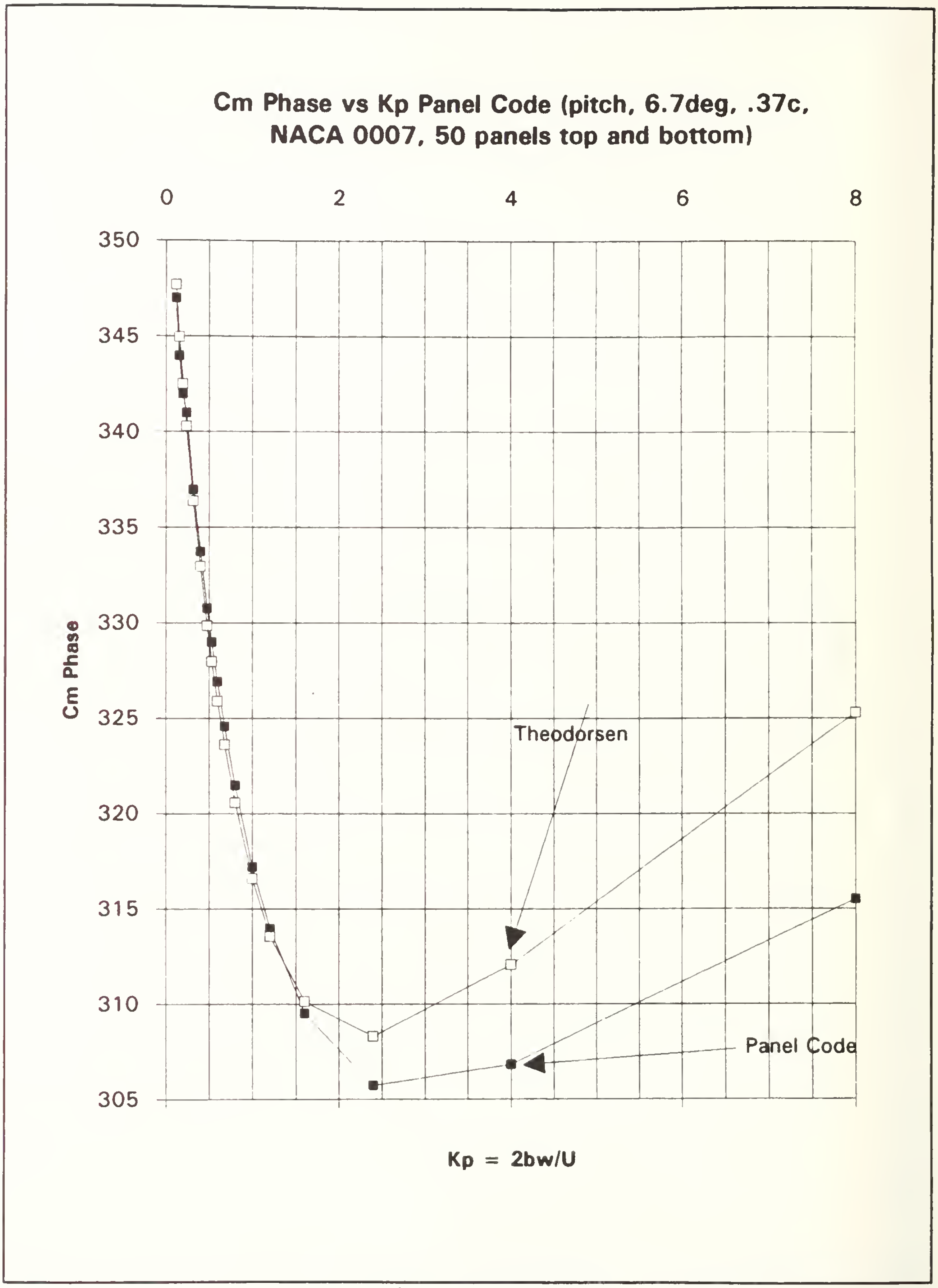

Figure 2.35 6.7 Degrees pitch C_M phase

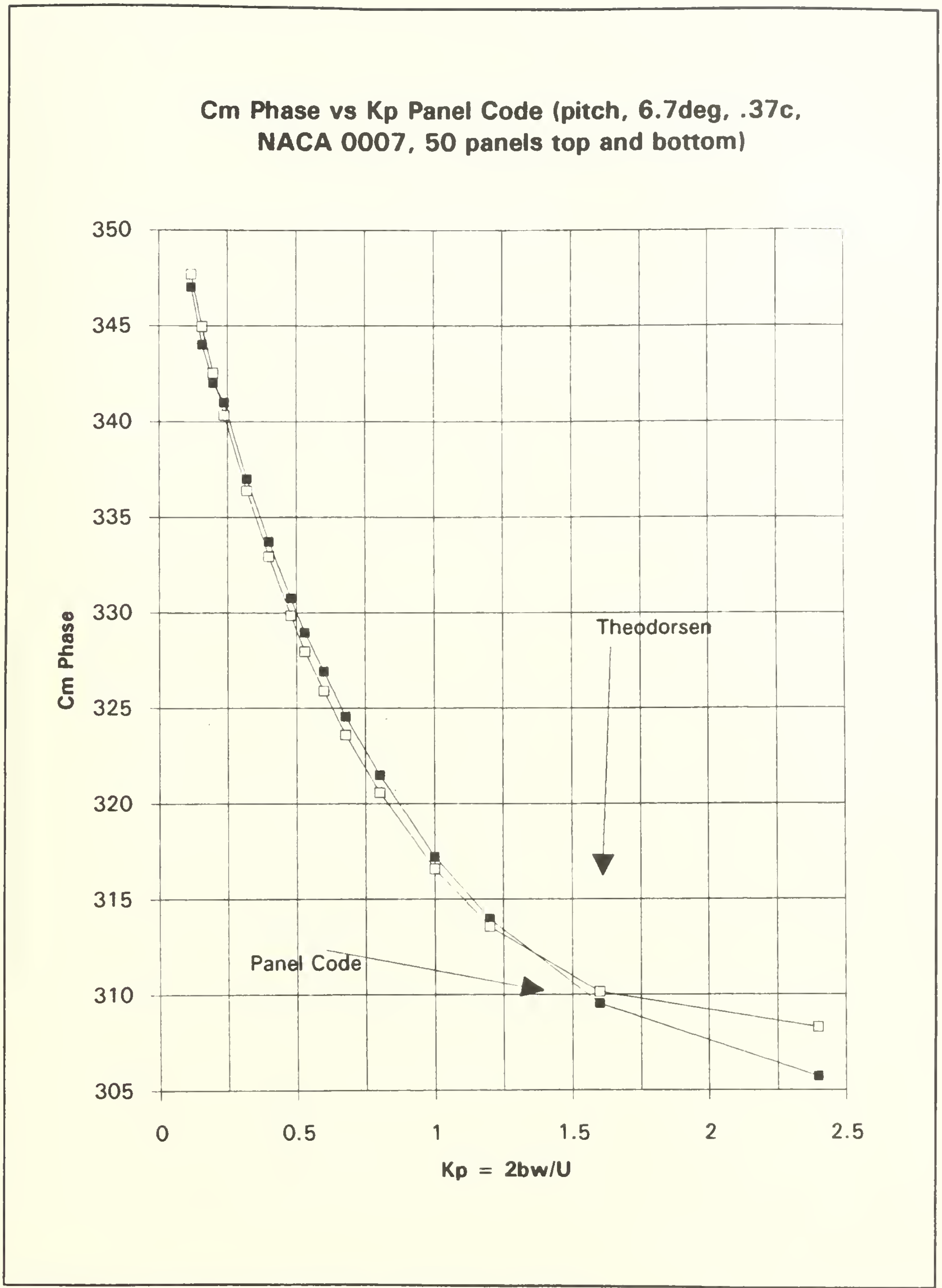

Figure 2.36 6.7 Degrees pitch C_M phase

			Comparison of Panel Cl Values (Plunge) with Theordorsen Results												
			(plunge .0833h/2b, .37c, NACA 0007, 75 panels,3 cyc65)												
			Kpanel (equal to 2 x Theordorsen Kt)				%DIFF taken wrt Theordorsen values.								
1/kt	Kpanel	Real pan.	Real theo.	% DIFF	Imag Pan.	Imag Theo.	% DIFF.	Mag Pan.	Mag Theo.	% DIFF.	Phase Pn.	Phase Th.	% DIFF.		
16.67	0.11998	-0.00854	-0.007088	20.81%	-0.05864	-0.056004	4.71%	0.059258	0.05644837	4.98%	261.714	262.806	0.42%		
12.5	0.16	-0.01234	-0.010103	22.15%	-0.07512	-0.0720518	4.26%	0.076127	0.07275881	4.63%	260.6713	262.0184	0.51%		
10	0.2	-0.0159	-0.0128	24.22%	-0.09048	-0.0871	3.88%	0.091866	0.0880355	4.35%	260.0332	261.6398	0.81%		
8.33	0.24	-0.01904	-0.015088	28.19%	-0.10494	-0.101284	3.61%	0.106653	0.10240164	4.15%	258.7163	261.5271	0.69%		
6.25	0.32	-0.02374	-0.018022	31.73%	-0.13164	-0.1277572	3.04%	0.133764	0.12902207	3.67%	259.7771	261.9706	0.84%		
5	0.4	-0.02608	-0.01854	40.67%	-0.15626	-0.15232	2.59%	0.158421	0.15344417	3.24%	260.5246	263.0802	0.96%		
4.17	0.48	-0.02602	-0.016641	58.36%	-0.1795	-0.17558	2.23%	0.181378	0.17636685	2.84%	261.752	264.5858	1.07%		
3.75	0.53	-0.02478	-0.014062	76.21%	-0.19348	-0.18989	1.89%	0.195058	0.1904092	2.44%	262.7074	265.7676	1.15%		
3.33	0.6	-0.02154	-0.009165	134.50%	-0.2127	-0.20883	1.85%	0.213788	0.20903191	2.28%	264.2174	267.4815	1.22%		
2.94	0.68	-0.015632	-0.001331	1074.46%	-0.234043	-0.230234	1.65%	0.234564	0.23023785	1.88%	266.1766	269.6688	1.29%		
2.5	0.8	-0.00282	0.01468	119.21%	-0.26558	-0.2617	1.48%	0.265595	0.26211141	1.33%	269.3916	273.2106	1.40%		
2	1	0.02874	0.05198	44.71%	-0.31742	-0.31294	1.43%	0.318718	0.31722762	0.47%	275.1736	278.4306	1.52%		
1.87	1.2	0.07234	0.10188	28.99%	-0.36932	-0.36352	1.60%	0.376338	0.37752658	0.31%	281.0824	285.656	1.60%		
1.25	1.6	0.19372	0.23742	18.41%	-0.47526	-0.46404	2.42%	0.513243	0.52124982	1.54%	292.1754	297.096	1.66%		
0.63	2.4	0.59614	0.6435	6.91%	-0.686452	-0.66572	3.11%	0.90265	0.92589168	2.51%	310.493	314.0277	1.13%		
0.5	4	1.85484	1.97276	5.98%	-1.20784	-1.07178	12.69%	2.213438	2.24610454	1.41%	326.9285	331.4852	1.37%		
0.25	8	6.013278	6.24694	2.83%	-3.3882	-2.1094	60.63%	8.699366	8.51243724	2.20%	337.0924	345.6525	2.48%		
Values for Kp equal to 2.4,4, and 8 above were calculated using 200 panels top and bottom and 4 cycles of 100 calculations															
The values below were calculated using 75 panels and 3 cyc 65calc.															
0.83	2.4	0.56626	0.6435	12.00%	-0.7011	-0.66572	5.31%	0.901217	0.82589166	2.66%	308.9269	314.0277	1.62%		
0.5	4	1.80844	1.97278	8.33%	-1.2444	-1.07178	16.11%	2.195218	2.24610454	2.22%	325.4879	331.4852	1.82%		
0.25	8	7.62628	8.24694	5.10%	-3.52086	-2.1094	66.91%	8.58178	8.51243724	0.81%	335.7781	345.6525	2.86%		
	Real pan.	Real theo.	Imag Pan.	Imag Theo.											

TABLE 2.6 PLUNGE h/2b=.0833 C_L COMPARISON

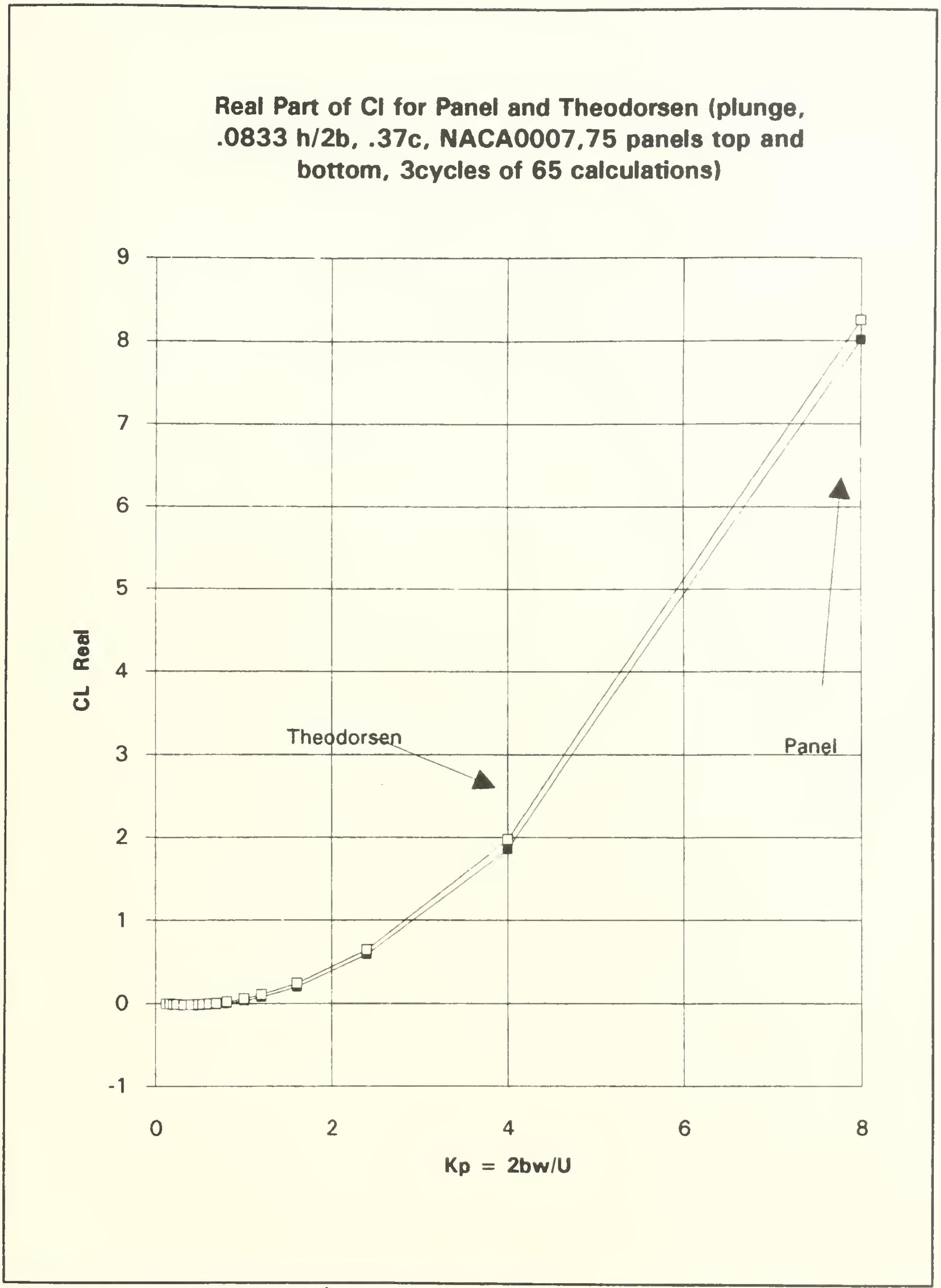

Figure 2.37 Plunge h/2b=.0833 C_L Re

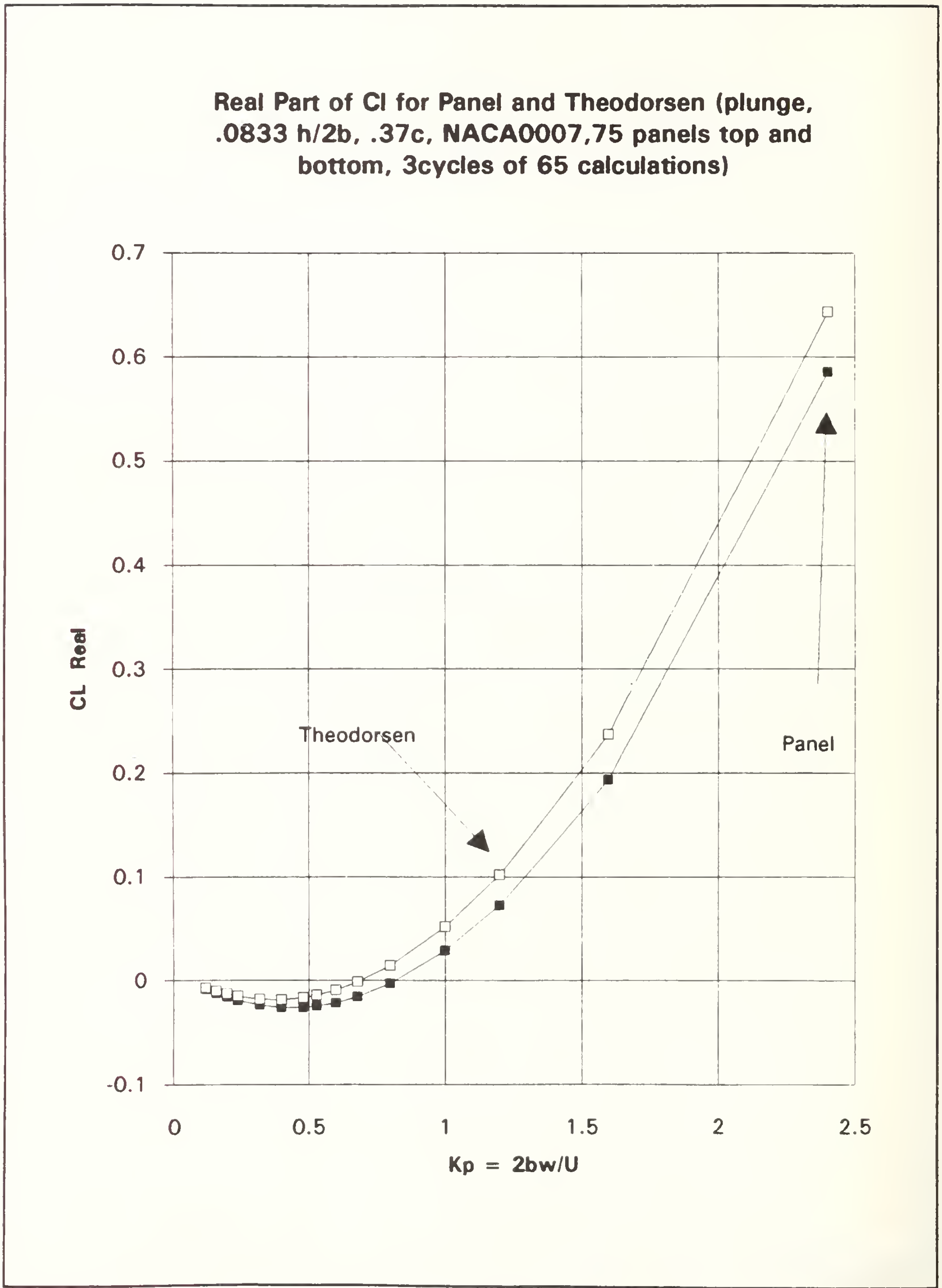

Figure 2.38 Plunge h/2b=.0833 C_L Re

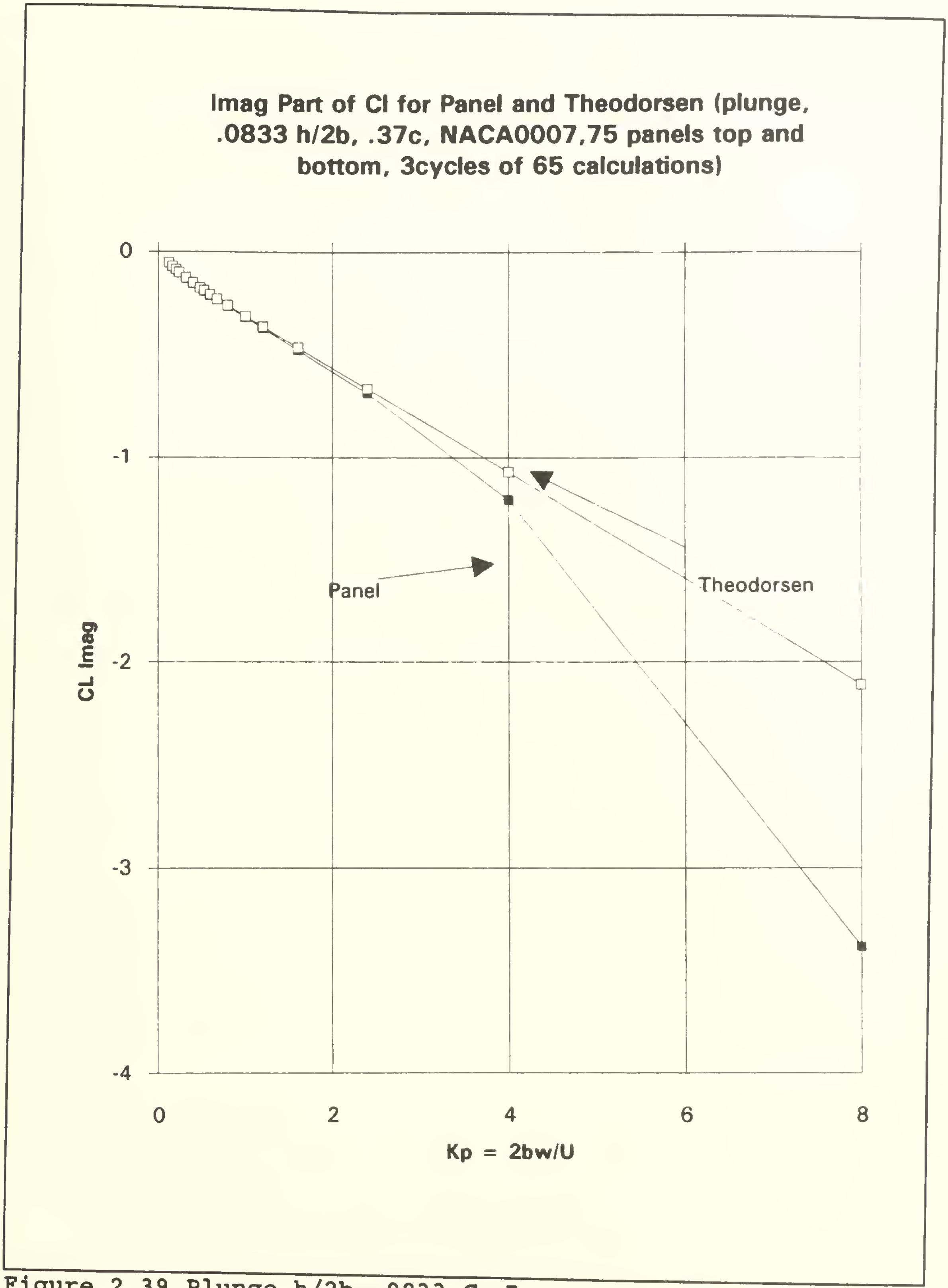

Figure 2.39 Plunge h/2b=.0833 C_L Im

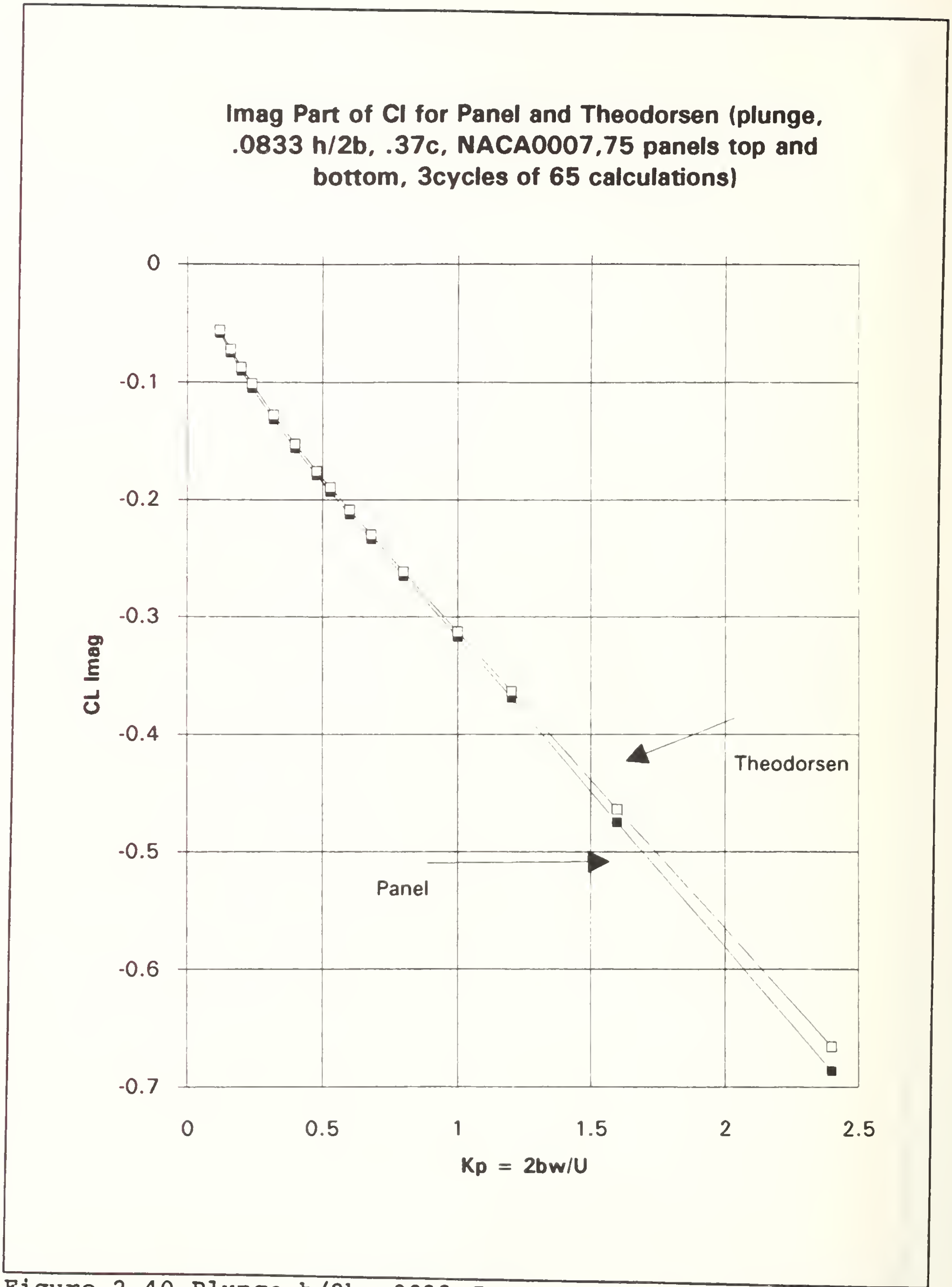

Figure 2.40 Plunge h/2b=.0833 C_L Im

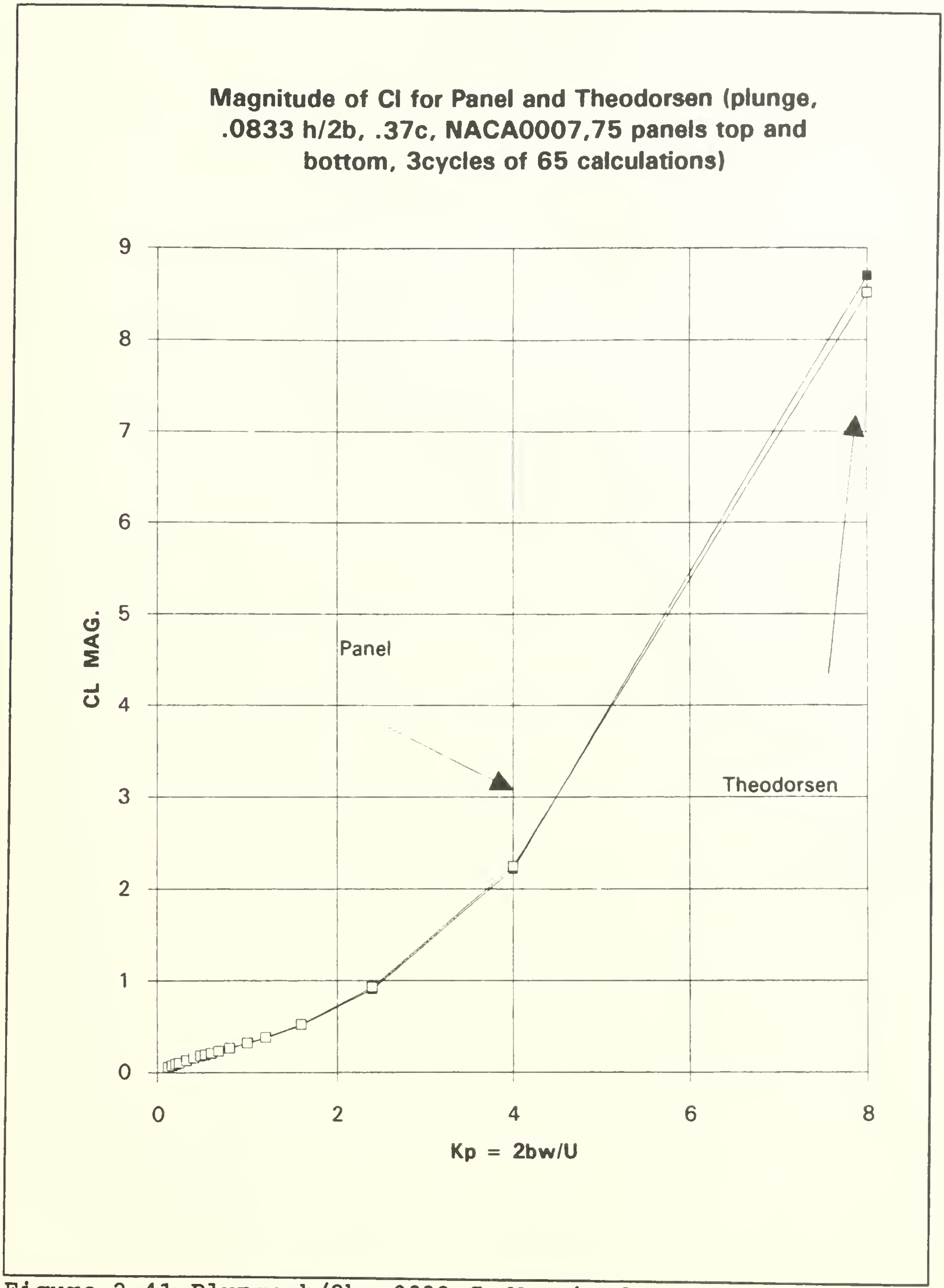

Figure 2.41 Plunge h/2b=.0833 C_L Magnitude

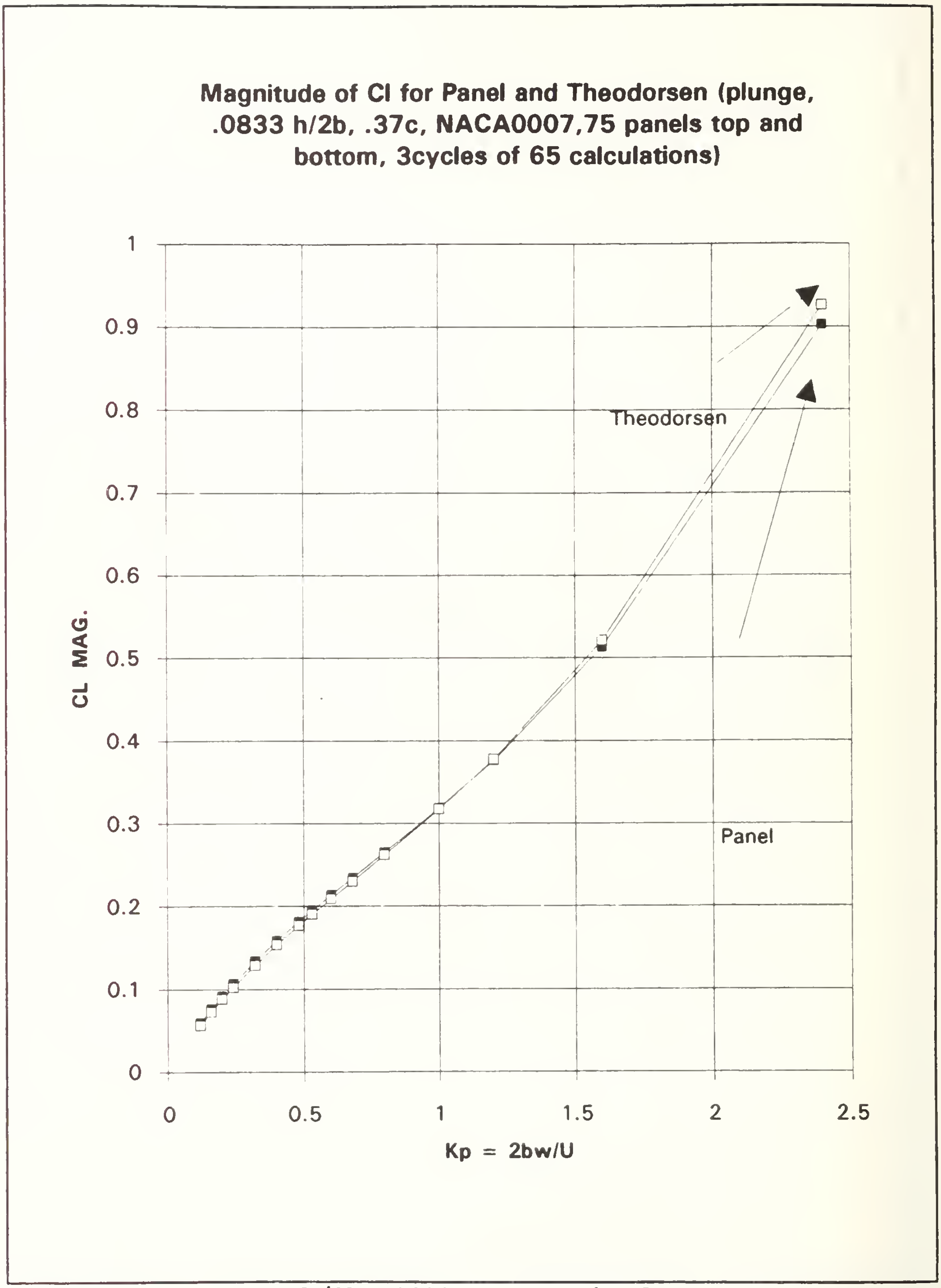

Figure 2.42 Plunge h/2b=.0833 C_L magnitude

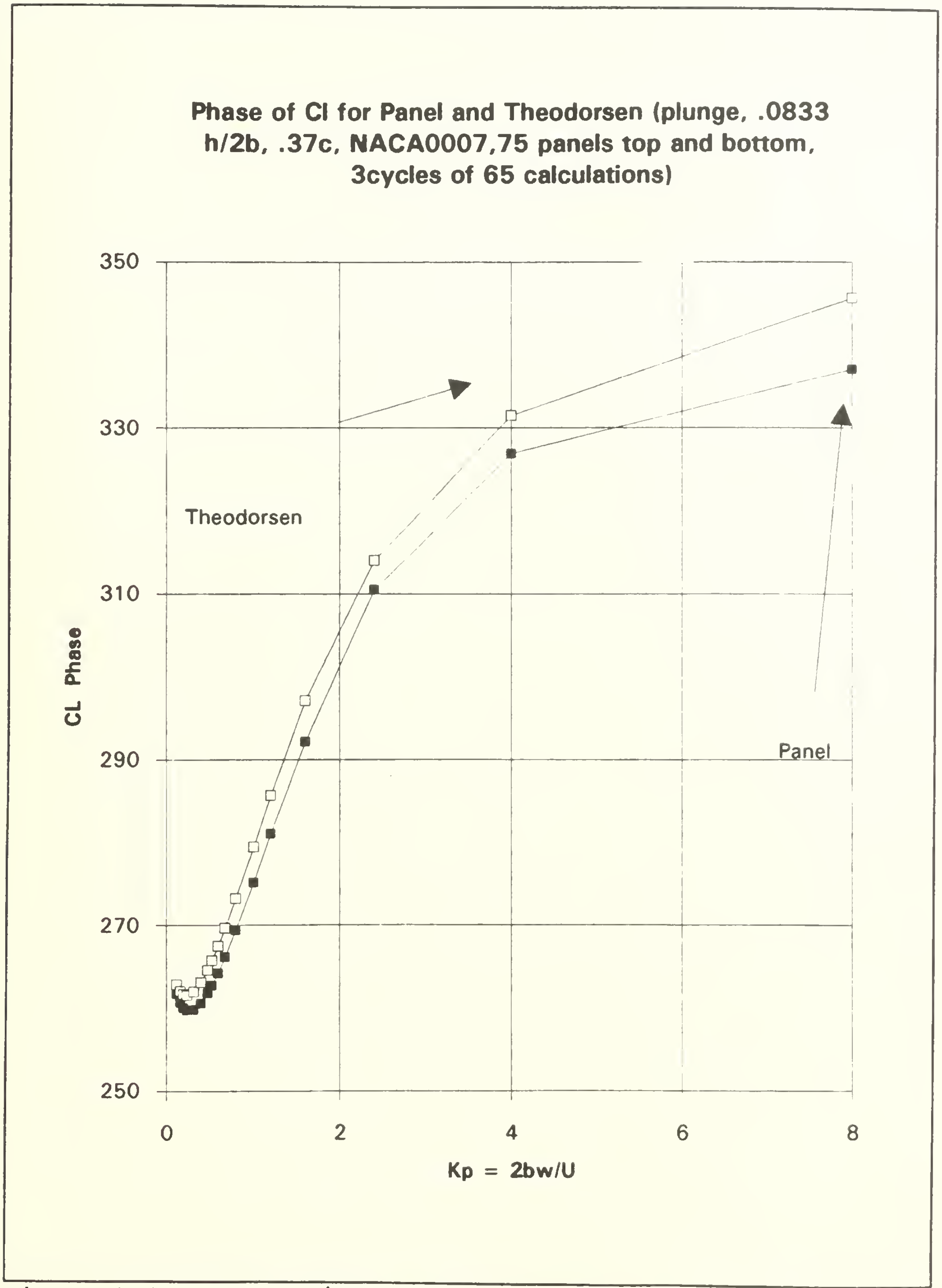

Figure 2.43 Plunge h/2b=.0833 C_L phase

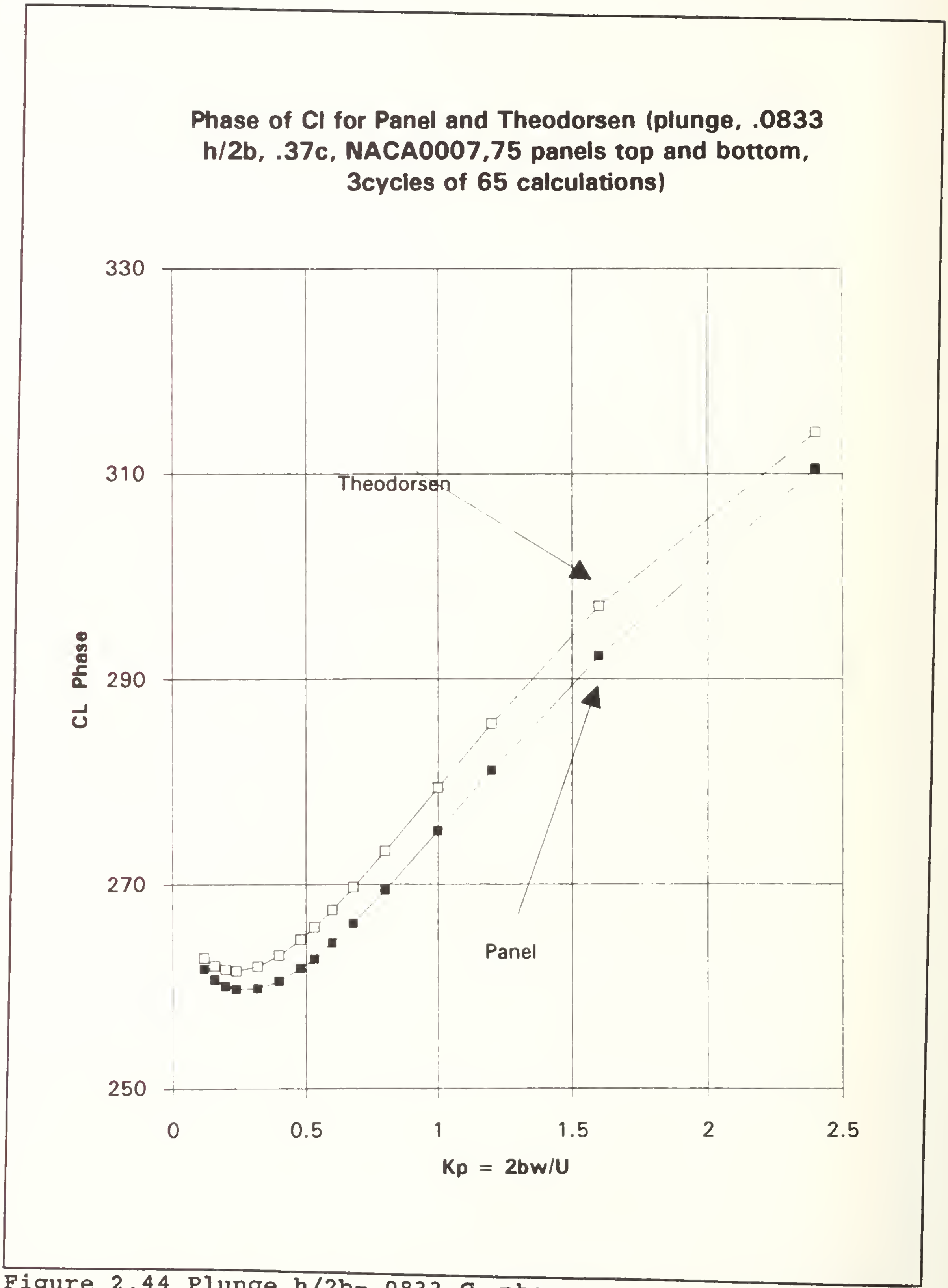

Figure 2.44 Plunge h/2b=.0833 C_L phase

			Comparison of Panel Cm Values (Plunge) with Theordorsen Results										
			(plunge .0833h/b. .37c. NACA 0007. 75 panels,3 cyc65)										
			Kpanel (equal to 2 x Theordorsen Kt)				%DIFF taken wrt Theordorsen values.						
1/kt	Kpanel	Real pan.	Real theo.	% DIFF.	Img Pan	Imag The	% DIFF.	Mag Pan.	Mag Theo.	% DIFF.	Phase Pn	Phase Th	% DIFF.
16.67	0.11998	0.00132	0.001319179	0.06%	0.00675	0.006721	0.44%	0.00687786	0.00684875	0.43%	78.9351	78.8945	0.05%
12.5	0.16	0.00202	0.00204733	1.33%	0.00865	0.008646	0.04%	0.00888273	0.00888531	0.03%	76.8555	76.6783	0.23%
10	0.2	0.00276	0.002844726	2.98%	0.01042	0.010451	0.30%	0.01077933	0.01083124	0.48%	75.1645	74.7732	0.52%
8.33	0.24	0.00354	0.00369484	4.19%	0.01209	0.012145	0.45%	0.01259761	0.01269456	0.76%	73.6798	73.0788	0.82%
6.25	0.32	0.00516	0.005512253	6.39%	0.0152	0.015331	0.85%	0.01605197	0.01629167	1.47%	71.249	70.2237	1.46%
5	0.4	0.00683	0.007459764	8.44%	0.01807	0.018279	1.14%	0.01931771	0.01974283	2.15%	69.2947	67.7996	2.21%
4.17	0.48	0.00857	0.009533759	10.11%	0.02081	0.02107	1.23%	0.02250558	0.02312655	2.69%	67.6171	65.6542	2.99%
3.75	0.53	0.0097	0.01098723	11.72%	0.02247	0.022787	1.39%	0.02447429	0.02529756	3.25%	66.6508	64.258	3.72%
3.33	0.6	0.01134	0.01287852	11.95%	0.02475	0.02506	1.24%	0.02722422	0.02817525	3.38%	65.3836	62.8008	4.11%
2.94	0.68	0.01328	0.01528568	13.10%	0.027295	0.027628	1.21%	0.03035548	0.03157482	3.86%	64.0503	61.0458	4.92%
2.5	0.8	0.01643	0.0191749	14.32%	0.03106	0.031403	1.09%	0.03513785	0.03679467	4.50%	62.1222	58.5917	6.03%
2	1	0.02232	0.026475126	15.69%	0.03722	0.037552	0.88%	0.04339943	0.04594666	5.54%	59.0498	54.8153	7.73%
1.67	1.2	0.02915	0.0348795	16.43%	0.04331	0.043623	0.72%	0.05220612	0.05585274	6.53%	56.0573	51.3552	9.16%
1.25	1.6	0.04591	0.055251155	16.91%	0.05529	0.055684	0.71%	0.07186593	0.0784436	8.39%	50.2955	45.2236	11.22%
0.83	2.4	0.09818	0.111201	11.71%	0.0800021	0.079887	0.14%	0.1266481	0.13692186	7.50%	39.1748	35.6935	9.75%
0.5	4	0.26237	0.286658	8.47%	0.1095213	0.128854	15.00%	0.28431041	0.31428687	9.54%	22.6572	24.2042	6.39%
0.25	8	1.06271	1.10392	3.73%	-0.021611	0.253136	109%	1.062926	1.1325711	6.15%	-1.165	12.915	109.02%
Values for Kp equal to 2.4.4.and 8 above were calculated using 200 panels top and bottom ad 4 cycles of 100 calculations.													
The below values were calculated using 75 panels and 3 cyc of 65 calc.													
0.83	2.4	0.09315	0.111201	16.23%	0.07777	0.079887	2.65%	0.121347	0.13692186	11.37%	39.8582	35.6935	11.67%
0.5	4	0.24712	0.28665824	13.79%	0.10401	0.128854	19.28%	0.26811635	0.31428709	14.69%	22.8257	24.2042	5.70%
0.25	8	0.9993	1.1039244	9.48%	-0.04788	0.253136	119%	1.00044639	1.13257539	11.67%	-2.7431	12.915	121.24%
Kp of 4 and 8 for CM img were redone using h/b=.01, .02,.04,.06 to better understand why the imag values became so different.													
These values of h/b were made smaller to account for the very high Kp.(NACA 0007,100 panels,3cyc65,.37c)													
h/b=.01.Imag	Imag Th.	%diff	h/b=.02.Imag p	Imag Th.	%diff		h/b=.04.Imag p	Imag Th.	%diff	h/b=.06.Imag	Imag Th.	%diff	
0.01536	0.01546	0.65%	0.0304	0.030937	1.74%		0.05862	0.06187	5.25%	0.08291	0.09281	10.67%	
0.02734	0.03039	10%	0.04886	0.060768	20%		0.06019	0.12107	50%	0.03441	0.18233	81%	

TABLE 2.7 PLUNGE h/2b=.0833 C_M COMPARISON

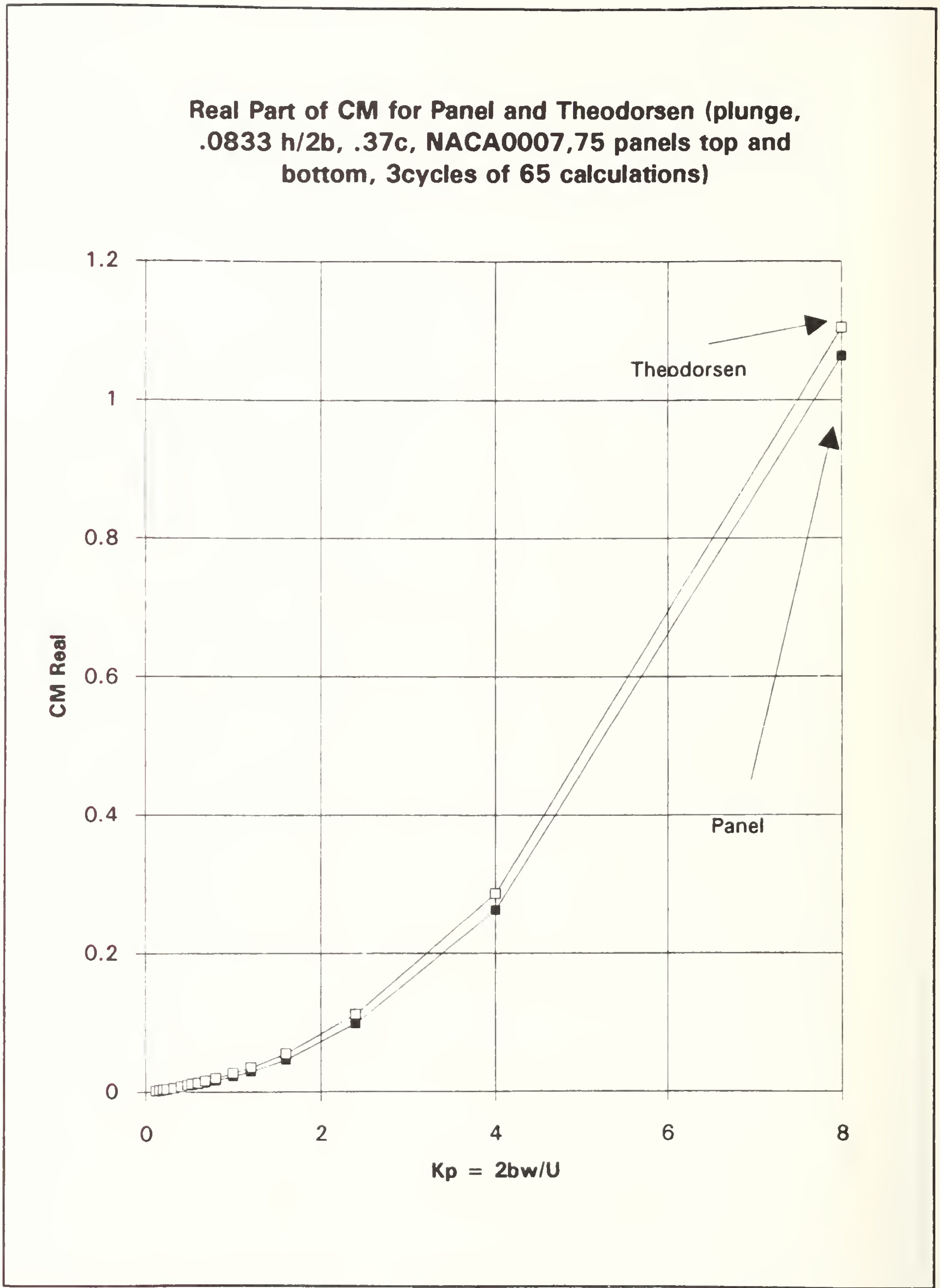

Figure 2.45 Plunge h/2b=.0833 C_M Re

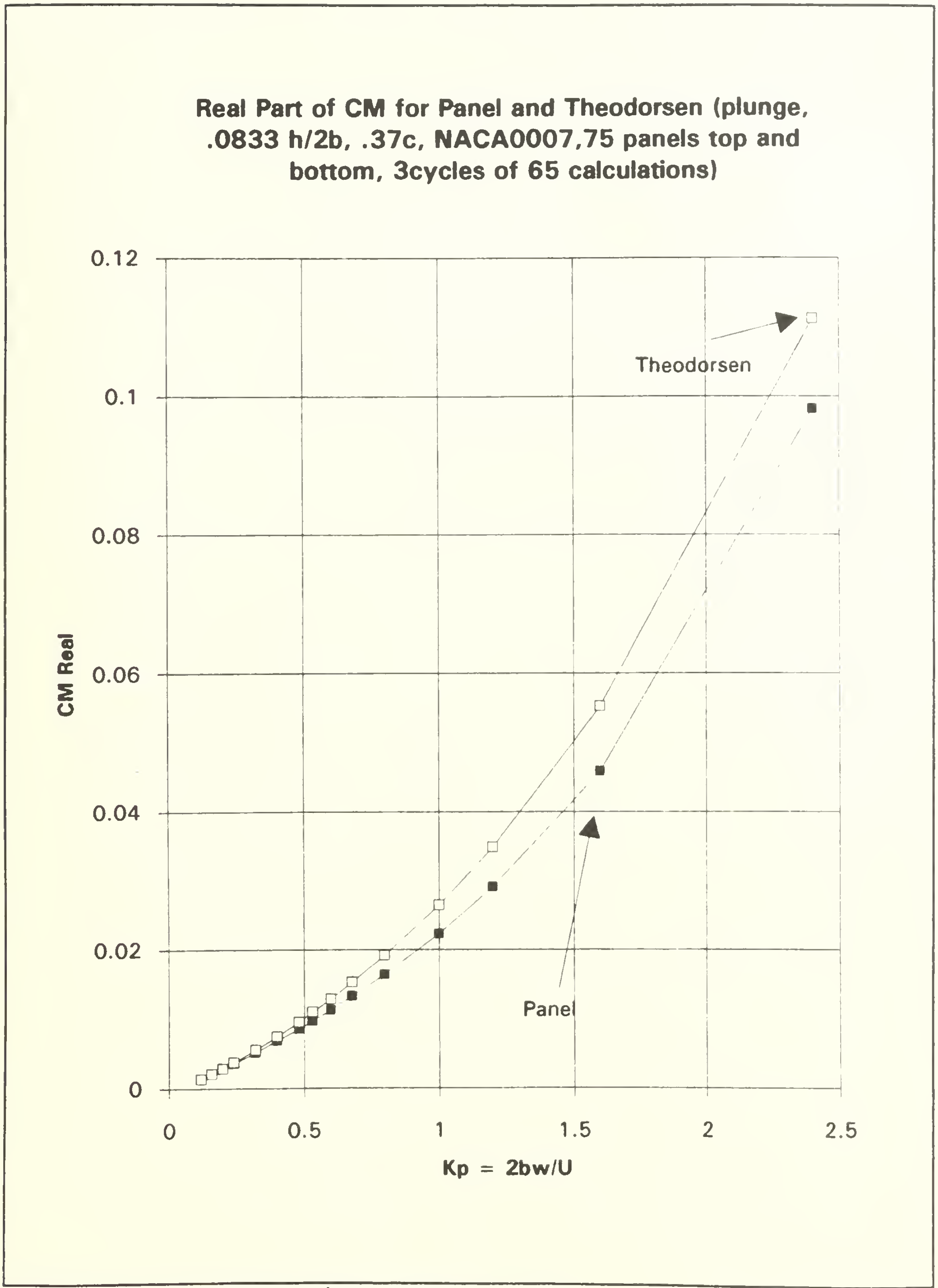

Figure 2.46 Plunge h/2b=.0833 C_M Re

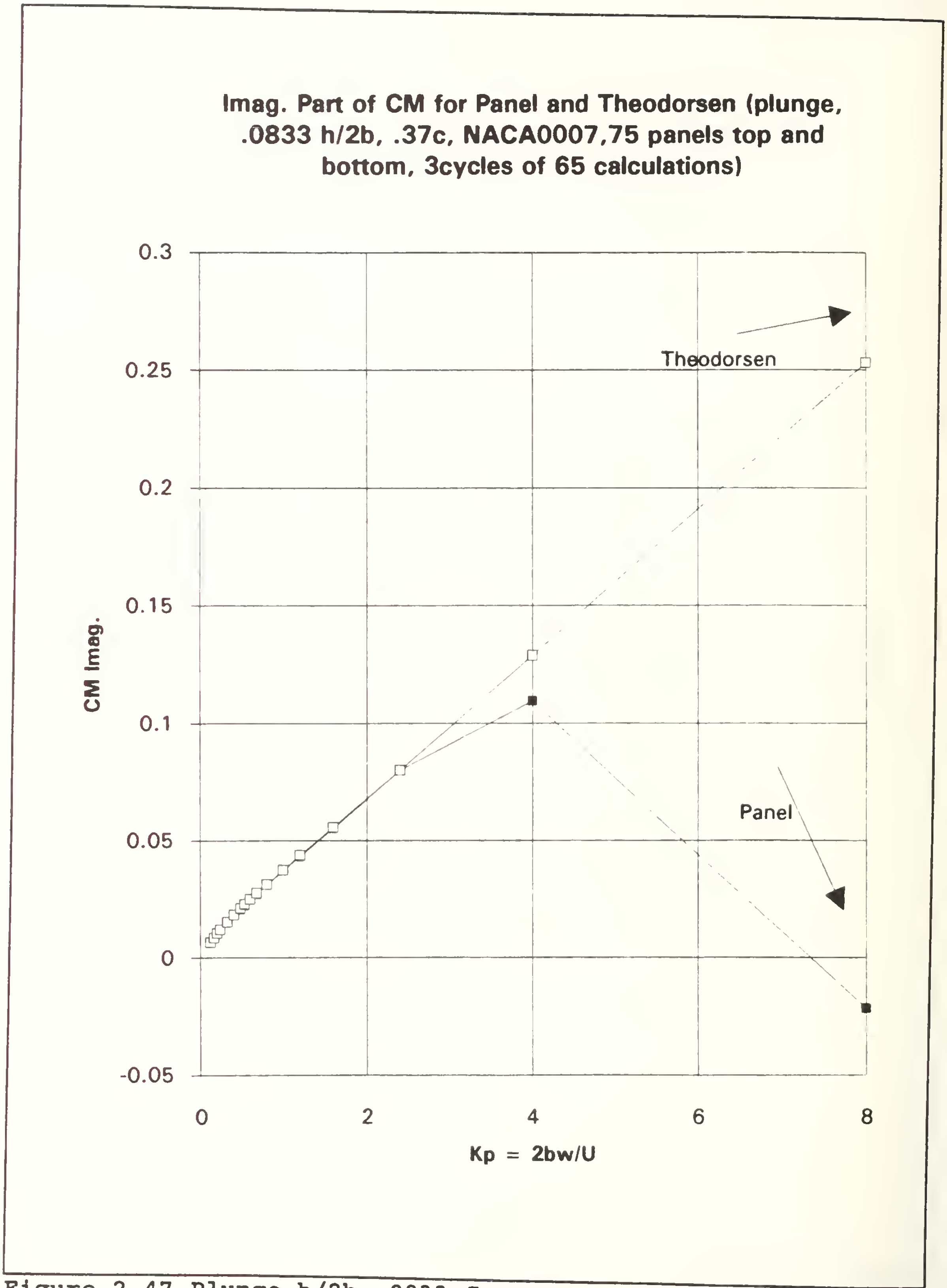

Figure 2.47 Plunge h/2b=.0833 C_M Im

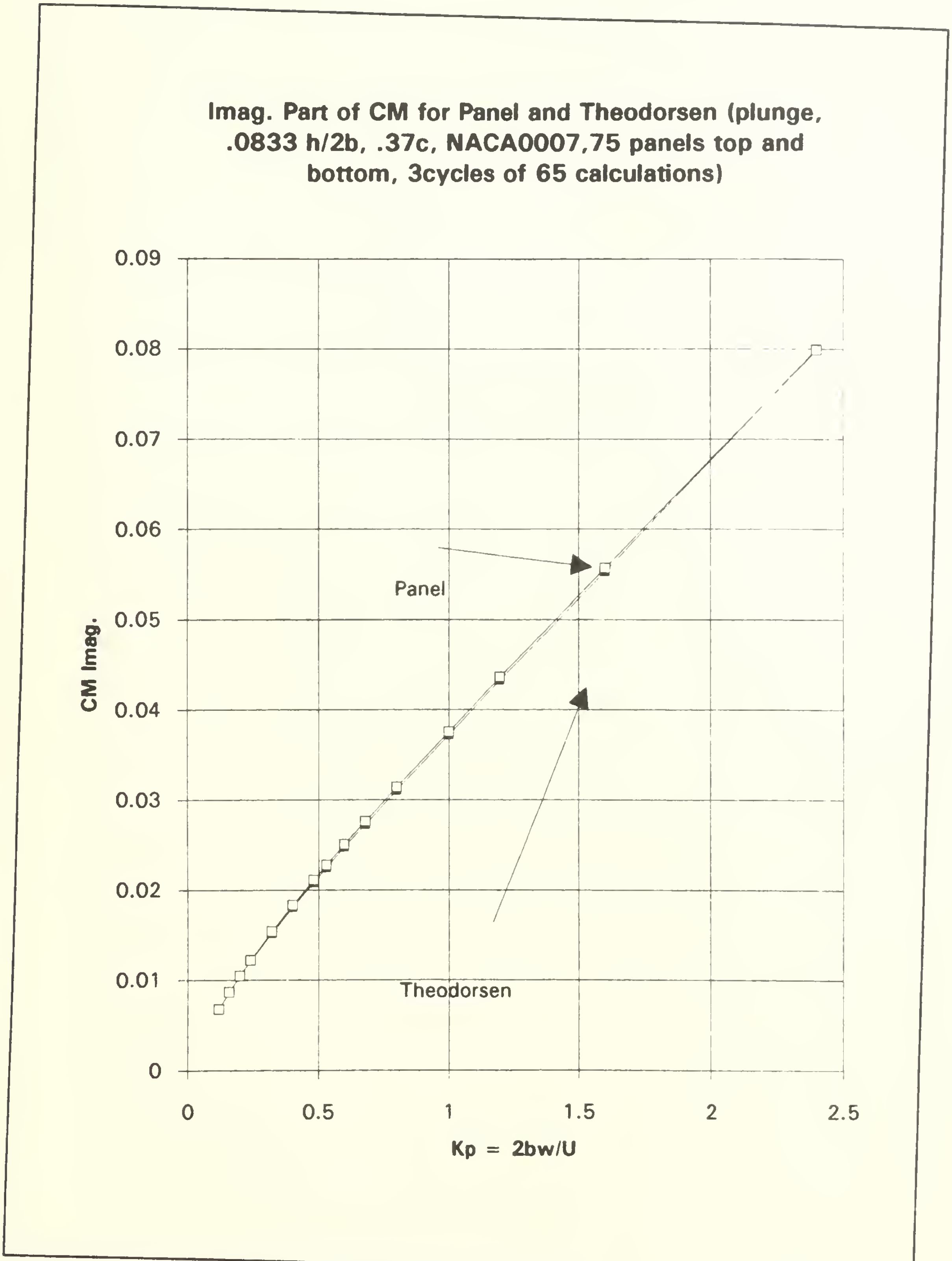

Figure 2.48 Plunge h/2b=.0833 C_M Im

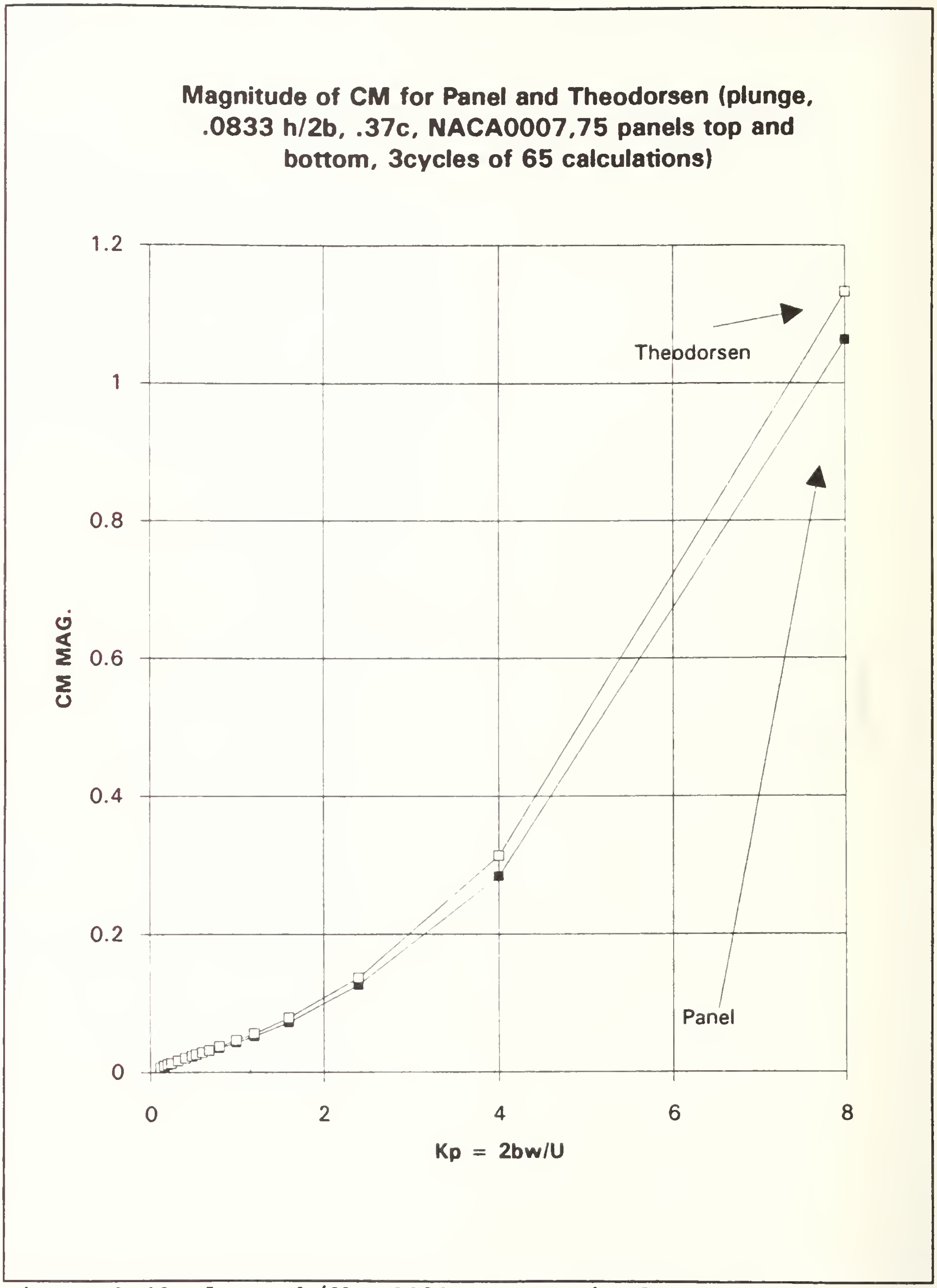

Figure 2.49 Plunge h/2b=.0833 C_M Magnitude

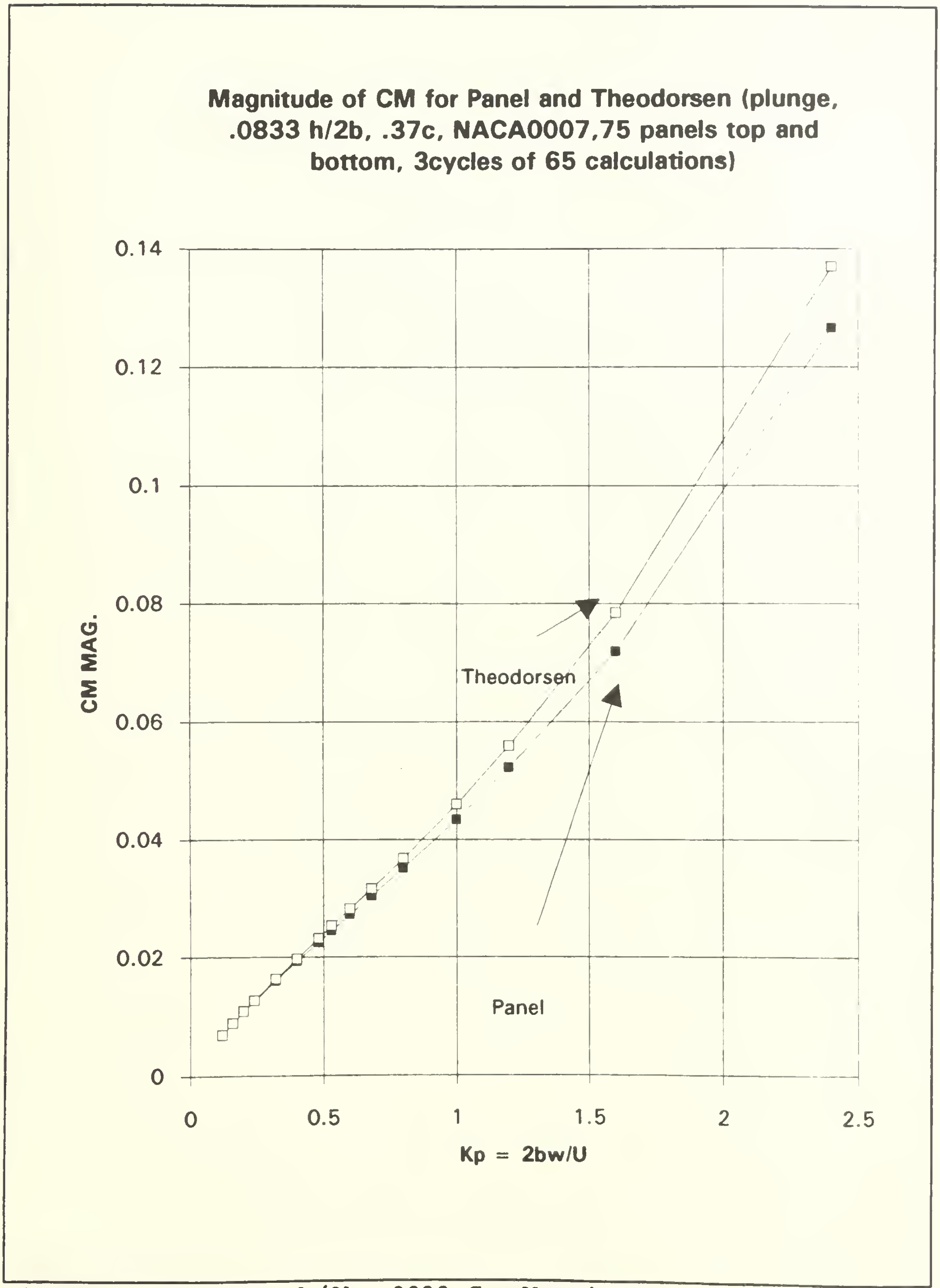

Figure 2.50 Plunge h/2b=.0833 C_M Magnitude

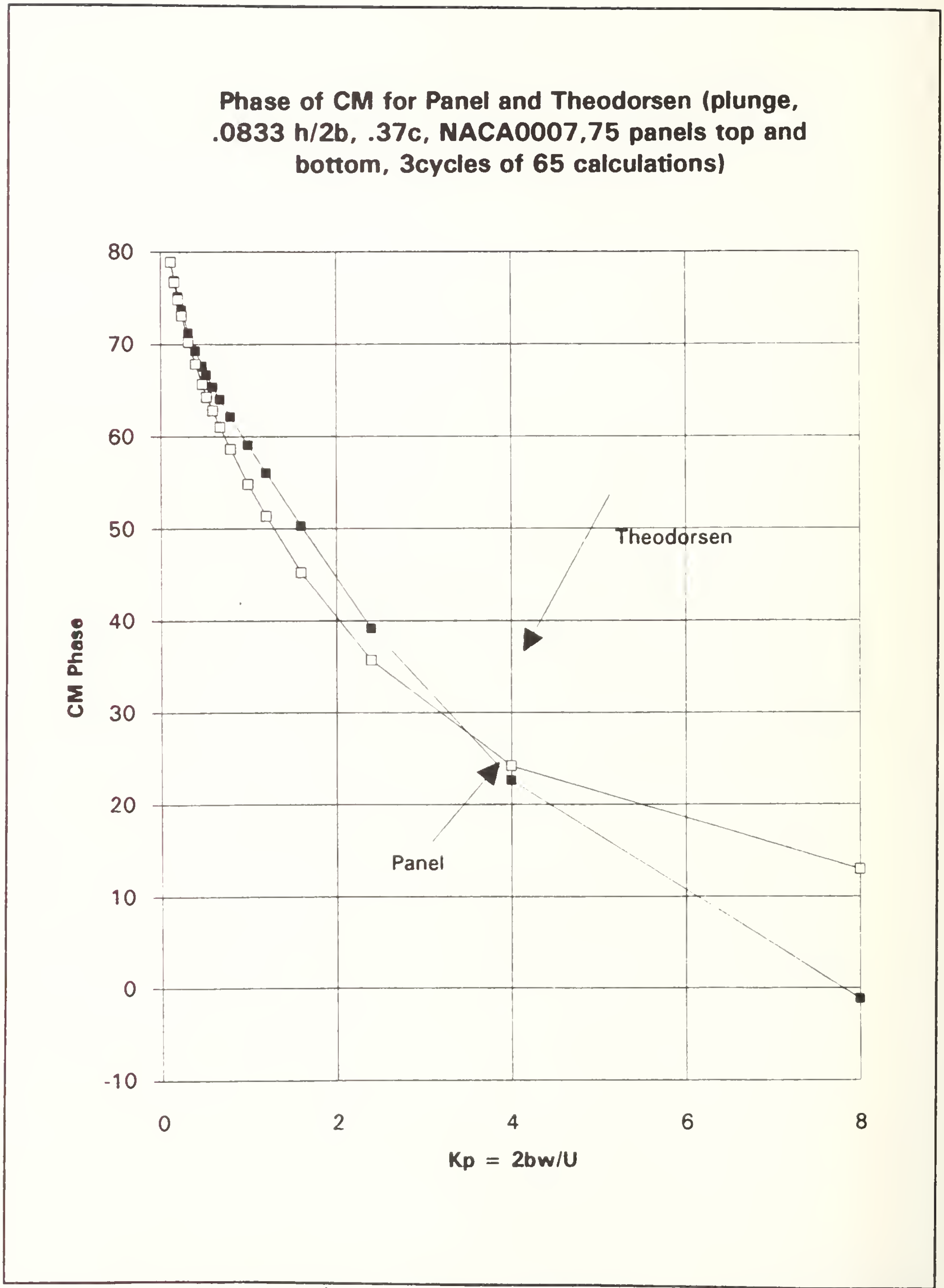

Figure 2.51 Plunge h/2b=.0833 C_M Phase

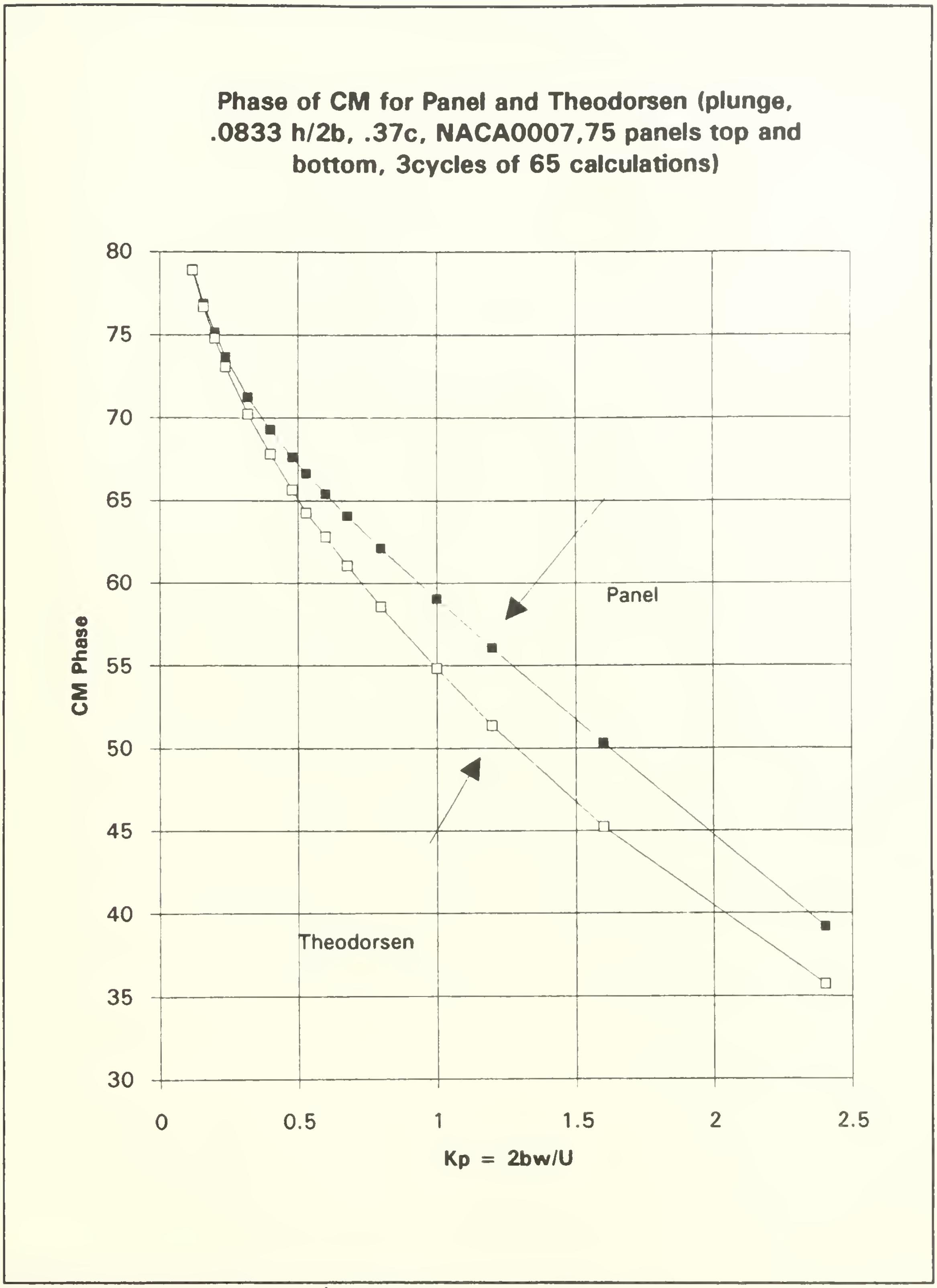

Figure 2.52 Plunge h/2b=.0833 C_M Phase

			Comparison of Panel Cm Values (Plunge) with Theordorsen Results										
			(plunge .01 h/2b, .37c, NACA 0007, 100 panels,3 cyc85)										
			Kpanel (equal to 2 x Theordorsen Kt)				%DIFF taken wrt Theordorsen values.						
1/kt	Kpanel	Real pan.	Real theo.	% DIFF.	Img Pan	Imag Theo.	% DIFF.	Mag Pan.	Mag Theo.	% DIFF.	Phase Pn.	Phase T	% DIFF.
18.67	0.11998	0.00016	0.000158365	1.03%	0.00061	0.00080678	0.40%	0.000826	0.000822	0.42%	78.828182	78.89	0.09%
12.5	0.18	0.00001	0.000245778	95.93%	0.00001	0.00103796	99.04%	1.41E-05	0.001067	98.87%	45	78.68	41.31%
10	0.2	0.00033	0.000341504	3.37%	0.00125	0.00125462	0.37%	0.001293	0.0013	0.57%	75.211322	74.77	0.59%
8.33	0.24	0.00043	0.000443558	3.08%	0.00145	0.00145798	0.55%	0.001512	0.001524	0.78%	73.482186	73.08	0.55%
6.25	0.32	0.00063	0.000661735	4.80%	0.00183	0.00184043	0.57%	0.001935	0.001958	1.04%	71.003346	70.22	1.11%
5	0.4	0.00083	0.00089553	7.32%	0.00216	0.00219439	1.57%	0.002314	0.00237	2.37%	68.980266	67.8	1.74%
4.17	0.48	0.00104	0.001144509	9.13%	0.00249	0.00252941	1.58%	0.002698	0.002778	2.80%	67.331136	65.65	2.55%
3.75	0.53	0.00117	0.001318995	11.30%	0.00269	0.00273553	1.68%	0.002933	0.003037	3.41%	66.493646	64.26	3.48%
3.33	0.8	0.00137	0.001546041	11.39%	0.00296	0.00300837	1.61%	0.003262	0.003382	3.57%	65.183516	62.8	3.78%
2.94	0.88	0.00181	0.001635018	12.26%	0.00327	0.00331871	1.41%	0.003645	0.00379	3.84%	63.786452	61.05	4.49%
2.5	0.8	0.001991	0.002301909	13.50%	0.00372	0.00376991	1.37%	0.004216	0.004417	4.51%	61.83111	58.59	5.53%
2	1	0.002704	0.003178288	14.93%	0.00446	0.00450806	1.05%	0.005216	0.005516	5.43%	58.77642	54.82	7.23%
1.87	1.2	0.00353	0.004187215	15.70%	0.0052	0.00523683	0.73%	0.006284	0.006705	6.28%	55.82521	51.36	8.70%
1.25	1.8	0.005553	0.006832792	16.28%	0.00887	0.00868475	0.19%	0.00868	0.009417	7.82%	50.22754	45.22	11.08%
0.83	2.4	0.011207	0.01334948	18.05%	0.00981	0.00959028	0.25%	0.014786	0.016437	10.17%	40.82597	35.89	13.82%
0.5	4	0.029326	0.034412725	14.78%	0.01536	0.0154887	0.71%	0.033104	0.03773	12.28%	27.6416	24.2	14.20%
0.25	8	0.115247	0.132523409	13.04%	0.02734	0.0303885	10.02%	0.118447	0.135963	12.88%	13.34668	12.92	3.34%

TABLE 2.8 PLUNGE h/2b=.01 C_M COMPARISON

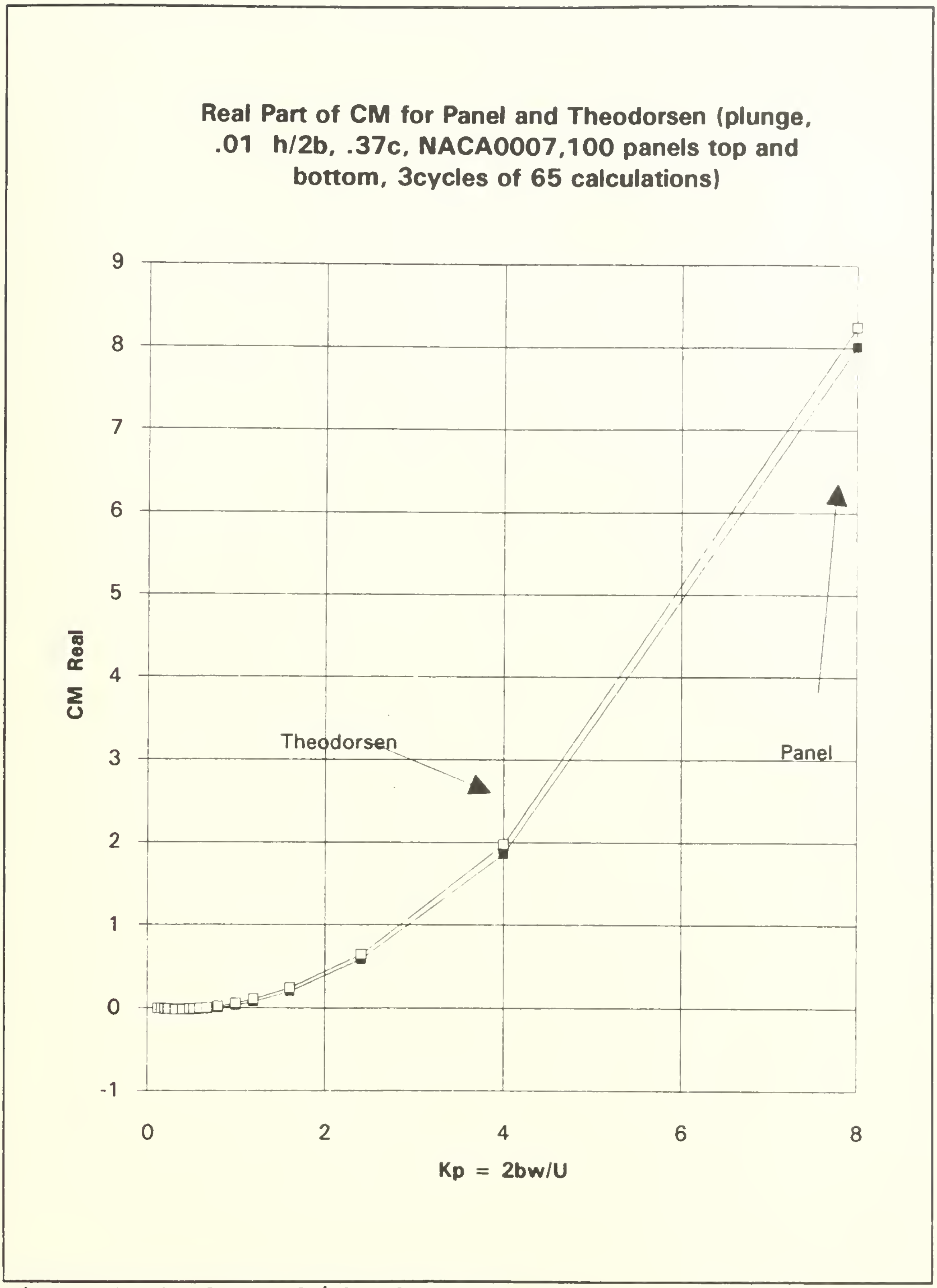

Figure 2.53 Plunge h/2b=.01 C_M Re

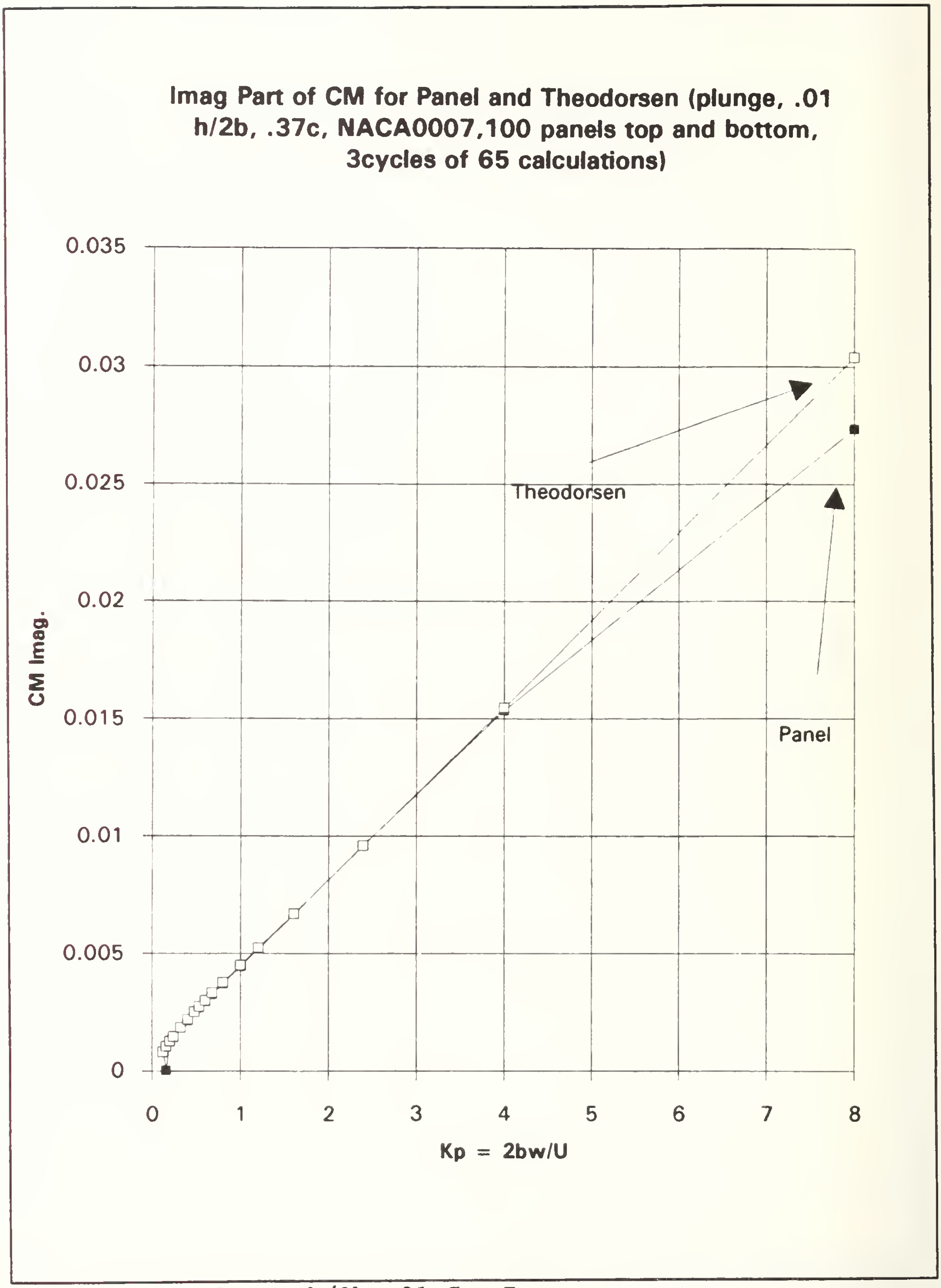

Figure 2.54 Plunge h/2b=.01 C_M Im

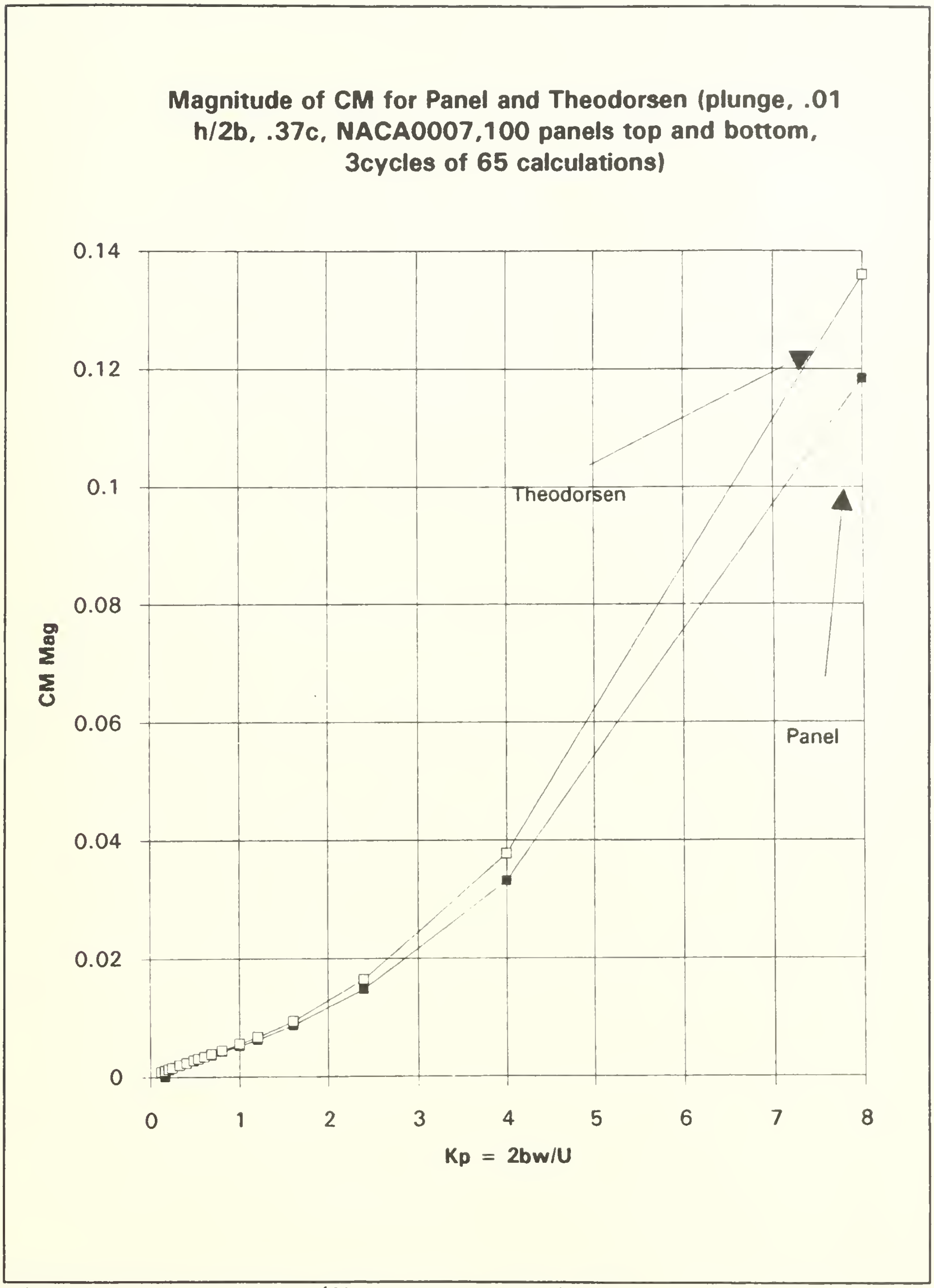

Figure 2.55 Plunge h/2b=.01 C_M Magnitude

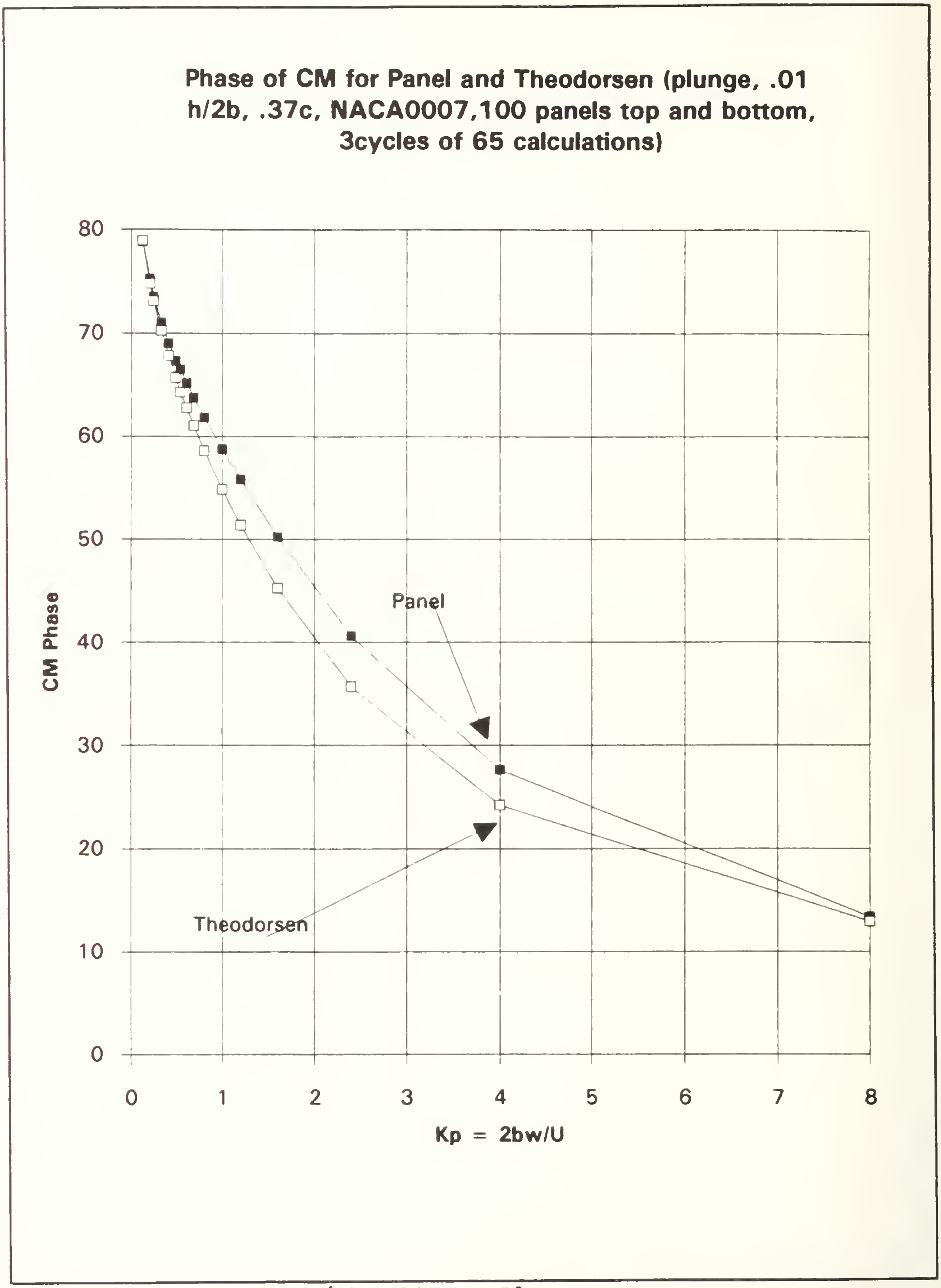

Figure 2.56 Plunge h/2b=.01 C_M Phase

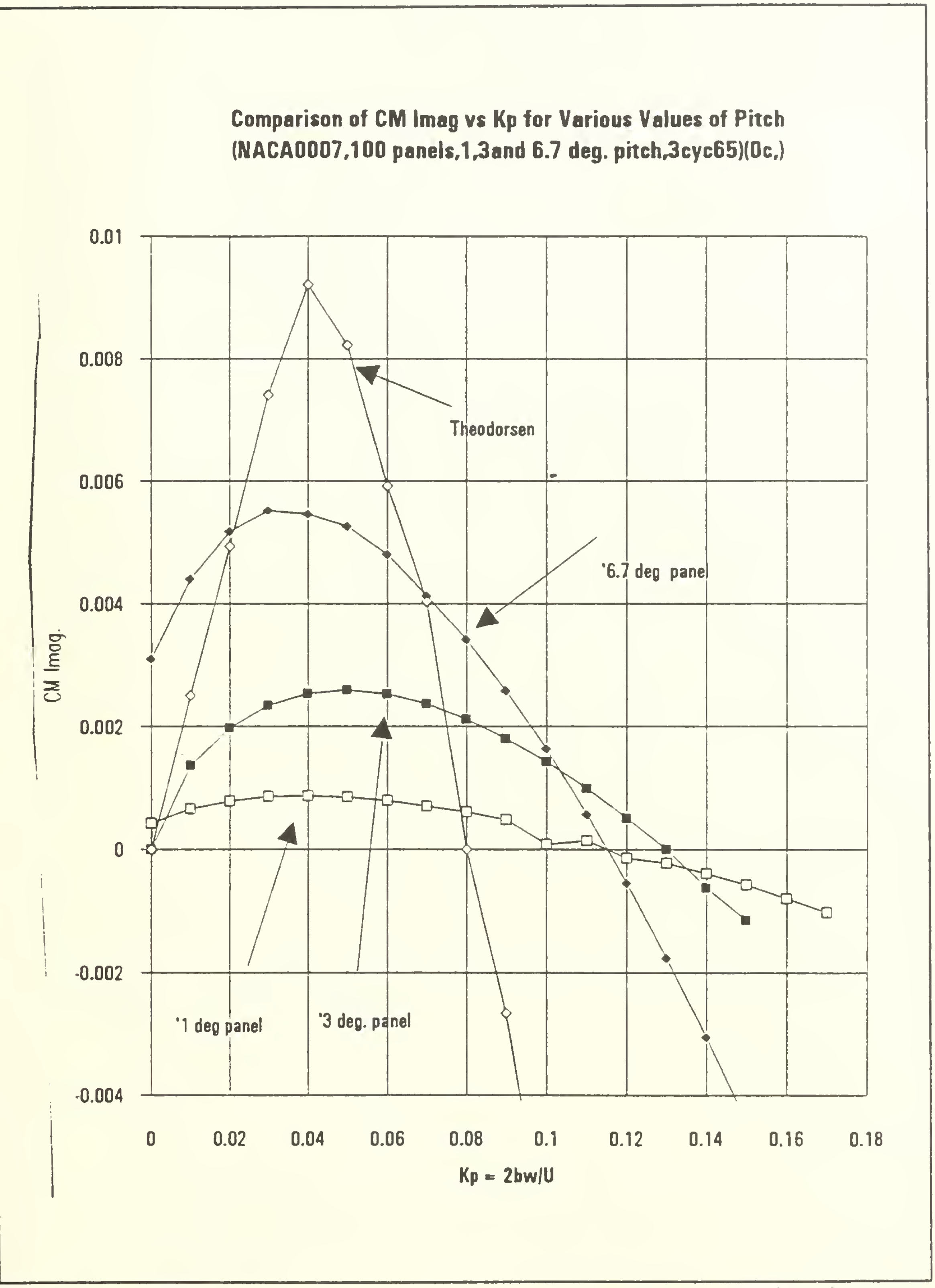

Figure 2.57 Pitch 0c. 1.0,3.0,and 6.7 degrees vs Theodorsen

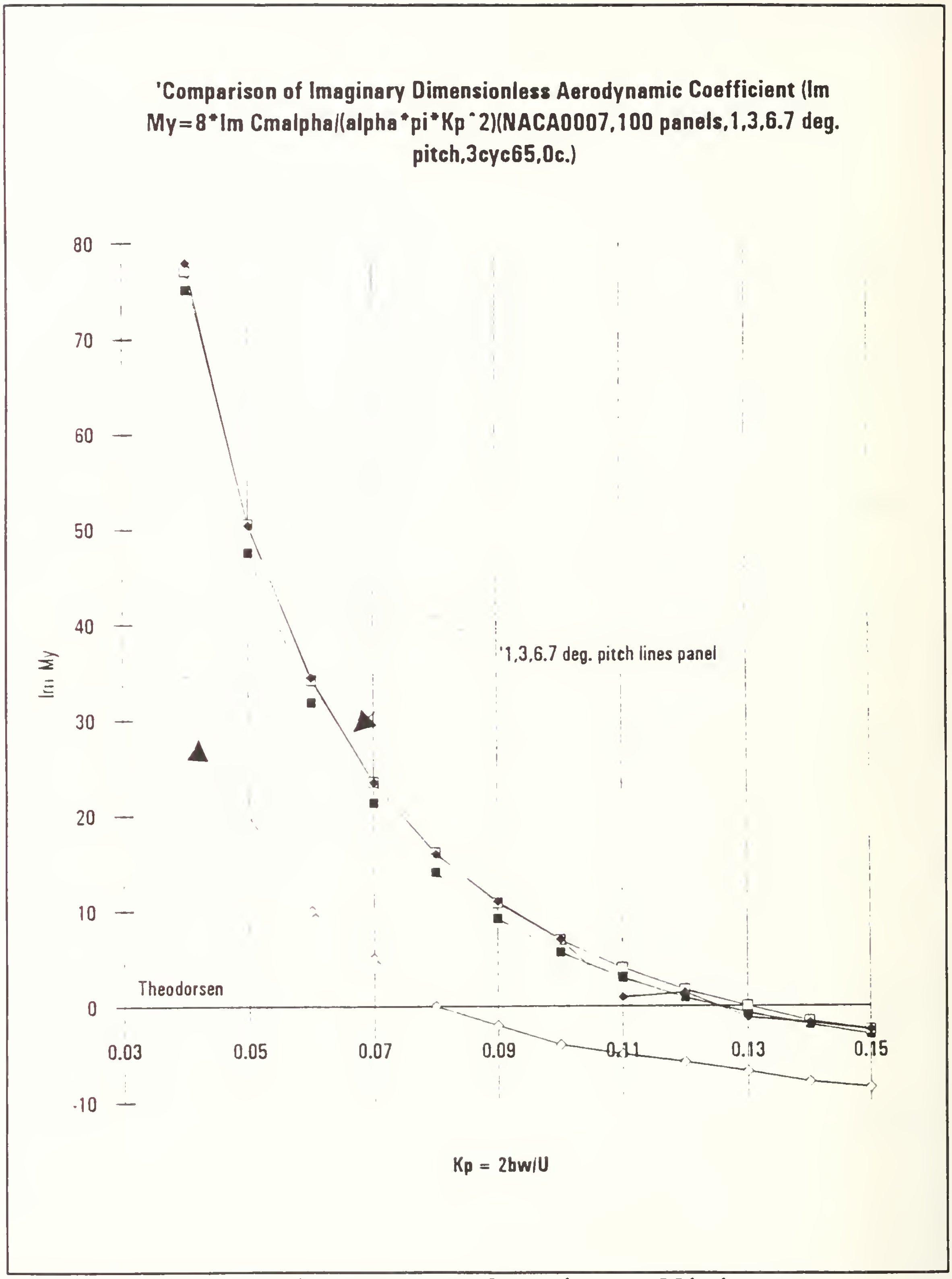

Figure 2.58 Dimensionless Aerodynamic Coefficient for 1.0,3.0,and 6.7 degrees

III. FLUTTER DETERMINANT

The proven accuracy of the UPOT Code enabled it to be used for the solution of the flutter determinant.

A. FLUTTER THEORY

In order to analyze the phenomenon of flutter, it is necessary to obtain the equations of motion of the system. To simplify the problem the assumption is made that the actual motion of the system can be considered a combination of fundamental wing bending, and fundamental wing torsion. The system can then be replaced by an equivalent system containing an airfoil section of unit span restrained by springs against independent vertical motion (bending),and torsion as illustrated in Figure 3.1. This paper will not consider the aileron hinge case so ß and c are set equal to zero. According to the class notes of M. Platzer [ref.1] the formulation proceeds as follows:

Consider the balance of the elastic, inertial and aerodynamic forces on a mass element:

- Total Inertial force: $-\int dm(h''+r\alpha'')=-(Mh''+S_\alpha\alpha'')$
  Mass: $M=\int dm$
  Static Moment about the elastic axis: $S_\alpha = \int rdm$
- The moments about the elastic axis are:

$$-\int r(h''+r\alpha'')\,dm = -(I_\alpha\alpha''+S_\alpha h'') \tag{3.1}$$

Mass moment of inertia about elastic axis

$$I_\alpha = \int r^2 dm$$

- Elastic restoring forces are: $-hC_h$ $-\alpha C_\alpha$

The Equations of motion therefore become:

$$\begin{aligned} h''M+\alpha''S_\alpha+hC_h &= L \\ \alpha''I_\alpha+h''S_\alpha+\alpha C_\alpha &= M \end{aligned} \tag{3.2}$$

Where: C_α = Torsional stiffness of the wing

C_h = Stiffness of the wing in translation (plunge)

M = Mass of the wing per unit span

These equations can be written in a different way by expressing the spring constants in terms of the natural frequencies. Consider the airfoil to be so restrained that only one degree of freedom is permitted. The equations of motion become:

$$\begin{aligned} Mh''+hC_h &= 0 \quad \text{so that} \quad \omega_h = \sqrt{\frac{C_h}{M}} \\ I_\alpha\alpha''I_\alpha+\alpha C_\alpha &= 0 \quad \text{so that} \quad \omega_h = \sqrt{\frac{C_\alpha}{I_\alpha}} \end{aligned} \tag{3.3}$$

Hence: $C_h = M\omega_h^2$ $C_\alpha = I_\alpha\omega_\alpha^2$

The small structural damping of metal aircraft may be approximated by a force that opposes the motion and is in phase with the velocity. One assumes therefore that the

magnitude of the damping is proportional to the elastic restoring force. Since the motion of the airfoil is harmonic at the critical flutter condition, the structural damping can be accounted for by replacing the terms:

hC_h with $hC_h(1+ig_h)$

αC_α with $\alpha C_\alpha(1+ig_\alpha)$

Where g_h and g_α are damping constants multiplied by i to ensure that the damping force is in phase with the velocities in the simple harmonic motion.

From equation 3.3 with:

$h(t) = he^{i\omega t}$ and $\alpha(t) = \alpha e^{i\omega t}$

We have:

$h'' = \omega^2 he^{i\omega t}$ and $\alpha'' = -\omega^2 \alpha e^{i\omega t}$

And the equations of motion become:

$$e^{i\omega t}(-\omega^2 hM-\omega^2\alpha S_\alpha+hC_h) = L \qquad (3.4)$$

$$e^{i\omega t}(-\omega^2\alpha I_\alpha-\omega^2 hS_\alpha+\alpha C_\alpha) = M \qquad (3.5)$$

The equations for the aerodynamic forces were given by Fung [ref.5] and are shown here:

$$L=\pi\rho b^3\omega^2(L_h\frac{h}{b}+[L_\alpha-(\frac{1}{2}+a)L_h]\alpha)e^{i\omega t} \qquad (3.6)$$

Equating equation 3.4 to 3.6 and 3.5 to 3.7 yields:

Substituting into equation 3.8 and 3.9 for C_h and C_α and using the following dimensional terms:

$$M=\pi\rho b^4\omega^2\left([M_h-(\frac{1}{2}+a)L_h]\frac{h}{b}+\right.$$
$$\left.[M_\alpha-(\frac{1}{2}+a)(L_\alpha+M_h)+(\frac{1}{2}+a)^2L_h]\alpha\right)e^{i\omega t} \tag{3.7}$$

$$(-\omega^2Mh-\omega^2\alpha S_\alpha+hC_h)=\pi\rho b^3\omega^2\left(L_h\frac{h}{b}+[L_\alpha-(\frac{1}{2}+a)L_h]\alpha\right) \tag{3.8}$$

$$(-\omega^2\alpha I_\alpha-\omega^2hS_\alpha+\alpha C_\alpha)=\pi\rho b^4\omega^2\left([M_h-(\frac{1}{2}+a)L_h]\frac{h}{b}+\right.$$
$$\left.[M_\alpha-(\frac{1}{2}+a)(L_\alpha+M_h)+(\frac{1}{2}+a)^2L_h]\alpha\right) \tag{3.9}$$

$$\mu=\frac{M}{\pi\rho b^2} \qquad x_\alpha=\frac{S_\alpha}{Mb} \qquad r_\alpha=\sqrt{\frac{I_\alpha}{Mb^2}} \tag{3.10}$$

The equations simplify and after bringing all terms to the left result in:

$$A\frac{h}{b}+B\alpha=0$$
$$D\frac{h}{b}+E\alpha=0 \tag{3.11}$$

This is a homogeneous equation whose solution is obtained if the flutter determinant is zero.

$$\begin{bmatrix} A & B \\ D & E \end{bmatrix}=0 \tag{3.12}$$

Where:

$$A=\mu[1-(\frac{\omega_\alpha}{\omega})^2(\frac{\omega h}{\omega_\alpha})^2(1+ig_h)]+L_h$$

$$B=\mu X_\alpha+L_\alpha-L_h(½+a)$$

$$D=\mu x_\alpha+½-L_h(½+a) \qquad (3.13)$$

$$E=\mu r_\alpha{}^2[1-(\frac{\omega_\alpha}{\omega})^2(1+ig_\alpha)]-½(½+a)+M_\alpha-L_\alpha(½+a)+L_h(½+a)^2$$

μ is the ratio of the mass of the wing to the mass of a cylinder of air of a diameter equal to the chord of the wing. ω_α and ω_h are the natural angular frequency (rad/sec) of torsional vibration around "a" (elastic axis) and the natural frequency in deflection, respectively. x_α is the location of center of gravity of the wing measured from a. ω is the circular frequency of wing vibration.

The relationships between the code and Theodorsen derived earlier in Chapter II can be used here to simplify the equations: (note: no damping in this case $g_\alpha=g_h=0$)

For A: manipulating equation 2.20,

$$L_h=\frac{2C_{Lh}}{\pi K_p^2(\frac{h}{2b})} \qquad (3.14)$$

resulting in:

$$A=\mu[1-(\frac{\omega_\alpha}{\omega})^2(\frac{\omega h}{\omega_\alpha})^2]+\frac{2C_{L\alpha}}{\pi K_p^2(\frac{h}{2b})} \qquad (3.15)$$

For B: manipulating equation 2.14,

$$L_\alpha - L_h(\tfrac{1}{2}+a) = \frac{4C_{L\alpha}}{\pi K_p^2 \alpha} \tag{3.16}$$

resulting in:

$$B = \mu x_\alpha + \frac{4C_{L\alpha}}{\pi K_p^2 \alpha} \tag{3.17}$$

For D: manipulating equation 2.28

$$L_\alpha - L_h(\tfrac{1}{2}+a) = \frac{4C_{Mh}}{\pi K_p^2 (\frac{h}{2b})} \tag{3.18}$$

resulting in:

$$D = \mu x_\alpha + \frac{4C_{Mh}}{\pi K_p^2 (\frac{h}{2b})} \tag{3.19}$$

For E: manipulating equation 2.24

$$-\tfrac{1}{2}(\tfrac{1}{2}+a) + M_\alpha - L_\alpha(\tfrac{1}{2}+a) + L_h(\tfrac{1}{2}+a)^2 = \frac{8C_{M\alpha}}{\alpha \pi K_p^2} \tag{3.20}$$

resulting in:

$$E = \mu r_\alpha^2 [1 - (\frac{\omega_\alpha}{\omega})^2] + \frac{8C_{M\alpha}}{\alpha \pi K_p^2} \tag{3.21}$$

The determinant is expanded to AE-BD=0, and the real and imaginary parts are set equal to zero. Substituting $(\omega_\alpha/\omega)^2 =$ X and solving the real (2 roots) and imaginary (1 root) equations for values of X corresponding to each reduced frequency value. These X values can be plotted as SQRT(X)

against K_p and any intersections of real and imaginary parts signify a flutter point.

Knowing that :

$$K_p = \frac{2b\omega}{U} \qquad and \qquad \sqrt{X} = \left(\frac{\omega_\alpha}{\omega}\right) \tag{3.22}$$

solve for $U_{critical}$

$$U_{critical} = \frac{2b\omega_\alpha}{K_p\sqrt{X}} \tag{3.23}$$

which is the critical flutter speed.

B. UPOTFLUT CODE

1. FORMULATION AND INPUT

The equations derived in the flutter theory section above were programmed into a FORTRAN subroutine and attached to the UPOT.f code. The UPOT code was modified first to enable it to conduct a frequency sweep of pitch and plunge simultaneously. The resulting frequency sweep pitch and plunge array data is then sent to the flutter subroutine which provides the values of SQRT(x) and K_p for plotting. The program also gives a best guess for the $U_{critical}$ based on the difference betweeen the real and imaginary SQRT (X) values. The input file UPOTFLUT.IN is very similar to the regular UPOT.IN file with the addition of actual physical properties of the system being analyzed. The user should start the

analysis in the pitch mode first (IOSCIL =1, ITRANS =0) to ensure complete coverage of all frequencies of interest. The following relations were taken from NACA TR-685 [ref.8] and should prove helpful in determining the physical properties needed for program operation.

κ = mass ratio = $\pi \rho b^2/M$

$\kappa = 1/\mu$

$x_\alpha = S_\alpha/Mb$

$r_\alpha{}^2 = I_\alpha/Mb^2$

2. OUTPUT

Outputs from the code have been limited to reduce the amount of computer space taken up by the code operation. A sample input and output file are contained in Figure 3.2. The following list describes the input/output files and the data they contain:

a. UPOTFLUT.IN The input file figure 3.2a

b. CL.d Same as UPOT.f output

c. CM.d Same as UPOT.f output

d. PHASE.d Same as UPOT.f output

e. CPSS.d Same as UPOT.f output

f. CPU005.d Same as UPOT.f output

g. PHZSWP.d This file contains $K_p, \phi_L, \phi_M, C_{L\alpha}, C_{M\alpha}$

h. PLHZSWP.d This file contains $K_p, \phi_L \phi_M, C_{Lh}, C_{Mh}$

i. PITCH.in This file contains K_p , $C_{L\alpha}$ Re, $C_{L\alpha}$ Im, $C_{M\alpha}$ Re, $C_{M\alpha}$N Im

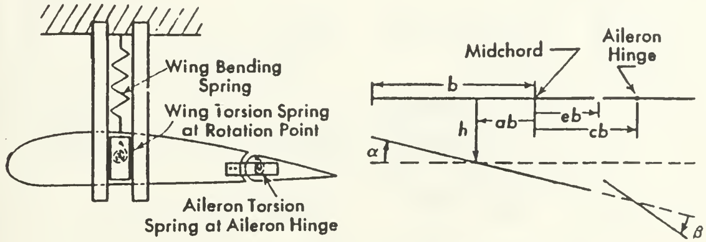

b = semichord (ft.)
cb = distance between midchord and aileron hinge, positive if aft of midchord (ft.)
eb = distance between midchord and aileron leading edge, positive aft of midchord (ft.)
ab = distance between rotation point (elastic axis) and midchord, positive if aft of midchord (ft.)
h = bending deflection of rotation point (elastic axis), positive downward (ft.)
α = angular deflection about rotation point (elastic axis), positive for leading edge up (radians)
β = angular deflection of aileron about aileron hinge relative to wing chord, positive for aileron leading edge up (radians)

Figure 3.1 Simplified System Geometry

```
stdin                                                    Page 1

  4
*****************************************************************
      AIRFOIL TYPE : NACA 0012 AIRFOIL
      NLOWER = 50 , NUPPER = 50
*****************************************************************
 IFLAG  NLOWER  NUPPER
 0        50    50
 AIRFOIL TYPE
  7
 IRAMP  IOSCIL   ALPI     ALPMAX       PIVOT
   0      1     -3.0      3.0          0.3
 FREQ   RFQSTP  RFQFNL
  .85     .01     .95
 IGUST  UGUST   VGUST
   0     0.      0.
 ITRANS  DELHX  DELHY  DELI  PHASE
   0    0.00   .0833  -.0833  0.00
 CYCLE  NTCYCLE      TOL
  3      65       0.005
 naot &  naot X aoa values multiplied by 10 (integer)
  2      05 10  20 25 39 50
 Semi-chord  Walpha   Wh     Mass
  6          90      72.0    .53789
 Ialpha     Salpha  Density
 4.84102    .645468   .002378
Comments...

IRAMP  0: n/a              RFREQ is based on full chord
       1: Straight ramp
       2: Modified ramp

IOSCIL 0: n/a              RFREQ is based on full chord
       1: Sinusoidal pitch, motion starts at min Aoa

ITRANS 0: n/a
       1: Translational harmonic oscillation

CYCLE  : # of cycles for oscillatory motions
        -In case of ramp, cycle=1.5 denotes airfoil is held
         at max aoa for the duration of .5 cycle
        -For steady state solution set it to 0

NTCYCLE: # of time steps for each cycle
          CYCLE*NTCYCLE is limited to 200 currently.

NAOT: # of input aoa for cp output
       - angles should be in increasing order,
       - for oscilatory motions angles should increase
         first, then decrease. Decreasing angles are for
         the return cycle..

SEMI-CHORD Half Chord in feet.

Walpha,Wh, uncoupled natural frequencies of the system in question.
           Walpha is pitch and Wh is plunge(HZ).

Mass       specific mass of the system in slugs/foot of span

Ialpha     Moment of Inertia of system about the elastic axis(a)
           per unit span length.
Salpha     Static moment of wing-aileron per unit span length

Density    Mass of air per unit of volume(slugs per ft^3)
```

Figure 3.2a UPOTFLUT.in example input file

```
stdin                                                          Page 1

    *************************************************************
         AIRFOIL TYPE : NACA 0012 AIRFOIL
         NLOWER = 50 , NUPPER = 50
    *************************************************************
 OSCILLATORY MOTION, IOSCIL    =           1



FREQ SWEEP
FREQ =    0.850000


                 PHASE SHIFT ANALYSIS
                  FREQ =    0.8500000
 w  0.8500000
 kp=  0.8500000    ifreq           1

 AMPLITUDE;  clamp, cmamp :  0.2316691      2.9221054E-02
 ioscil =            Oitrans =            0
 PHASE;      clp,    cmp   :   202.4033      -63.70797
 AVERAGE DRAG, TOTAL DRAG :   1.5930884E-03  0.1051438
 ETAS, WBAR                :  -0.1430808     -1.1134184E-02


                 PHASE SHIFT ANALYSIS
                  FREQ =    0.8500000
 w  0.8500000
 kp=  0.8500000    ifreq           1

 AMPLITUDE;  clamp, cmamp :  0.2779089      2.2117507E-02
 ioscil =            Oitrans =            1
 PHASE;      clp,    cmp   :   270.5030       37.10253
 AVERAGE DRAG, TOTAL DRAG :  -6.2051453E-03 -0.4095396
 ETAS, WBAR                :   0.1050769     -0.1181067



FREQ SWEEP
FREQ =    0.860000


                 PHASE SHIFT ANALYSIS
                  FREQ =    0.8600000
 w  0.8600000
 kp=  0.8600000    ifreq           2

 AMPLITUDE;  clamp, cmamp :  0.2317267      2.9490557E-02
 ioscil =            Oitrans =            0
 PHASE;      clp,    cmp   :   202.8760      -63.85251
 AVERAGE DRAG, TOTAL DRAG :   1.5921656E-03  0.1050829
 ETAS, WBAR                :  -0.1398697     -1.1383206E-02


                 PHASE SHIFT ANALYSIS
                  FREQ =    0.8600000
 w  0.8600000
 kp=  0.8600000    ifreq           2

 AMPLITUDE;  clamp, cmamp :  0.2804866      2.2494521E-02
 ioscil =            Oitrans =            1
 PHASE;      clp,    cmp   :   270.7843       36.79393
 AVERAGE DRAG, TOTAL DRAG :  -6.3188463E-03 -0.4170439
 ETAS, WBAR                :   0.1047920     -0.1205979



FREQ SWEEP
FREQ =    0.870000


                 PHASE SHIFT ANALYSIS
                  FREQ =    0.8700000
 w  0.8700000
```

Figure 3.2b UPOTFLUT example output file

stdin Page 2

```
kp=  0.8700000    ifreq           3

AMPLITUDE;  clamp, cmamp :  0.2317936      2.9765518E-02
ioscil =             Oitrans =           0
PHASE;       clp,    cmp    :   203.3604      -64.02047
AVERAGE DRAG, TOTAL DRAG :   1.5893428E-03  0.1048966
ETAS, WBAR                :  -0.1365460     -1.1639614E-02


                 PHASE SHIFT ANALYSIS
                  FREQ =    0.8700000
w  0.8700000
kp=  0.8700000    ifreq           3

AMPLITUDE;  clamp, cmamp :  0.2830637      2.2874046E-02
ioscil =             Oitrans =           1
PHASE;       clp,    cmp    :   271.0655       36.47753
AVERAGE DRAG, TOTAL DRAG :  -6.4334869E-03 -0.4246101
ETAS, WBAR                :   0.1045149     -0.1231114



FREQ SWEEP
FREQ =    0.880000


                 PHASE SHIFT ANALYSIS
                  FREQ =    0.8800000
w  0.8800000
kp=  0.8800000    ifreq           4

AMPLITUDE;  clamp, cmamp :  0.2318744      3.0037180E-02
ioscil =             Oitrans =           0
PHASE;       clp,    cmp    :   203.8330      -64.15525
AVERAGE DRAG, TOTAL DRAG :   1.5880425E-03  0.1048108
ETAS, WBAR                :  -0.1335113     -1.1894441E-02


                 PHASE SHIFT ANALYSIS
                  FREQ =    0.8800000
w  0.8800000
kp=  0.8800000    ifreq           4

AMPLITUDE;  clamp, cmamp :  0.2856959      2.3258235E-02
ioscil =             Oitrans =           1
PHASE;       clp,    cmp    :   271.3546       36.17284
AVERAGE DRAG, TOTAL DRAG :  -6.5488103E-03 -0.4322215
ETAS, WBAR                :   0.1042214     -0.1256711



FREQ SWEEP
FREQ =    0.890000


                 PHASE SHIFT ANALYSIS
                  FREQ =    0.8900000
w  0.8900000
kp=  0.8900000    ifreq           5

AMPLITUDE;  clamp, cmamp :  0.2319494      3.0311935E-02
ioscil =             Oitrans =           0
PHASE;       clp,    cmp    :   204.3115      -64.29196
AVERAGE DRAG, TOTAL DRAG :   1.5859993E-03  0.1046759
ETAS, WBAR                :  -0.1304959     -1.2153637E-02


                 PHASE SHIFT ANALYSIS
                  FREQ =    0.8900000
w  0.8900000
kp=  0.8900000    ifreq           5

AMPLITUDE;  clamp, cmamp :  0.2883391      2.3644408E-02
```

Figure 3.2c UPOTFLUT example output file

```
 ioscil =            Oitrans =            1
 PHASE;       clp,    cmp    :   271.6436       35.87401
 AVERAGE DRAG, TOTAL DRAG :  -6.6649993E-03 -0.4398900
 ETAS, WBAR                :   0.1039310      -0.1282581



FREQ SWEEP
FREQ =    0.900000


                  PHASE SHIFT ANALYSIS
                   FREQ =    0.9000000
 w  0.9000000
 kp=  0.9000000    ifreq           6

 AMPLITUDE;  clamp, cmamp :  0.2320280      3.0592278E-02
 ioscil =            Oitrans =            0
 PHASE;       clp,    cmp    :   204.7803      -64.43259
 AVERAGE DRAG, TOTAL DRAG :   1.5828811E-03  0.1044701
 ETAS, WBAR                :  -0.1274617      -1.2418482E-02


                  PHASE SHIFT ANALYSIS
                   FREQ =    0.9000000
 w  0.9000000
 kp=  0.9000000    ifreq           6

 AMPLITUDE;  clamp, cmamp :  0.2909827      2.4039967E-02
 ioscil =            Oitrans =            1
 PHASE;       clp,    cmp    :   271.9288       35.58691
 AVERAGE DRAG, TOTAL DRAG :  -6.7821071E-03 -0.4476191
 ETAS, WBAR                :   0.1036481      -0.1308680



FREQ SWEEP
FREQ =    0.910000


                  PHASE SHIFT ANALYSIS
                   FREQ =    0.9100000
 w  0.9100000
 kp=  0.9100000    ifreq           7

 AMPLITUDE;  clamp, cmamp :  0.2321466      3.0865142E-02
 ioscil =            Oitrans =            0
 PHASE;       clp,    cmp    :   205.2529      -64.61227
 AVERAGE DRAG, TOTAL DRAG :   1.5800473E-03  0.1042831
 ETAS, WBAR                :  -0.1245367      -1.2687406E-02


                  PHASE SHIFT ANALYSIS
                   FREQ =    0.9100000
 w  0.9100000
 kp=  0.9100000    ifreq           7

 AMPLITUDE;  clamp, cmamp :  0.2936268      2.4440434E-02
 ioscil =            Oitrans =            1
 PHASE;       clp,    cmp    :   272.2159       35.29980
 AVERAGE DRAG, TOTAL DRAG :  -6.9000078E-03 -0.4554005
 ETAS, WBAR                :   0.1033707      -0.1335003



FREQ SWEEP
FREQ =    0.920000


                  PHASE SHIFT ANALYSIS
                   FREQ =    0.9200000
 w  0.9200000
 kp=  0.9200000    ifreq           8
```

Figure 3.2d UPOTFLUT example output file

```
AMPLITUDE:  clamp, cmamp :  0.2322759       3.1138692E-02
loscil =            0ltrans =               0
PHASE;        clp,    cmp   :   205.7373       -64.69626
AVERAGE DRAG, TOTAL DRAG :   1.5782372E-03  0.1041637
ETAS, WBAR                :  -0.1218763      -1.2949497E-02

                   PHASE SHIFT ANALYSIS
                    FREQ =   0.9200000
w  0.9200000
kp=  0.9200000    1freq           8

AMPLITUDE:  clamp, cmamp :  0.2962705       2.4841587E-02
loscil =            0ltrans =               1
PHASE;        clp,    cmp   :   272.5011        35.01268
AVERAGE DRAG, TOTAL DRAG :  -7.0186830E-03 -0.4632331
ETAS, WBAR                :   0.1030987      -0.1361546


FREQ SWEEP
FREQ =   0.930000


                   PHASE SHIFT ANALYSIS
                    FREQ =   0.9299999
w  0.9299999
kp=  0.9299999    1freq           9

AMPLITUDE:  clamp, cmamp :  0.2324548       3.1417310E-02
loscil =            0ltrans =               0
PHASE;        clp,    cmp   :   206.2080       -64.82713
AVERAGE DRAG, TOTAL DRAG :   1.5755624E-03  0.1039871
ETAS, WBAR                :  -0.1191657      -1.3221607E-02

                   PHASE SHIFT ANALYSIS
                    FREQ =   0.9299999
w  0.9299999
kp=  0.9299999    1freq           9

AMPLITUDE:  clamp, cmamp :  0.2989171       2.5250332E-02
loscil =            0ltrans =               1
PHASE;        clp,    cmp   :   272.7901        34.72948
AVERAGE DRAG, TOTAL DRAG :  -7.1382108E-03 -0.4711219
ETAS, WBAR                :   0.1028326      -0.1388317


FREQ SWEEP
FREQ =   0.940000


                   PHASE SHIFT ANALYSIS
                    FREQ =   0.9399999
w  0.9399999
kp=  0.9399999    1freq          10

AMPLITUDE:  clamp, cmamp :  0.2326474       3.1699076E-02
loscil =            0ltrans =               0
PHASE;        clp,    cmp   :   206.6846       -64.94821
AVERAGE DRAG, TOTAL DRAG :   1.5715322E-03  0.1037211
ETAS, WBAR                :  -0.1164358      -1.3496989E-02

                   PHASE SHIFT ANALYSIS
                    FREQ =   0.9399999
w  0.9399999
kp=  0.9399999    1freq          10

AMPLITUDE:  clamp, cmamp :  0.3015640       2.5659967E-02
loscil =            0ltrans =               1


 PHASE;        clp,    cmp   :   273.0792        34.44823
 AVERAGE DRAG, TOTAL DRAG :  -7.2587137E-03 -0.4790751
 ETAS, WBAR                :   0.1025746      -0.1415304
  Number of Kp Values                   =   10
  Plunge Value/Full Chord (h/2b)        =    0.0833
  Alpha                                 =    3.0000
  PIVOT POINT (a) Of Elastic Axis       =   -0.4000
  Half Chord (b)                        =    6.0000
  Alpha Uncoupled Nat. Freq.            =   90.0000
  Plunge Uncoupled Nat. Freq            =   72.0000
  I alpha                               =        4.8410
  S alpha                               =    0.6455
  Mass                                  =    0.5379
  Air Density                           =    0.0024
  Mass Ratio                            =        2.0000
  Dist. To Wing CG Aft of Elas. Axis=    0.2000
 Kp crit   =  0.9000000
 DIFF      =  1.1507273E-03
 SQRTX     =  0.9579428
 U crit    =   1252.684
```

Figure 3.2e UPOTFLUT example output file

j. PLUNGE.in This file contains K_p, C_{Lh} RE, C_{Lh} IM, C_{mh} RE, C_{Mh} IM

k. FLUTPLOT.d This file contains K_p,SQRT(x) Re, SQRT(X) RE, SQRT(X) IM

3. VALIDATION

The program was tested against some sample cases to check for code validity. The first case was taken from reference 6 example #1, p. 236. Figures 3.3 and 3.4 show plots of the FLUTPOT.d file. Figure 3.3 shows the initial look over a wide range of K_p and after finding the approximate flutter location Figure 3.4 shows a closer look at the K_p range of interest. This example calculated a $U_{critical}$ of 161.985 ft/sec. which compares favorably to the example value of 162 ft/sec. The next example was taken from NACA TR-685 [ref.8] case #1 p. 8. Figures 3.5 and 3.6 again show the initial and final looks for this analysis. The example called for a $U_{critical}$ of 567 miles/hr and the program returned a value of 570 miles/hr. Next, the code was tested over a range of ω_h/ω_α ratios as done in NACA TR-685, p11., graph I-A(a). Figure 3.7 shows the comparison between the two methods.

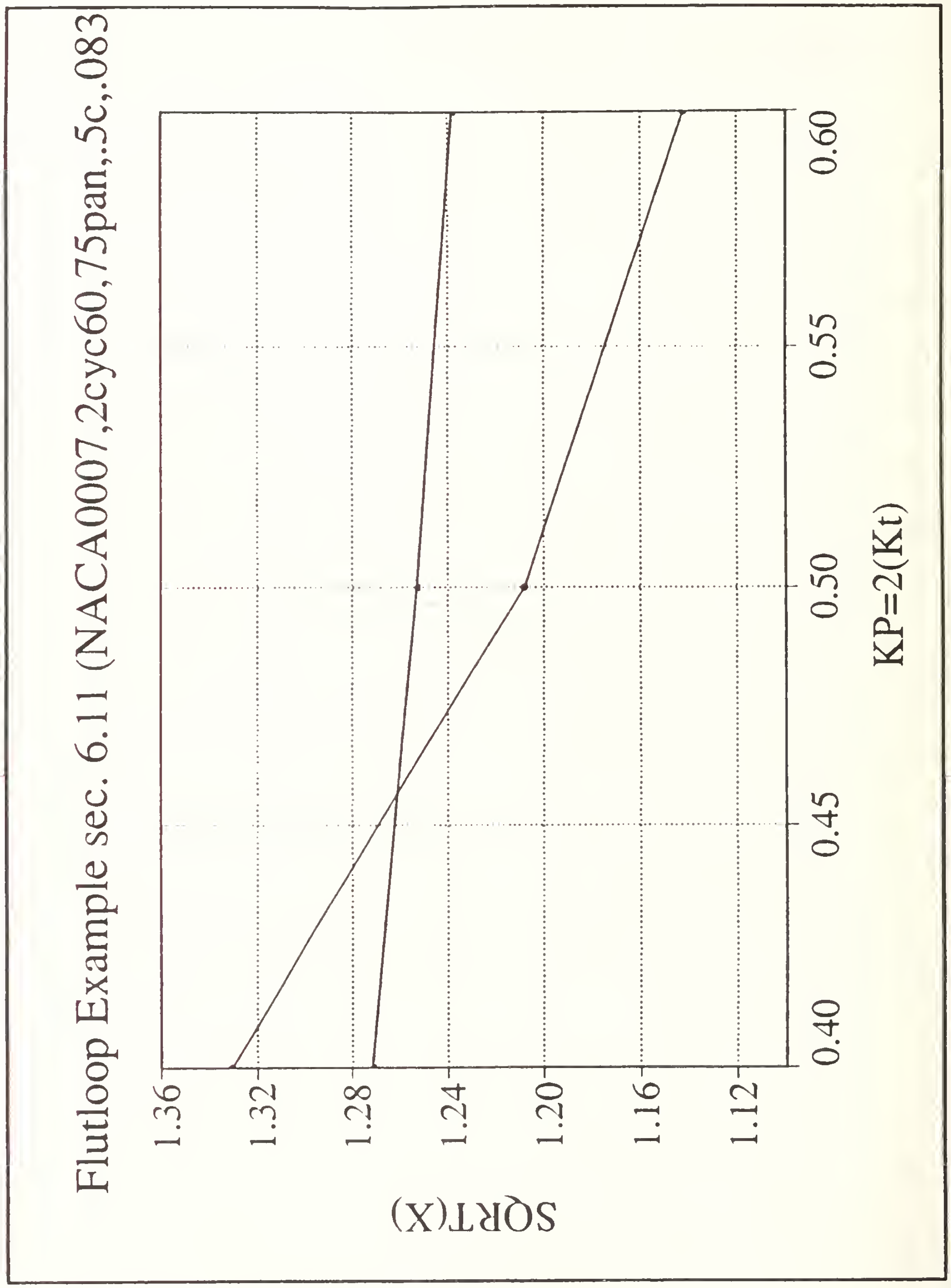

Figure 3.3 Initial look at flutter, example 1

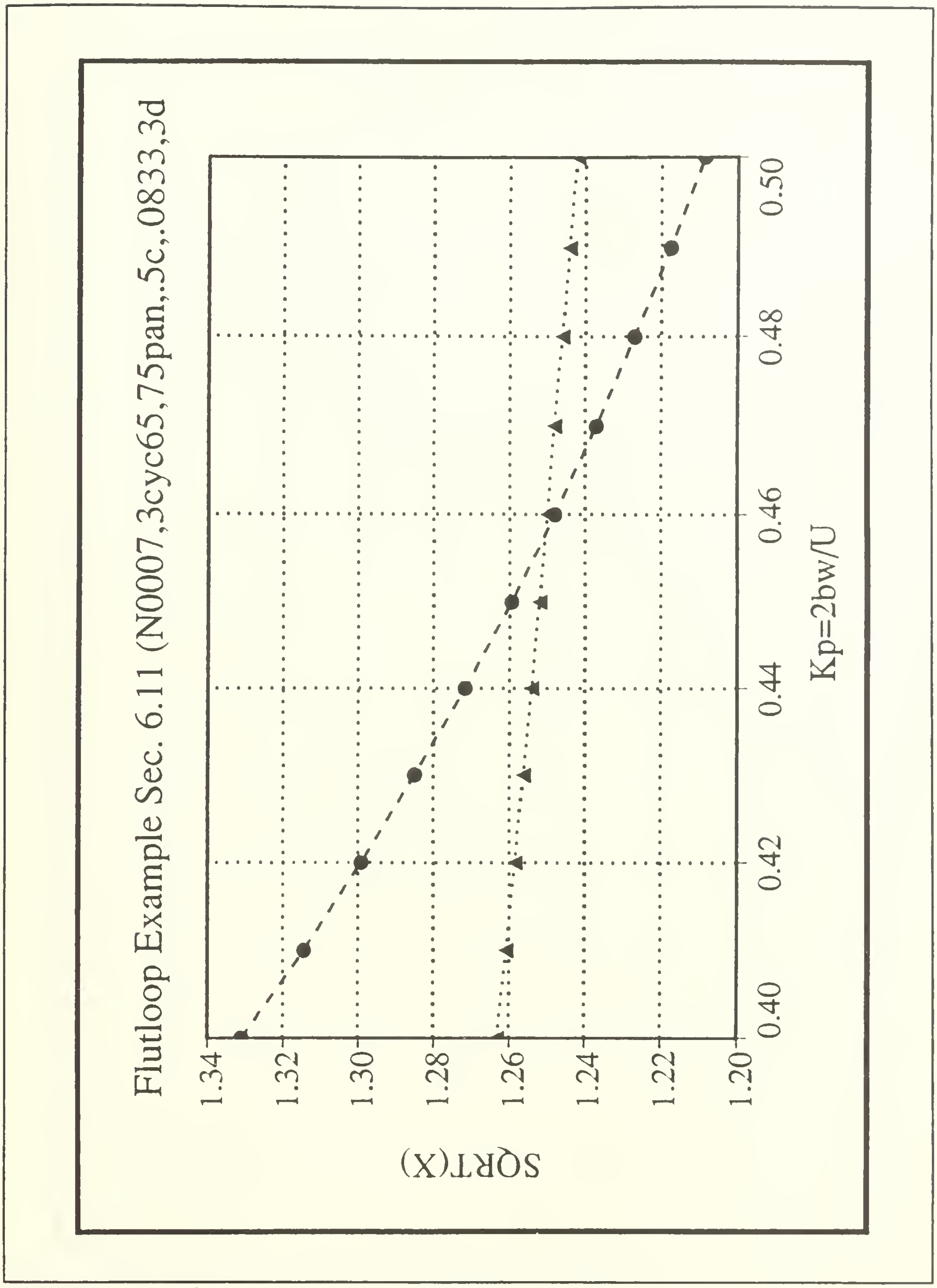

Figure 3.4 Final look at flutter, example 1

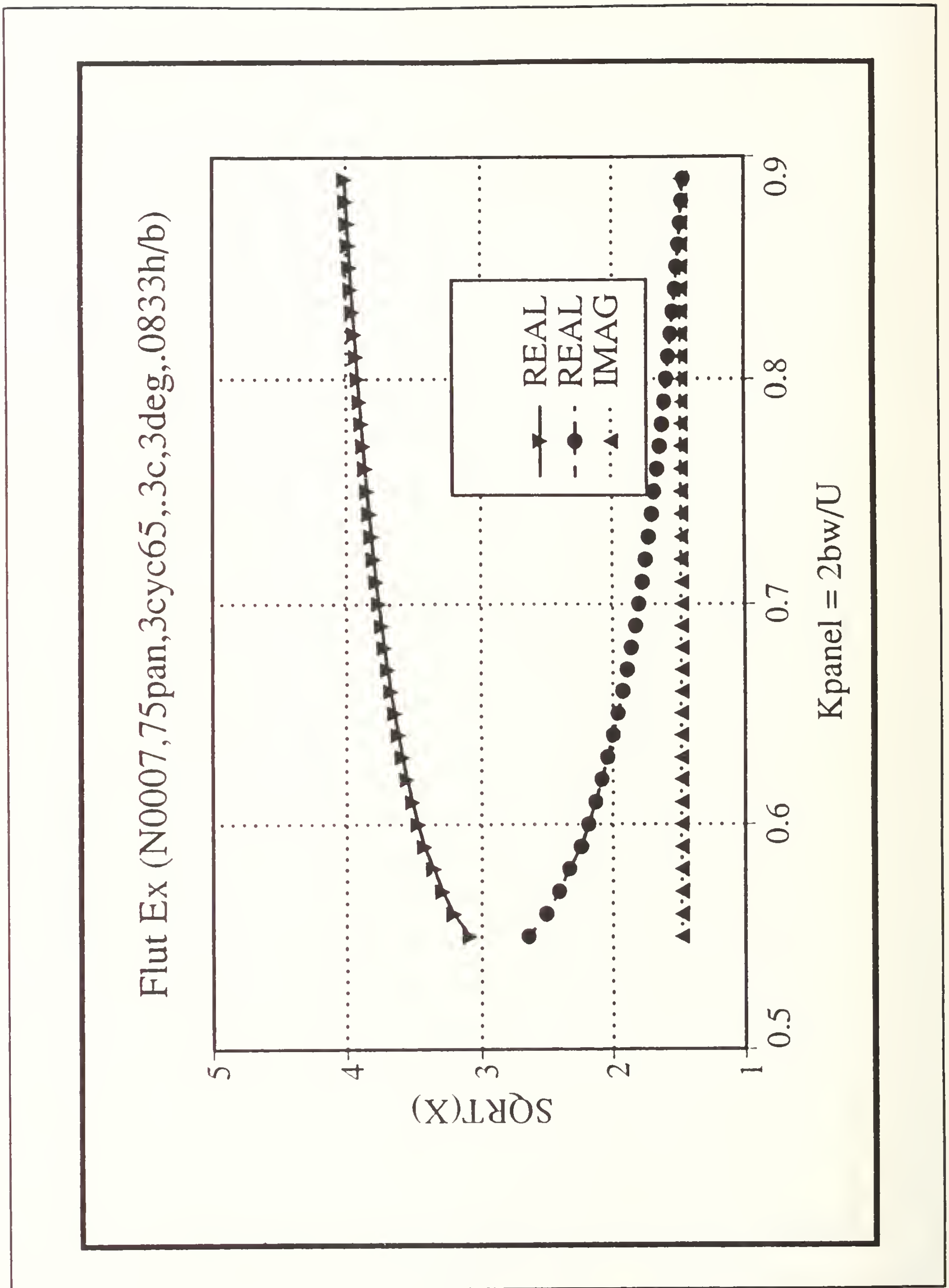

Figure 3.5 Initial look at flutter, example 2

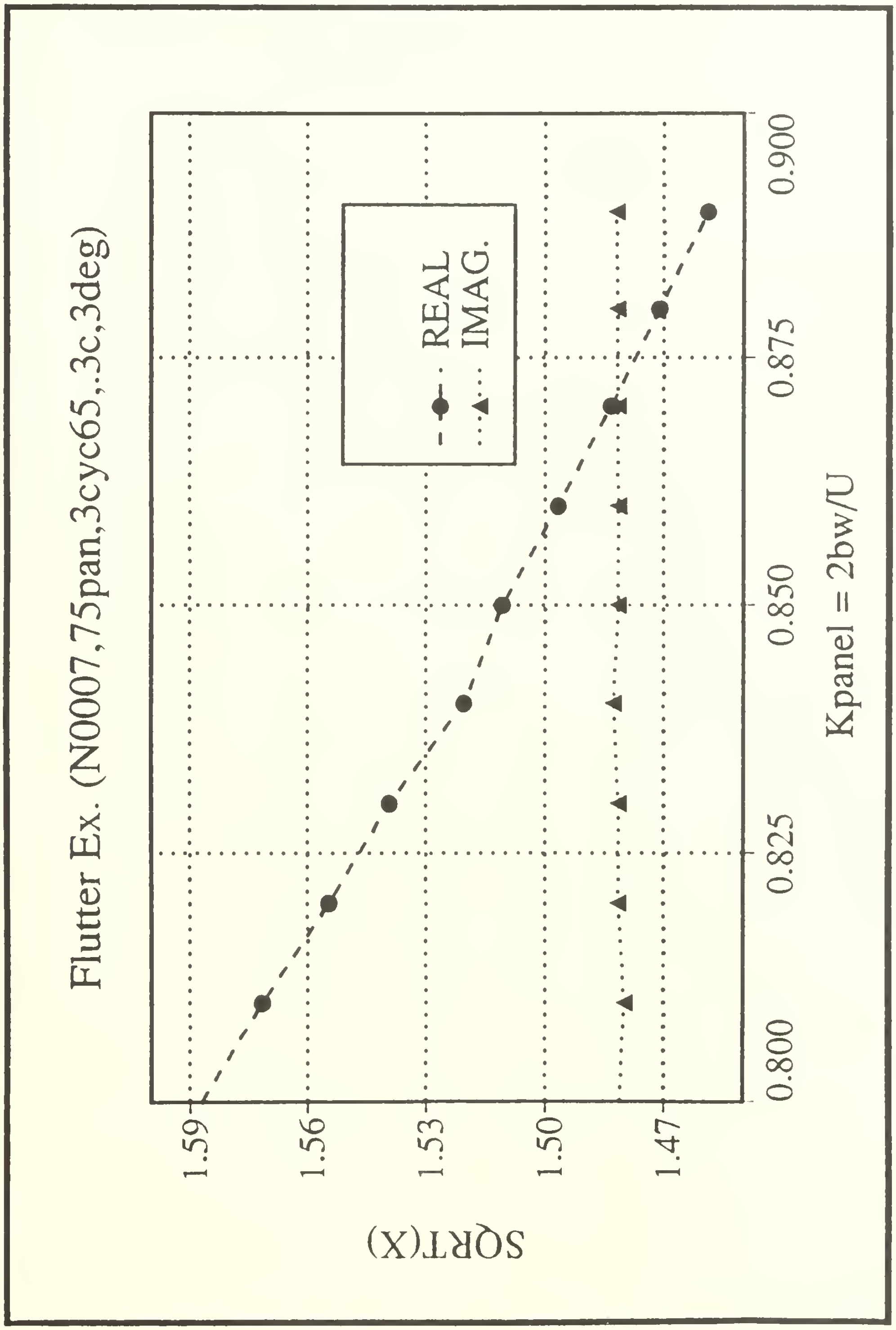

Figure 3.6 Final look at flutter, example 2

Mechanism of Flutter .The affects of changing the ratio of plunge and pitch natural frequencies.				
	Panel code vs Theo.	(NACA0007, 50panels, 3deg, h/2b=.0833, 3cyc65calc.,)		
	(Mass= .53789 slugs/ft, Ialpha=4.84102, Salpha=.645468,b= ft, std day air density)			
Wh/Walpha	Panel Ucrit.(ft/sec)	Panel (-Ucrit/bWalpha)	Theo (-Ucrit/bWalpha)	%Diff wrt Theo.
0.0111	896.6013	-1.66	-1.7	2.35%
0.2	925.5568	-1.713994	-1.72	0.35%
0.4	960.3143	-1.7783598	-1.8	1.20%
0.5	994.4232	-1.84152	-1.9	3.08%
0.6	1036.167	-1.9188	-2.04	5.94%
0.7	1107.237	-2.060438	-2.22	7.64%
0.8	1252.889	-2.32016	-2.42	4.13%

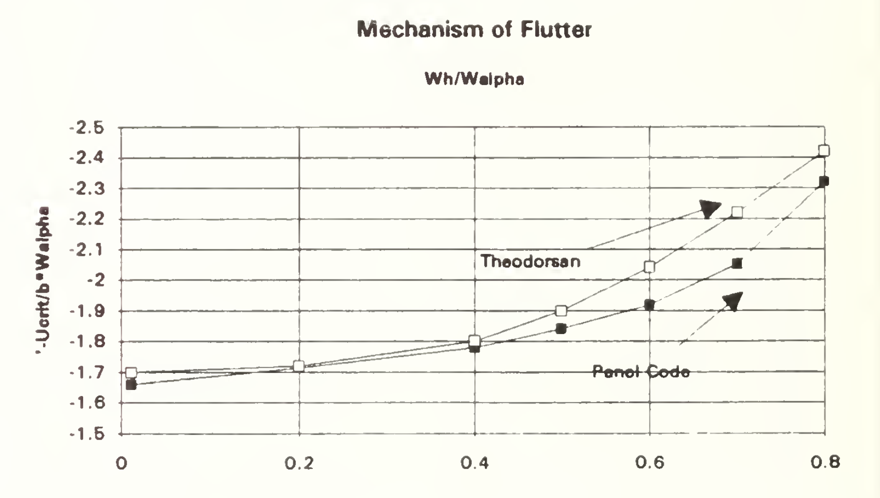

Figure 3.7 ω_h/ω_α Calculations

IV. FLOW VISUALIZATION EXPERIMENT

A. INTRODUCTION

The purpose of this experiment was to document the production of thrust by a plunging airfoil. This was a preliminary experiment to better understand the vortex pattern produced by a plunging airfoil, and to examine the production of thrust using smoke flow visualization techniques.

An explanation of what constitutes a propulsive vortical signature along with smoke flow visualization of the propulsive vortical patterns is given in Reference 7. In this reference, the explanation is given by contrasting the vortical pattern produced by a cylinder (drag) with the vortical pattern produced by a plunging airfoil (thrust). The cylinder produced a vortical sheet where the top row of vortices rotated clockwise and the bottom row of vortices rotated counterclockwise. This pattern induces a velocity component in the upstream direction (Biot-Savart law). In contrast, the plunging airfoil produced a clockwise rotating vortex sheet on the bottom row. This pattern induces a velocity component in the downstream direction. Reproduction of the flow visualization data from Reference 7 is shown in Figure 4.1.

Figure 4.1 View of flow over cylinder (top) and plunging airfoil (bottom) [Ref. 7]

B. THEORY

A comparison was done using the incompressible panel code, U2DIIF. The purpose of this study was to examine the vortical pattern produced by the panel code, and determine if the vortical signature matched experimental results. The input to the panel code was set up to best match the conditions of the experiment described in the next section. The panel code was run using a plunge amplitude, h/2b equal to .1977, a reduced frequency of 1.8 and a zero mean AOA. The results of the vortical pattern are shown in Figure 4.2. Aside from the starting vortex, this is clearly a thrust producing vortical sheet. Furthermore, the vortical pattern is similar to that produced by the experiment shown in Figures 4.10 and 4.11.

C. EXPERIMENTAL SETUP

1. Plunging Airfoil

The plunging airfoil used in this paper was originally a wing taken from the rotor of a model helicopter. The wing was attached to a MB250 Shaker Table as shown in Figure 4.3 The wing was made from a NACA0007 airfoil section and consisted of a 2.45" chord and a 22" span. The wing was built from a foam core and finished with a layer of graphite epoxy composite for added fatigue strength. The airfoil's drive mechanism was a MB 250 Shaker Table capable of 1" total

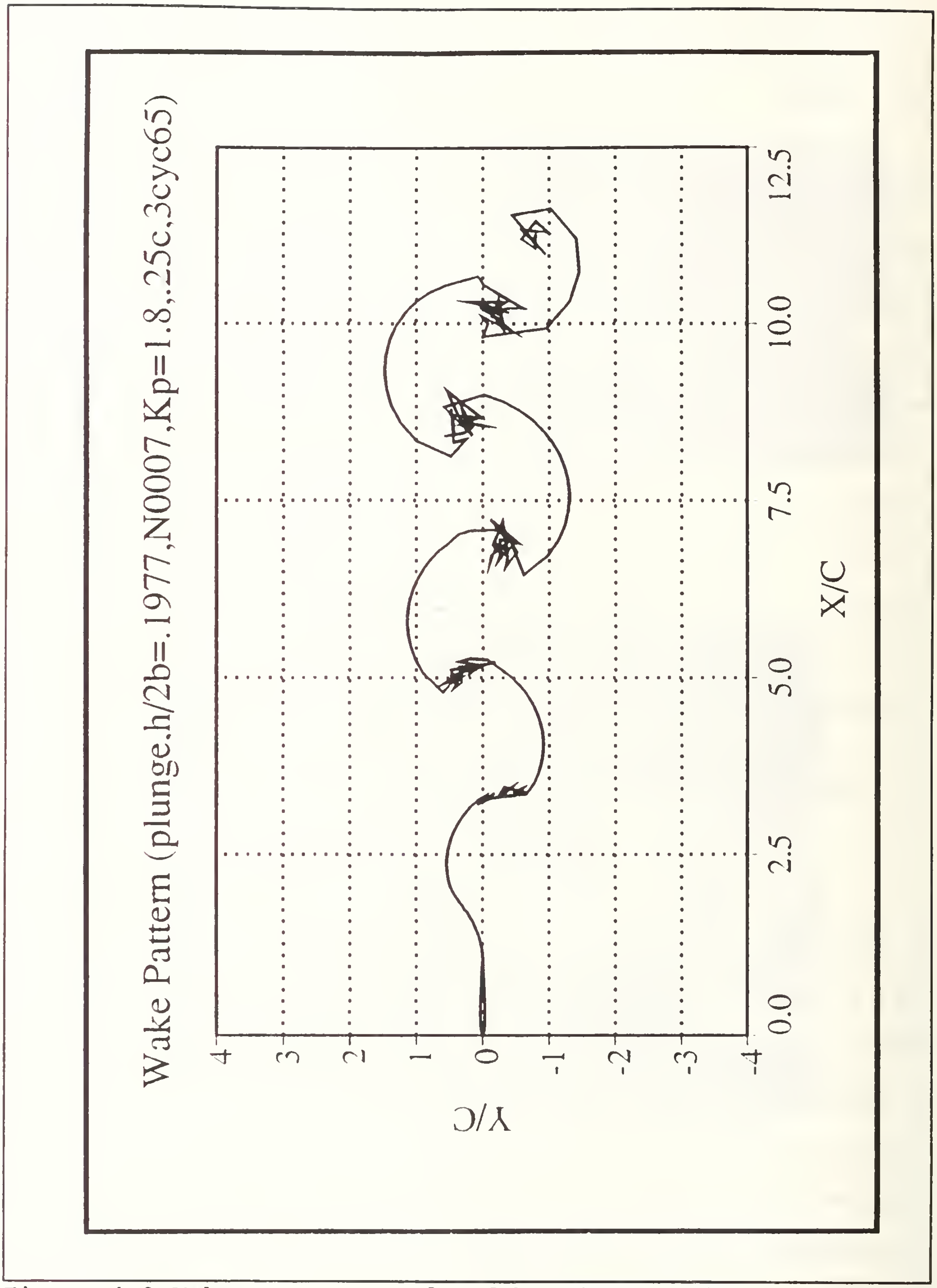

Figure 4.2 Wake pattern produced by U2DIIF code

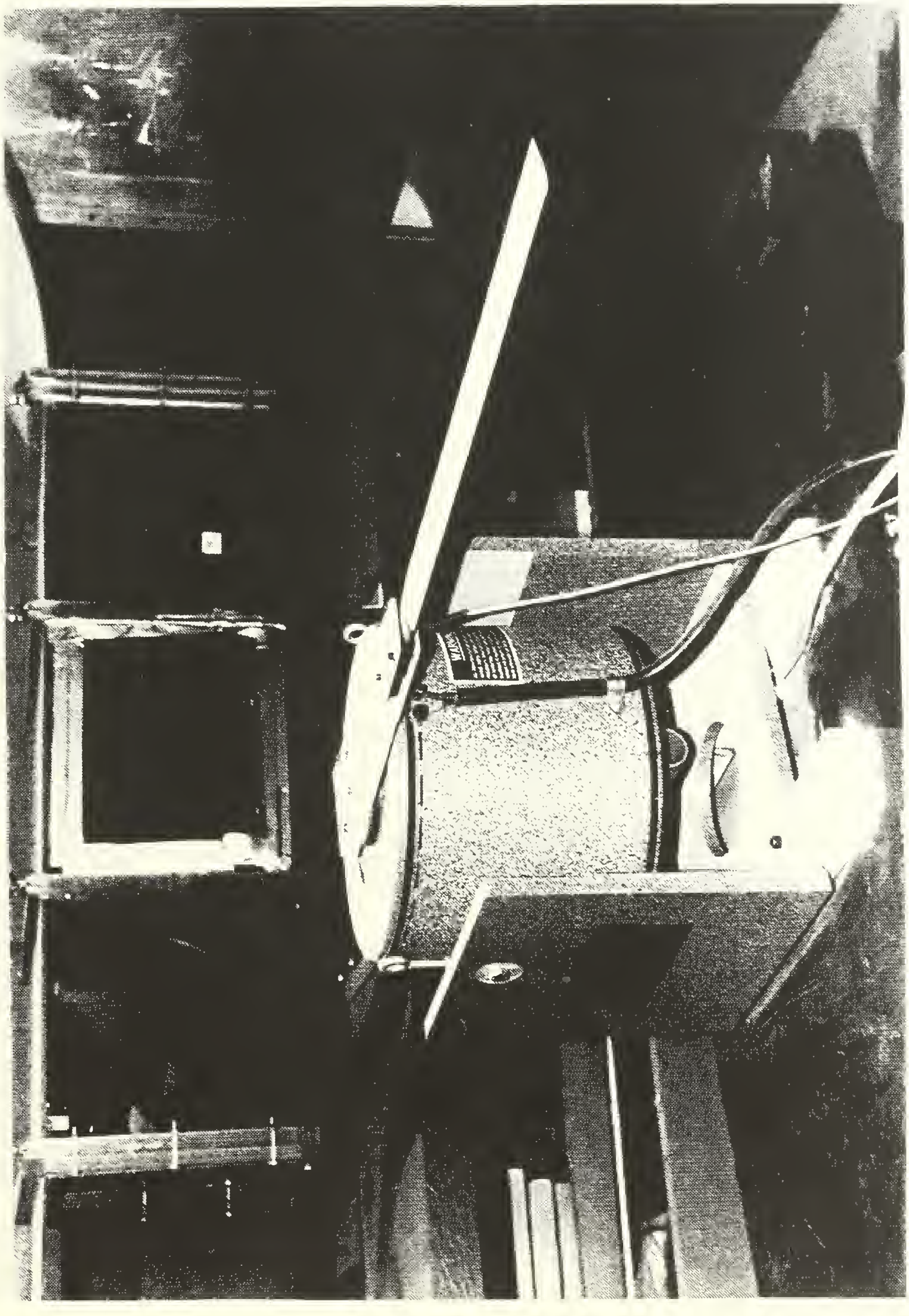

Figure 4.3 Shaker table with wing

deflection. The Shaker Table was limited only by resonance frequencies of the wing which occurred around 20 Hz or 1200 rpm.

2. WIND TUNNEL

The wind tunnel used in this experiment was a very low speed, low turbulence smoke tunnel. It is made of plexiglass walls and a contraction ratio of 2.8:1. The motor provides wind tunnel velocities between 0 and 10 feet per second (fps). The smoke was created using a Rosco smoke generator and piped into the tunnel in the test section using a small seven tube smoke rake constructed for this experiment. Figure 4.4 is a photograph of the wind tunnel and smoke rake used in this experiment.

D. TEST PROCEDURE

Testing was conducted in the low speed smoke tunnel under several different conditions. The speeds of the tunnel were approximately 1.04 fps, 1.47 fps, and 1.56 fps (measured visually). These low speeds allowed good pictures and the ability to get higher reduced frequencies without calling for too high a load on the wing. The actual plunging harmonic frequencies ranged from 1 to 15 Hz and amplitudes from 1/16" to 1" peak to peak. The tunnel was initially turned off and the Shaker Table turned on with stagnant smoke in the tunnel. The purpose was to see if the
plunging airfoil would draw the smoke through the tunnel like

Figure 4.4 Tunnel and smoke rake

a fan, thus showing the production of thrust by the plunging airfoil.

Photos were taken using a Nikon 35mm camera and Kodak TMAX-400 ASA black and white film. The shutter speed was set to 1/125 seconds with an aperture setting of 4.0 for the light conditions. Film developing time was optimized at 9 minutes at 75 degrees F.

E. RESULTS AND DISCUSSION

The result for the tunnel off condition flow visualization experiment was as expected. The wing in fact accelerated the smoke in its vicinity.

The result of the additional rake flow visualization experiments are shown in Figures 4.5-4.14. Figure 4.5 shows the stationary airfoil at zero degree AOA. The Reynolds number (based on airfoil chord) is 10,000. It can be seen that the airfoil produces a small wake with the boundary layer mostly attached. Figures 4.6 through 4.14 show the vortical wake flow patterns produced by plunge oscillations at various frequencies as indicated. Most of these pictures reveal the propulsive vortical street pattern discovered in Reference 7. Previous experiments by Neace, [ref.9] found that the tunnel was too small for the airfoil size used, but the airfoil size for the present experiment seemed to be optimum, as seen by the long trail of vortices. The vortical patterns show that the bottom vortex is rotating clockwise, and the top vortex is

Figure 4.5 Steady airfoil 1.56 ft/s

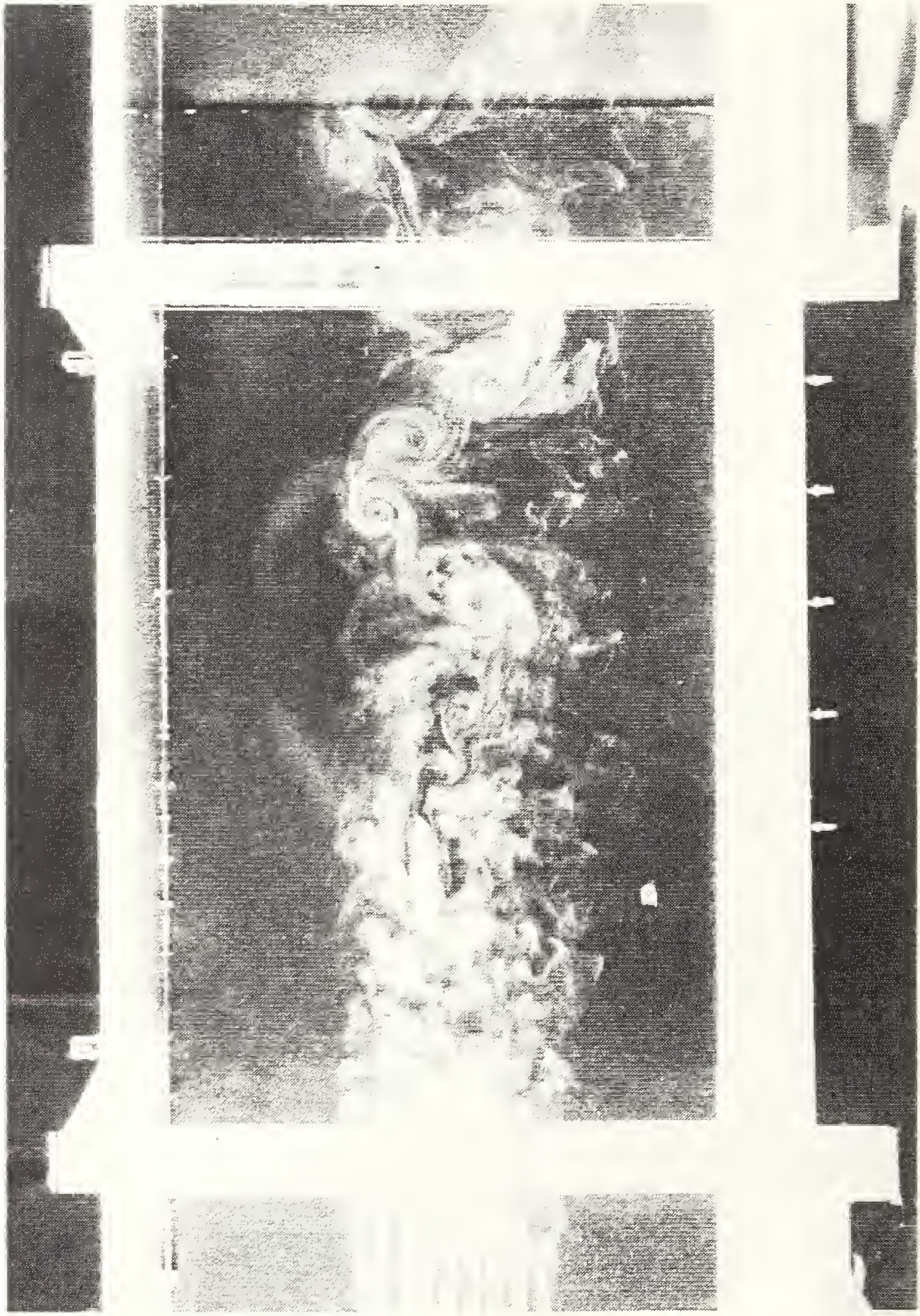

Figure 4.6 K_p = 1.8008, h/2b=.1977, 1.56 ft/s

Figure 4.7 K_p = 2.467, h/2b=.10204, 1.56 ft/s

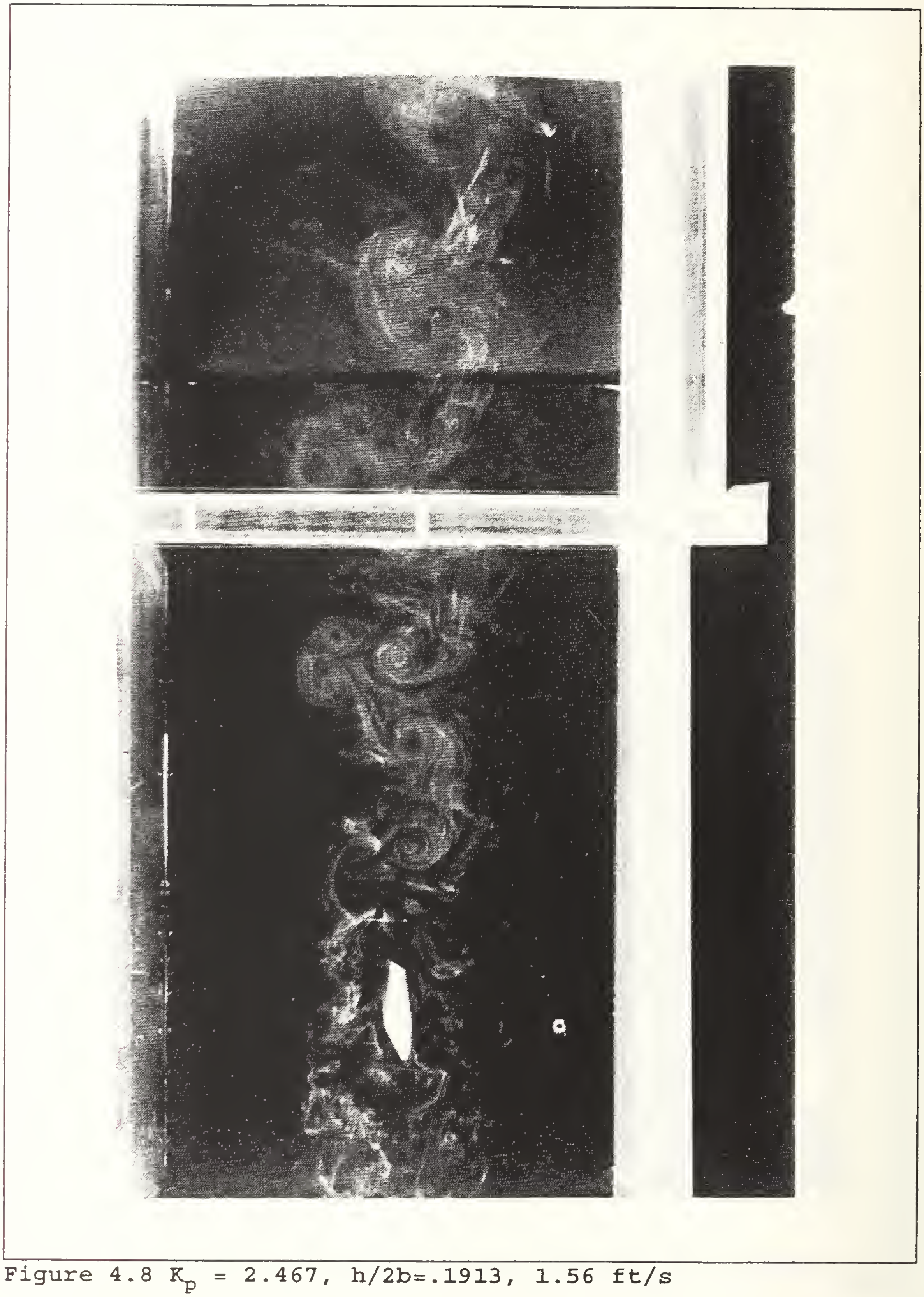

Figure 4.8 K_p = 2.467, h/2b=.1913, 1.56 ft/s

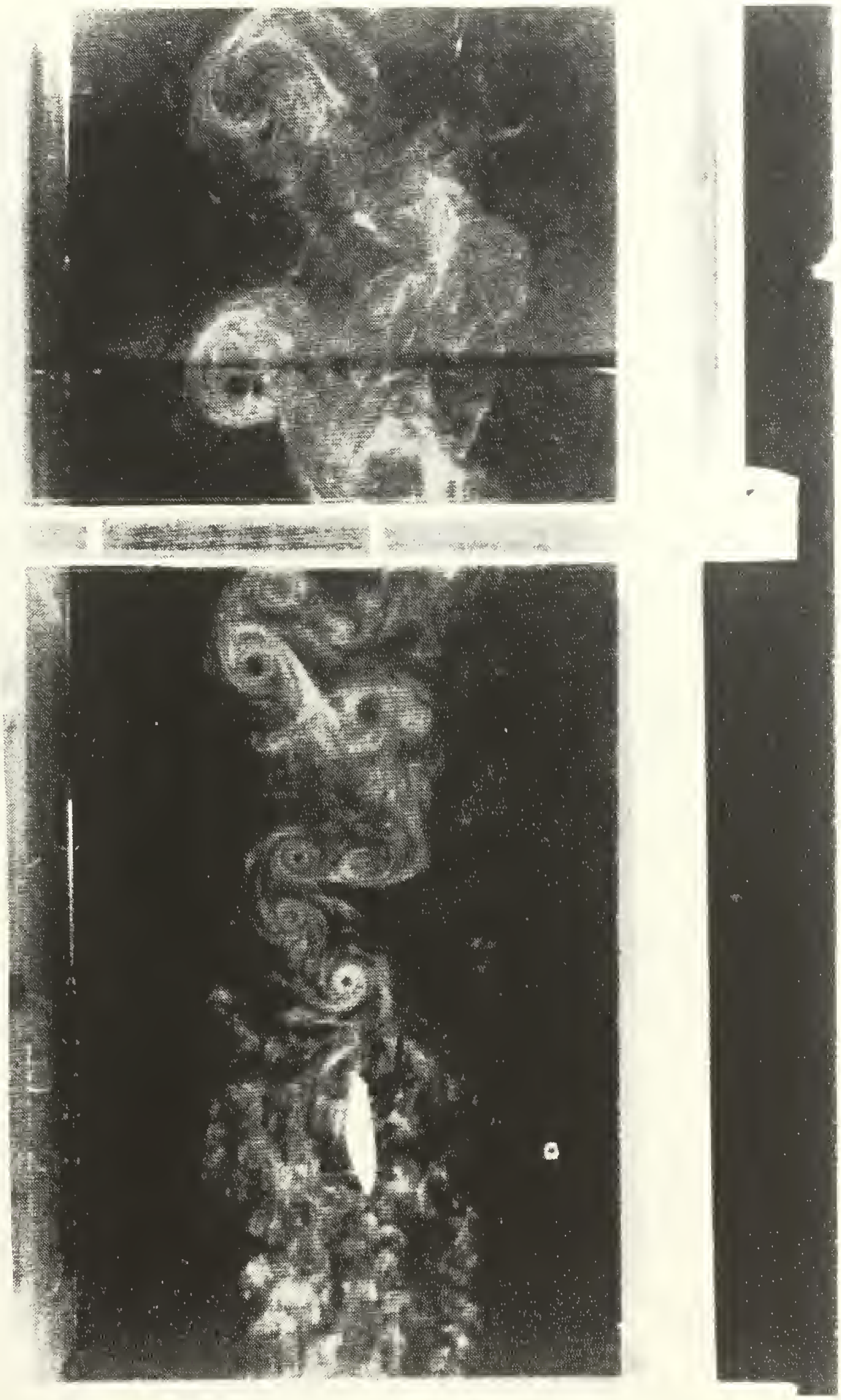

Figure 4.9 K_p = 4.112, h/2b=.14031, 1.56 ft/s

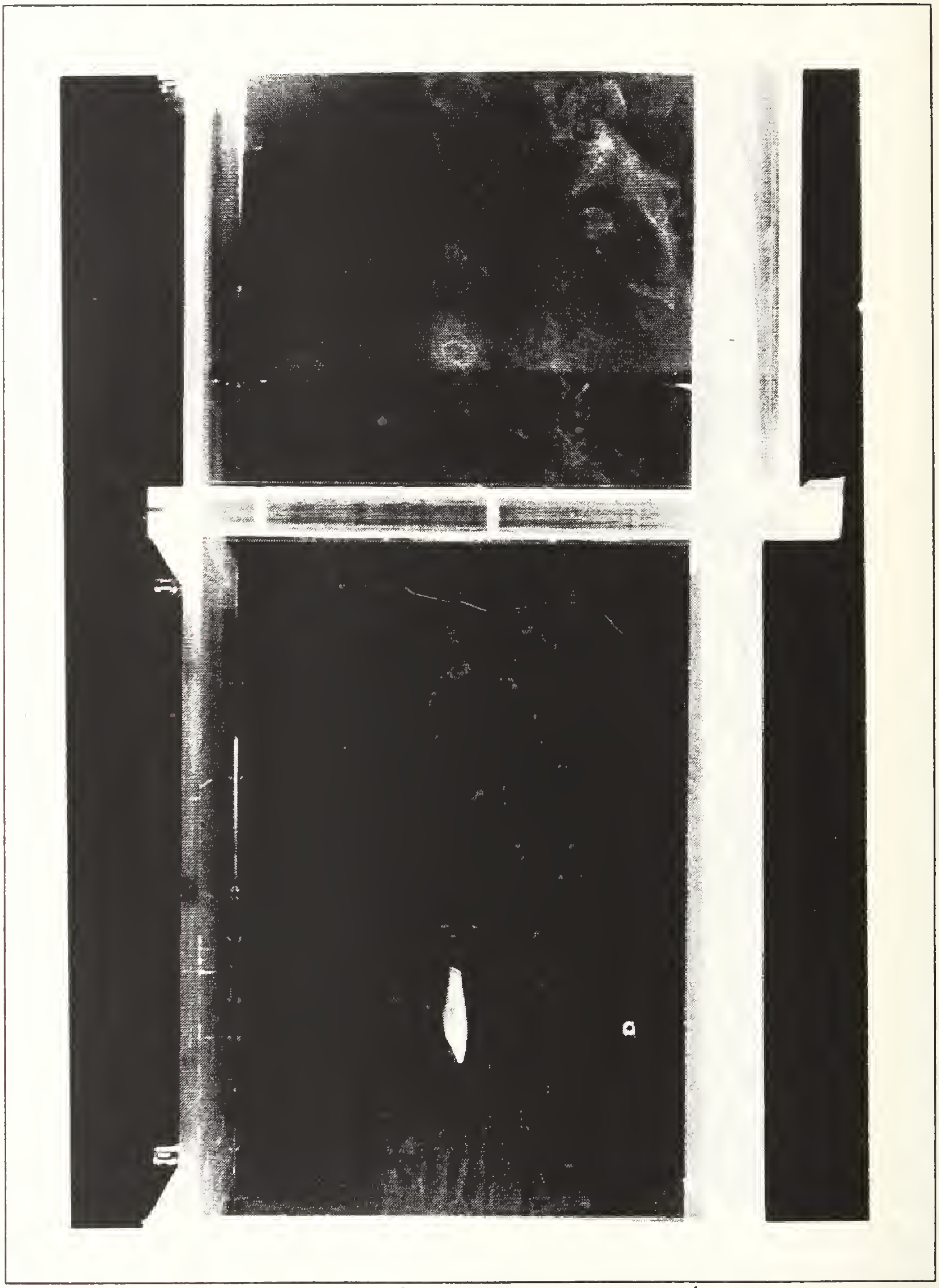

Figure 4.10 K_p = 6.167, h/2b=.05102, 1.56 ft/s

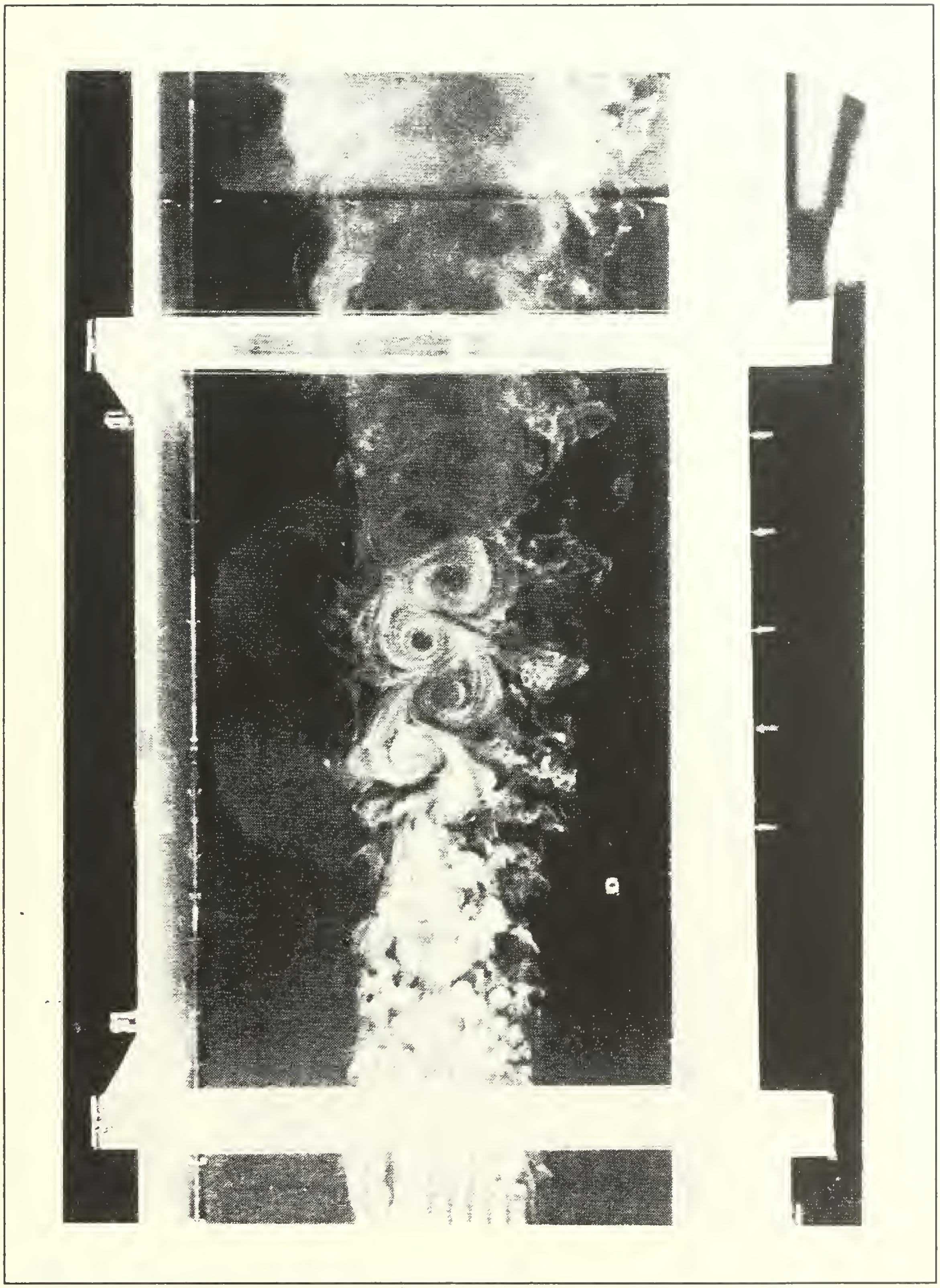

Figure 4.11 K_p = 6.753, h/2b=.1084, 1.56 ft/s

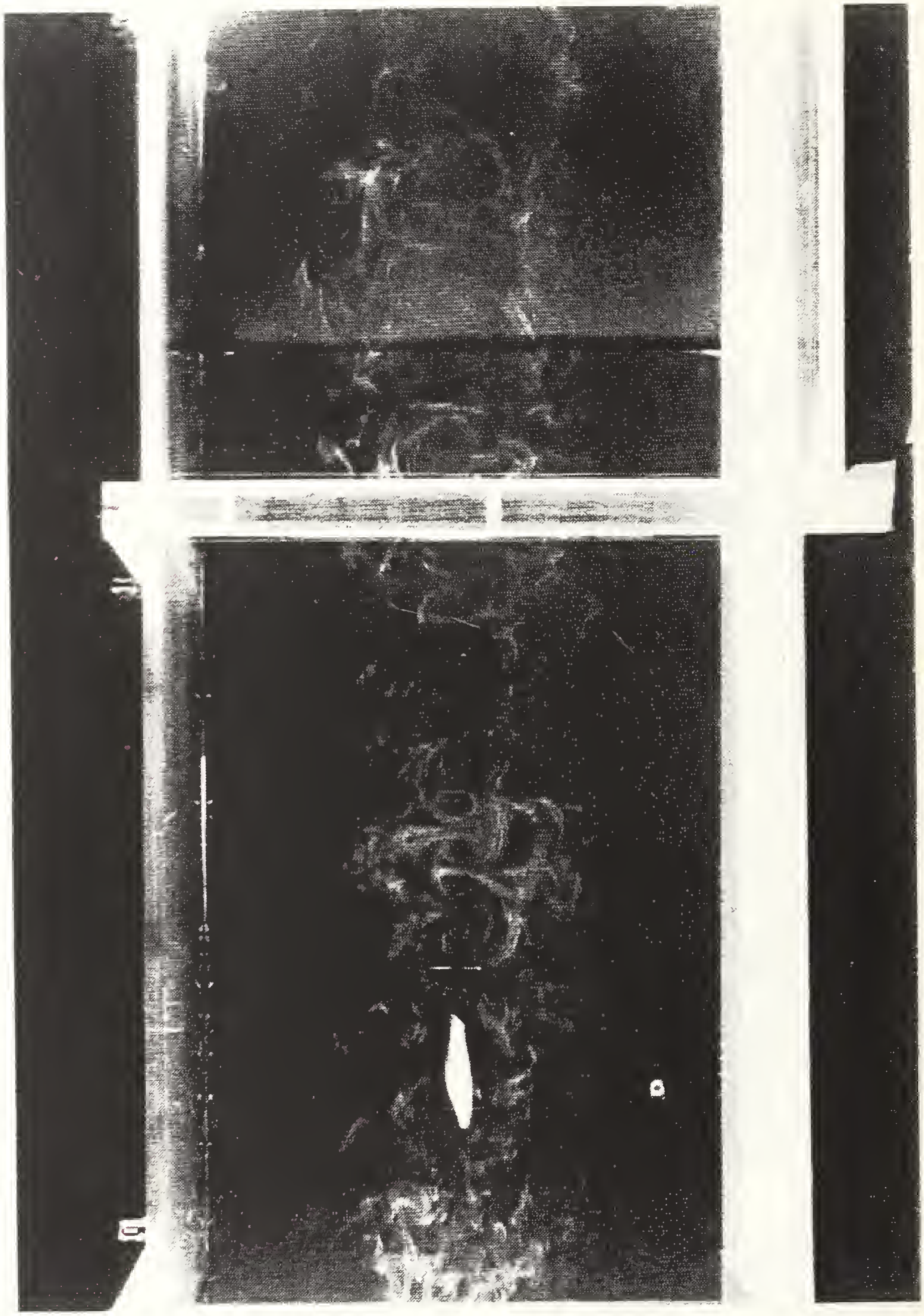

Figure 4.12 K_p = 7.401, h/2b=.03826, 1.56 ft/s

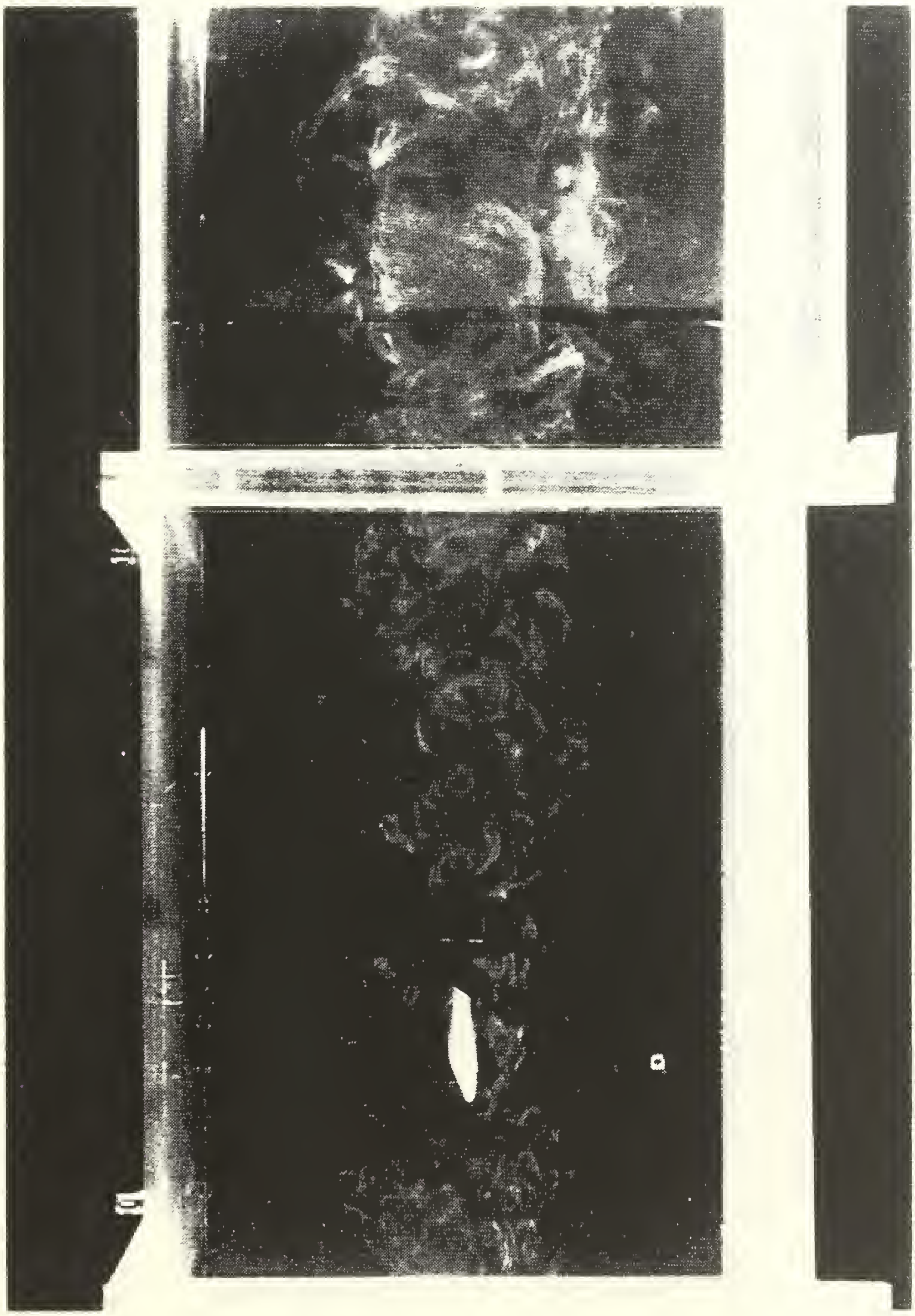

Figure 4.13 K_p =8.223, h/2b=.01913, 1.56 ft/s

Figure 4.14, K_p=12.335, h/2b=.01775, 1.56 ft/s

rotating counterclockwise, which is a thrust producing vortical sheet. It can be seen in the pictures that the frequency greatly affects the vortical strength (size). Increasing the frequency leads to an increase in wake vorticity.

V. LIFT ENHANCEMENT PRODUCED BY A PLUNGING AIRFOIL

A. THEORY

Chapter IV demonstrated the propulsive capability of a plunging airfoil. The production of thrust implies the generation of a jet flow which, in turn, may be utilized as a boundary layer control device. Therefore, an additional test was conducted in the NPS smoke tunnel in order to explore the feasibility of this concept.

B. SETUP

The same NACA0007 plunging wing was used as in chapter IV with a different driving mechanism. The wing was mounted to an ELECTRO-SEIS Model 113 Shaker Table by APS Dynamics, Inc. The shaker was located below the test section of the NPS smoke tunnel (Figure 5.1). The plunging airfoil was mounted to struts at both ends to prevent excessive bending while plunging. The large airfoil is a cambered profile taken from the rotor of a full size helicopter (13" chord, 2" Thickness, modified NACA airfoil, Reynolds Number of 52,000). The wing is suspended from the tunnel ceiling as shown in the flow pictures. The design allowed for full movement of the big wing to position it in the vicinity of the plunging airfoil.

C. WIND TUNNEL

This study used the Naval Postgraduate School's flow visualization wind tunnel. The tunnel is an open-circuit one, with air entering an inlet that measures 4.5 m X 4.5 m (15'X15'). As the air enters the tunnel, it passes through a 7.5-cm long honeycomb. A 9:1 ratio square contraction cone directs the flow into a test section that is 1.5 m X 1.5 m (5'X5'), and 6.7 m (22') long, as seen in Figure 5.2. The flow is then exhausted into the atmosphere through a fan, which uses variable pitch blades to control the speed of the flow. The speed control toggle switch is located right below the red and green on/off switch located in the left side of the tunnel control room. The tunnel speed was determined using a digital manometer which was verified for accuracy (Figure 5.3).

An observation booth is located on the side of the tunnel. A glass window, 1.6 m X 1.1 m (5.2' X 3.4'), provides the primary viewing area from the observation room and a second one, 0.4 m X 1.23 m (1.33'X4'), is located in the tunnel's roof. The main viewing window had sufficient area for most of the photography, with the top window used for illumination. A circular turntable was located on the floor of the test section [ref.11] which allowed for easy access to the shaker table. The walls and floor of the test section were flat black for low light reflectivity.

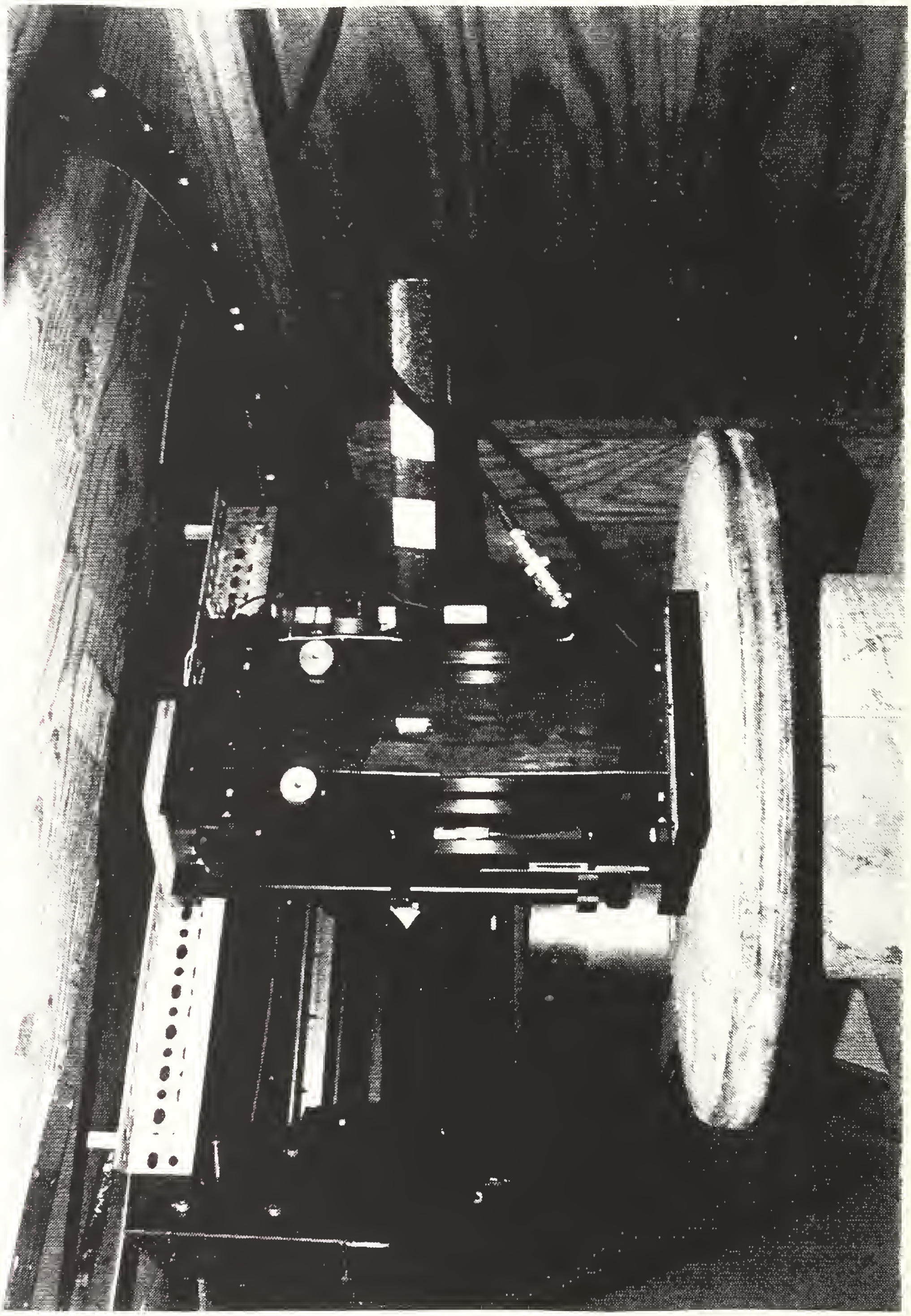

Figure 5.1 Shaker table setup below tunnel

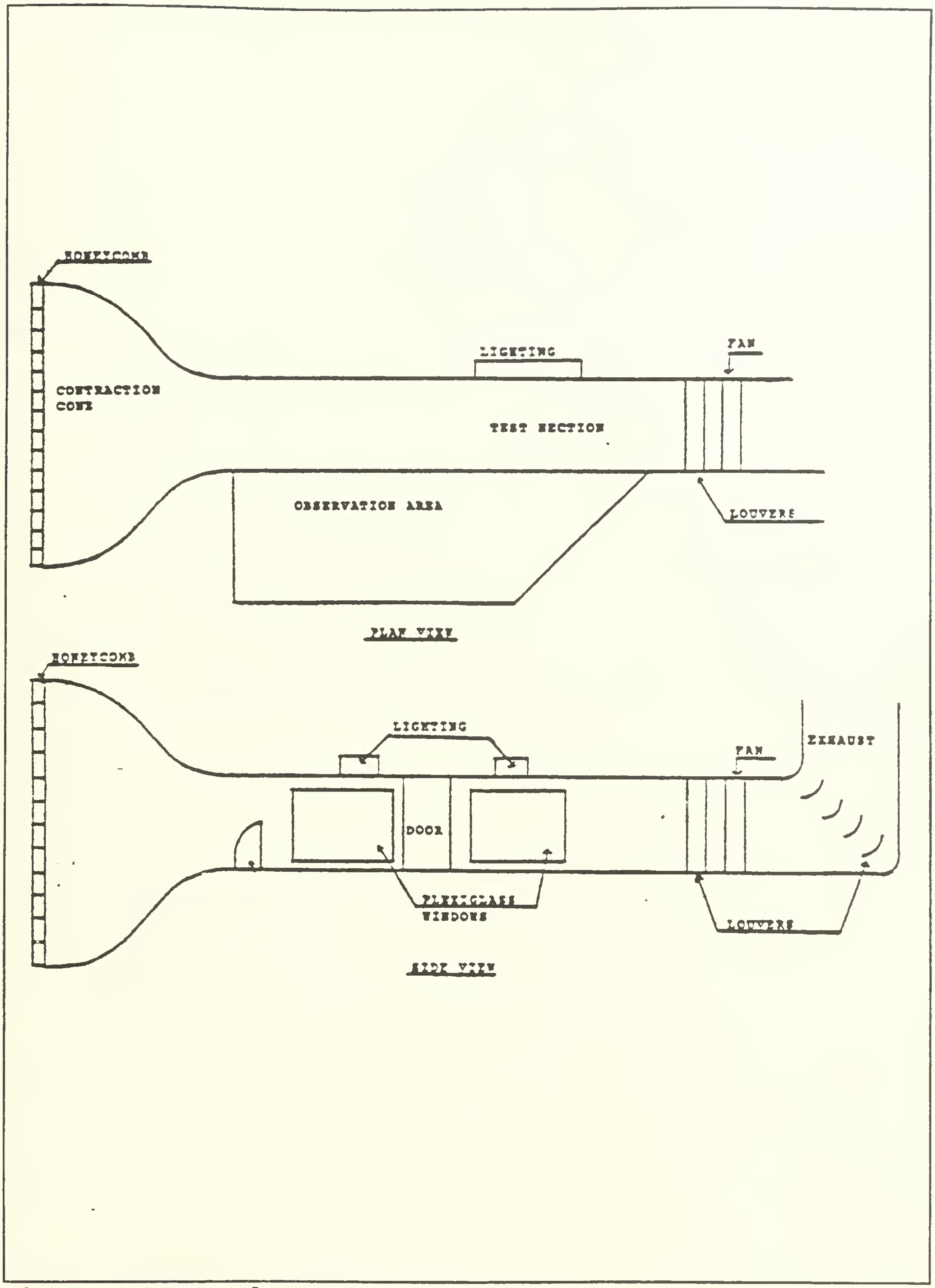

Figure 5.2 Tunnel Layout

	Tunnel Velocity Speed Check			
Comparing the digital manometer speed indications against known				
Aerolab Wind Tunnel readings (3 readings taken at each value)				
Digital reading	Aerolab reading	Dig. Vel.	Aero. Vel.	% Diff fm Acad.
(in H20)	(cm H20)	ft/s	ft/s	
0.0175	0.05	9.2815	9.845	5.72%
0.04	0.1	14.0338	13.9229	0.80%
0.0835	0.2	20.2735	19.69	2.96%
0.131	0.3	25.397	24.115	5.32%
0.173	0.4	29.1845	27.8459	4.81%
0.22	0.5	32.912	31.132	5.72%
0.263	0.6	35.985	34.1	5.53%
0.343	0.8	41.095	39.38	4.36%
0.43	1	46.013	44.028	4.51%
0.662	1.5	57.09	53.92	5.88%

Figure 5.3 Tunnel speed check

D. SMOKE GENERATION

The smoke was generated in the Rosco smoke/fog machine. Many different smoke injection techniques were tried but with less than satisfactory results. Smoke rakes were first tried outside the tunnel with the tube number varying from 2 to 30 tubes. The tubes were inserted in the honeycomb and also separated different distances from the inlet of the tunnel. The rake was also tried inside the test section with very bad results (smoke dispersed immediately). Problems ranged from lack of smoke and turbulence when enough smoke was present. The Rosco machine at its lowest setting was producing a very high smoke volume and whenever the flow was restricted by a smoke rake the smoke production went way down. The final technique adopted was very simple. The smoke output was sent directly from the machine to a 1" nozzle which was manually waved at the entrance of the tunnel to make a steady cloud. The steady cloud was gradually pulled into the tunnel, producing a thick smoke sheet in the test section.

E. PHOTOGRAPHY

Photos were taken using a Nikon 35mm camera and Kodak TMAX-400 ASA black and white film. The film speed was set to 1/250 seconds with an aperture setting of 4.0 for the light conditions. Film developing time was optimized at 9 minutes at 75 degrees F.

F. EXPERIMENTAL PROCEDURES

The first step involved a look at the large airfoil to verify normal flow patterns (Figure 5.4 and 5.5) and find the AOA for initial trailing edge separation (Figure 5.6). Next, the plunging airfoil was placed in the tunnel by itself and a run was made to verify the propulsive capability in the larger tunnel at higher speeds. As seen in Figure 5.7, the airfoil produced a drag vortical flow. Figure 5.8 and 5.9 shows the propulsive pattern of the propulsive airfoil. Finally, the two airfoils were placed in close relative position to see the interference effect between the two airfoils.

G. RESULTS AND DISCUSSION

Several airfoil position combinations were studied, as shown in Figures 5.10 through 5.15. Figure 5.10 and 5.11 show the plunging airfoil located at approximately .65 chord of the large airfoil. Figure 5.12 through 5.15 show the plunging airfoil located at approximately .75 chord.

The differences between the plunging on and off condition were not easy to see with the eye but pictures indeed showed some differences between the two conditions. A shortcoming of this experiment was the inability of the plunging airfoil to run parallel with the large airfoil. Additionally, sizing of and relative positioning of the two airfoils was not optimized to give best results. The two airfoils were chosen from the resources available and time constraints prevented a more

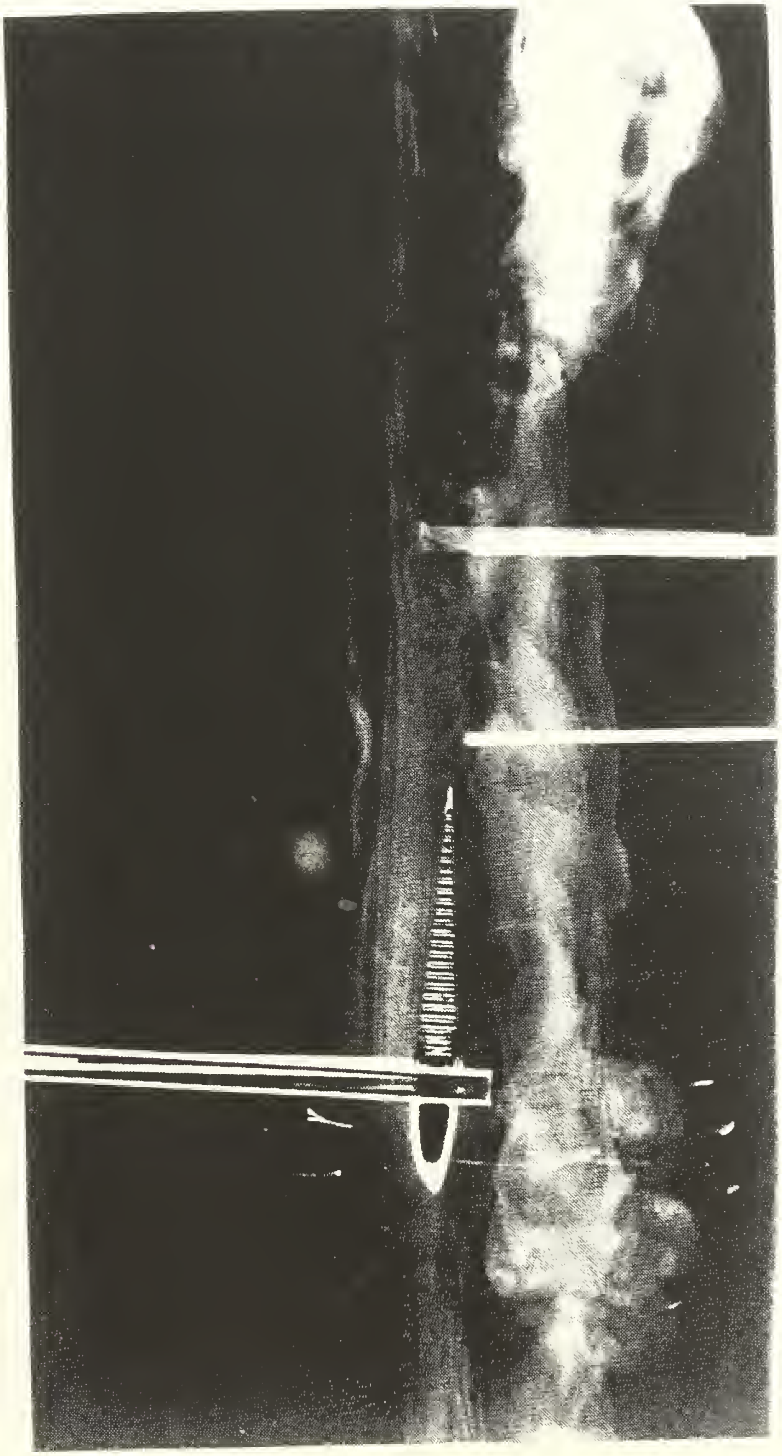

Figure 5.4 Large airfoil at zero AOA

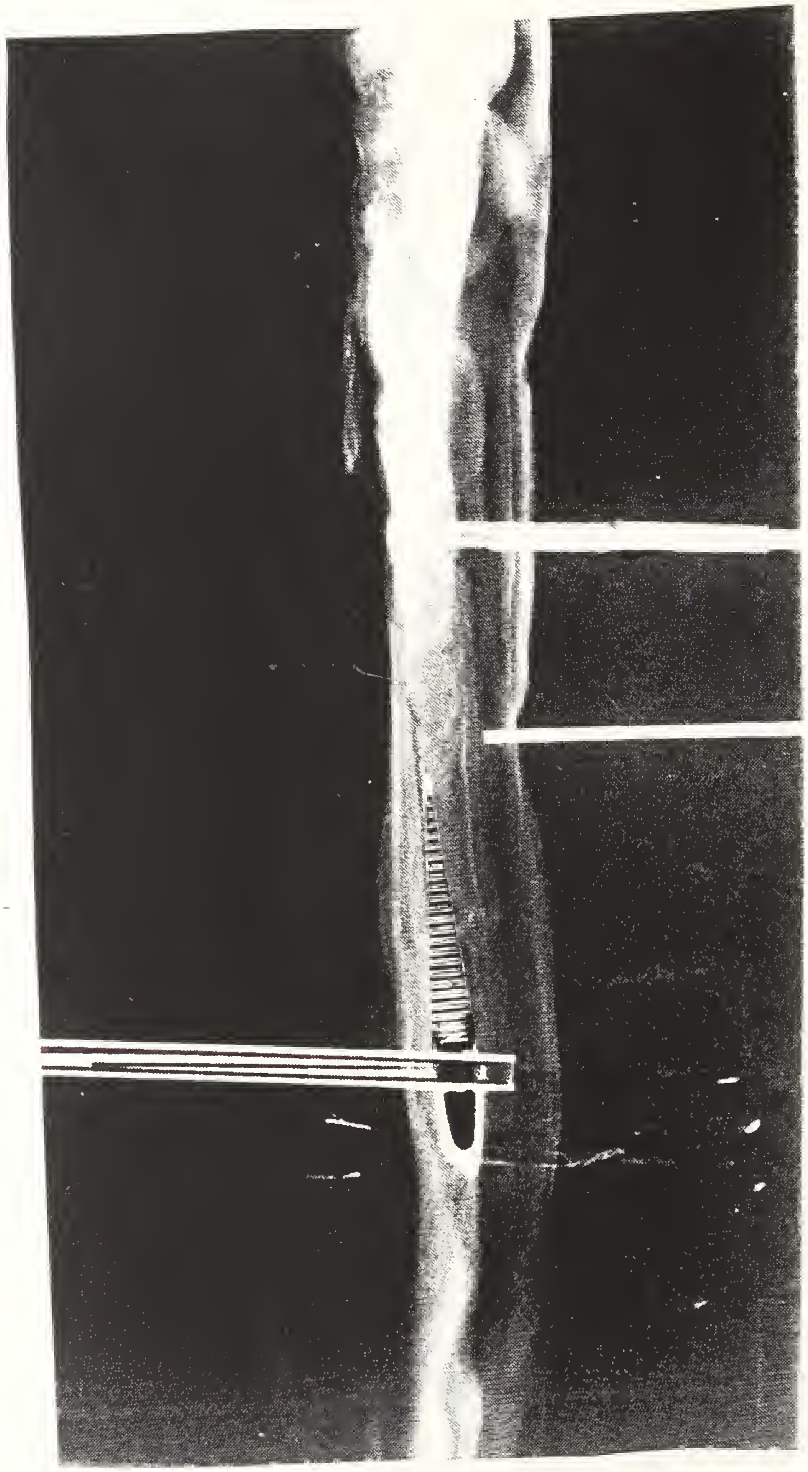

Figure 5.5 Large airfoil at 10 degrees AOA

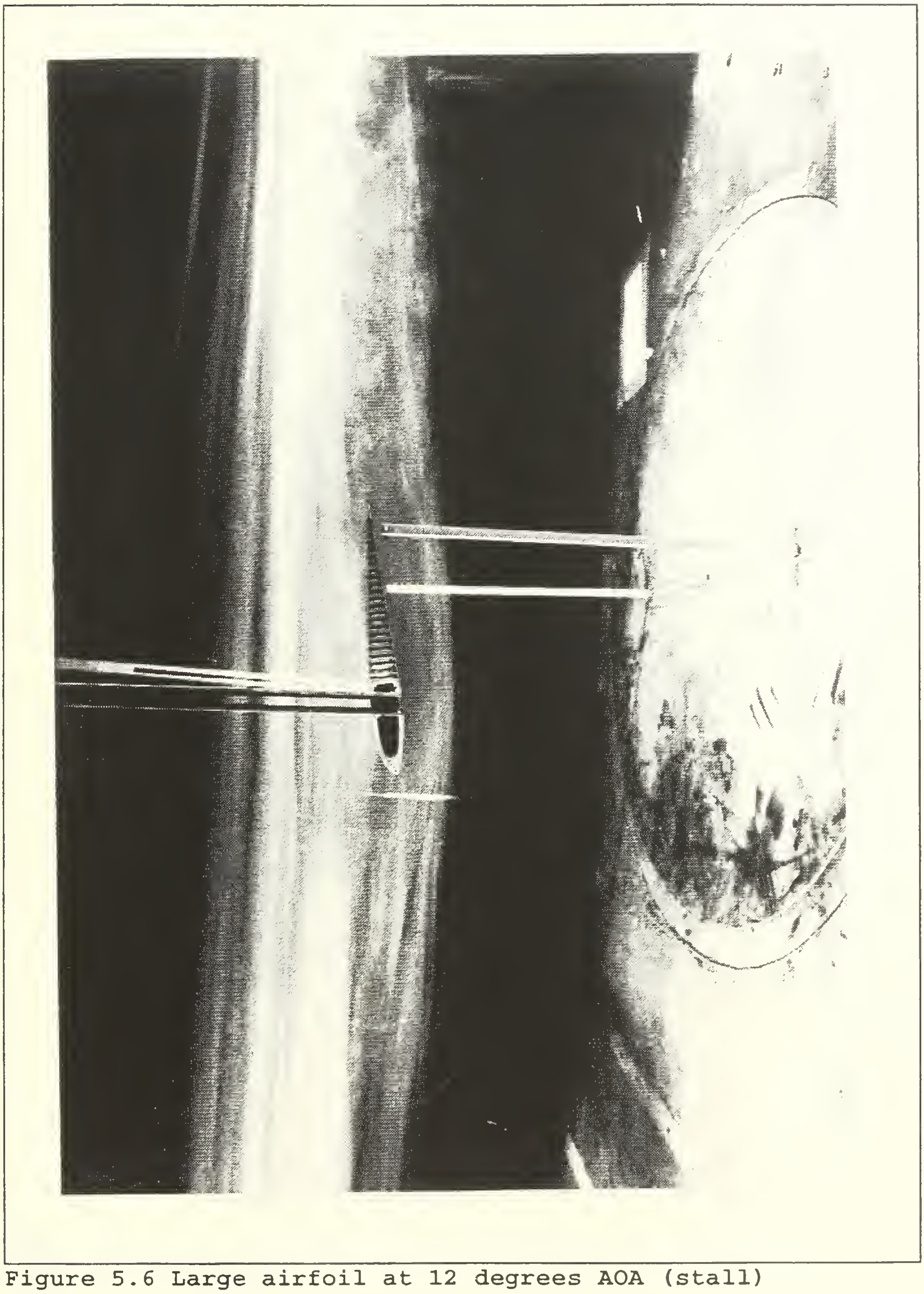

Figure 5.6 Large airfoil at 12 degrees AOA (stall)

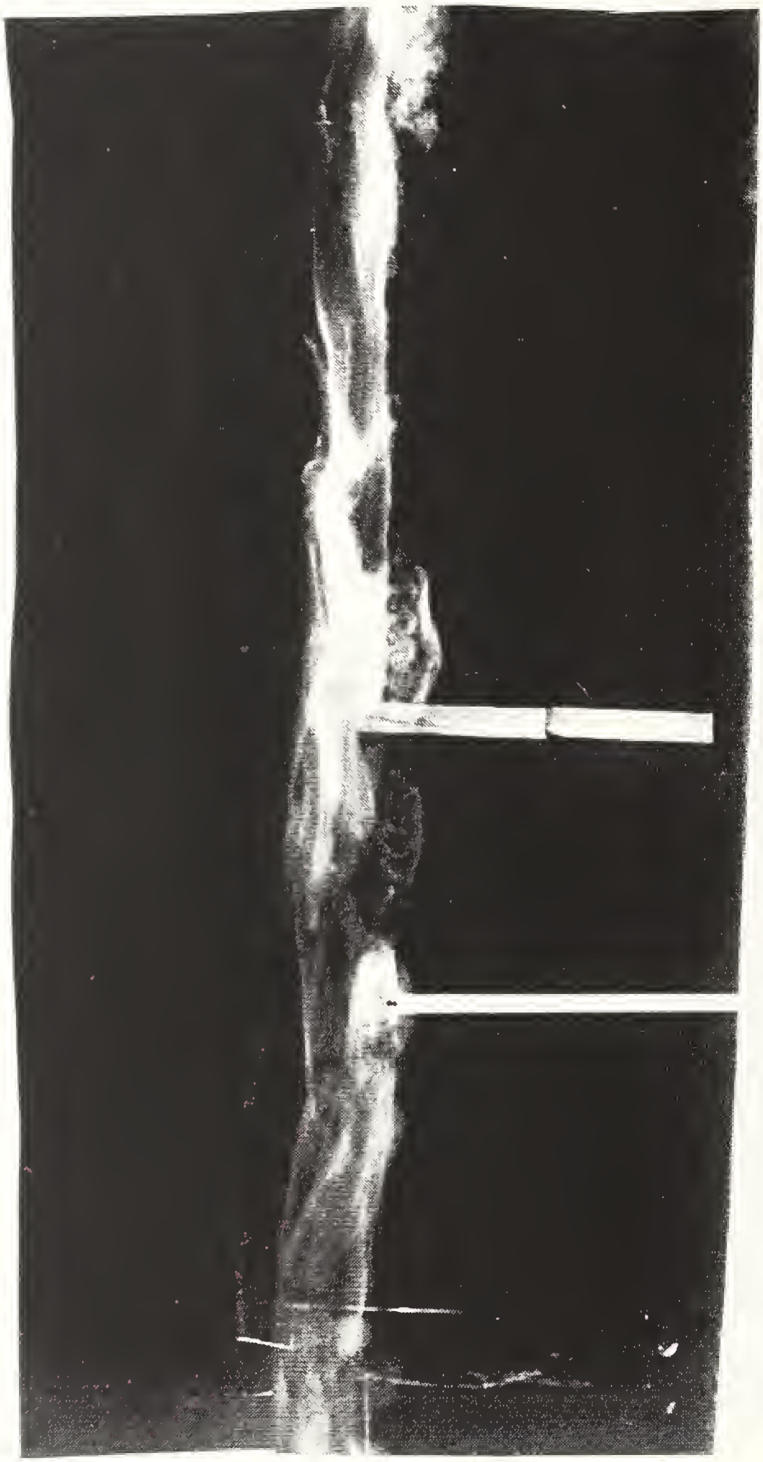

Figure 5.7 Plunge airfoil steady

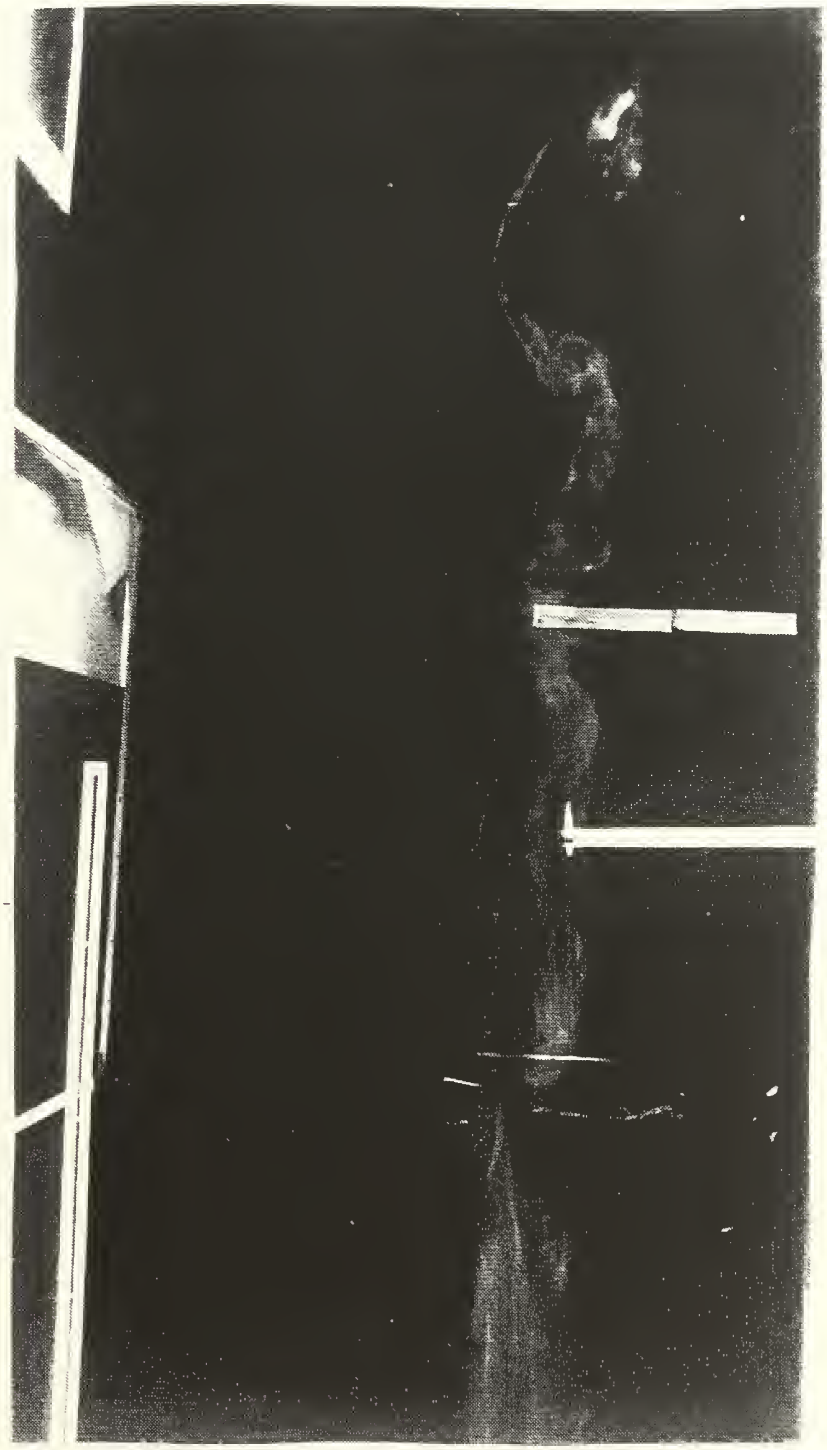

Figure 5.8 Plunging airfoil K_p=1.71

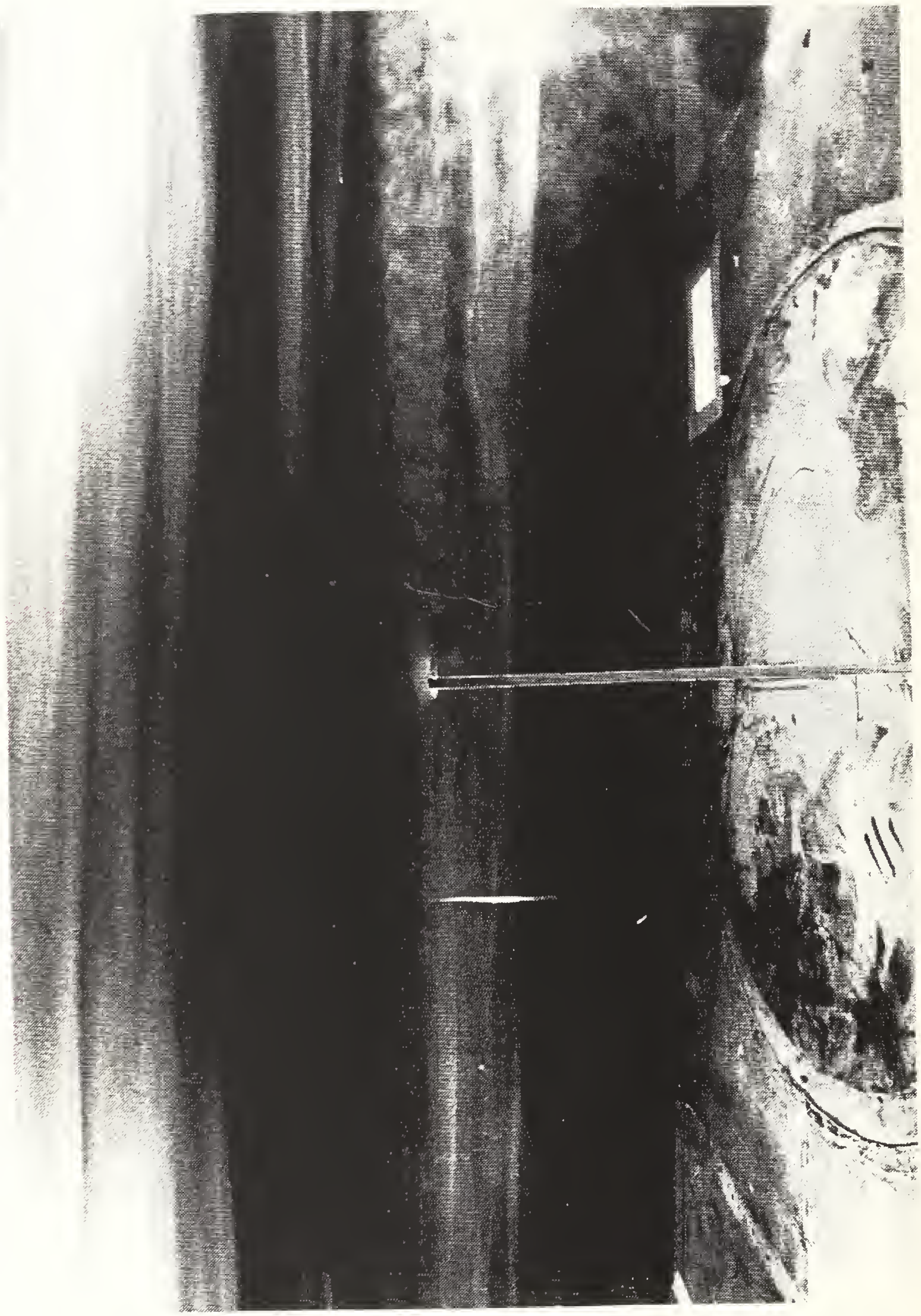

Figure 5.9 Plunging airfoil K_p=3.42

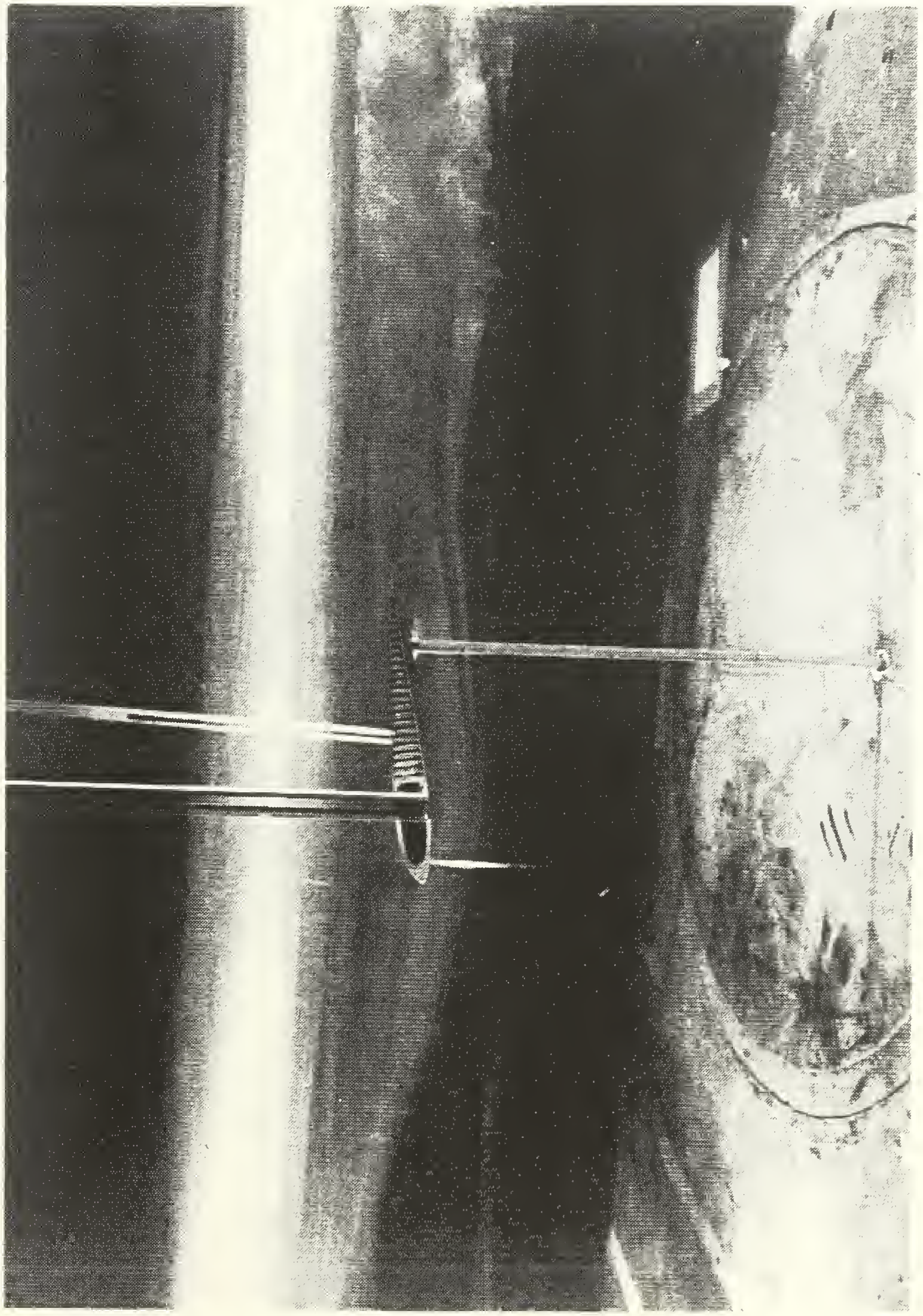

Figure 5.10 Large airfoil at 12 degrees AOA, steady plunging airfoil position 1

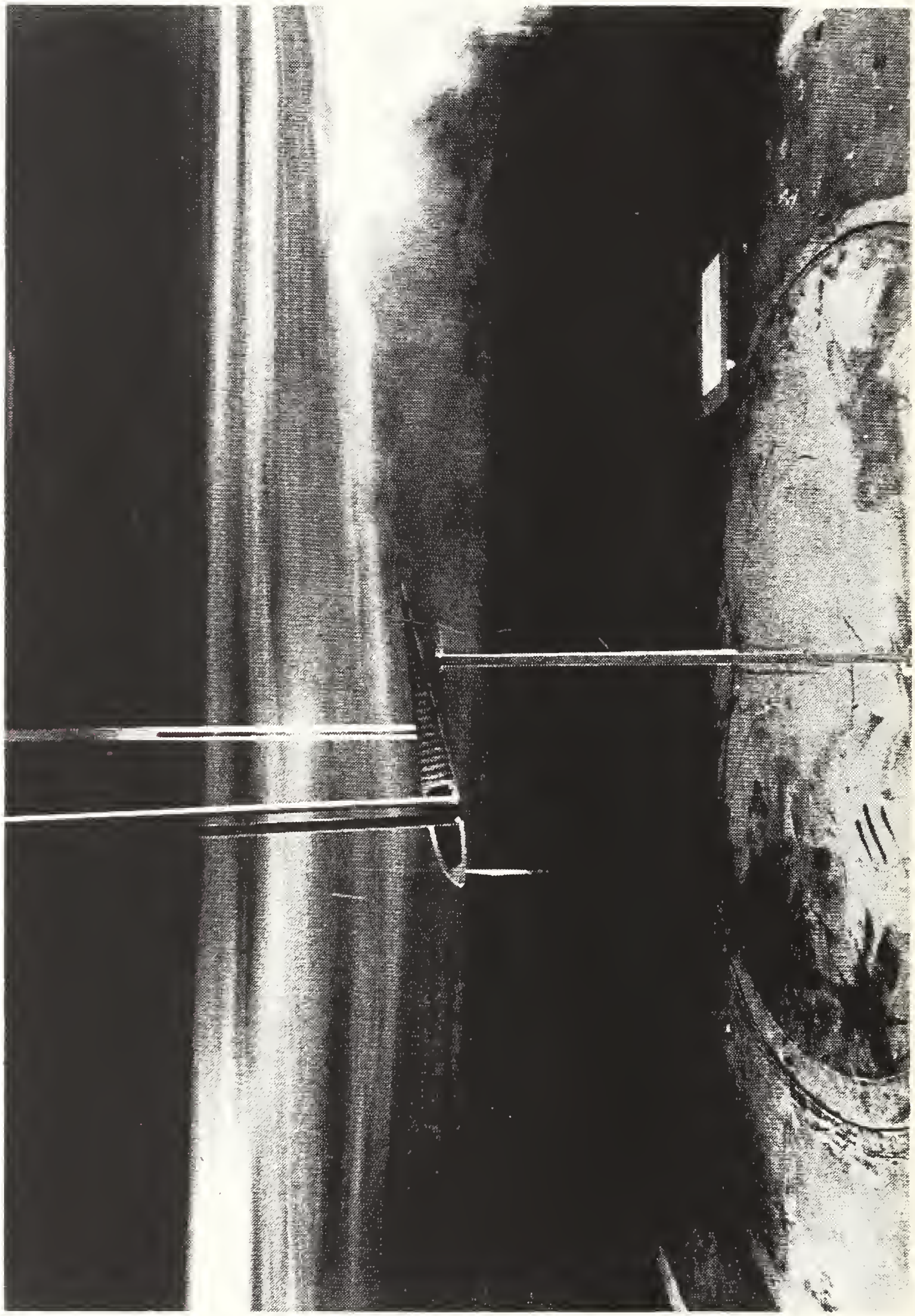

Figure 5.11 Large airfoil at 12 degrees AOA, plunging airfoil K_p=3.42, position 1

Figure 5.12 Large airfoil at 12 degrees AOA, plunging airfoil steady, position 2

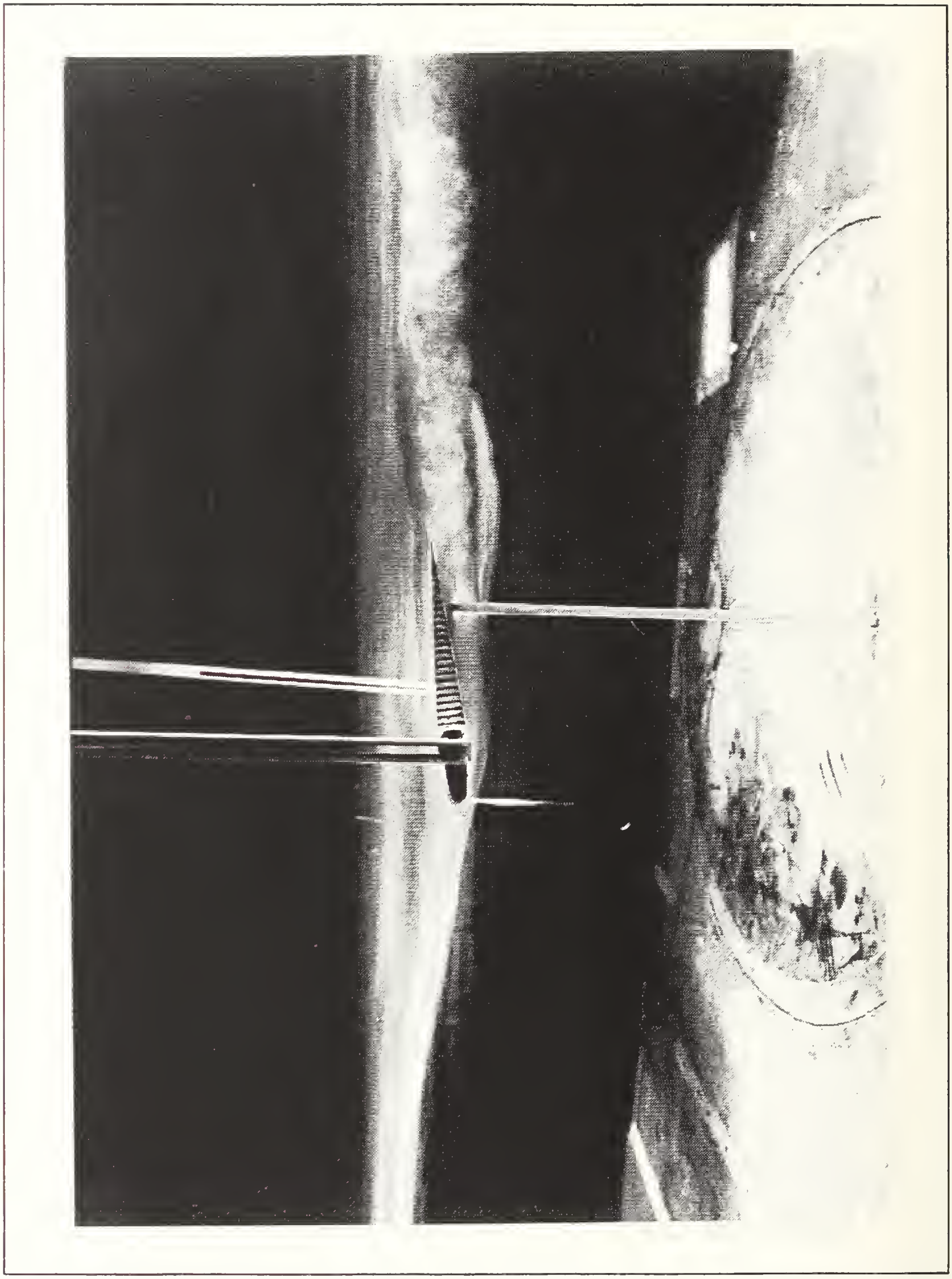

Figure 5.13 Large airfoil at 12 degrees AOA, plunging airfoil K_p=3.42, position 2

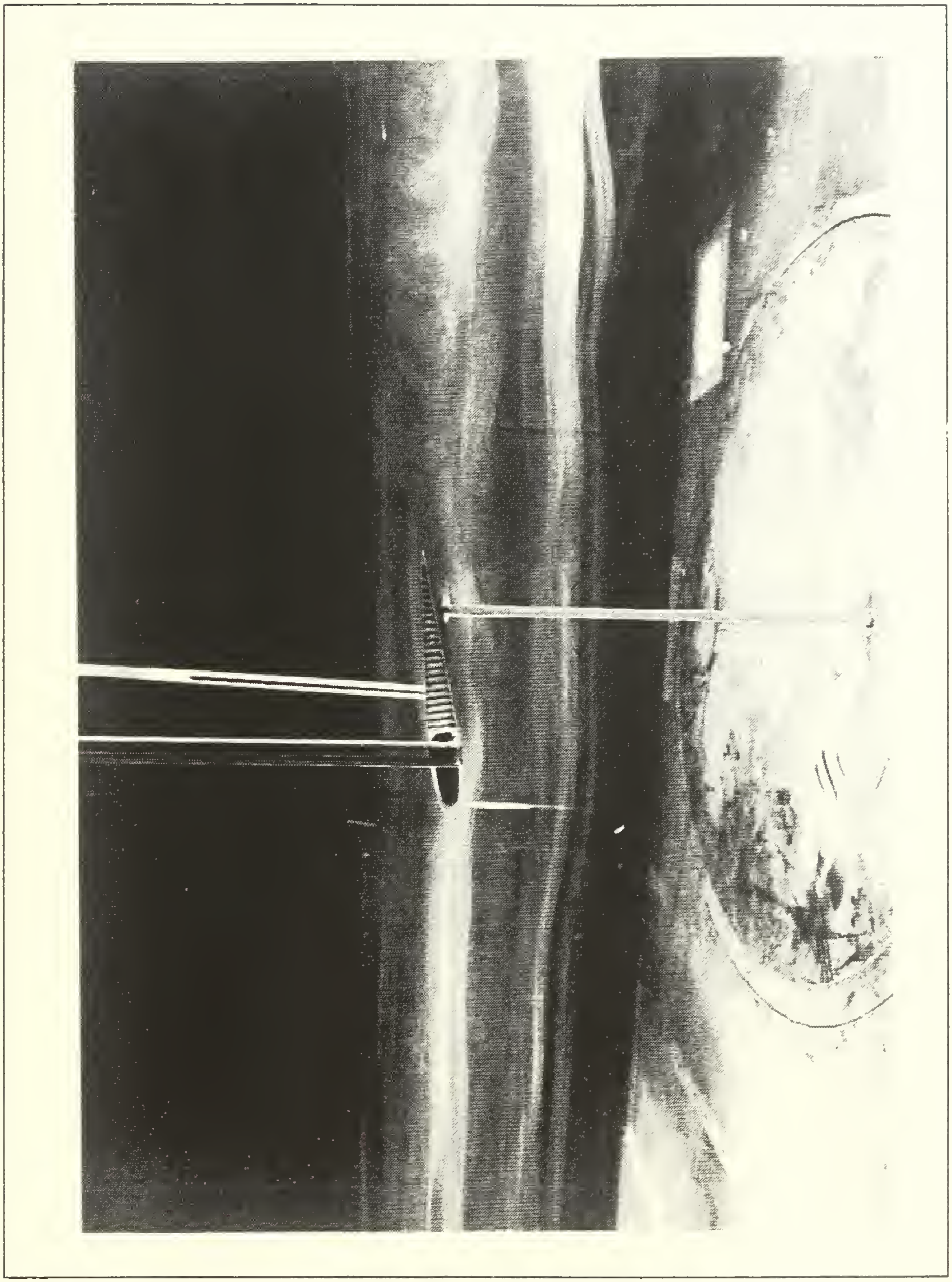

Figure 5.14 Large airfoil at 14 degrees AOA, plunging airfoil steady, position 2

Figure 5.15 Large airfoil at 14 degrees AOA, plunging airfoil K_p=3.42, position 2

detailed investigation of the interference effects between the two airfoils.

VI. CONCLUSIONS AND RECOMMENDATIONS

A. SINGLE AIRFOIL ANALYSIS

The modified version of U2DIIF (UPOT) can perform aerodynamic calculations over any range of reduced frequencies. The nonlinear theory presented here for harmonic motion, and the phase relationships that exist between the airfoil motion and the aerodynamic forces have been extensively verified by comparison with Theodorsen's linear theory. Furthermore, this panel code was applied to the analysis of incompressible bending-torsion airfoil flutter. Again, excellent agreement with the classical Theodorsen analysis was obtained.

Access to faster computational means is recommended to shorten the time needed to predict the flutter points. The code should be modified to incorporate three-dimensional calculations which would help solve more difficult flutter problems.

B. FLOW VISUALIZATION EXPERIMENTS

The flow visualization experiment successfully showed the development of thrust produced by a plunging airfoil. The enhanced lift experiment, on the other hand, was not a complete success. The smoke visualization presented difficulties that were not satisfactorily overcome. As a

result, the pictures taken were somewhat inconclusive. Futhermore, the angle of attack of the oscillating airfoil could not be changed thus making it difficult to achieve a flow condition conducive to lift enhancement.

It is recommended that further experiments be conducted in the low speed smoke tunnel with a shaker table capable of moving an airfoil at harmonic frequencies near 40 HZ. Additionally, the airfoil must be modified to allow change of AOA. Finally, the Rosco smoke machine output volume must be modified to permit much lower smoke output. This final point proved to be the single largest detriment to the visualization experiment.

LIST OF REFERENCES

1. Platzer,M.F.,*Class Lecture Notes*, Naval Postgraduate School,Monterey,California,Sep 1991.

2. Teng,N.H.,*The Development of a Computer Code (U2DIIF) for the Numerical Solution of Unsteady,Inviscid and Incompressible Flow over an Airfoil*,Master's Thesis,Naval Postgraduate School,Monterey,California,Jun 1987,pp. 1-135

3. Ashley,H.,Bislinghoff,R.L.,Halfman,R.L.,*Aeroelasticity*, Addison Wesley,1957.

4. Hess, J.L. and Smith, A.M.O. *Calculation of Potential Flow about Arbitrary Bodies*, Progress in Aeronautical Sciences, Vol. 8, Pergamon Press, Oxford, 1966,pp1-138.

5. Fung, Y.C., *The Theory of Aeroelasticity*, Dover, 1969,pp455-463.

6. Scanlan, Robert H., Rosenbaum, Robert, *Introduction to the Study of Aircraft Vibration and Flutter*, The Macmillan Company, 1960, pp. 192-204.

7. Freymouth,P., *Propulsive Vortical Signature of Plunging and Pitching Airfoils*, AIAA Journal,Vol. 26, No. 7, Jul 1988,pp. 881-883.

8. Theodorsen,T.,Garrick,T.E., *Mechanism of Flutter*, NACA TR-685,1940.

9. Neace,K.S., *A Computational and Experimental Investigation of the Propulsive and Lifting Characteristics of Oscillating Airfoils and Airfoil Combinations in Incompressible Flow*, Aeronautical and Astronautical Engineer's Thesis, Naval Postgraduate School, Monterey,California, Sep. 1992.

10. Theodorsen,T., *General Theory of Aerodynamic Instability and the Mechanism of Flutter, NACA TR-496*, 1934

11. Rhoades, Mark M., *A Study of the Airwake Aerodynamics over the Flight Deck of an AOR Model Ship*, Master's Thesis, Naval Postgraduate School, Monterey, California, Sep. 1990.

INITIAL DISTRIBUTION LIST

		No. Copies
1.	Defense Technical Information Center Cameron Station Alexandria VA 22304-6145	2
2.	Library, Code 052 Naval Postgraduate School Monterey CA 93943-5002	2
3.	Chairman, Code AA/CO Naval Postgraduate School Monterey, California 93943-5000	1
4.	Dr. M.F. Platzer Dept. of Aeronautics and Astronautics, Code AA/PL Naval Postgraduate School Monterey, California 93943-5000	6
5.	Dr. S.K. Hebbar Dept. of Aeronautics and Astronautics, Code AA/HB Naval Postgraduate School Monterey, California 93943-5000	2
6.	Dr. E. Tuncer Dept. of Aeronautics and Astronautics, Code AA/ET Naval Postgraduate School Monterey, California 93943-5000	1
7.	LCDR. Peter J. Riester 1129 Manchester Avenue Norfolk, Virginia 23508	1